

Version 6 Performance and Test Report

AIRS/AMSU/HSB Version 6 Level 2 Performance and Test Report

Edited by:

H. Van T. Dang, Bjorn Lambrightsen, and Evan Manning

Contributions by:

Evan Manning¹, Sun Wong¹, Frederick Irion¹, H. Van T. Dang¹, Glynn Hulley¹, Joel Susskind², Lena F. Iredell², John M. Blaisdell², Gyula Molnar², Bjorn H. Lambrightsen¹, Brian H. Kahn¹, Xiaozhen Xiong³, Juying Warner⁴, Baijun Tian¹, Larrabee Strow⁵, Joao Teixeira¹

¹Jet Propulsion Laboratory, California Institute of Technology

²NASA Goddard Space Flight Center

³NOAA

⁴ Dept. of Atmospheric & Oceanic Sciences, University of Maryland

⁵Physics Department, UMBC



December, 2012

Version 1.2

JPL

Jet Propulsion Laboratory
California Institute of Technology
Pasadena, CA

Submit Questions to:

<http://airs.jpl.nasa.gov/AskAirs>

Version 6 Performance and Test Report

Table of Contents

1. EXECUTIVE SUMMARY.....	11
2. INTRODUCTION.....	13
3. TEST RESULTS.....	14
3.1 GENERAL TREND/YIELD TESTING	14
3.1.1 Trends over all retrieved fields.....	14
3.1.2 Yield and Spurious Bias Trends of $T(p)$ and $q(p)$	20
3.1.3 Temperature and Water Vapor Retrieval Accuracy as a Function of Yield.....	21
3.2 WATER VAPOR DATA PRODUCTS FOR AIRS/AMSU AND AIRS-ONLY LAYER PRODUCT	33
3.3 TEMPERATURE BIAS AND BIAS TRENDS COMPARED WITH PREPQC RADIOSONDES.....	37
3.4 SURFACE AIR TEMPERATURE	49
3.5 LAND AND POLAR SURFACE TEMPERATURE AND EMISSIVITY	54
3.6 OCEAN SURFACE TEMPERATURE AND EMISSIVITY	70
3.7. MICROWAVE SURFACE PRODUCTS	80
3.8. CLOUD TOP PROPERTIES	83
3.9. CLOUD PHASE AND ICE CLOUD PROPERTIES	92
3.10. OUTGOING LONGWAVE RADIATION.....	99
3.11. TRACE GASES.....	105
3.11.1 Methane	105
3.11.2 Carbon Monoxide.....	113
3.11.3 Ozone.....	122
3.12. TROPOPAUSE PRESSURE AND HEIGHT	128
3.13. HEIGHT OF TOP OF BOUNDARY LAYER.....	132
3.14. CLOUD CLEARED RADIANCES	134
3.15. SO ₂ BRIGHTNESS TEMPERATURE AND FLAG	141
3.16. DUST DETECTION	143
3.17. LAYER TO LEVEL TRANSFORMATION.....	144
4. APPENDIX A: PRODUCT TABLES	147
4.1. STANDARD PRODUCTS ('AIRX2RET').....	147
4.2. SUPPORT PRODUCTS ('AIRX2SUP').....	158
4.3. CLOUD CLEARED RADIANCES ('AIRICCF')	195

Version 6 Performance and Test Report

Table of Tables

Table 1. 7-Day Mean Statistics Tropospheric Temperature Metric (TTM)	29
Table 2. TSurfStd statistics over sea-ice pixels for Jan. 2007 day and night.	67
Table 3. Annual global trend.....	103
Table 4. Relative biases of V5, V6, and V6-AIRS only total ozone compared to OMI, filtered by quality flags, for sunlit observations of Feb. 24, 2007. The upper rows are unweighted averages, while the lower rows are averages weighted by cos(latitude).	124

Table of Figures

Figure 1. Total retrieved methane by latitude zone (y axis) for different stratifications. (a) sea night, (b) sea day, (c) land night, (d) land day.....	15
Figure 2 Difference in V6.0.2 AIRS+AMSU retrieved global monthly methane between 2003 and 2011. a) January b) April c) July d) October.....	16
Figure 3 Difference in V6.0.2 retrieved global monthly methane between Jan 2003 and Jan 2011. a) AIRS+AMSU. b) IR-Only.....	17
Figure 4 . Total retrieved carbon monoxide by latitude zone (y axis) for different stratifications. (a) sea night, (b) sea day, (c) land night, (d) land day.....	18
Figure 5 Difference in mean monthly retrieved carbon monoxide between 2003 and 2011. a) January b) April c) July d)October	19
Figure 6. Difference in V6.0.2 retrieved monthly carbon monoxide between January 2003 and January 2011 a) AIRS+AMSU b) IR-Only	19
Figure 7. Global trends of water vapor and temperature bias.....	21
Figure 8. Focus day statistics: Temperature	24
Figure 9. Focus day statistics: Water vapor	25
Figure 10. Focus day statistics: QC comparison.....	26
Figure 11. T(p) RMS error for different ensembles (water vapor)	28
Figure 12. Same as previous figure but for precipitable water	30
Figure 13. Spatial distribution of a pseudo-Level-3 seven day field of accepted cases of total precipitable water.....	32
Figure 14 Geographical distributions of specific humidity (in g/kg) on Jan 15, 2007 in the layers of 250-300 (top row), 400-500 (middle row), and 700-850 hPa (bottom row) for the V5 (left column), V6 Layer, and V6 Layer TqJ	

Version 6 Performance and Test Report

Level-3 products. The plots are the averages of the ascending and descending soundings of specific humidity. The missing data are in black color.....	34
Figure 15 Comparison of the AIRS Level-2 specific humidity vertical profiles to the measurements of dedicated sondes in the tropics (left column, 30°S-30°N), mid-latitudes (middle column, 30°-60°N), and polar region (right column, 60°-90°N). All sondes' profiles from 2002 to 2007 are included in these plots and the numbers of samples are shown on the right axis of each panel. The top row is for profiles without quality control being applied, the middle row is for profiles selected by quality flags less or equal to 1, and the bottom row is for profiles selected by quality flags equal to 0. The black solid lines are the sonde profiles, the red solid lines are the V5 specific humidity, the blue solid lines are the V6 specific humidity (layer product), and the blue dash-dotted lines are the V6 infrared-only retrievals of specific humidity.	36
Figure 16 Locations of AIRS – radiosonde matchups for December 2005-January-February 2006 (left panel), and June, July, August 2006 (right panel).....	42
Figure 17 Zonally-averaged comparisons of AIRS minus operational radiosonde temperatures (left panels), number of sondes in zonal bin (middle panels), and AIRS minus radiosonde modified by the AIRS averaging kernel as in Equation 2. Data are from December 2005 through February 2006. Note that the right panels have a shorter temperature scale than the left panels.....	43
Figure 18 Zonally-averaged comparisons of V5 and V6 AIRS minus operational radiosonde temperatures (left panels), number of sondes in zonal bin (middle panels), and AIRS minus radiosonde modified by the AIRS averaging kernel as in Equation 2. Data are from June, July and August 2006. Note that the right panels have a shorter temperature scale than the left panels.	44
Figure 19 Zonally-averaged comparisons of AIRS V6-Regular (using AMSU in the retrieval) and V6 AIRS-only (without AMSU) minus radiosonde temperatures (left panels), and AIRS-only minus AIRS-regular on the right panels. Data are from December 2005 through February 2006. Note that the right panels have a shorter temperature scale than the left panels.....	45
Figure 20 Zonally-averaged comparisons of AIRS V6-Regular (using AMSU in the retrieval) and V6 AIRS-only (without AMSU) minus radiosonde temperatures (left panels), and AIRS-only minus AIRS-regular on the right panels. Data are from June through August 2006. Note that the right panels have a shorter temperature scale than the left panels.	46
Figure 21 Zonally averaged temperature bias drift of V5 and V6 AIRS minus operational radiosondes (left panel), and minus sondes modified by the AIRS	

Version 6 Performance and Test Report

averaging kernel as in Equation 2 (right panel). Trends were calculated by linear, least squares fitting though calendar month data from 2004 through 2011, with the average slope over all months shown above. The thinner lines are the standard deviation of the average slope at each pressure level.	47
Figure 22 Zonally averaged temperature bias trends of AIRS V6-Regular (using AMSU in the retrieval) and V6 AIRS-only (without AMSU) minus operational radiosondes (left panels), and AIRS-only minus AIRS-Regular (right panels). Trends were calculated by linear, least squares fitting though calendar month data from 2004 through 2011, with the average slope over all months shown above. The thinner lines are the standard deviation of the average slope at each pressure level.	48
Figure 23. Location of PrepQC radiosondes that are matched to AIRS ocean cases.	50
Figure 24. Location of PrepQC radiosondes that are matched to AIRS land cases.	50
Figure 25. Land and Ocean scenes showing AIRS V5 and V6 showing the average deviation from sondes per latitude band. Also the number of matchups between AIRS and sondes per latitude band.	51
Figure 26. Land cases of AIRS V5 and V6 showing the average deviation from sondes per latitude band for day and night cases.....	53
Figure 27. AIRS percent yield for Jan. 2007 based on TSurfStd_QC using QC=0 (best), 1 (good), 2 (bad) for (a) AIRS V5 graybody surfaces, (b) AIRS V5 bare surfaces, (c) AIRS V6 graybody surfaces, and (d) AIRS V6 bare surfaces.....	55
Figure 28. AIRS surface temperature estimated error, TSurfStdErr, versus quality control, TSurfStd_QC for global AIRS/AMSU retrievals during Jan. 2007.....	55
Figure 29. Mean monthly TSurfStd during Jan. 2007 for day-time (left) and night-time (right) AIRS/AMSU V6 retrieval using QC=(0,1).....	56
Figure 30. Monthly standard deviation of TSurfStd during Jan. 2007 for day-time (left) and night-time (right) AIRS/AMSU V6 retrieval using QC=(0,1).....	57
Figure 31. Mean monthly day (left) night-time (right) differences between AIRS/AMSU and AIRS IR-only V6 LST for Jan. 2007 using QC=(0,1).	58
Figure 32. Mean monthly day-time differences between AIRS V5 and MODIS v4.1 LST for Jan. 2007 using QC=(0,1).	58
Figure 33. Mean monthly day-time differences between AIRS V6 and MODIS v4.1 LST for Jan. 2007 using QC=(0,1).	59
Figure 34 Mean monthly emisIRStd at 2632 cm-1 during Jan. 2007 for day-time (left) and night-time (right) AIRS/AMSU V6 retrieval using QC=(0,1).....	61

Version 6 Performance and Test Report

Figure 35 Monthly standard deviation of emisIRStd at 2632 cm ⁻¹ during Jan. 2007 for day-time (left) and night-time (right) AIRS/AMSU V6 retrieval using QC=(0,1).....	61
Figure 36. Distributions of AIRS V5 (left panels) and V6 (right panels) global daytime emissivities at 820 cm ⁻¹ for Jan. 2007 using QC=(0,1).....	62
Figure 37. Diurnal (day-night) shortwave emissivity differences for AIRS V5 (left panels) and V6 (right panels) at 2632 cm ⁻¹ for Jan. 2007 using QC=(0,1). Diurnal differences are reduced by more than a factor of two in V6, although some unphysical differences are reduced by more than a factor of two in V6, although some unphysical differences are still evident (e.g. Australia).....	63
Figure 38. AIRS mean emissivity spectra from 2003-2006 over the Grand Erg Oriental validation site in Algeria for V5 (left) using the NOAA surface regression first guess, and V6 (right) using the UW-Madison MODIS baseline-fit emissivity database. Improvement in emissivity spectral shape and absolute magnitude versus ASTER emissivity at this site is clearly seen.	64
Figure 39. Mean monthly day (left) night-time (right) differences between AIRS/AMSU and AIRS IR-only V6 shortwave emissivity (2632 cm ⁻¹) for Jan. 2007 using QC=(0,1)	65
Figure 40. Maximum values of SurfClass from 6-12 Jan. 2007 for AIRS V6 (left) and V5 (right) for daytime (top) and night-time (bottom).....	66
Figure 41. Same as Figure 40 except results are for the AIRS IR-only retrieval.	66
Figure 42. AIRS/AMSU V6 (top rows), V5 (middle rows), and AIRS V6 IR-only (bottom rows) surface emissivity for three channels (820, 1163, 2632 cm ⁻¹) for sea-pixels classified by SurfClass during July 2007 for day and night-time data.....	69
Figure 43 Surface skin temperature difference for seven days with combined night and day time data for 50S to 50N over non-frozen ocean.....	70
Figure 44 Difference between AIRS and ECMWF surface skin tempareture for V5 and V6.	72
Figure 45 Mean difference between AIRS and Masuda emissivity for 950 cm ⁻¹ . 74	
Figure 46 Mean difference between AIRS and Masuda emissivity for 2400 cm ⁻¹ . 75	
Figure 47 Standard deviation of Emissivity at 950 cm ⁻¹	76
Figure 48 Standard deviation of Emissivity at 2400 cm ⁻¹	77
Figure 49 Mean difference between daytime and nighttime emissivities for 950 cm ⁻¹ and 2400 cm ⁻¹	78

Version 6 Performance and Test Report

Figure 50 Mean difference in Emissivity between night and day for different AIRS versions.....	79
Figure 51. AMSU-A channel 5 brightness temperature: 9/14/2002 (left); 4/21/2011 (right)	81
Figure 52. Retrieved surface emissivity at 50.3 GHz, 4/21/2011: V5 (left); V6 (center); V6-V5 (right)	81
Figure 53. Retrieved surface emissivity at 50.3 GHz, 9/14/2002: V5 (left); V6 (center); V6-V5 (right)	82
Figure 54. Distributions of Cloud Top Height over ocean for day/night from AIRS, CALIPSO, and CloudSat for V5 and V6 single and double cloud layer as determined by AIRS.....	84
Figure 55. Distribution of Cloud Top Height over Land for AIRS, CALIPSO, and CloudSat during day/night scenes of either single or double cloud layer as determined by AIRS V5/V6.....	86
Figure 56. Average AIRS deviation from CALIPSO CTH per 10 degree latitude band for V5/V6 LAND/OCEAN and DAY/NIGHT scenes.....	86
Figure 57. Distribution of V5 and V6 Cloud Top Temperature and Cloud Top Pressure of the top and bottom layer along with the values weighted by the Effective Cloud Fraction.....	88
Figure 58. Showing the top layer effective cloud coverage changes from V5 to V6 given the changes in the top layer of cloud top pressure from V5 to V6.89	89
Figure 59 Comparing AIRS/AMSU and AIRS-ONLY CTP retrieval in V6.0.2. A) For single layer as determined by AIRS/AMSU, comparing top layer CTP AIRS/AMSU top layer CTP of AIRS-ONLY B) For double layer as determined by AIRS/AMSU, comparing top layer CTP AIRS/AMSU top layer CTP of AIRS-ONLY. C) Comparing the bottom layer CTP of AIRS/AMSU to AIRS-ONLY	90
Figure 60 Distribution of the CTP between AIRS/AMSU and AIRS-ONLY retrieval.....	91
Figure 61 Histogram of new cloud products.....	96
Figure 62 Difference between AIRS and CERES global and clear sky OLR.	100
Figure 63 Time series of global and clear sky OLR.	102
Figure 64 Global temperature trends.	104
Figure 65 Comparison of DOFs in V6 and V5 for the case on March 27, 2010.	107
Figure 66 Comparison of the area of averaging kernels function with latitude (upper panel is V5 and the lower panel is for V6) on March 27, 2010.	108

Version 6 Performance and Test Report

Figure 67 The retrieved total column of CH ₄ from V6 and V5 on March 27, 2010 (ascending only)	109
Figure 68 The retrieved CH ₄ at 400 hPa from V6 and V5 on March 27, 2010 (ascending only)	110
Figure 69 Latitudinal gradient of CH ₄ at 400 and 800 hPa from HIPPO-3 aircraft measurement (red triangle) in March/April, 2010, and its comparison with one day retrievals from V5 (black line) and V6 (green line) on March 27, 2010 (left two panels). Right panel is from V6 using all collocated AIRS and HIPPO-1 observations.....	110
Figure 70 Validation of CH ₄ retrieval (V5) in layer between 286 – 496 hPa using HIPPO-1,-2,-3 aircraft measurement data. N=101 is the number of data points between the two blue dash lines.	111
Figure 71 Same as Figure 4a but for AIRS V6. The correlation and bias and RMS error in V6 is much smaller than V5.....	111
Figure 72 Monthly variation of CO used as the first guess for AIRS retrieval of CO.	115
Figure 73 Yields of CO for different quality flags.....	116
Figure 74 Global total column CO for day and night for V5 and V6 and their differences.	118
Figure 75 Error estimates CO retrieval at 506 mb for day and night of V5 and V6.	119
Figure 76 Profiles of CO mixing ratio.	120
Figure 77 Relative bias of Versions 5, 6, and 6 AIRS-only and Version 3 OMI total ozone for Feb. 24, 2007.	123
Figure 78 AIRS-OMI relative difference vs AIRS-AMSRe ocean surface temperature difference for Feb. 24, 2007.	124
Figure 79 Version 5 AIRS-OMI relative ozone bias vs combined cloud-top pressure (top panel) and number of observations in bin (bottom panel) for sunlit observations of Feb. 24, 2007. Dots are colored by the total cloud fraction. The combined cloud-top pressure is the sum of the retrieved pressures weighted by the cloud fraction in each cloud layer.....	125
Figure 80 Version 6 AIRS-OMI relative ozone bias vs combined cloud-top pressure (top panel) and number of observations in bin (bottom panel) for sunlit observations of Feb. 24, 2007. Dots are colored by the total cloud fraction. The combined cloud-top pressure is the sum of the retrieved pressures weighted by the cloud fraction in each cloud layer.....	126
Figure 81 Version 6 AIRS only-OMI relative ozone bias vs combined cloud-top pressure (top panel) and number of observations in bin (bottom panel) for sunlit observations of Feb. 24, 2007. Dots are colored by the total cloud	

Version 6 Performance and Test Report

fraction. The combined cloud-top pressure is the sum of the retrieved pressures weighted by the cloud fraction in each cloud layer.....	127
Figure 82. The AIRS tropopause pressure (TropPres) for the ascending node of January 1st, 2007. The upper panel is for V5 and the lower panel is for V6.....	129
Figure 83. The AIRS tropopause temperature (TropTemp) for the ascending node of January 1 st , 2007. The upper panel is for V5 and the lower panel is for V6.....	130
Figure 84. The AIRS tropopause height (TropHeight) for the ascending node of January 1 st , 2007. The upper panel is for V5 and the lower panel is for V6.....	131
Figure 85 Monthly average (January 2003) PBL height (in pressure, hPa) for the AIRS+AMSU operational version 6 retrieval system.....	133
Figure 86 Monthly average (January 2003) PBL height (in pressure, hPa) for the AIRS-only operational version 6 retrieval system.	133
Figure 87 Map of cloud cleared radiance quality for Feb. 25, 2012. Good=blue, Better=green, Best=red.	135
Figure 88 Bias histograms of cloud-cleared versus sea-surface temperature between \pm 60 deg latitude. Also shown is the AIRS Calibration Data Set (ACDS) “very” clear bias histogram and the ACDS bias over land (versus ECMWF land surface temperatures).	136
Figure 89 Comparison of widths of AIRS V5 and V6 covariances versus kernal function widths near 850 mbar. Also shown in the ECMWF 850 mbar covariance.	136
Figure 90 Similar bias histograms as in Figure 88 but now for combined latitudes of 30N-60N and 30S-60S and only for “Good” cloud-cleared radiances. The ACDS clear bias histogram is shown for reference. Clearly the cloud-cleared radiances contain significant cloud contamination.	137
Figure 91 Bias histograms for cloud-cleared ocean radiances for 30-70 deg N/S but subsetted for observations (according to L2 Supplemental product) with cloud fraction ranging from 25-50%.	138
Figure 92: Bias and standard deviations for cloud-cleared and clear scenes for \pm 60 degrees, ocean, night.	139
Figure 93: Zoom of Figure 92.....	140
Figure 94. AIRS V6 SO ₂ flags (left panel) shown with the absolute values of the brightness temperature differences compared against the Aura/OMI SO ₂ total columns (DU) (right panel) over Reykjavik, Iceland on May 27, 2011	142
Figure 95 Layer and level profile comparison of water vapor from the support product.....	145

Version 6 Performance and Test Report

Figure 96 Layer and level profile comparison of water vapor from the support product.....146

Version 6 Performance and Test Report

1. Executive Summary

This test report characterizes the various AIRS core data product differences going from V5 to V6, and in many instances provides comparisons to other well validated data sources such as radiosondes. The report also features newly developed data products which are still being researched and tested to see if they are within reasonable range of well-established data sources. This document is used as a litmus test to detect errors before the release of V6 and as groundwork for which validation can be carried out afterwards. The report does not touch on much of the changes in algorithm between versions, just the results of the differences in data values. To get a detailed description of the algorithm changes, please refer to the V6 Algorithm Theoretical Basis Document. The report also does not delve much into the reasons for the differences in data values between V5 and V6 and the anomalies in V6, it only states what the differences and anomalies are. The reasons behind the anomalies will be hypothesized and analyzed in a subsequent validation report.

In V5, bias trends in temperature, water vapor, and the low altitude clouds were significant, but in V6 they have been greatly reduced when compared to ECMWF, radiosondes, and other remote sensing data. The yield for temperature and water vapor profile has been improved to reflect a subset of the data targeted for data assimilation needs and another that has a better yield to be used for climate studies. The AIRS cloud top products have seen greater agreement with CALIPSO and CloudSat when looking at cloud detection and also the top height of a cloud layer as indirectly reported by AIRS.

The surface temperature and emissivity over land, ocean, and Polar Regions have seen significant improvements, especially reflected in the more reasonable range values between night and day for emissivity. This has probably led to an improvement in the comparison of surface air temperature with radiosondes for many latitude bands.

Carbon monoxide and methane have seen improvements in the trends and comparison to direct measurements from aircraft instruments. For total column ozone, V6 is a slight improvement over V5, but there are still problems when the surface skin temperature does not compare well to AMSR-E or the scene has a significant cloud amount.

Top height of the boundary layer and cirrus cloud products are new research products produced in V6 and currently residing in the Support products. They

Version 6 Performance and Test Report

have been tested for this report to see how reasonable they look, but they will be more rigorously validated in the validation report.

The removal of the failed AMSU-A channel 5 from Version 6 has improved the retrievals and yields of the core products in the years since AMSU-A channel 5 ceased to function properly. Since AMSU performance continues to degrade, it may become necessary to switch to AIRS-only retrievals in the future. Therefore, AIRS-only retrievals of water vapor and temperature profiles are also addressed in this report.

Version 6 Performance and Test Report

2. Introduction

Unless otherwise stated, “Version 6” refers to V6.06 and is generally compared to V5.0.16.0. Occasionally, “Version 4” may also be referenced, which then refers to V4.0.9.0.

The test results can be found in Section 3. The reader should not interpret the analyses as validation but rather as indicators of the characteristics of the products and how they differ from those in the previous version. Additional information can be found in the User guides.

The AIRS product files contain a large number of parameters, ranging from quality flags to retrieved data values. Complete lists of the parameters can be found in Appendix A, where the range of values assumed by each parameter is also listed. Only a small subset of these parameters, representative of the core retrieved variables, have been tested and assessed. This includes the thermodynamic quantities (temperature, humidity, cloud parameters), trace gases (except for CO₂, which will be reported on in a separate report), and surface parameters. The reader is referred to the table of contents.

One of the new features in V6 is that parameters that have previously been determined as layer averages are now also determined at pressure levels. This is essentially done by interpolation with smoothing kernels. This mathematical transformation leads to occasional strange results for water vapor profiles with inversions, typically near the surface. A section of the test report is dedicated to this.

Version 6 Performance and Test Report

3. Test Results

3.1 General Trend/Yield Testing

Tester and point of contact unless noted otherwise: Joel Susskind

3.1.1 Trends over all retrieved fields

Tester and Point of Contact: Evan Manning

In order to find any large trends in AIRS retrieved products, an automated process looked for trends in AIRS+AMSU V6.0.2.0 data for every January from 2003-2011 using the January nadir data set. Best-fit linear trends were calculated separately for day vs. night, land vs. ocean, and 18 10-degree latitude zones. The results were then manually screened for significance by visually checking for coherent patterns. Coherent patterns need to show an almost monotonic progression year-to-year and also need to display similar patterns across regimes.

Only methane and carbon monoxide fields complied with the coherence screening. It is notable that temperature and water vapor did deviate from the coherent pattern even though in section 4.3 there are indications of trends in temperature. That is because those trends are smaller than interannual variation and so can only be reliably measured with reference to ground truth data. This check uses no ground truth and so can only detect trends that are larger than interannual variation.

Figure 1 shows the difference in total methane for different stratifications from baseline 2003 levels. The trend is nearly uniform in space and time. The measured trend amounts to $\sim +0.2\%/\text{year}$. A similar analysis of V5 data shows a much smaller trend, $\sim +0.05\%/\text{year}$. Team methane expert Xiaozhen Xiong of NOAA believes that the trend as measured by V6 is consistent with changes in global methane concentrations measured by other instruments.

Version 6 Performance and Test Report

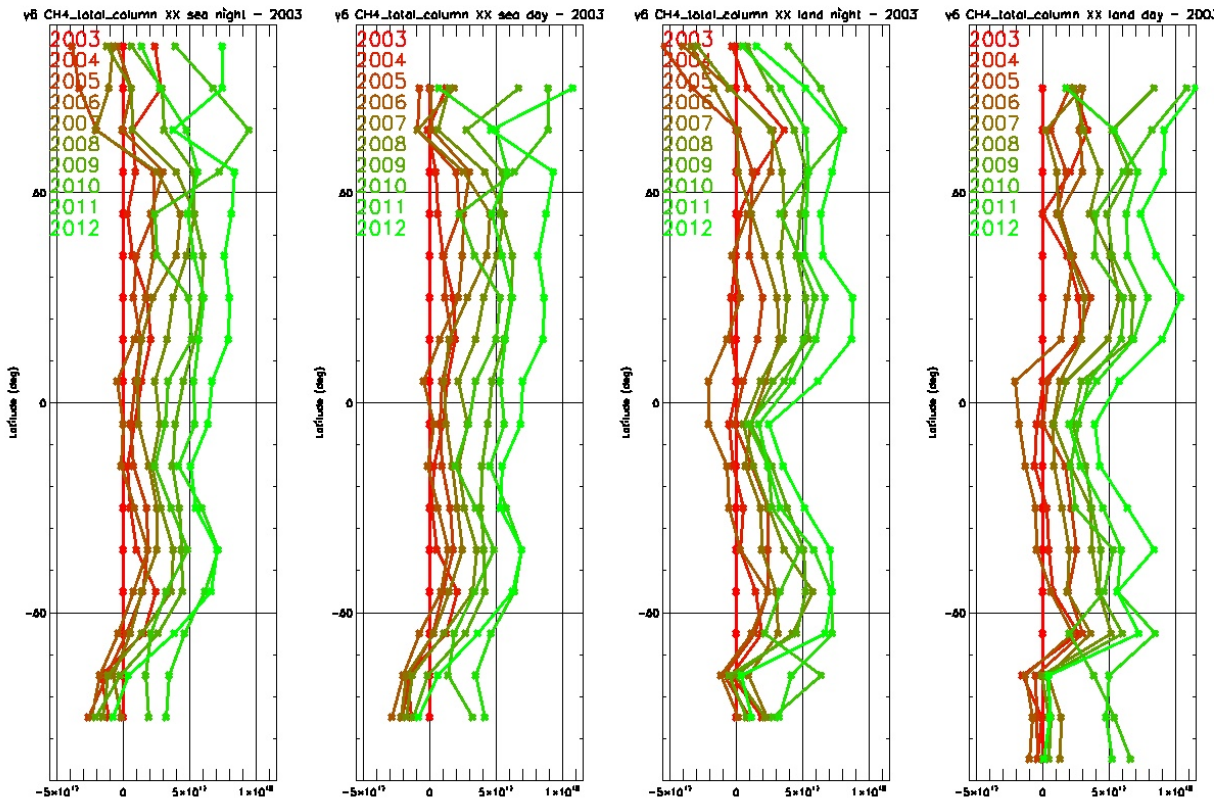


Figure 1. Total retrieved methane by latitude zone (y axis) for different stratifications. (a) sea night, (b) sea day, (c) land night, (d) land day

We investigate this trend with more spatial resolution but without the year-by-year temporal resolution by looking at differences between mean monthly total methane burden for key months in 2011 minus the same month in 2003. Interannual variation shows up as regional variation, but the global difference is fairly constant. Figure 2 shows these differences for January, April, July, and October.

Version 6 Performance and Test Report

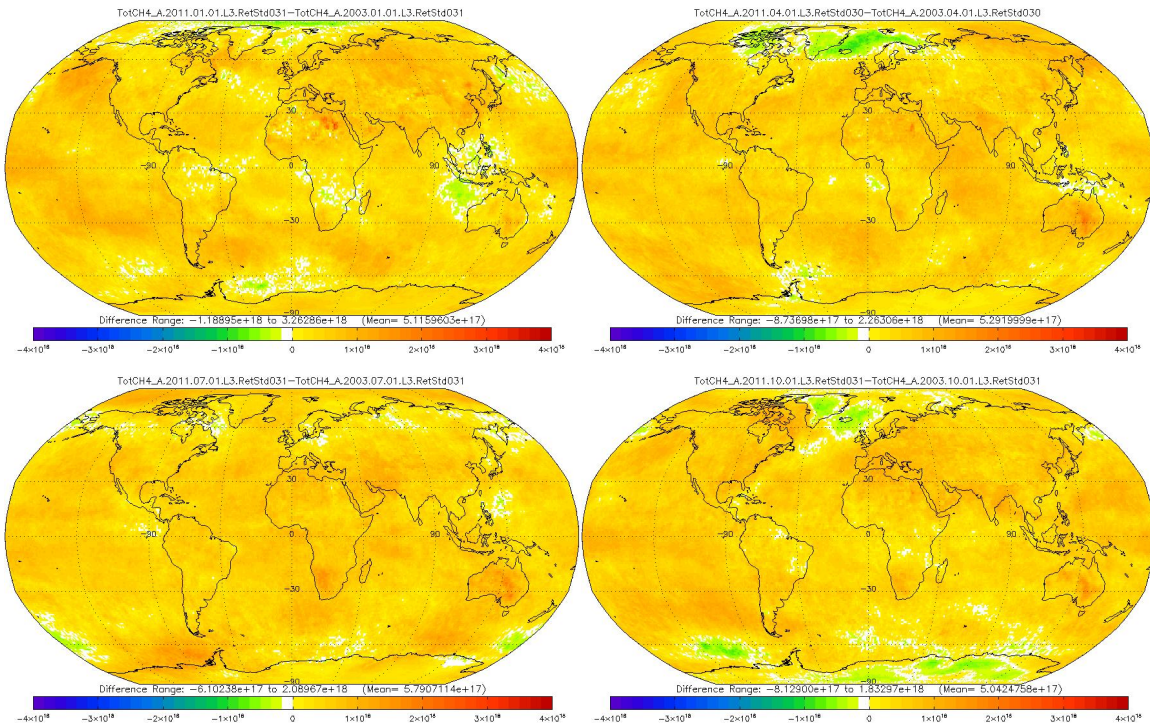


Figure 2 Difference in V6.0.2 AIRS+AMSU retrieved global monthly methane between 2003 and 2011. a) January b) April c) July d) October

Monthly global images can also be used to check for significant differences in global trend between the AIRS+AMSU and IR-Only variants of V6.0.2 retrieval.

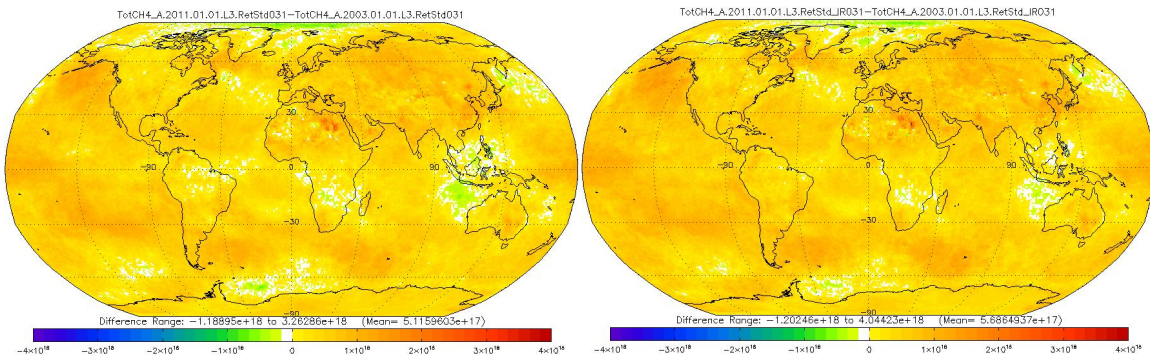


Figure 3 Difference in V6.0.2 retrieved global monthly methane between Jan 2003 and Jan 2011. a) AIRS+AMSU. b) IR-Only.

compares the differences for Jan 2011 minus Jan 2003. No significant change is seen.

Version 6 Performance and Test Report

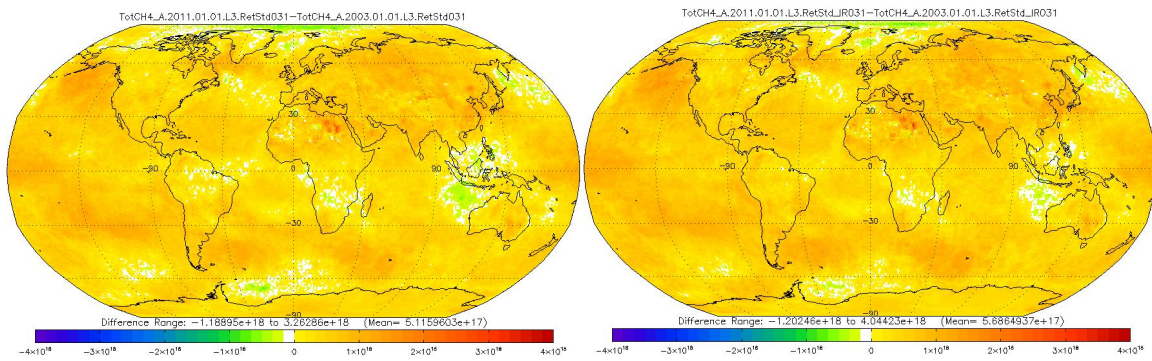


Figure 3 Difference in V6.0.2 retrieved global monthly methane between Jan 2003 and Jan 2011. a) AIRS+AMSU. b) IR-Only.

Figure 4 shows the difference in V6.0.2 AIRS+AMSU retrieved total carbon monoxide for different stratifications from baseline 2003 levels. This trend is not as uniform in space or time as the methane trend, but does show coherent patterns. The global mean measured trend amounts to ~-0.05%/year. A similar analysis of V5 data gives a slightly smaller trend of ~-0.04%/year. Team carbon monoxide expert Juying Warner of UMBC believes that the trend measured by V6 is consistent with changes in global carbon monoxide concentrations measured by other instruments.

Version 6 Performance and Test Report

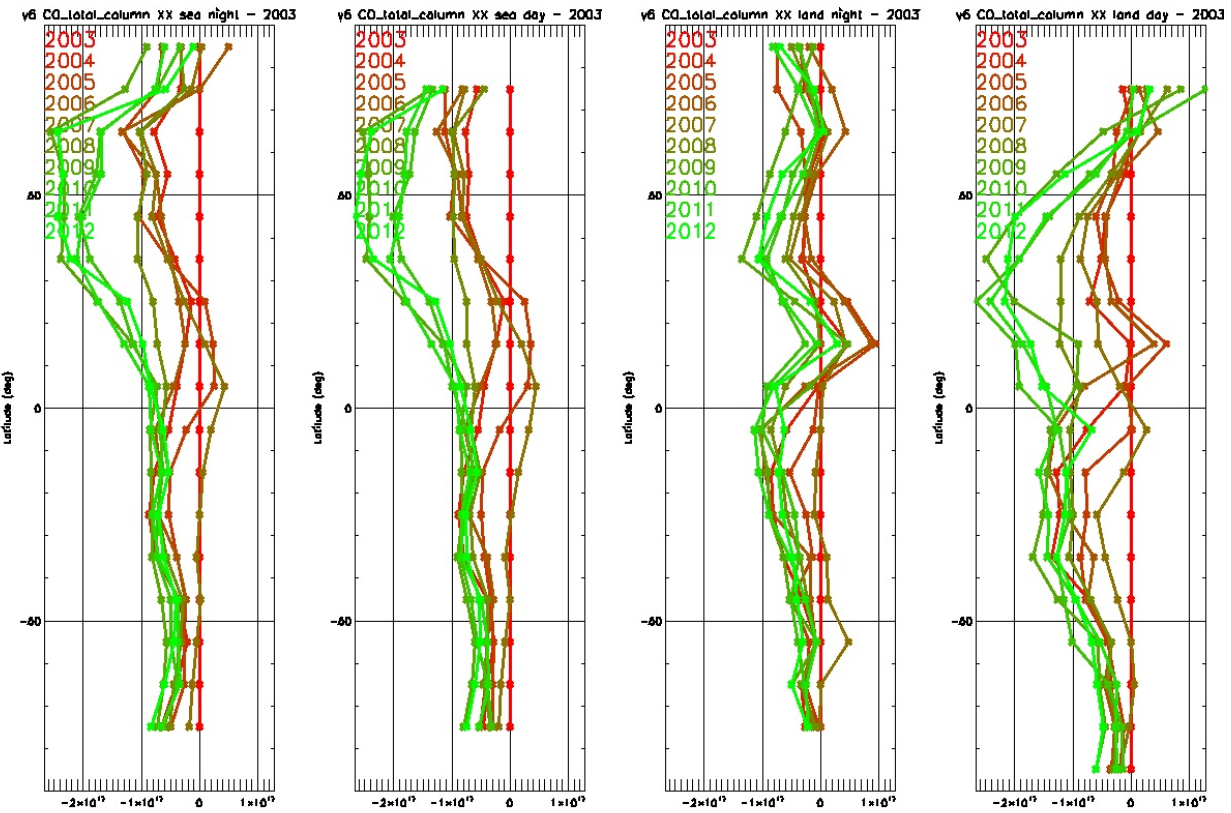


Figure 4 . Total retrieved carbon monoxide by latitude zone (y axis) for different stratifications. (a) sea night, (b) sea day, (c) land night, (d) land day

As with methane, we also look at differences in mean monthly retrieved CO between 2003 and 2011. In this case we see significant changes in the spatial pattern between months, but the change in global mean is similar.

Version 6 Performance and Test Report

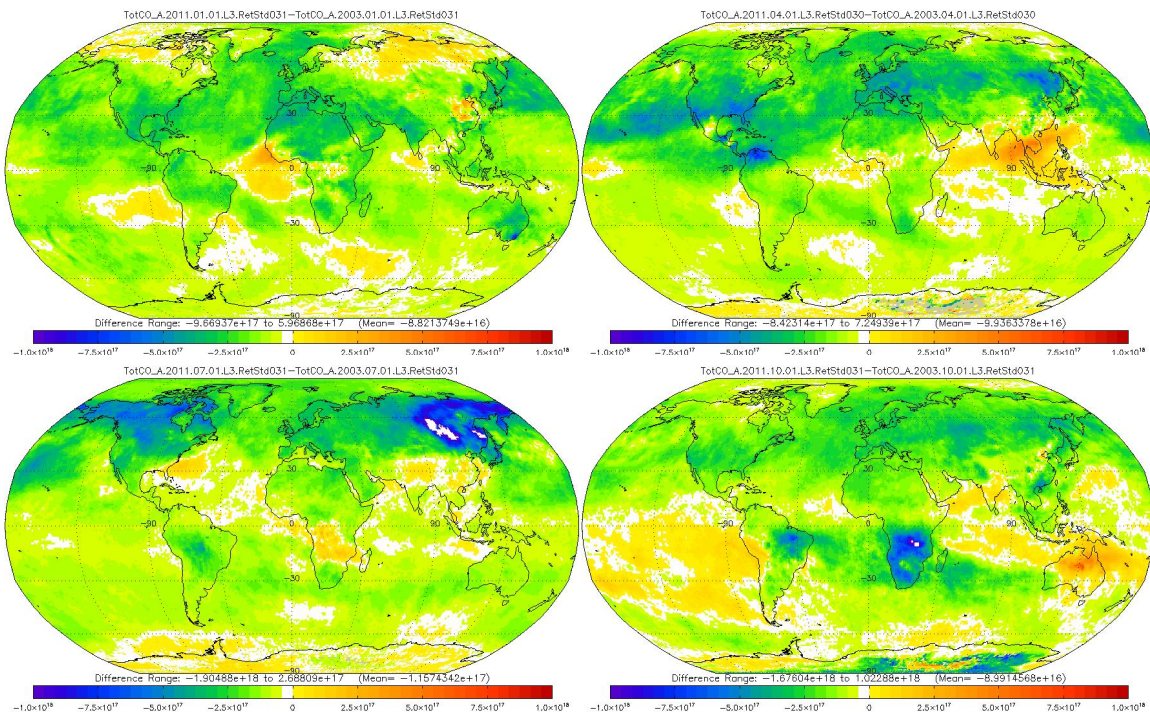


Figure 5 Difference in mean monthly retrieved carbon monoxide between 2003 and 2011.
a) January b) April c) July d) October

Figure 6 shows differences in global trend between the AIRS+AMSU and IR-Only variants of V6.0.2 retrieval for Jan 2011 minus Jan 2003. No significant change is seen.

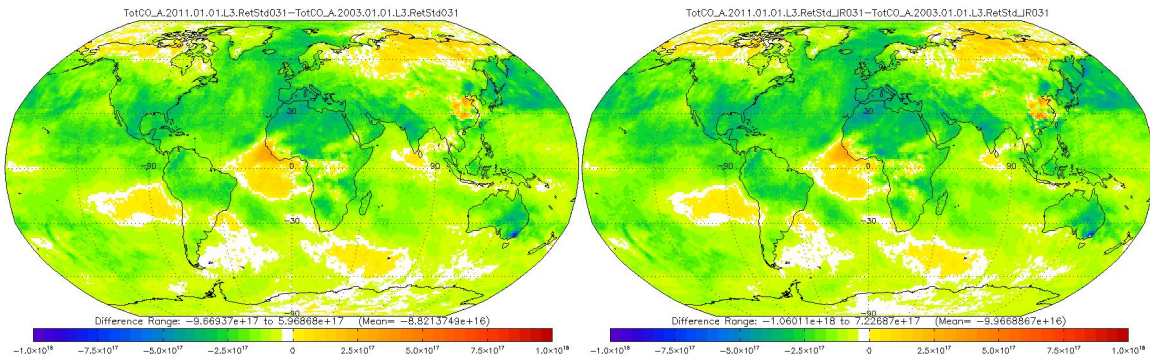


Figure 6. Difference in V6.0.2 retrieved monthly carbon monoxide between January 2003 and January 2011 a) AIRS+AMSU b) IR-Only

Version 6 Performance and Test Report

3.1.2 Yield and Spurious Bias Trends of T(p) and q(p)

Version-5 retrievals have been found to have two very undesirable characteristics with regard to trends, both of which were considered to be critical to correct in Version-6. The first was that the % yield of accepted retrievals was found to be decreasing over time (negative yield trend). The second was that the mean difference of QC'd retrieved temperatures from collocated truth values were found to be changing over time as well, especially beneath 300 mb (spurious bias trend). In this section, we examine yield and spurious bias trends of Version-5 and Version-6 products. We computed volumes of these trends by taking the slope of the linear least squares fit passing through the values of the appropriate parameter for each of the seven days as a function of time.

Figure 7 shows these trends as a function of pressure for Version-5, Version-6, and Version-6 AO. All results are for cases with Climate QC (Standard QC for Version-5) because trends are most significant with regard to the generation of Level-3 products used for climate research. It is apparent that Version-6 has eliminated the substantial negative tropospheric temperature profile yield trends, on the order of 1% per year, which were found in Version-5. In addition, the Version-6 negative T(p) bias trends beneath 500 mb are much smaller than those of Version-5, which were on the order of -0.05K/yr. The negative q(p) bias trends found in Version-5 are also substantially reduced in Version-6. It is interesting to note that the spurious q(p) bias trends found in Version-5, as a function of pressure, tend to follow those of T(p) in sign. This is consistent with physics in that a spuriously cold temperature solution (trend) result lowers computed radiance for water vapor channels. If the retrieved temperature is too low, the solution for q(p) will result in a lowered retrieved water amount so as to raise the radiances computed using the incorrect value of T(p) in order to match the observed radiance, resulting in a spurious negative low value (or negative trend) of q(p). This lowered q(p) (trend) subsequently gives too high a computed radiance in the window channels used to compute cloud parameters, which subsequently results in increased values of retrieved cloud fraction, and finally a spurious increasing cloud trend.

Version 6 Performance and Test Report

Global Trends 7-Day

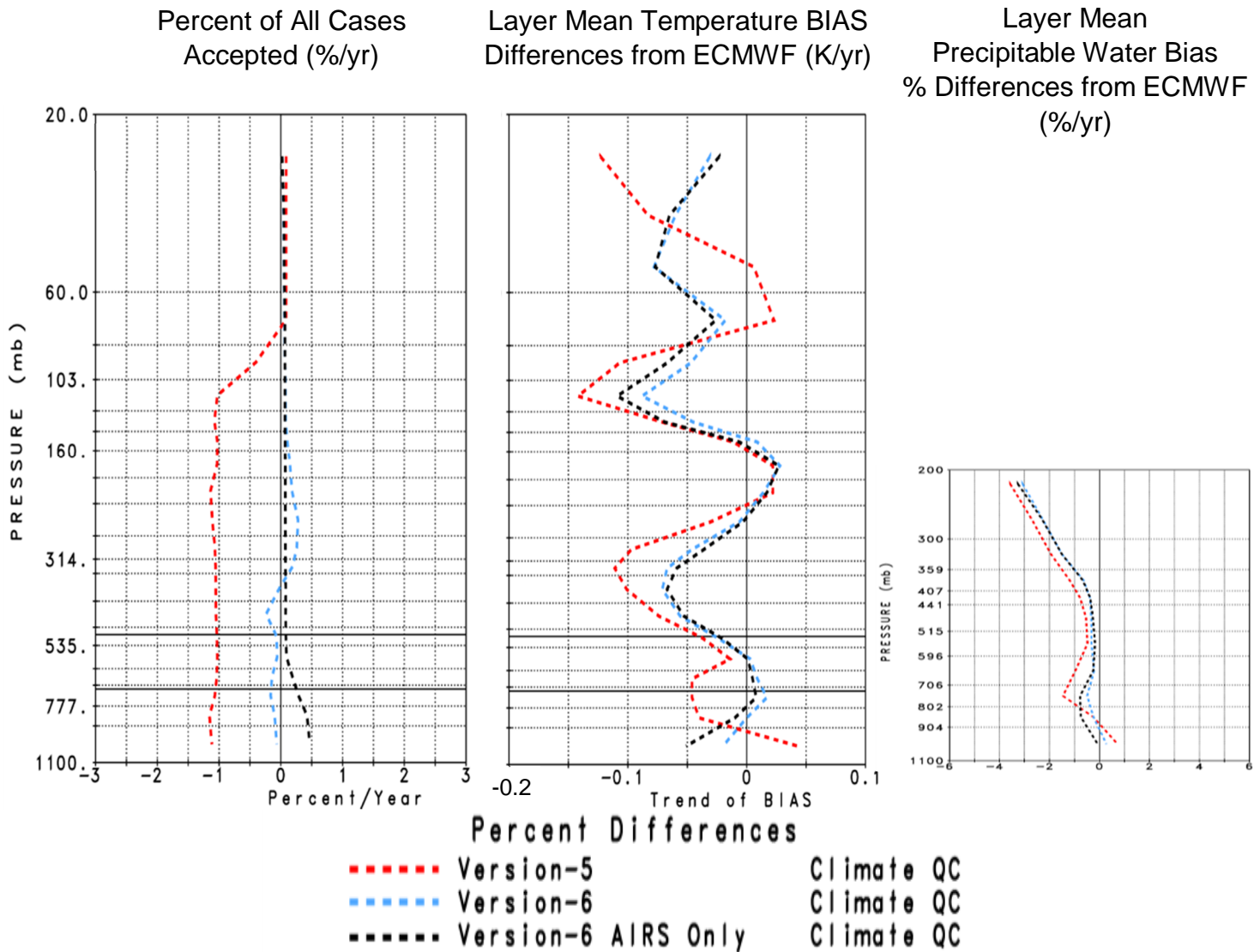


Figure 7. Global trends of water vapor and temperature bias.

3.1.3 Temperature and Water Vapor Retrieval Accuracy as a Function of Yield

Figure 8 shows statistics of the differences of QC'd Version-5 and Version-6 retrievals from collocated ECMWF truth for a globle ensemble of cases taken over the 7 focus days. Panel (a) shows the percentage of QC'd cases accepted

Version 6 Performance and Test Report

as a function of height, panel (b) shows RMS differences of 1 km layer mean temperatures from collocated ECMWF truth, and panel (c) shows biases of QC'd 1 km layer mean differences from ECMWF. Statistics are shown for six sets of results. Results for Version-5 retrievals are shown in red, results for Version-6 retrievals (called V6.02) are shown in blue, and results for Version-6 AIRS Only retrievals (called V6.02 AO) are shown in black. Version-5 did not have QC'd AIRS Only retrievals. Two sets of curves are shown for each experiment, each using different QC thresholds. Version-5 had only one set of QC thresholds, called standard thresholds. These Version-5 thresholds were chosen so as to provide a middle ground between the highest accuracy, which would be optimal for Data Assimilation purposes, and the highest yield (best spatial coverage), which would be optimal for Climate purposes. Experience using Version-5 products showed that Standard QC thresholds were optimal for neither purpose. For example, Data Assimilation experiments using Version-5 retrievals that passed a tighter set of QC thresholds than found in the official Version-5 system, resulted in significantly improved forecasts compared to those passing the looser Standard QC thresholds. The solid red lines in Figure 8, and subsequent figures, shows statistics of Version-5 retrievals passing the tighter QC threshold, which we refer to as Tight QC threshold, and the dashed red lines show equivalent statistics for the ensemble of Standard Version-5 retrievals. Version-6 uses two different sets of thresholds, a very tight set of thresholds newly optimized for Data Assimilation purposes ($QC=0$), and a substantial looser set of thresholds optimal for Climate purposes ($QC=1$). As with Version-5, the solid lines show V6 and V6 AO results using the Data Assimilation (DA) QC thresholds, and the dashed lines show results using the Climate thresholds. Level-3 gridded products utilize all cases passing Climate QC.

In Version-5, all retrievals are either accepted or rejected above 70 mb based on use of different types of tests, even before the QC procedures are applied. One of the tests that eliminates consideration of the entire temperature profile, and flags the entire profile with $QC=2$ (do not use), is that the retrieved cloud fraction is over 90%. Roughly 83% of Version-5 retrievals pass the initial screening procedure, but none of them are in near overcast conditions. Version-5 retrievals with Tight QC have considerably lower yield than those with Standard QC below 200 mb, with correspondingly smaller RMS errors, on the order of 1K beneath 300 mb. There is no appreciable difference in Version-5 bias errors compared to ECMWF found using either set of QC thresholds.

Version-6 does not apply any test which eliminates the entire temperature profile, other than the requirement that the retrieval runs to completion. Version-6 retrievals using DA thresholds have roughly 1K RMS errors throughout the

Version 6 Performance and Test Report

atmosphere, with a yield which is much higher than Version-5 Tight down to about 500 mb. The yield of Version-6 retrievals with DA QC is lower than that of Version-5 Tight beneath 500 mb, but with a considerable improvement in mid-lower tropospheric temperature RMS errors, with values less than 1K, which is believed to be optimal for Data Assimilation purposes. The yield of Version-6 retrievals with Climate QC is extremely high throughout the atmosphere, with a value of about 83% at the surface. Achievement of this very high yield is extremely valuable in the generation of more representative Level-3 products which are used for Climate data sets. RMS errors of Version-6 retrievals with Climate QC are better than, or comparable to those of, Version-5 Standard down to about 700 mb, but with a much higher yield. Beneath 700 mb, Version-6 Climate QC RMS errors are somewhat larger than those of Version-5 Standard, but the Version-6 results are essentially unbiased, which is the more important statistic with regard to the generation of the Level-3 products used for Climate research. QC'd results for Version-6 AO are roughly comparable to those of Version-6 but with a somewhat lower yield near the surface.

Version 6 Performance and Test Report

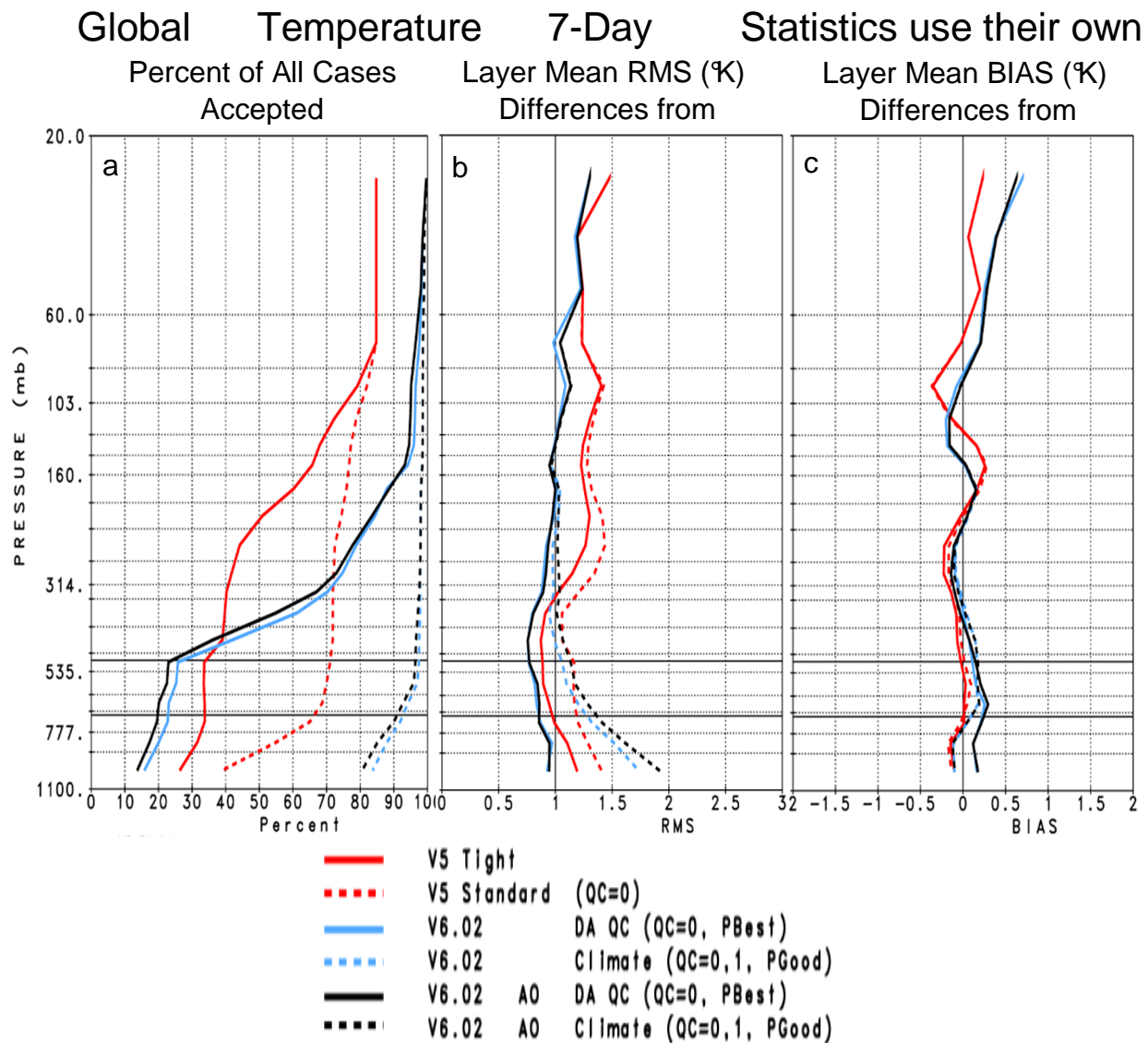


Figure 8. Focus day statistics: Temperature

Version 6 Performance and Test Report

Figure 9 shows analogous results comparing QC'd 1 km layer precipitable water to that of collocated values of ECMWF. Figure 9 contains results for only Version-5 retrievals and Version-6 retrievals. Results are shown only up to 200 mb, above which water vapor retrievals are considered to be of minimal validity, and are not included in the Standard Product data set. The relative results regarding Version-5 and Version-6 are analogous to those found for T(p). Version-6 q(p) retrievals with DA QC are considerably improved over those of Version-5 in the lower troposphere. This improvement is at least partially a result of the improved values of T_s , ε_v in Version-6 compared to Version-5. As with T(p), Version-6 q(p) retrievals with Climate QC are unbiased, have high accuracy, and contain almost complete spatial coverage.

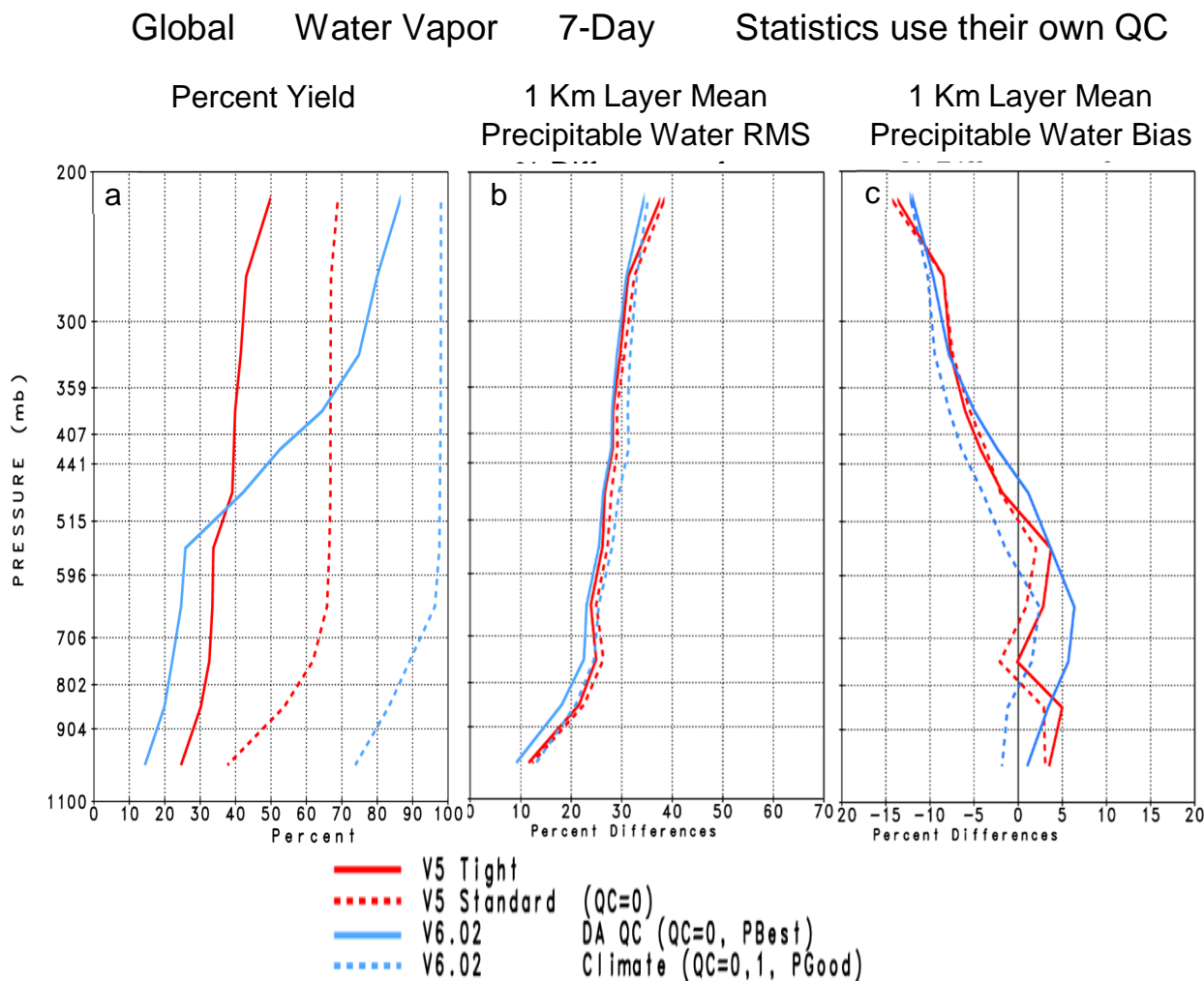


Figure 9. Focus day statistics: Water vapor

Version 6 Performance and Test Report

Figure 10 shows analogous results comparing QC'd Version-6 $q(p)$ retrievals with those of Version-6 AO. As in the case of $T(p)$, Version-6 AO water vapor retrievals are somewhat poorer than those of Version-6, but are still of very high quality. Part of this degradation results from loss of the information in Version-6 AO contained in the two channels of AMSU-A2, which are very sensitive to boundary layer water vapor over ocean.

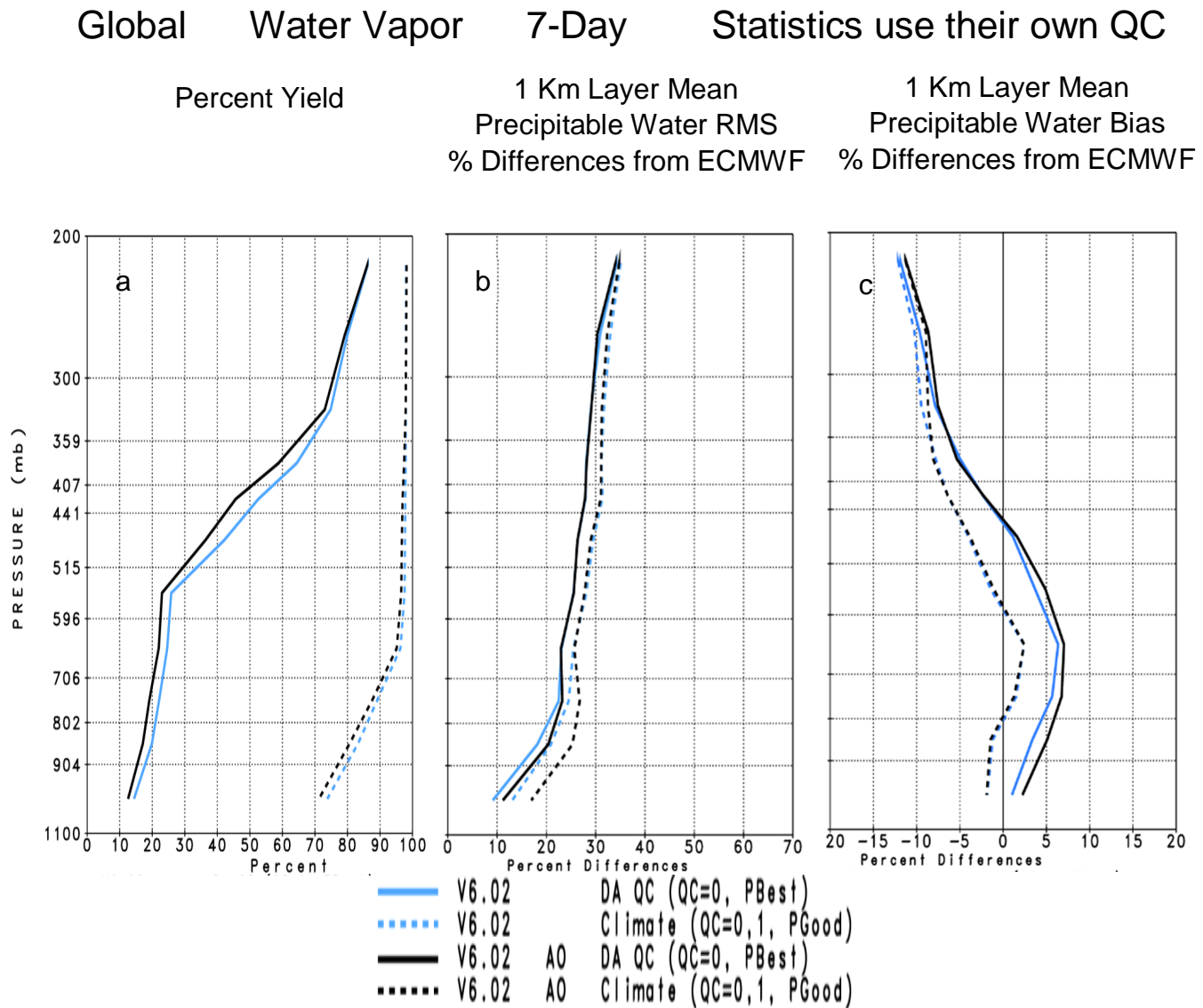


Figure 10. Focus day statistics: QC comparison

Version 6 Performance and Test Report

Figure 8 to Figure 10 provide very important information about the accuracy of Quality Controlled retrievals obtained by different retrieval systems each using their own QC procedures. Indeed, the ability of a different retrieval system to perform QC is a critical part of that retrieval system, especially in the generation of Level-3 products. Figure 8 to Figure 10 do not tell the whole story about the relative accuracy of the retrievals obtained in Version-5 and Version-6 however, because results are shown for different ensembles of cases. Figure 11 compares RMS T(p) errors of Version-6 and Version-5 retrievals when evaluated on common ensembles of cases. Results for two such ensembles are shown: an ensemble of relatively easier (less cloudy) cases given by those cases accepted in Version-5 using Tight QC (shown in solid lines); and an ensemble including much more difficult (more cloudy) cases given by those cases accepted in Version-6 using Climate QC, shown in dashed lines. As previously, Version-6 RMS errors are shown in blue and Version-5 RMS errors are shown in red. Version-6 retrievals for the easier (solid line) cases are more accurate than those of Version-5 at all levels, but the degree of improvement below 500 mb is relatively small for these cases. The accuracy of Version-5 retrievals degrades much more rapidly than those of Version-6 for the harder cases (dashed lines). In fact, it is for this reason that the Version-5 retrieval system did not use relaxed QC thresholds that would have provided much for higher yields to be used in the generation of Level-3 products.

Version 6 Performance and Test Report

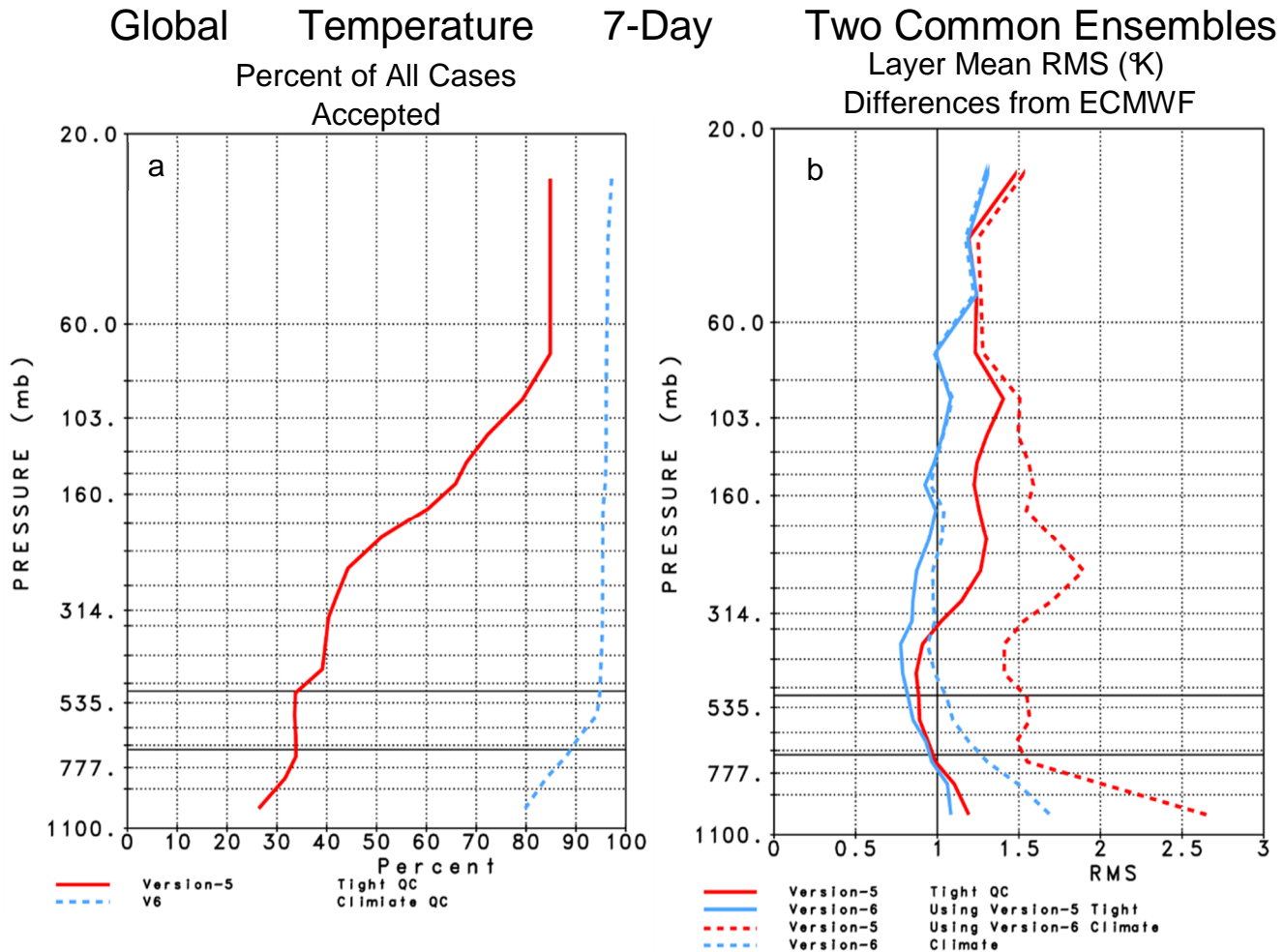


Figure 11. $T(p)$ RMS error for different ensembles (water vapor)

All results shown so far have been for a global ensemble of cases. **Table 1** contains a breakdown of two temperature profile statistics, the Tropospheric Temperature Metric (TTM) and the Boundary Layer Metric (BLM), evaluated over different spatial regions: global; land 50°N to 50°S ; ocean 50°N to 50°S ; poleward of 50°N ; and poleward of 50°S . In this table, TTM represents the mean RMS $T(p)$ error over all 1km layers from the surface to 100 mb, and BLM represents the mean RMS $T(p)$ error over the 6 lowest 0.25 km layers from the surface. TTM and BLM results for Version-5 and Version-6 retrievals evaluated over the Version-5 Tight ensemble are shown in **Table 1A**, and evaluated over the Version-6 Climate QC ensemble are given in **Table 1B**.

Version 6 Performance and Test Report

***Table 1. 7-Day Mean Statistics Tropospheric Temperature Metric (TTM)
and Boundary Layer Metric (BLM)***

1A. Cases in Common Using the Version-5 Tight Ensemble										
	Global		Land +/- 50°		Ocean +/-50°		Poleward of 50°N		Poleward of 50°S	
	TTM	BLM	TTM	BLM	TTM	BLM	TTM	BLM	TTM	BLM
Version-5	1.10	1.29	1.19	1.71	1.04	1.13	1.14	1.50	1.31	1.76
Version-6.02	0.92	1.16	0.94	1.49	0.86	0.98	0.96	1.47	1.20	1.69

1B. Cases in Common Using the Version-6.02 Climate Ensemble										
	Global		Land +/- 50°		Ocean +/-50°		Poleward of 50°N		Poleward of 50°S	
	TTM	BLM	TTM	BLM	TTM	BLM	TTM	BLM	TTM	BLM
Version-5	1.67	2.57	1.82	2.78	1.65	2.48	1.53	2.39	1.72	2.72
Version-6.02	1.11	1.67	1.06	1.75	1.03	1.34	1.12	1.93	1.32	2.02

Version-6 T(p) retrievals are superior to those of Version-5 with regard to both metrics in all spatial regions. It is important to note the improvement of Version-6 Boundary Layer Temperatures compared to Version-5 especially over land, even for the easier ensemble of cases. This improvement over land is at least in part a result of the improved values of land surface temperature and surface spectral emissivity over land. Improvement of boundary layer temperatures was one of stated goals of Version-6, which indeed has been accomplished. The improvement of boundary layer temperatures is even more pronounced when evaluated over the ensemble of much more difficult cases.

Version 6 Performance and Test Report

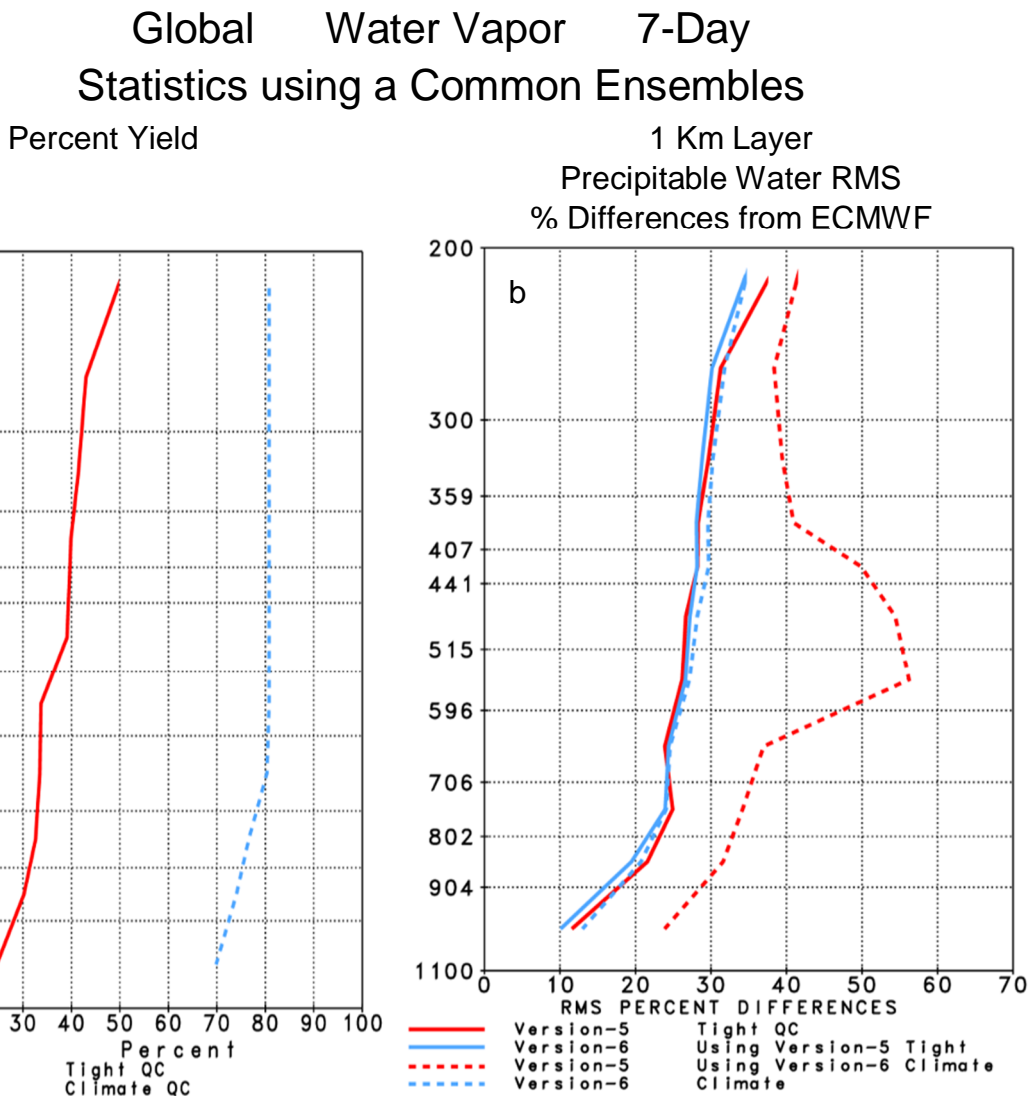


Figure 12. Same as previous figure but for precipitable water

Figure 12 is analogous to Figure 11, but shows yields and RMS differences from ECMWF of 1km layer precipitable water for Version-5 and Version-6 retrievals evaluated over the same common ensembles of cases used for T(p) and shown in Figure 11. As in the case of T(p), layer integrated lower tropospheric water vapor is more accurate in Version-6 than in Version-5 for the easier sets of cases, and layer integrated tropospheric water vapor in all layers is much more accurate in Version-6 for the more comprehensive ensemble of cases passing Version-6 Climate QC thresholds.

Version 6 Performance and Test Report

Figure 13 shows the spatial distribution of a pseudo-Level-3 seven day field of accepted cases of total precipitable water, W_{TOT} , flagged to be of climate quality (QC=0,1). We refer to this spatial distribution as a pseudo-Level-3 product because the seven days are not contiguous in time. In Version-6, W_{TOT} is flagged to be of climate quality if the water vapor profile passes the climate QC test down to the surface. Version-5 uses a different procedure to determine if W_{TOT} is of climate quality. The values shown for Version-6 and Version-5 represent the ensemble mean difference, for all accepted cases within that grid box, of the retrieved value of W_{TOT} from the collocated ECMWF value of W_{TOT} . Grid points in which no accepted values of W_{TOT} were found for any of the seven days, either daytime or nighttime, are shown in gray. Statistically, Version-6 seven day mean values of W_{TOT} are considerably more accurate than those of Version-5, both with regard to global mean bias and as well as to the standard deviation of the errors. Even more important from the climate perspective, spatial coverage of the seven day mean Version-6 product, with 99.89% of the grid boxes filled, is much more complete than that of Version-5, with 96.12% of grid boxes filled. Moreover, the 3.88% of grid boxes for which no accepted soundings were generated in Version-5 tend to come in spatially coherent groups in oceanic areas where low clouds tend to exist.

Version 6 Performance and Test Report

7-Day Surface Total Precipitable Water (cm) Retrieved minus ECMWF AM/PM Average

Version-6.02

Version-5

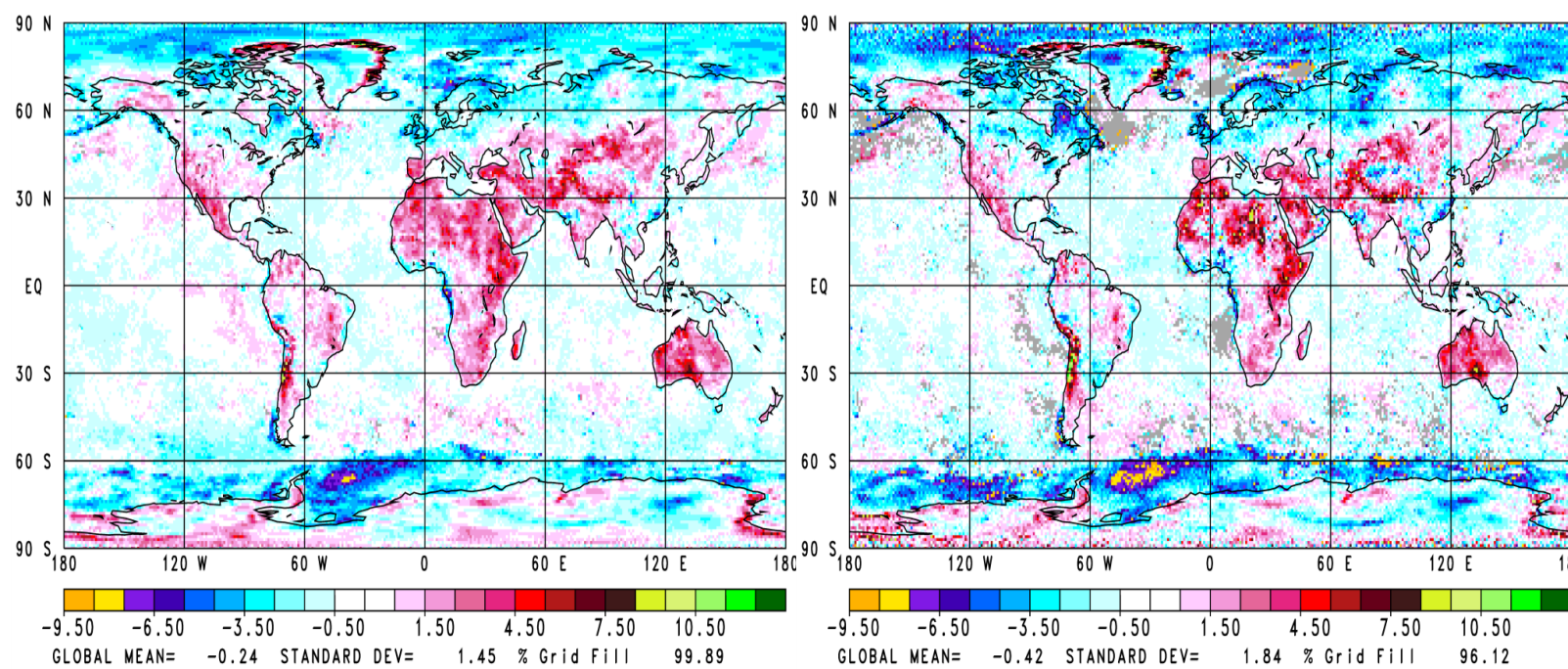


Figure 13. Spatial distribution of a pseudo-Level-3 seven day field of accepted cases of total precipitable water

Version 6 Performance and Test Report

3.2 Water Vapor Data Products for AIRS/AMSU and AIRS-ONLY Layer Product

Tester and Point of Contact: Sun Wong

Data Product	Description
H2O_MMR (L3)	
H2OCDSup (L2)	
H2OCDSup (L2 infrared-only)	

AIRS V6 Level-3 (L-3) dataset contains two specific humidity products that are on standard AIRS pressure layers. One is the layer product similar to the original layer product in V5, and one is the layer TqJ product for which the quality control at any layer is the same as that at the surface. Consequently, the layer product will have higher yields at higher altitudes compared to the yields of the layer TqJ product, while the yields of the TqJ product are uniform in the vertical dimension. Figure 14 compares the V6 L-3 specific humidity to the V5 L-3 specific humidity. Both V6 products have higher yields than the V5 product at all levels. The improved yields in the V6 products enhance the datasets' ability to capture the fine structure of water vapor transport caused by synoptic scale dynamical systems. Locations of extrema of specific humidity are better resolved in the V6 products. The V6 specific humidity well captures the dynamical structure of the atmosphere when compared to the MERRA product (not shown). The V6 product underestimates the spatial variability of specific humidity, because of the smaller maxima due to the sampling issue over the cloudy or heavily precipitating area. Although the layer TqJ has a smaller yields than the yields of the layer product, it can still capture features of the spatial structure of the layer product.

Version 6 Performance and Test Report

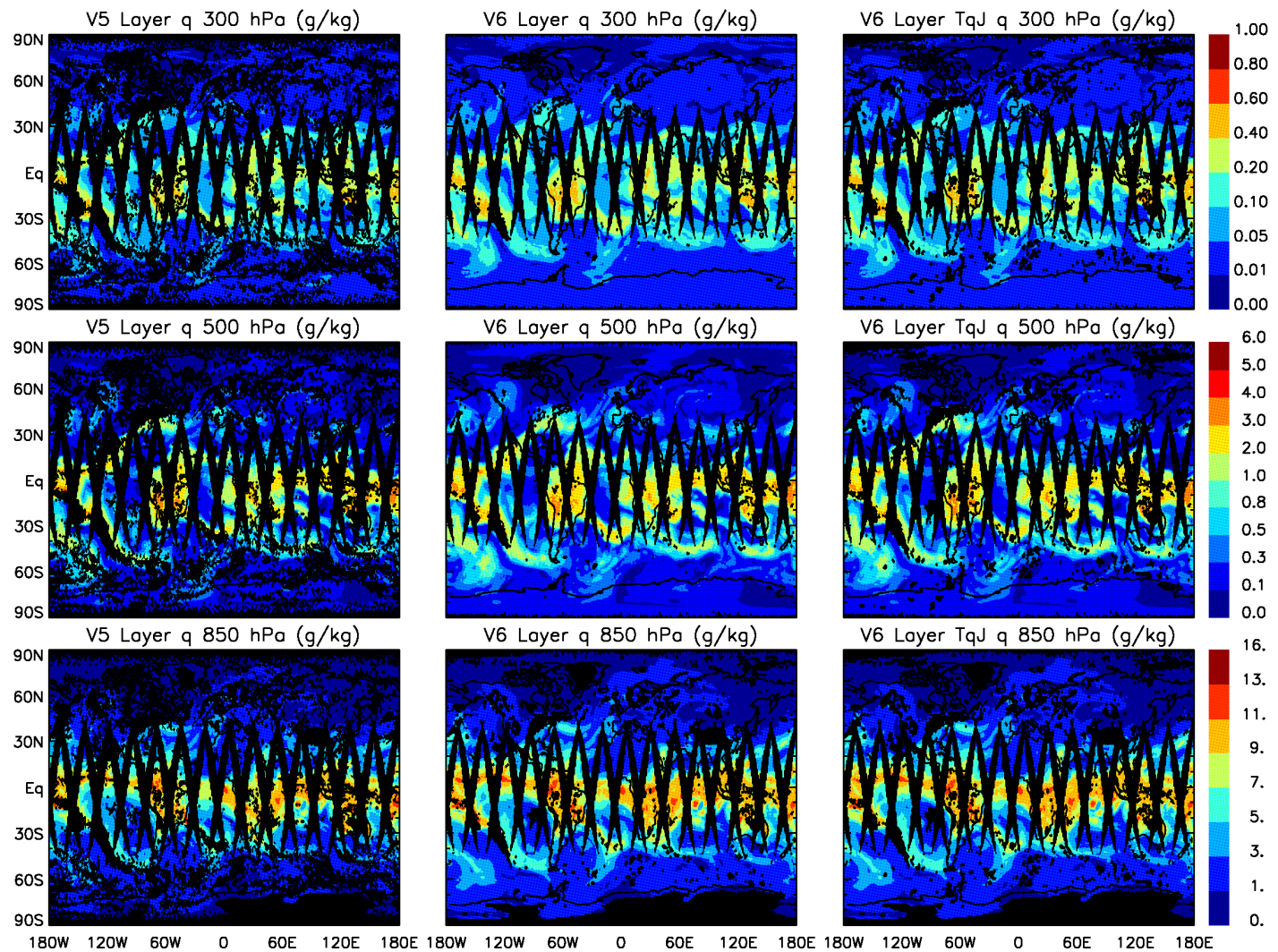
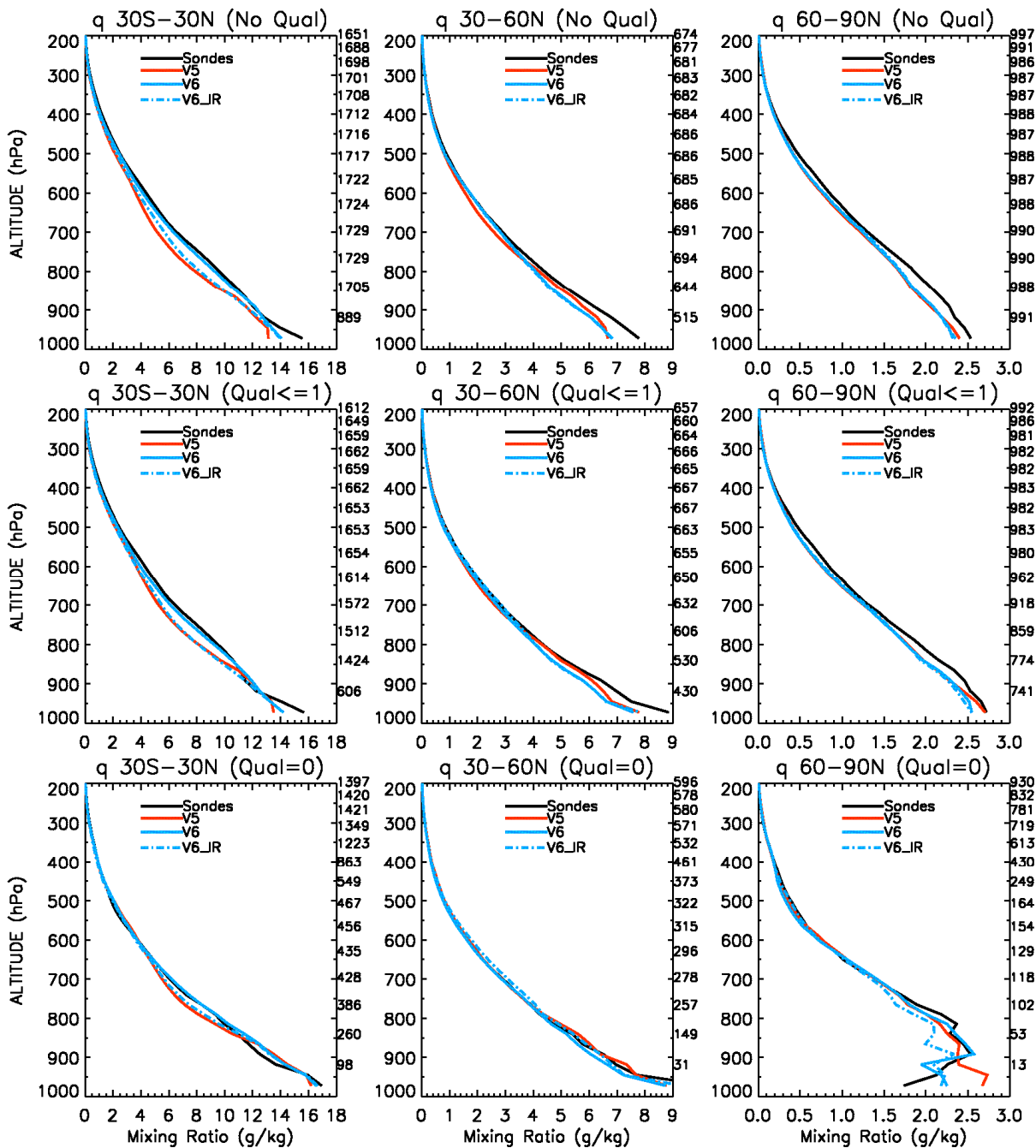


Figure 14 Geographical distributions of specific humidity (in g/kg) on Jan 15, 2007 in the layers of 250-300 (top row), 400-500 (middle row), and 700-850 hPa (bottom row) for the V5 (left column), V6 Layer, and V6 Layer TqJ Level-3 products. The plots are the averages of the ascending and descending soundings of specific humidity. The missing data are in black color.

Version 6 Performance and Test Report



Version 6 Performance and Test Report

Figure 15 Comparison of the AIRS Level-2 specific humidity vertical profiles to the measurements of dedicated sondes in the tropics (left column, 30°S-30°N), mid-latitudes (middle column, 30°-60°N), and polar region (right column, 60°-90°N). All sondes' profiles from 2002 to 2007 are included in these plots and the numbers of samples are shown on the right axis of each panel. The top row is for profiles without quality control being applied, the middle row is for profiles selected by quality flags less or equal to 1, and the bottom row is for profiles selected by quality flags equal to 0. The black solid lines are the sonde profiles, the red solid lines are the V5 specific humidity, the blue solid lines are the V6 specific humidity (layer product), and the blue dash-dotted lines are the V6 infrared-only retrievals of specific humidity.

Figure 15 shows the vertical profiles of the V5 and V6 Level-2 specific humidity compared to the measurements by dedicated sondes. The quality control applied to the middle and the bottom rows are those for the V6 layer product. The V6 specific humidity is closer to the observed values than the V5 specific humidity in the middle troposphere, in particular when the quality flag of 0 is applied as the quality control. When the quality flag of less or equal to 1 is used as the quality control, the AIRS specific humidity (both V5 and V6) is smaller than the observed values below about 800 hPa.

Figure 15 also shows the infrared-only retrievals of specific humidity (the dash-dotted lines). In many situations, its behavior is very similar to the V6 layer product. In the tropical middle troposphere, the infrared-only retrievals are closer to the V5 specific humidity and much smaller than the sonde values.

Version 6 Performance and Test Report

3.3 Temperature bias and bias trends compared with PREPQC radiosondes

Tester and Point of Contact: Frederick (Bill) Irion

Versions 5.0.14 and 6.02 AIRS and AIRS-only (without AMSU) retrieved temperatures (on the 100-level support grid) were compared against radiosonde observations in the National Centers for Environmental Prediction (NCEP) quality-controlled final observation (PREPQC) data files. The latter are from operational radiosondes mostly launched near 00 and 12 hrs GMT, with some launched near 6 and 18 hrs GMT. In addition to temperature, pressure and (often) specific humidity observations, the data records contain codes relating to quality control, correction methodology, radiosonde type etc., which were used in filtering the data before comparison to AIRS retrieval. To test and compare Version 5 and 6 AIRS temperature retrievals, we matched radiosonde data to AIRS observations and calculated zonally-averaged differences as a function of pressure.

Radiosonde data were filtered by the following criteria:

1. For each pressure/temperature observation within a sonde profile:
 - (a) If the “Temperature Program Code” (TPC) was 8, indicating that virtual temperature was given (T_V), the sensible temperature (T_s) was calculated from the formula:
$$T_s = \frac{T_V}{1 + 0.608Q}$$
where T_V , T_s are in Kelvin, and Q is the specific humidity using the same mass units (e.g., kg H₂O/kg dry air, not mg H₂O/kg dry air).
(b) A single-level observation (but not necessarily the whole profile) would be rejected if either the “Temperature Quality Marker” (TQM), or the “Pressure Quality Marker” (PQM) was greater than 2.
(c) An observation would be kept if the “Temperature Program Code” (TPC) and “Temperature Reason Code” (TRC) were matched as follows:
 (TPC = 8 and TRC = 1) (Virtual temperature reported calculated from sensible temperature and specific humidity), or
 (TPC = 1 and TRC = 100) (Temperature and quality marker unchanged from original values read into program “prepdata.”), or
 (TPC = 6 and TRC = 1) (Rawinsonde has had a radiation bias correction with temperature and/or height recalculated),
 otherwise the observation would be rejected.
2. An entire sonde profile would be rejected if
 - (a) the instrument type (ITP) was

Version 6 Performance and Test Report

- 2 through 6, 8, or 9 (not radiosondes), or
- 90 (radiosonde type unknown), or
- 100 through 109, or 112 through 225 (vacant, “not vacant”, or reserved fields), or
 - (b) Accepted sonde temperature levels did not reach altitudes above the 90 mb level or altitudes below the 700 mb level, or
 - (c) A height gap in the accepted temperature observations was greater than 5 km (calculated from pressures assuming a 7km scale height).

For these comparisons, AIRS observations were land-only, and had to be made within 1 hour and 100 km of a sonde launch. (Note that this can lead to multiple AIRS observations matched to the same sonde profile.) Both daytime and nighttime observations are included, however comparisons are mostly at 0° in longitude and points eastward over Europe due to launch of sondes near noon GMT and the (ascending) 1:30PM equator crossing time of AQUA satellite. Figure 16 illustrates the locations of coincident observations used for bias calculations during JJA 2006.

As the quality control flag algorithms have changed between AIRS V5 and V6, we selected a simple approach to maximize the number of coincidences while still avoiding poor retrievals: The only filters for AIRS data was that the surface temperature quality flag (“Qual_Surf” for V5, “TSurfStd_QC” for V6) had to be 0 or 1 (“best” or “good”), and both Version 5 and 6 retrievals for a matched sonde had to be successful. We did not use AIRS quality flags for temperature profiles in filtering AIRS observations.

Radiosonde data were interpolated (by log pressure) to the AIRS 100-level vertical pressure grid prior to comparison. For direct measurements between AIRS and radiosonde temperatures, we did not extrapolate radiosonde data beyond their original range.

In addition to direct comparisons between AIRS and radiosonde temperature profiles, we have also applied AIRS temperature averaging kernels to the radiosonde data (“kerned sondes”). The averaging kernel, \mathbf{A} (a matrix), contains information on the vertical smoothing and sensitivity of a retrieval, and is calculated for each retrieved AIRS profile (both in Version 5 and 6). Put simply, it relates the change of a retrieved state vector, $\hat{\mathbf{x}}$, to a change in the “true” state vector, \mathbf{x} :

$$\mathbf{A} = \frac{\partial \hat{\mathbf{x}}}{\partial \mathbf{x}} \quad (1)$$

We apply the AIRS averaging kernel to the sonde data on the 100-level AIRS support grid as follows:

$$\mathbf{x}_{est} = \mathbf{x}_0 + \mathbf{T} \mathbf{A} \mathbf{T}' (\mathbf{x}_T - \mathbf{x}_0) \quad (2)$$

where: \mathbf{x}_{est} is the temperature profile as AIRS “should have” seen it given its sensitivity to the *a priori* and limited vertical resolution,

Version 6 Performance and Test Report

\mathbf{x}_0 is the *a priori* temperature profile,
 \mathbf{x}_T is the radiosonde profile,
 \mathbf{A} is the averaging kernel,
 \mathcal{T} is a matrix describing the retrieval trapezoids (see Susskind *et al.* [2003]), and
 $\mathcal{T}' = [\mathcal{T}^T \mathcal{T}]^{-1} \mathcal{T}^T$ is the least-squares inverse of \mathcal{T} .

Details on the calculation of \mathbf{A} for AIRS retrievals can be found in Maddy *et al.* [2008].

Note that as sondes do not extend to the lower pressures of the AIRS gridding, retrieved AIRS temperatures are used to fill in missing elements of \mathbf{x}_T (e.g., pressures below the sonde burst); comparisons of temperatures between AIRS and kerned sondes may not be reliable in the mid-to-upper stratosphere since we are combining in-situ and AIRS remote measurements as ‘truth’ for this region. We also note that the AIRS averaging kernel is only calculated for the last step of the ‘physical retrieval,’ and does not account for information contained in the neural-network derivation of the *a priori* temperature profile for the V6 retrieval or the fast eigenvector regression [Goldberg *et al.*, 2003] used in the V5 retrieval.

AIRS minus Radiosonde Bias Calculation

To test changes in AIRS temperature retrievals between Version 5 and 6, we selected two three-month intervals, and binned comparisons on polar, mid-latitude and tropical latitudes. Figure 17 compares results for DJF 05/06. The left panels are the averages of profile temperature differences between AIRS (V5 in red, V6 in blue) and sonde observations. The middle column shows the number of observations in each bin. The right panels show differences of AIRS to ‘kerned sonde temperatures,’ that is, sonde temperatures that been modified by the AIRS averaging kernel as in Eq. 2. Rows are by latitude bins.

The left panels generally show a reduction in the bias from V5 to V6 between AIRS and sondes in the middle troposphere and lower stratosphere, with an improvement in the RMS error. Retrieval biases are mostly within 1K except for 90°S-60°S, where a ~1.5K high bias can be seen around 200mb. Indeed, V6 produces a ‘zig-zag’ bias upwards from the middle troposphere with biases ranging from ~ -0.5K to 1.5K, where V5 biases had a large spike at 200mb. While cold biases can be seen in the boundary layer at all latitudes except 30°S-30°N, V6 produces a colder bias than V5 in the boundary layer in the winter hemisphere (60°N-90°N and 30°N-60°N bins). However, we again note that we have only applied surface temperature quality control flags to filter our data, and not profile temperature flags.

Version 6 Performance and Test Report

The right panels compare AIRS to ‘kerned sonde temperatures.’ (Note that the right panels have a shorter temperature scale on the abscissa.) Again, AIRS V6 shows improvement over V5 except in the boundary layer in the northern hemisphere, and retrievals are within $\pm 1\text{K}$ of the kered sonde.

Figure 18 compares biases for JJA 2006. Again, the bias comparisons on the left panels show V6 improvements over V5 for most pressures, except for the tropical lower stratosphere, and the southern polar region. Excluding the $90^\circ\text{S}-60^\circ\text{S}$ bin, biases tend to be within 1K except in the boundary layer from $60^\circ\text{N}-90^\circ\text{N}$, and $60^\circ\text{S}-30^\circ\text{S}$ where cold biases greater than -1K can be seen. For the $90^\circ\text{S}-60^\circ\text{S}$ bin, zig-zag biases can be seen that are significantly larger during the austral winter months than what could be seen during the austral summer in Figure 17. In the $90^\circ\text{S}-60^\circ\text{S}$ bin, a significantly different bias pattern can be seen in comparing AIRS to sondes on the left panel, and AIRS to kered sondes on the right, indicating that shortcomings in both the *a priori* and the AIRS physical retrieval contribute to large biases.

We compare biases of ‘Version 6 Regular’ (that is, retrievals that include AMSU microwave data), and ‘Version 6 AIRS-only’ (without AMSU data) for DJF 05/06 in Figure 19. The left panels of Figure 19 are biases against sondes as in Figure 17 and Figure 18, while the right panels difference V6 AIRS-only and V6 regular. Biases are similar, with differences between them tending to be less than 0.2K except at polar latitudes, and near the surface. Similar biases, and bias differences, can be seen for JJA 2006 in Figure 20.

AIRS Bias Drift Calculation

To calculate and compare any temperature bias drifts in Versions 5 and 6 AIRS retrievals, sonde profiles were filtered and matched to AIRS in the same manner described above, but this time for all available matchups from the beginning of 2004 through the end of 2011. (Dates after 2003 were used to avoid any ‘jumps’ resulting from calibration changes after the AIRS on-orbit shutdown of October 29 to November 14, 2003.) To avoid seasonal effects skewing the result, data were binned by calendar month, with the date of each matched observation set to the year+fraction-of-year. (For example, Feb 1, 2009 at 00:00GMT would have the date 2009.084931.) Data were then binned by pressure level, and a linear least-squares fit of the bias vs. the fractional date was calculated. The slopes from each calendar month were then averaged, and this average is presented in Figure 21 for each latitude bin and pressure. AIRS comparisons against sondes are on the left panels, and AIRS against kered sondes are on the right. The thin lines show the standard deviation of the monthly averaged slope on each pressure level.

Version 6 Performance and Test Report

Version 6 shows significant improvements in the bias drift over V5 in most regions except 90°S-60S, with the absolute value of all drifts reduced below 0.05K/yr. For the 60°N-90°N bin, a slightly larger drift can be seen in the lower troposphere, but remains below 0.05K/yr. Drifts for the southern polar region remain largely the same, except for the region between 700 and 400 mb, where a slight negative drift in V5 is mirrored by a slight positive drift in V6.

Figure 22 compares the bias drifts between V6 AIRS-only and AIRS-regular retrievals. The right hand panels show the differences in the drifts. While the drifts are generally similar, AIRS-only drifts tend to be less than AIRS-regular at or just above 100 mb in all latitude bins, and tend to be greater in the middle to upper troposphere except in southern polar region.

Acknowledgement:

We thank Eric Maddy for helpful discussions on this issue.

References:

Maddy, E. S. and C. D. Barnet, Vertical Resolution Estimates in Version 5 of AIRS Operational Retrievals, *IEEE Trans. Geosci. Remote Sens.*, 46(8), 2375-2384, 2008.

Susskind, J., C. D. Barnet, and J. Blaisdell, Retrieval of atmospheric and surface parameters from AIRS/AMSU/HSB data in the presence of clouds, *IEEE Trans. Geosci. Remote Sens.*, 41(2), 390–409, 2003.

Goldberg M. D., Y. Qu, L. McMillin, W. Wolf, L. Zhou, and M. Divakarla, 2003: AIRS near-real-time products and algorithms in support of operational numerical weather prediction. *IEEE Trans. Geosci. Remote Sens.*, 41(2), 379–399.

Version 6 Performance and Test Report

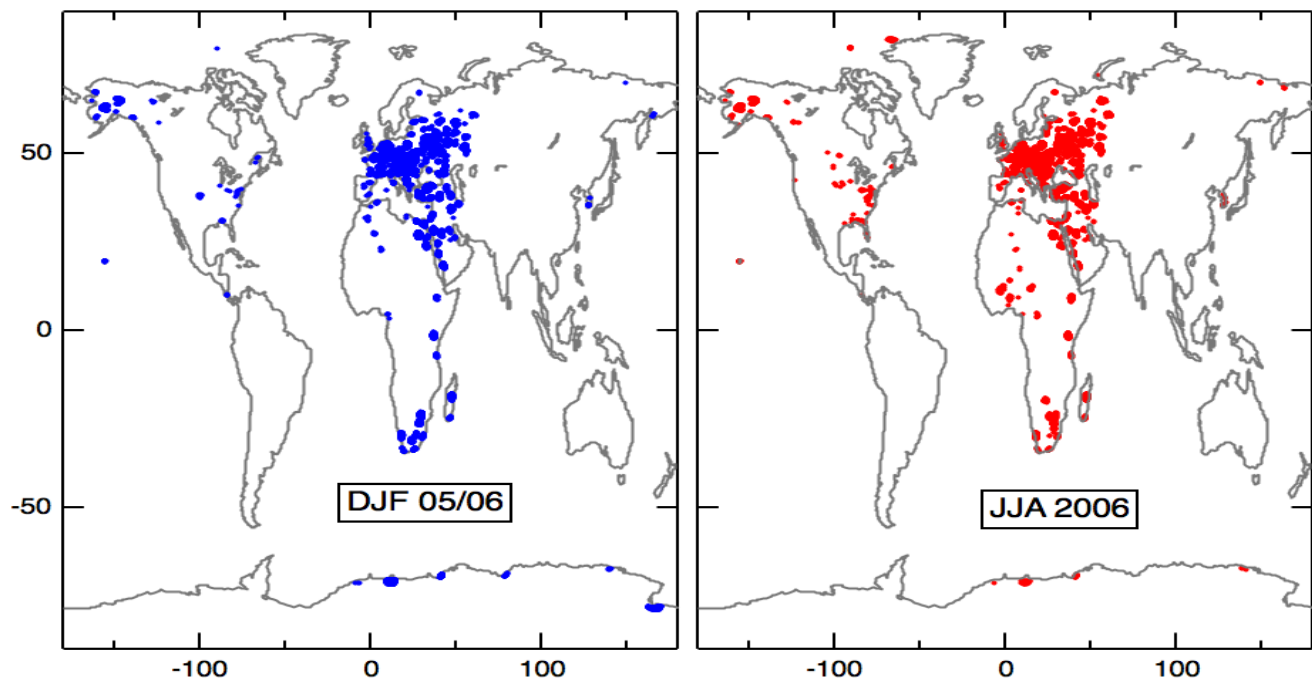
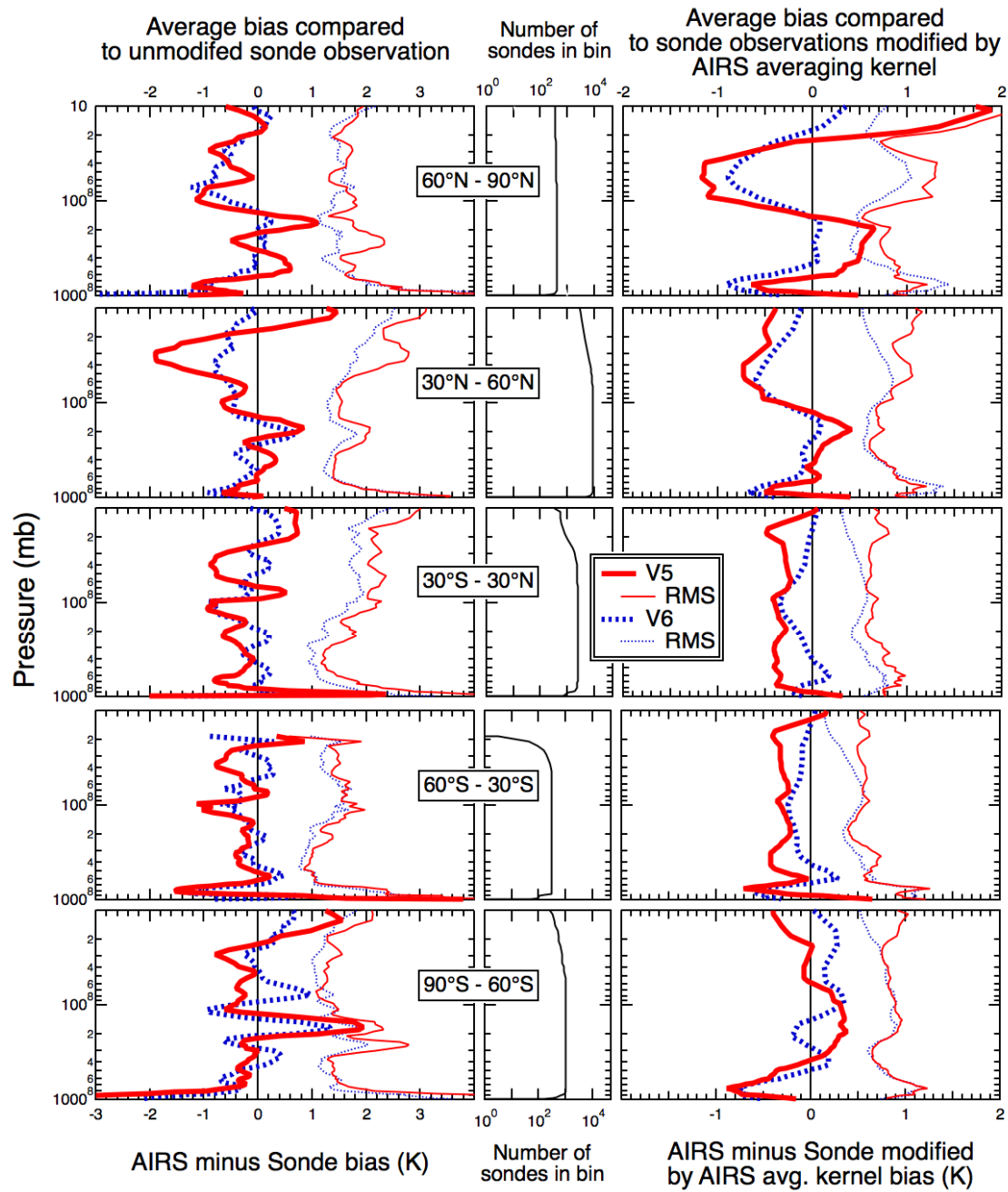


Figure 16 Locations of AIRS – radiosonde matchups for December 2005-January-February 2006 (left panel), and June, July, August 2006 (right panel).

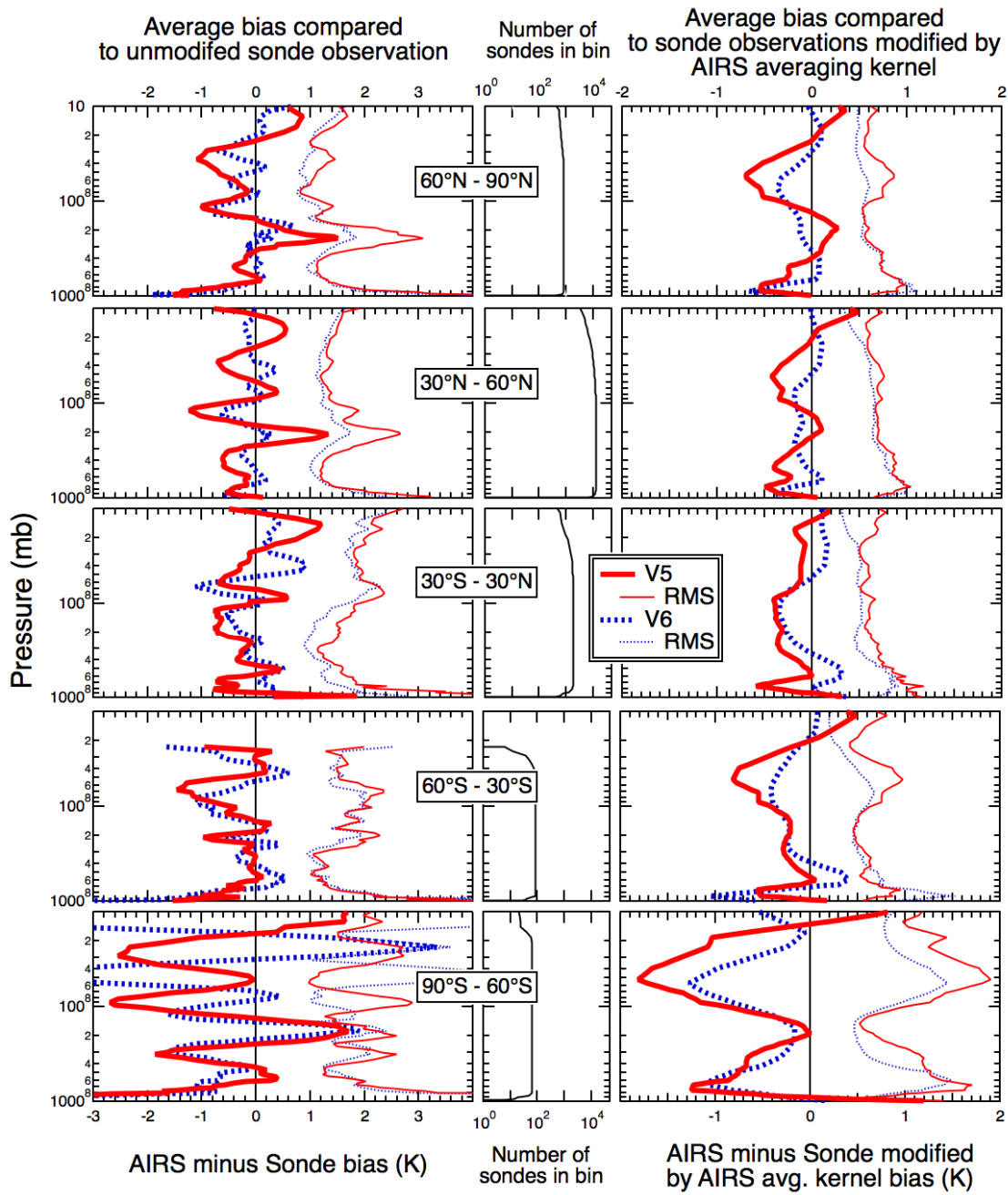
Version 6 Performance and Test Report



DJF 05/06

Figure 17 Zonally-averaged comparisons of AIRS minus operational radiosonde temperatures (left panels), number of sondes in zonal bin (middle panels), and AIRS minus radiosonde modified by the AIRS averaging kernel as in Equation 2. Data are from December 2005 through February 2006. Note that the right panels have a shorter temperature scale than the left panels.

Version 6 Performance and Test Report



JJA 06

Figure 18 Zonally-averaged comparisons of V5 and V6 AIRS minus operational radiosonde temperatures (left panels), number of sondes in zonal bin (middle panels), and AIRS minus radiosonde modified by the AIRS averaging kernel as in Equation 2. Data are from June, July and August 2006. Note that the right panels have a shorter temperature scale than the left panels.
Page 44

Version 6 Performance and Test Report

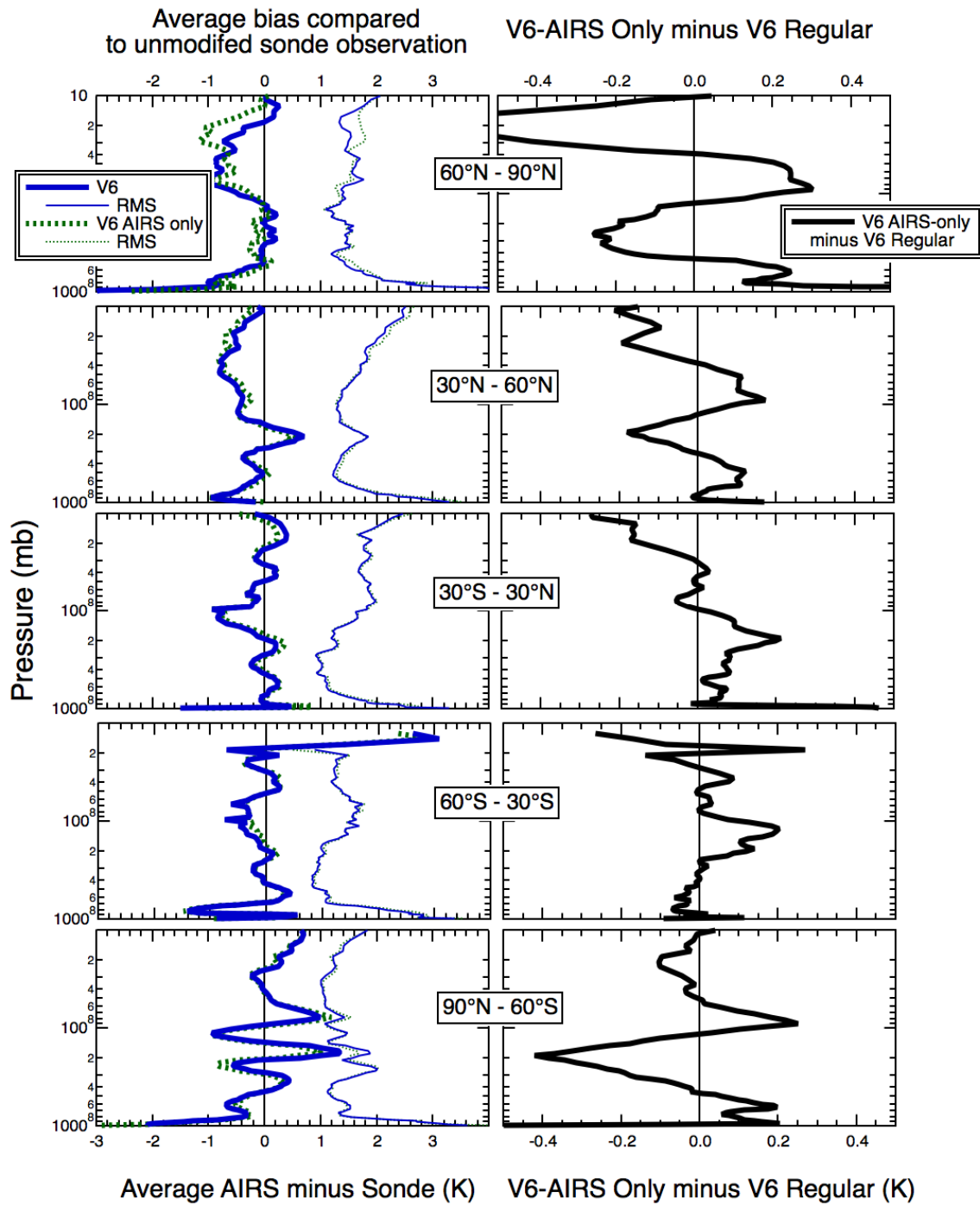


Figure 19 Zonally-averaged comparisons of AIRS V6-Regular (using AMSU in the retrieval) and V6 AIRS-only (without AMSU) minus radiosonde temperatures (left panels), and AIRS-only minus AIRS-regular on the right panels. Data are from December 2005 through February 2006. Note that the right panels have a shorter temperature scale than the left panels.

Version 6 Performance and Test Report

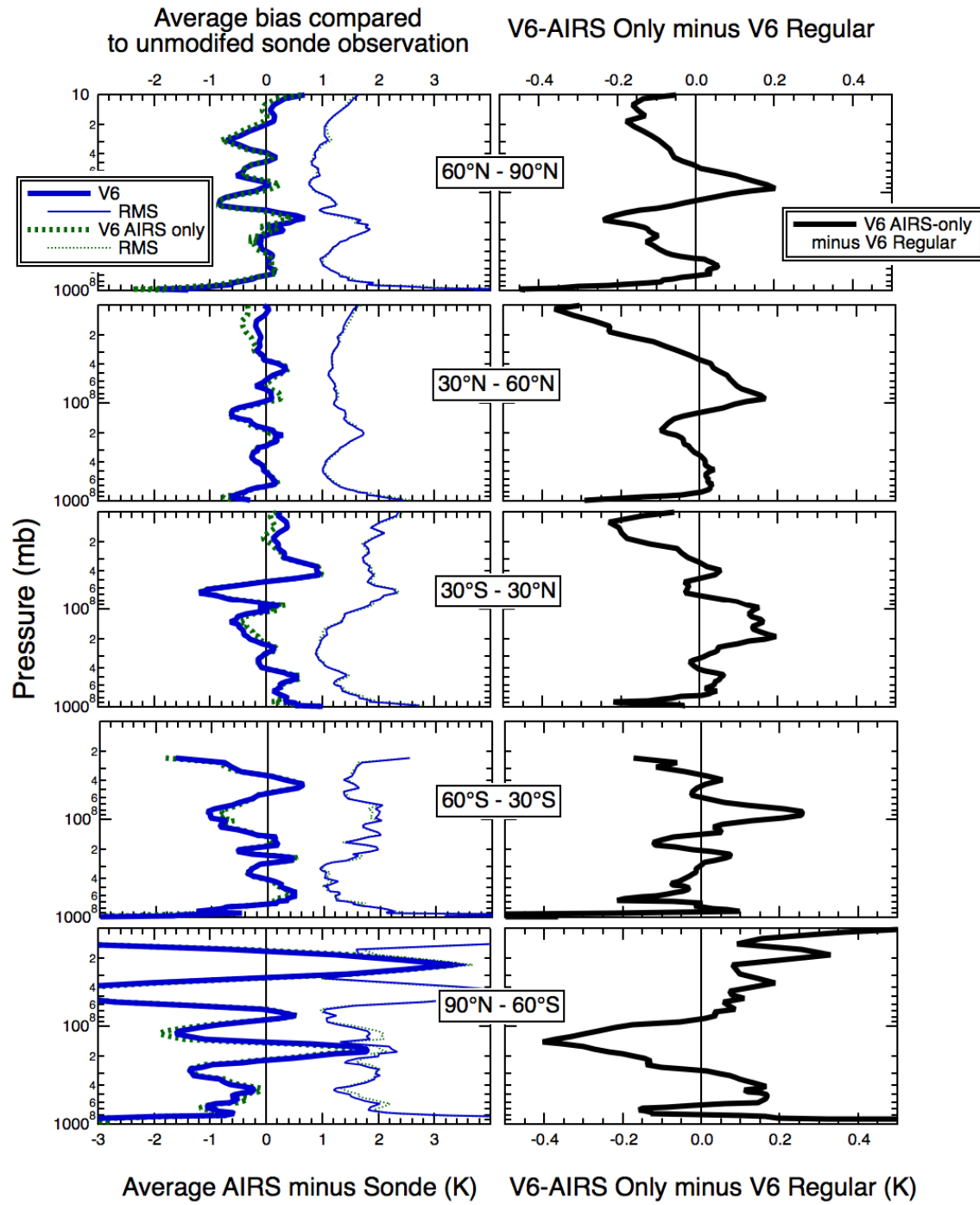


Figure 20 Zonally-averaged comparisons of AIRS V6-Regular (using AMSU in the retrieval) and V6 AIRS-only (without AMSU) minus radiosonde temperatures (left panels), and AIRS-only minus AIRS-regular on the right panels. Data are from June through August 2006. Note that the right panels have a shorter temperature scale than the left panels.

Version 6 Performance and Test Report

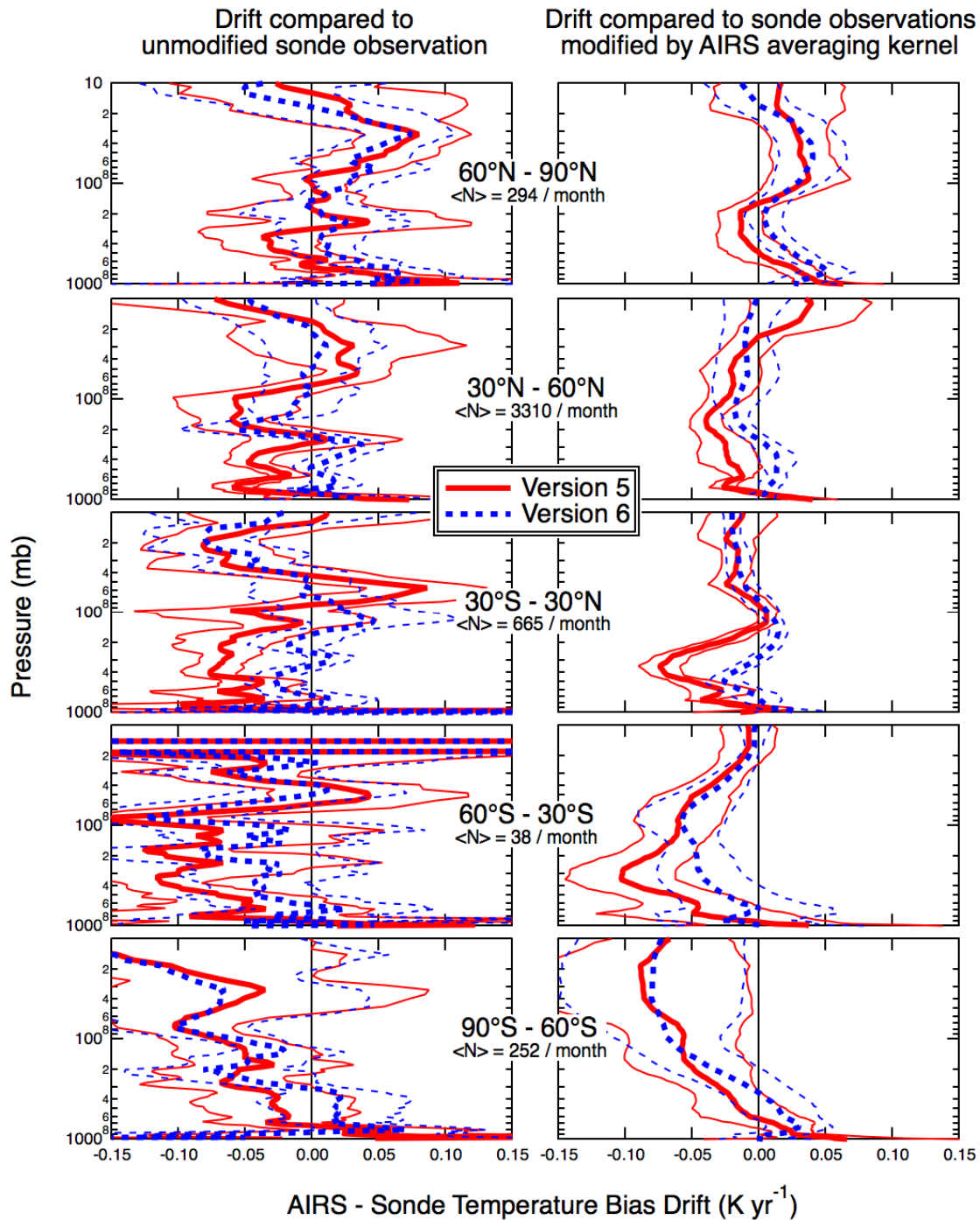


Figure 21 Zonally averaged temperature bias drift of V5 and V6 AIRS minus operational radiosondes (left panel), and minus sondes modified by the AIRS averaging kernel as in Equation 2 (right panel). Trends were calculated by linear, least squares fitting through calendar month data from 2004 through 2011, with the average slope over all months shown above. The thinner lines are the standard deviation of the average slope at each pressure level.

Version 6 Performance and Test Report

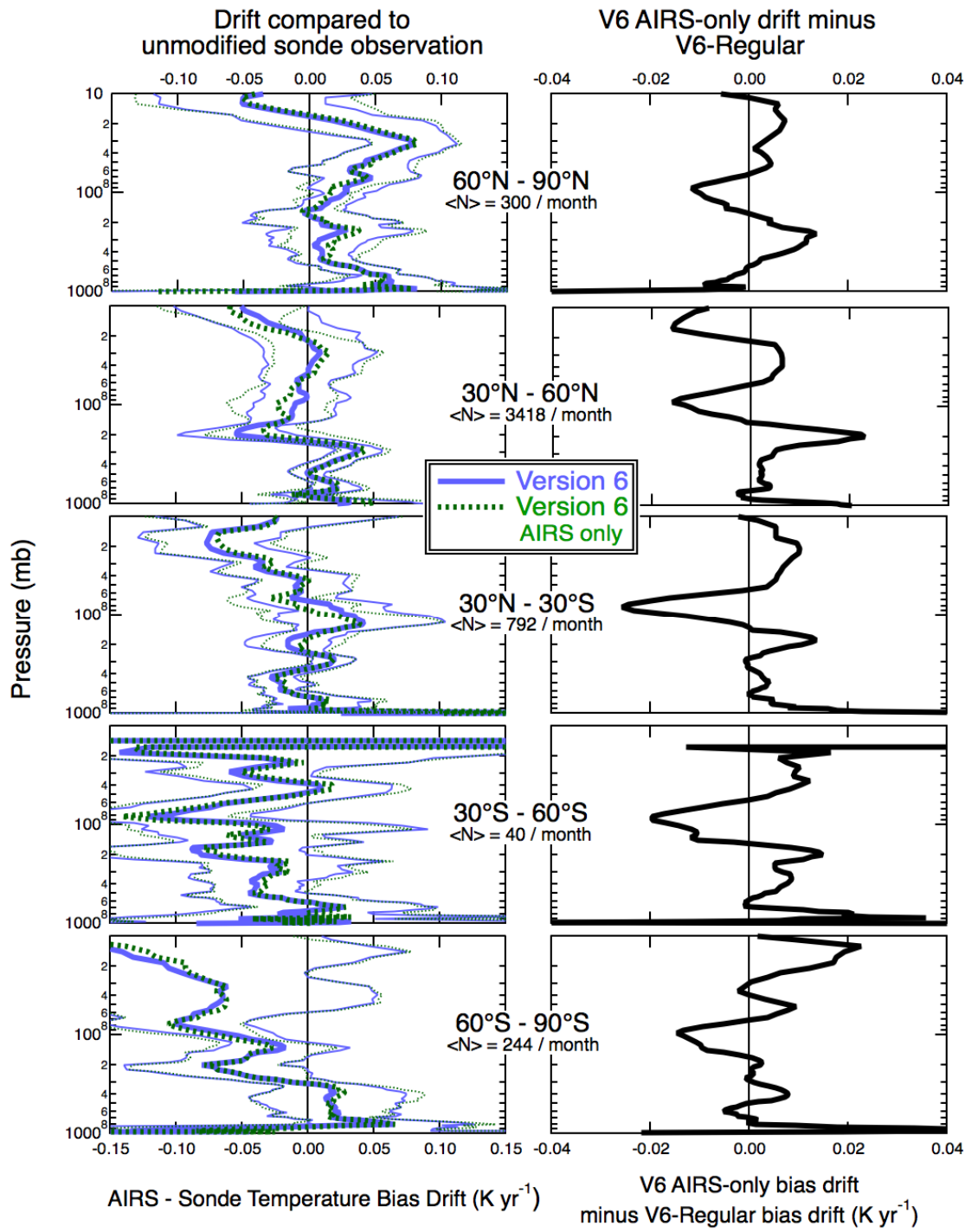


Figure 22 Zonally averaged temperature bias trends of AIRS V6-Regular (using AMSU in the retrieval) and V6 AIRS-only (without AMSU) minus operational radiosondes (left panels), and AIRS-only minus AIRS-Regular (right panels). Trends were calculated by linear, least squares fitting through calendar month data from 2004 through 2011, with the average slope over all months shown above. The thinner lines are the standard deviation of the average slope at each pressure level.

Version 6 Performance and Test Report

3.4 Surface Air Temperature

Tester: H. Van Dang

Data Product	Description
TSurfAir	Surface air temperature
TSurfAir_QC	Quality control of surface air temperature
TSurfAirErr	Error estimate of surface air temperature

Surface air temperature is derived from the two air temperature levels in the support product where one is above the surface and the other level is either very close on top or below the surface pressure. The two support air temperatures levels are weighted and summed to give the surface air temperature. The AIRS V5 and V6 (V6.0.2) surface air temperature are compared to PrepQC sondes values. The sondes report air temperature as it ascends the atmosphere and it does not necessarily reflect the air temperature that AIRS reports at the surface and so the PrepQC sonde temperatures have been linearly interpolated with the logarithm of the pressures to AIRS surface pressure level for comparison to AIRS. Since the sondes are only in specific locations, the results of the testing of this data product should not be extrapolated too wildly to other regions. The following are figures showing where over ocean and land we have the sondes and the number of sondes launched from September to December of 2002 for comparisons.

Version 6 Performance and Test Report

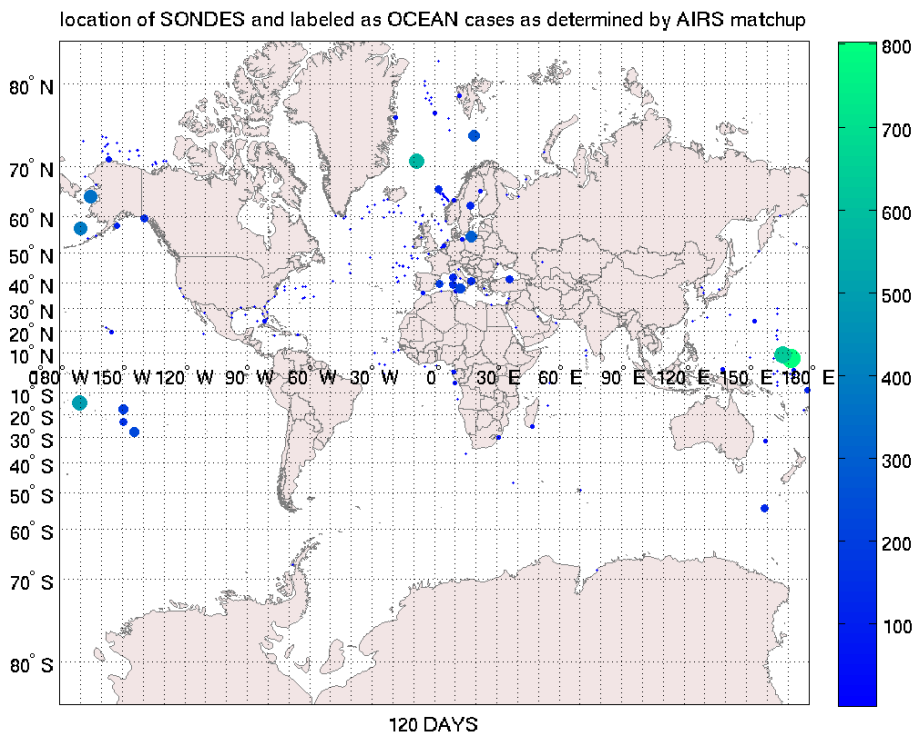


Figure 23. Location of PrepQC radiosondes that are matched to AIRS ocean cases.

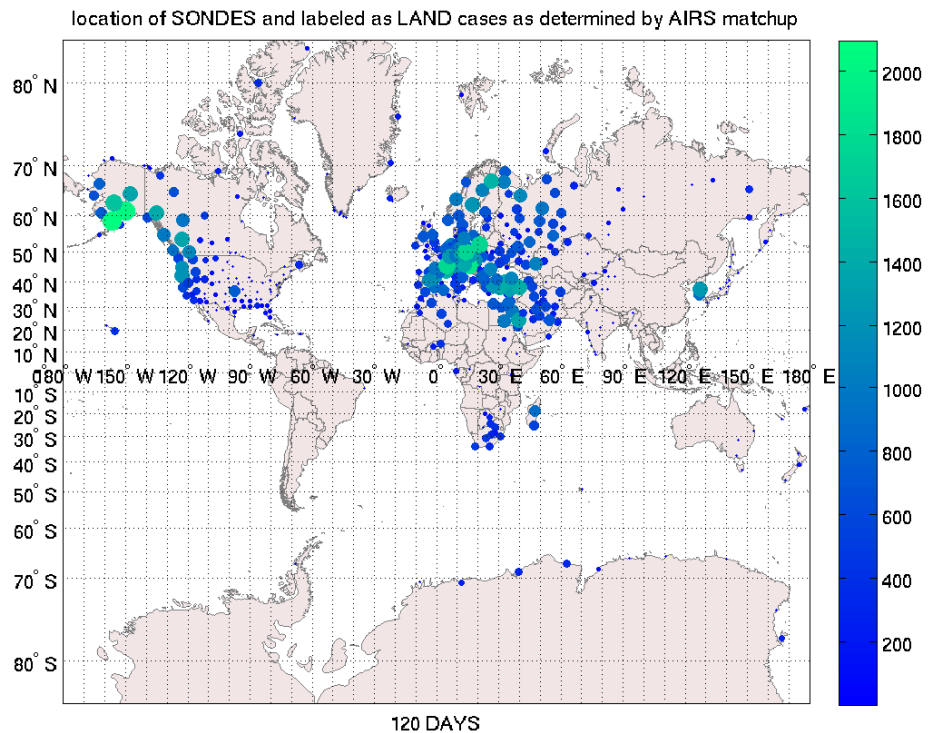


Figure 24. Location of PrepQC radiosondes that are matched to AIRS land cases.

Version 6 Performance and Test Report

There exists many more land comparisons with sondes than there are with ocean cases. Land cases mostly occur in the northern hemisphere. This is not a thorough validation exercise and so the testing is carried out to see if there are any glaring errors that need to be caught before the release of the product. The following are the results of the comparison.

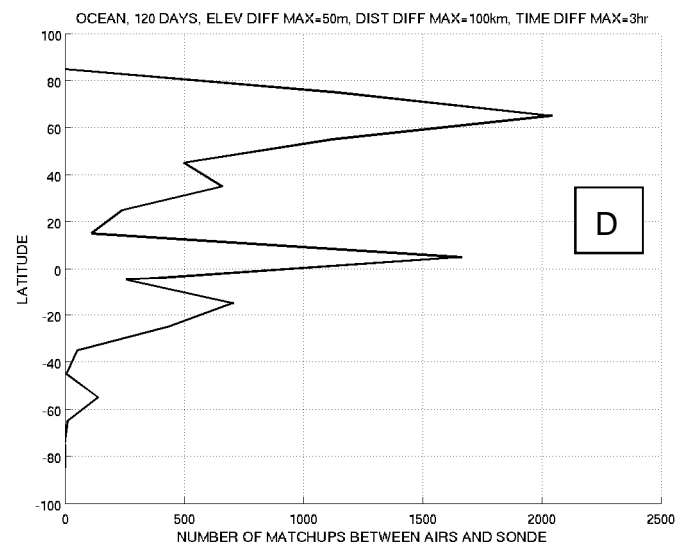
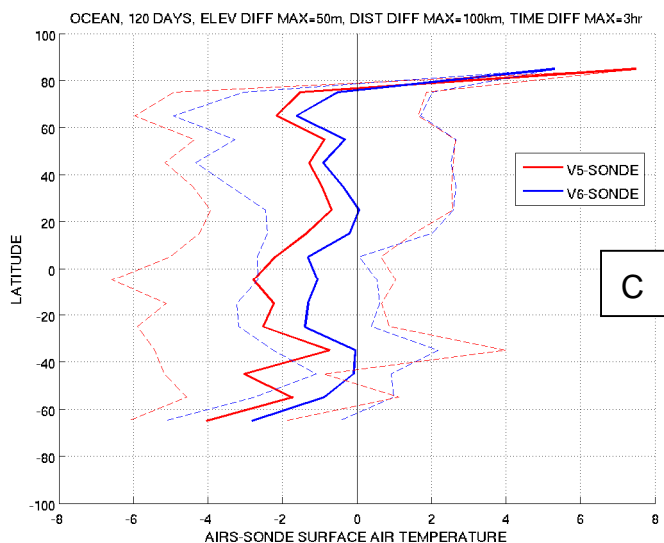
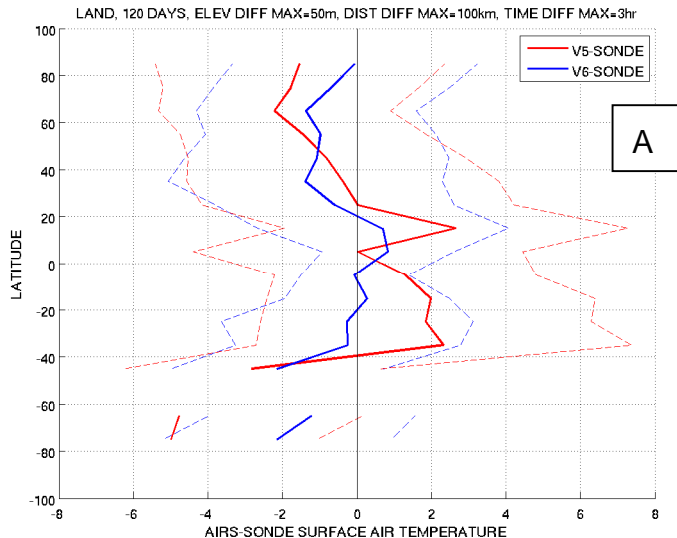


Figure 25. Land and Ocean scenes showing AIRS V5 and V6 showing the average deviation from sondes per latitude band. Also the number of matchups between AIRS and sondes per latitude band.

Version 6 Performance and Test Report

In Figure 25, the right column shows the number of comparisons between AIRS V5 and V6 with sondes that existed for the 120 days that were looked at per latitude band for land cases on the upper figure, and ocean cases in the lower image. On the left column of figures is the difference between AIRS V5/V6 with sonde surface air temperature per 10 degrees latitude band for land in the upper image and for ocean in the lower image. For ocean cases over most latitude bands, V6 deviates less from the sondes than V5 does. When looking at land cases and concentrating only in the northern hemisphere where most of the data exists, for latitude=[20,50] degrees, V5 values appears to be closer to sondes and for latitude=[50,70], V6 appears to compare better to sondes.

Figure 26 below is similar to the previous image except that the differences between AIRS and sondes are separated into day and night scenes. Looking at only the northern hemisphere where the average differences (thicker lines) are more representative due to a larger data set, it is very apparent that day time differences between AIRS V5/V6 with sondes are larger for night time scenes over land. For day time scenes over land, V5 and V6 difference with sondes are very similar. The thinner lines are the average +/- the standard deviation of AIRS minus sondes surface air temperature with the colors corresponding to AIRS version and day/night scenes.

Version 6 Performance and Test Report

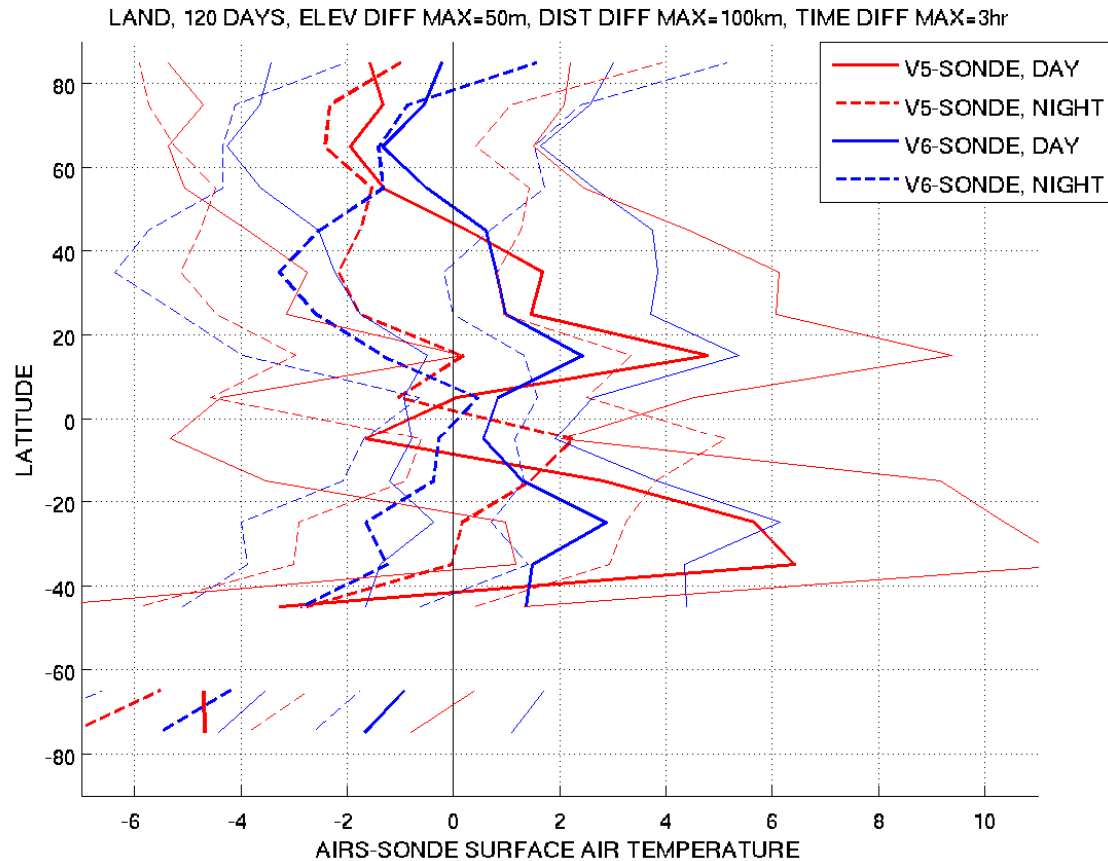


Figure 26. Land cases of AIRS V5 and V6 showing the average deviation from sondes per latitude band for day and night cases.

Version 6 Performance and Test Report

3.5 Land and Polar Surface Temperature and Emissivity

Tester and Point of Contact: Glynn Hulley

Data Products	Description
TSurfStd	Surface skin temperature
TSurfStd_QC	Surface skin temperature quality control
TSurfStdErr	Surface skin temperature standard error
SurfClass	Surface type classification
freqEmis	Frequencies of selected hinge-points in wavenumber
emisIRStd	Spectral surface emissivity at 39 nominal hinge-points
emisIRStd_QC	Spectral surface emissivity quality control
emisIRStdErr	Spectral surface emissivity standard error

This section will describe the AIRS V6 surface property products defined in Table 1 including testing of these products. For testing of the V6 product, a mean monthly AIRS dataset for January 2007 was chosen for the analysis. Products are tested using a variety of metrics including; 'geophysical smell test' - do the retrieved values make physical sense; range checks - do the quantities fall between physically defined values (e.g. emissivity should not be greater than 1); standard deviation - what regions have larger variations and why. The V6 products are further compared with the V5 product and the MODIS MYD11 LST and emissivity products. The majority of the testing is done for the AIRS/AMSU retrieval using QC = (0,1), but comparisons are also shown with the AIRS IR-only retrieval

Quality Indicators

In V5 **Qual_Surf** was used to describe quality indicators for the **TSurfStd** and **emisIRStd** products. In V6, each product has its own quality control, e.g. **TSurfStd_QC**, **emisIRStd_QC**, but the philosophy has not changed (i.e. 0=best, 1=good, 2=bad). In theory **TSurfStd_QC** and **emisIRStd_QC** should yield the same results since these two variables are retrieved simultaneously. The pie charts in Figure 27 show V5 and V6 global percentage yield (QC=0,1,2) from **Qual_Surf** for AIRS/AMSU retrievals during Jan. 2007 for two cases: bare surfaces (emissivity at 1205 cm-1) <0.85) and graybody surfaces such as snow, ice, vegetation (emissivity at 1205 cm-1>0.85). The statistics indicate a higher percentage of good retrievals (QC=0,1) in V6 for both arid and graybody surface types, with the most pronounced difference occurring for bare surfaces due to an

Version 6 Performance and Test Report

improved first guess emissivity spectral shape. Figure 28 shows an example of the standard error in TSurfStd, termed **TSurfStdErr**, versus the quality control, **TSurfStd_QC**. This is a good check to see if larger errors correlate with poorer quality (QC=2), as they should. On each box, the central mark is the median, the edges of the box are the 25th and 75th percentiles, the whiskers extend to the most extreme data points not considered outliers, and outliers are plotted individually. For both V5 and V6, TSurf errors are below 2K for QC=0, but in V6 the errors for QC=1 are much better constrained than in V5, which has similar distributions of errors for QC=1,2 extending up to 15 K. In V6 there is much better correlation between estimated error and QC. Similar results were obtained for the emissivity product, **emisIRStdErr**, not shown here.

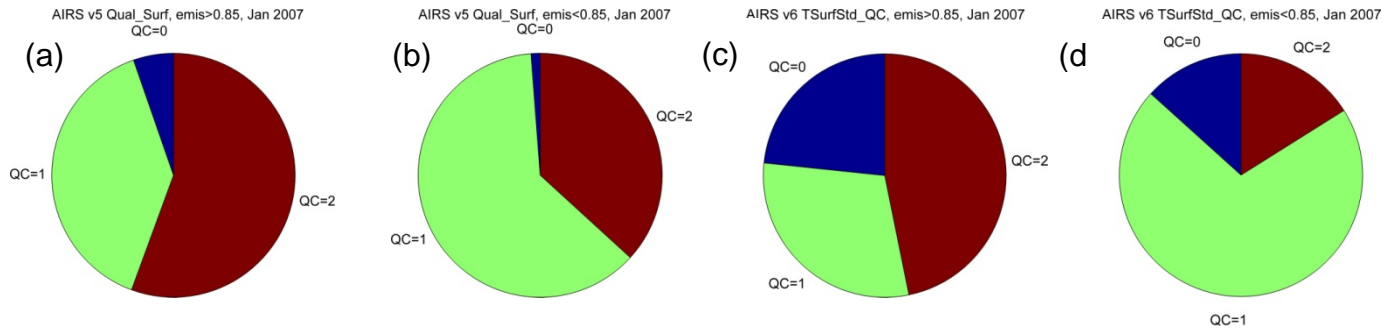


Figure 27. AIRS percent yield for Jan. 2007 based on **TSurfStd_QC** using QC=0 (best), 1 (good), 2 (bad) for (a) AIRS V5 graybody surfaces, (b) AIRS V5 bare surfaces, (c) AIRS V6 graybody surfaces, and (d) AIRS V6 bare surfaces.

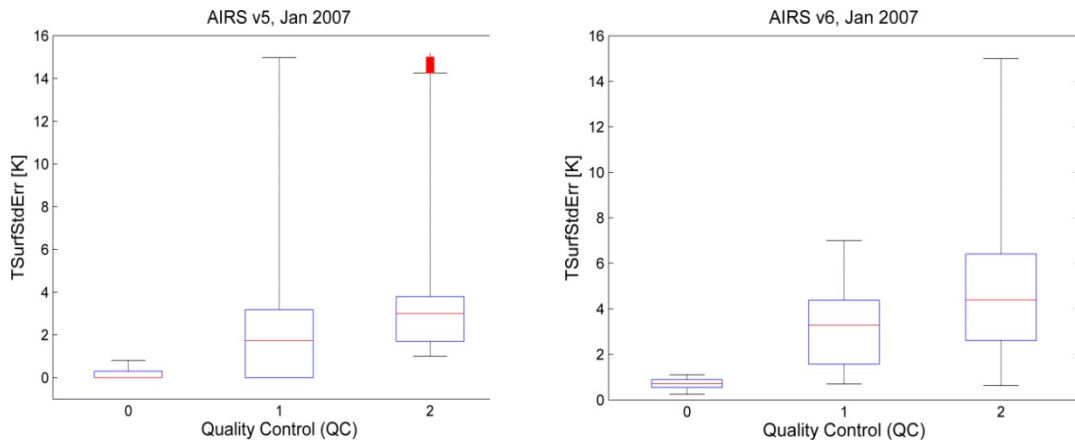


Figure 28. AIRS surface temperature estimated error, **TSurfStdErr**, versus quality control, **TSurfStd_QC** for global AIRS/AMSU retrievals during Jan. 2007.

Version 6 Performance and Test Report

TSurfStd

The **TSurfStd** product represents the 'skin' temperature of the Earth's surface, which usually represents the top few micrometers of the surface. For the remainder of the document we will refer to it as the land surface temperature (LST). Although retrieved simultaneously, the LST is independent of the emissivity and varies with solar irradiance history and local weather conditions. Changes made to the AIRS V6 surface retrieval are summarized in Susskind et al. (2008). Figure 29 shows the mean monthly day-time and night-time LST for Jan. 2007 retrieved with the AIRS/AMSU V6 algorithm. The temperatures appear within normal ranges for all regions and time of year, i.e. the hottest temperatures of up to 340 K are found over the Australian deserts during the summer and coldest temperatures <240 K over the northern polar regions during wintertime. Equatorial regions have the smallest diurnal differences while desert regions have much larger diurnal cycles as expected. The monthly standard deviations in LST shown in Figure 30 are generally below 5 K but can be as large as 15 K over Greenland, parts of Alaska and Australia. These variations are unreasonably high and are most likely due to cloud clearing issues in the retrieval, particularly when viewing low-level clouds over Polar Regions.

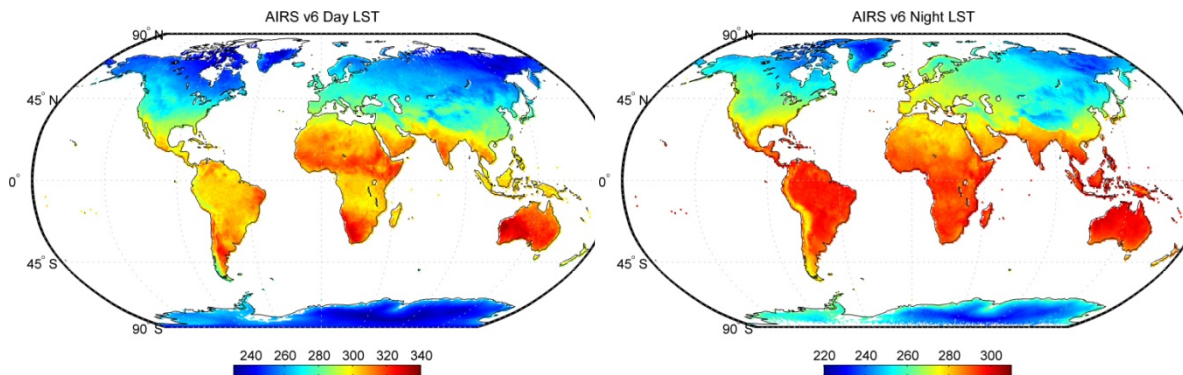


Figure 29. Mean monthly TSurfStd during Jan. 2007 for day-time (left) and night-time (right) AIRS/AMSU V6 retrieval using QC=(0,1).

Version 6 Performance and Test Report

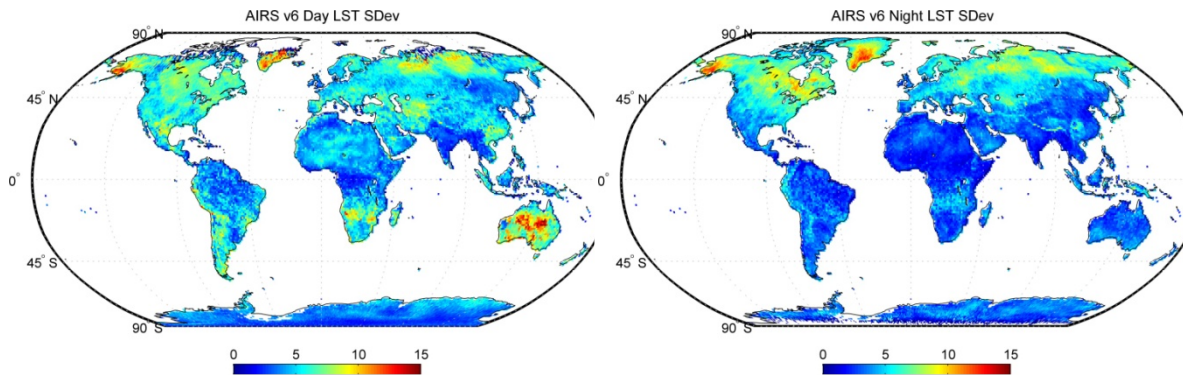


Figure 30. Monthly standard deviation of $T_{SurfStd}$ during Jan. 2007 for day-time (left) and night-time (right) AIRS/AMSU V6 retrieval using QC=(0,1).

Night-time variations are smaller than expected, except over Greenland and Alaska similar to the day-time results.

Figure 31 shows LST differences for day (left) and night (right) between the AIRS/AMSU retrieval and the AIRS (IR-only) retrieval. Generally the differences are small and below the 1 K level, but can be as large as 5 K over snow/ice covered regions such as Quebec, Canada (day and night), Greenland (day only) and parts of Europe (day and night). These differences are most likely cloud-related since with AMSU, retrievals under more difficult cloud conditions are possible. Users should therefore pay attention to the QC and estimated error when using this product over polar regions and under more difficult cloud situations.

Figure 32 shows comparisons between mean monthly AIRS V5 day-time LST and MODIS LST (MYD11C3 v4.1 product). The mean global bias is less than 1 K with an RMSD of around 3 K. The largest differences occur primarily over desert regions in North Africa and Australia (>10 K). Figure 33 shows corresponding differences between AIRS V6 and MODIS LST. The mean bias is negative but still less than 1 K. The RMSE is slightly higher at 4 K when compared to V5. However, this does not necessarily imply V6 is worse than V5. Rather differences with MODIS are primarily a function of differences in retrieval type (MODIS uses day/night algorithm), spatial resolution (MODIS is 5 km), and sampling (MODIS is clear-sky only). In V6,

Version 6 Performance and Test Report

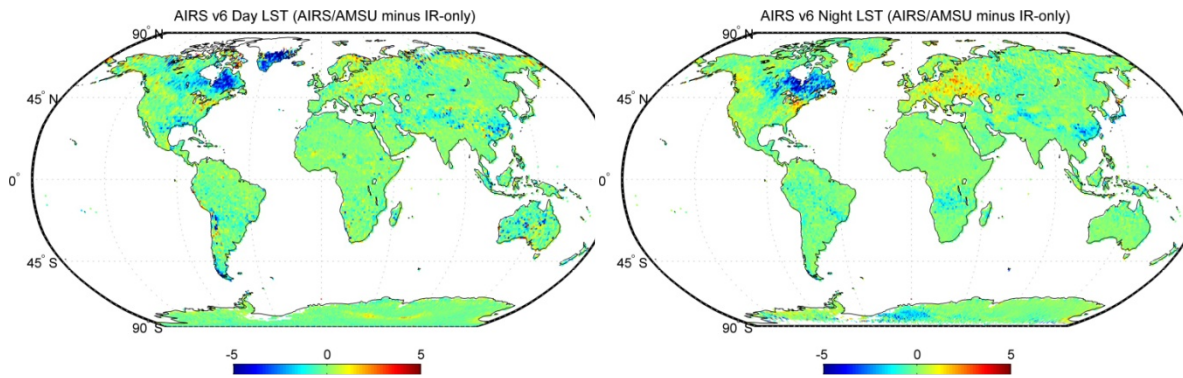


Figure 31. Mean monthly day (left) night-time (right) differences between AIRS/AMSU and AIRS IR-only V6 LST for Jan. 2007 using QC=(0,1).

biases with MODIS over North Africa and Australia are lower when compared to V5, but are larger in other areas (e.g. Greenland). Nevertheless a 'sanity' check with a baseline product such as MODIS is useful in that it identifies over what areas and types of conditions the largest changes between different product versions occur.

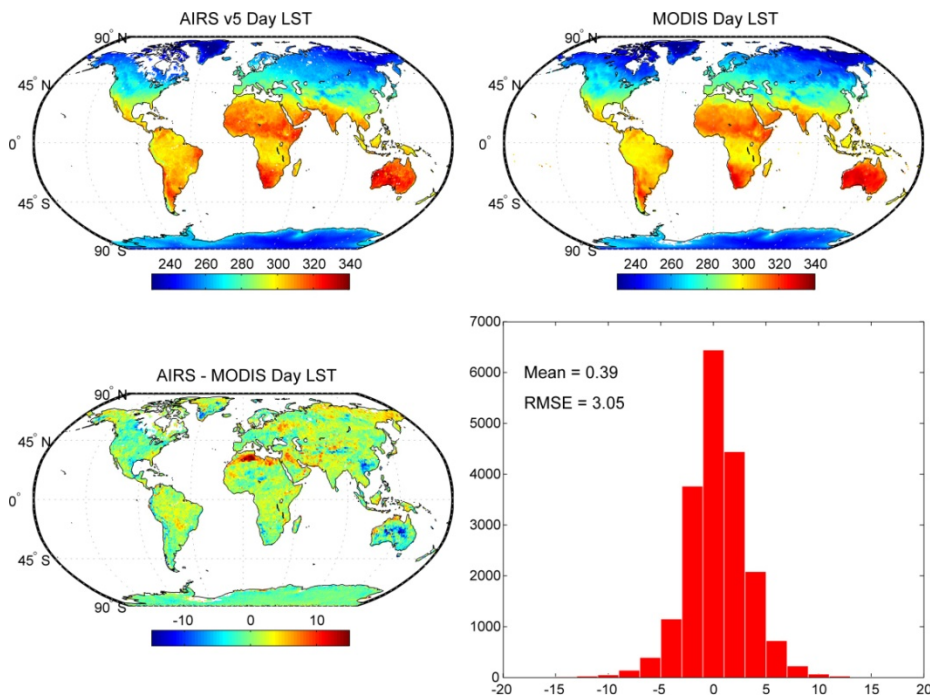


Figure 32. Mean monthly day-time differences between AIRS V5 and MODIS v4.1 LST for Jan. 2007 using QC=(0,1).

Version 6 Performance and Test Report

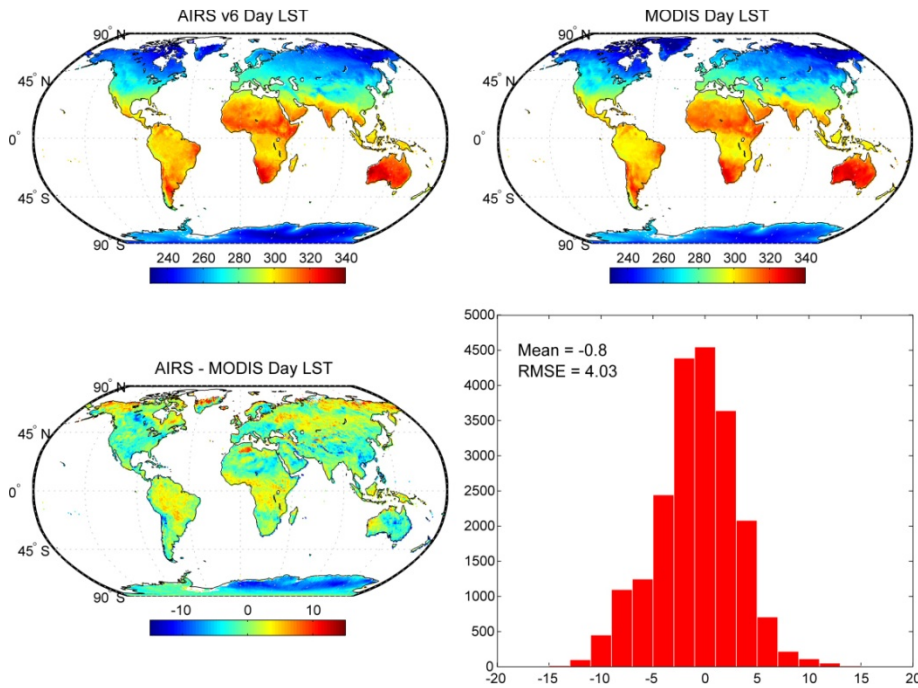


Figure 33. Mean monthly day-time differences between AIRS V6 and MODIS v4.1 LST for Jan. 2007 using QC=(0,1).

emisIRStd

The emissivity of an isothermal, homogeneous emitter is defined as the ratio of the actual emitted radiance to that emitted from a black body at the same thermodynamic temperature. The emissivity is an intrinsic property of the Earth's surface and is independent of the LST. For most natural Earth surfaces between 3-12 μm , emissivity ranges from ~0.65 to close to 0.99.

Figure 34 shows AIRS V6 retrieved shortwave emissivity at 2632 cm⁻¹ (3.8 μm) for day and night-time data. Emissivities less than 0.85 are typical for most desert areas due to the strong quartz absorption feature between 8-9.5 μm range, whereas the emissivity of vegetation, water and ice cover are generally greater than 0.95 and spectrally flat in the 3-12 μm spectral range. Differences between day and night emissivity should be small, and depend on factors such as dew, rainfall and snow/ice melt which increases soil moisture content and hence emissivity. Figure 34 shows shortwave emissivities correlate well spatially both day and night but the day-time emissivities are generally higher than at night,

Version 6 Performance and Test Report

particularly over vegetated regions. The emissivity standard deviations in Figure 35 during Jan. 2007 show largest daytime variations over deserts up to 0.1 (10%), due to improper modeling of shortwave reflected solar radiation in the retrieval. This was discussed in detail in Hulley et al. (2009). Nighttime variations are less over deserts but show large signal over boreal regions of northern Eurasia and North America.

Emissivities in the longwave 820 cm-1 region should normally be stable and invariant and range from ~0.92-0.99, and at the AIRS product resolution of 50km should not drop below about 0.94, except over mafic rocks such as pure basalt regions. Figure 36 shows mean monthly AIRS V5 and V6 emissivities, zonal means, and histogram distributions at 820 cm-1 for Jan. 2007. In V5, the surface retrieval produced many unphysical emissivity values, either greater than 1 independent of wavelength, or less than 0.9 in the longwave region. The V5 zonal mean plots in Figure 36 show regions of unphysical values below 0.94 in the equatorial regions and many pixels with emissivities less than 0.9 in the histogram plot. In V6 these issues have been resolved and retrieved emissivities are now well constrained between 0.94-1 in the longwave region, except for a few outliers over northern Australia and eastern parts of Brazil.

A big issue with the V5 surface retrieval was that diurnal emissivity differences were very large, particularly in the shortwave region (2632 cm-1) due to residual effects of improper solar reflection modeling. Figure 37 shows AIRS V5 and V6 diurnal emissivity differences at 2632 cm-1 and their distributions. In V5 the differences can be as large as 0.3 (30%) in emissivity, and are largest over desert regions of North Africa and the Arabian Peninsula. In V6 these differences have been substantially reduced and now range between -0.1 and 0.1. These differences can be physical, for example due to nighttime condensation on the surface from dew over arid regions; however, over Australia where V6 has the largest differences, these seem unphysical. The improved diurnal stability in V6 is a result of several major changes to the retrieval methodology discussed in Susskind et al. (2008). The changes include a new channel selection, retrieving LST. The changes include a new channel selection, retrieving LST using shortwave channels alone, and holding this fixed in the longwave emissivity retrieval, and improved solar reflection modeling.

Version 6 Performance and Test Report

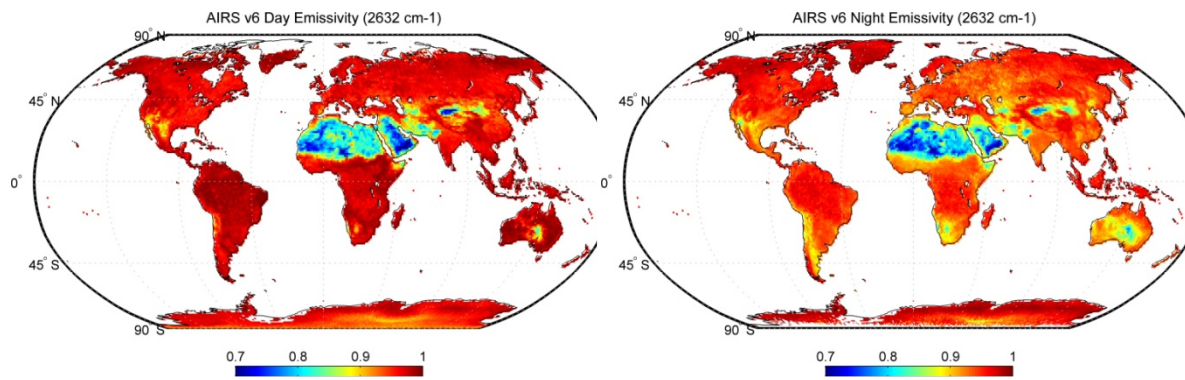


Figure 34 Mean monthly emisIRStd at 2632 cm⁻¹ during Jan. 2007 for day-time (left) and night-time (right) AIRS/AMSU V6 retrieval using QC=(0,1).

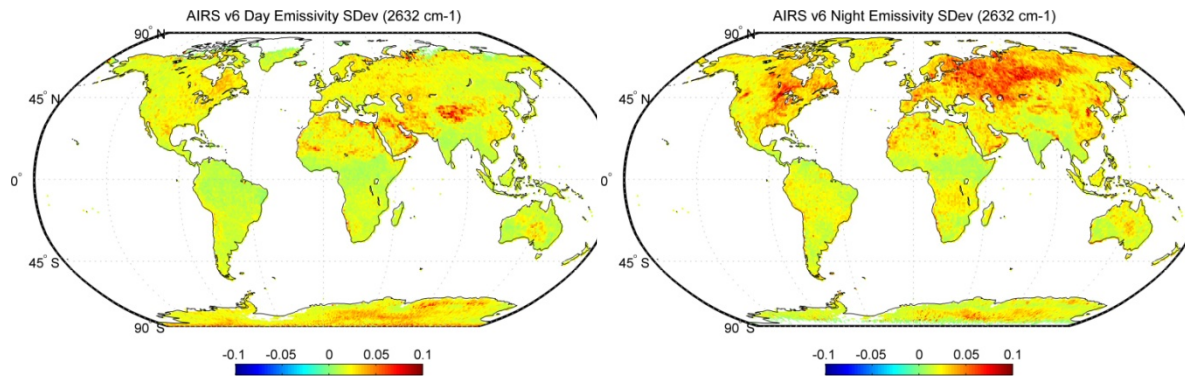


Figure 35 Monthly standard deviation of emisIRStd at 2632 cm⁻¹ during Jan. 2007 for day-time (left) and night-time (right) AIRS/AMSU V6 retrieval using QC=(0,1).

Version 6 Performance and Test Report

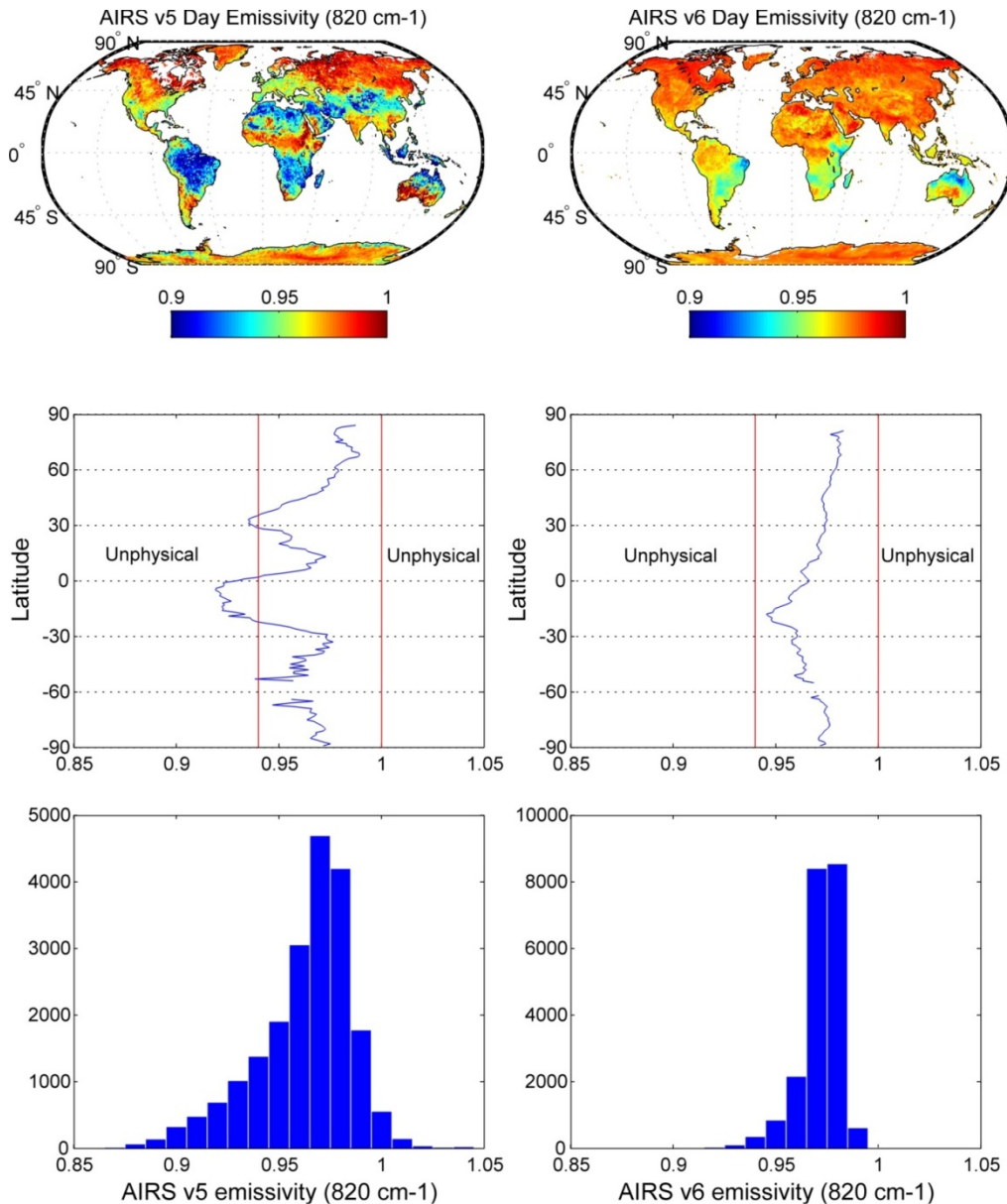


Figure 36. *Distributions of AIRS V5 (left panels) and V6 (right panels) global daytime emissivities at 820 cm⁻¹ for Jan. 2007 using QC=(0,1).*

Improvements in spectral shape due to a better first guess emissivity can be clearly seen in Figure 38 which shows AIRS mean spectra for V5 (left) and V6 (right) from 2003-2006 over the Grand Erg Oriental, Algeria including first guess and ASTER emissivity spectra. In this plot the 5 ASTER narrow-bands from 8-12 μm have been fit using a hyperspectral principal component model (black line). Solid errorbars show temporal variation and solid lines show mean values at the

Version 6 Performance and Test Report

selected hinge-points (solid circles). In V5 the NOAA regression first guess starts off with unphysical emissivities <0.6 in the shortwave and <0.9 in the longwave, resulting in emissivity being too low with poor spectral shape in the final retrieval when compared to ASTER (black line). In V6, the MODIS first guess starts very close to ASTER and there is improved spectral shape in the shortwave region. The final retrieval fits the ASTER spectra to

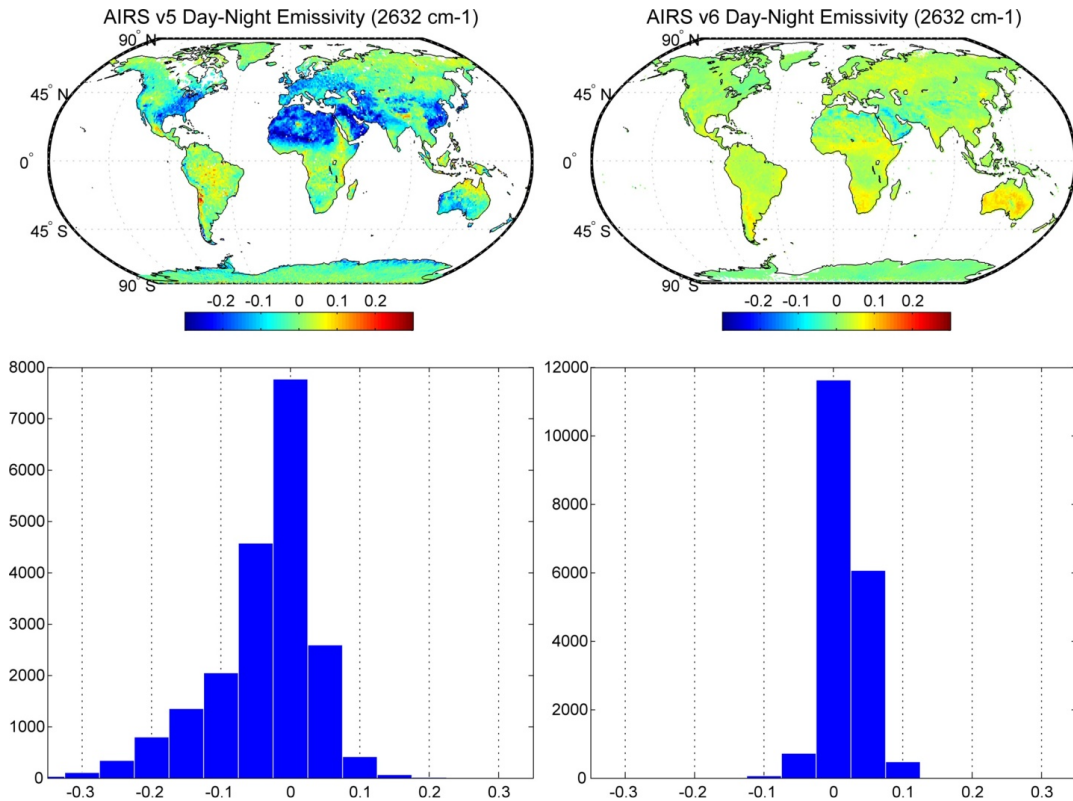


Figure 37. Diurnal (day-night) shortwave emissivity differences for AIRS V5 (left panels) and V6 (right panels) at 2632 cm-1 for Jan. 2007 using QC=(0,1). Diurnal differences are reduced by more than a factor of two in V6, although some unphysical differences are still evident (e.g. Australia).

within a few percent, however the quartz doublet (8-10 μm) is not represented well because MODIS only has one piece of information in this region (band 29).

Figure 39 shows emissivity differences for day (left) and night (right) between the AIRS/AMSU retrieval and the AIRS (IR-only) retrieval for the shortwave channel (2632 cm-1). Generally the emissivity differences are small for both day and night, with RMSEs of 0.006 (0.6%) and 0.005 (0.05%) respectively, but can be as

Version 6 Performance and Test Report

large as 0.2 (20%) both day and night. For example over the Taklamakan desert in China there are large daytime differences, even although the corresponding LST differences are small. For nighttime data, differences are slightly larger with the largest variations distributed over more diverse areas, e.g. boreal forests of northern Eurasia, over parts of Canada, and China.

The surface emissivity retrieval is set to have minimum limits of 0.65 (shortwave) and 0.92 (longwave). Emissivity retrievals that fall below these limits are generally considered unphysical values at AIRS spatial resolution (50km). However, on occasion emissivity values below these limits will be reported for Q0 (best) and Q1 (good) quality flags when there is a valid MODIS first guess emissivity that is unusually low, most likely due to cloud contamination. The logic for the minimum emissivity limit is as follows: For a valid MODIS first guess, the min allowable emissivity is $\min(\text{MODIS} - \Delta\epsilon, 0.65)$ for the shortwave, and $\min(\text{MODIS} - \Delta\epsilon, 0.92)$ for the longwave. The $\Delta\epsilon$, or 'maxchange' values are set to 0.25 (shortwave) and 0.1 (longwave), and set the limits to which the retrieval can move off the MODIS first guess.

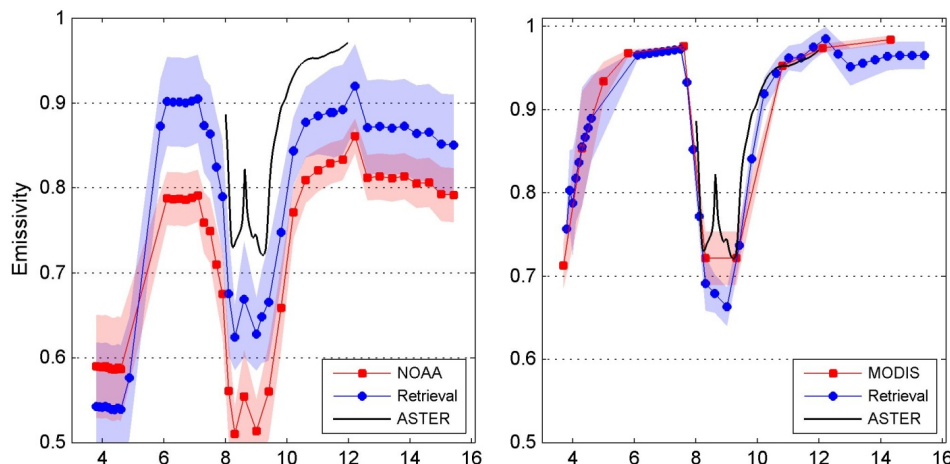


Figure 38. AIRS mean emissivity spectra from 2003-2006 over the Grand Erg Oriental validation site in Algeria for V5 (left) using the NOAA surface regression first guess, and V6 (right) using the UW-Madison MODIS baseline-fit emissivity database. Improvement in emissivity spectral shape and absolute magnitude versus ASTER emissivity at this site is clearly seen.

Version 6 Performance and Test Report

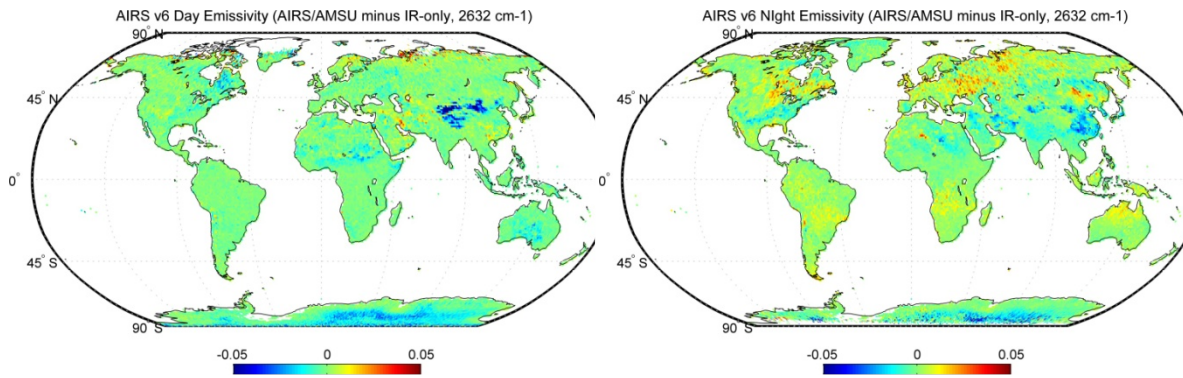


Figure 39. Mean monthly day (left) night-time (right) differences between AIRS/AMSU and AIRS IR-only V6 shortwave emissivity (2632 cm⁻¹) for Jan. 2007 using QC=(0,1).

SurfClass, freqEmis, and Sea-Ice

SurfClass is used in the physical retrieval to assign values for the emissivity first guess based on land cover type. Surface types are set by thresholding microwave (MW) and/or infrared (IR) data. SurfClass is identical to the **MWSurfClass** product when MW only data is used. Figure 40 shows the maximum AIRS V6 and V5 day and night-time SurfClass values for 6-12 Jan 2007 using the AIRS/AMSU retrieval. The daytime V5 and V6 results are very similar and surface assignments appear normal. For night-time, there appear to be anomalies over parts of the Sahara desert, Arabian Peninsula and Chile where snow classifications have been incorrectly set for both V5 and V6. Figure 41 shows the SurfClass product for AIRS IR-only retrievals. With the loss of microwave data (AMSU 4, 5) surface classification is more challenging, but daytime IR-only classes match up well with the AIRS/AMSU, except for at night where misclassifications appear over the Sahara desert, parts of Spain and in the US snow cover extends too far south.

Frequencies for retrieved surface emissivity and reflectivity, **freqEmis**, are arranged in order of increasing frequency. In V5 only the first **numHingeSurf** elements were valid, and so this could vary from one retrieval to the next, however in V6 the same list of 39 frequencies are always set in the retrieval.

Version 6 Performance and Test Report

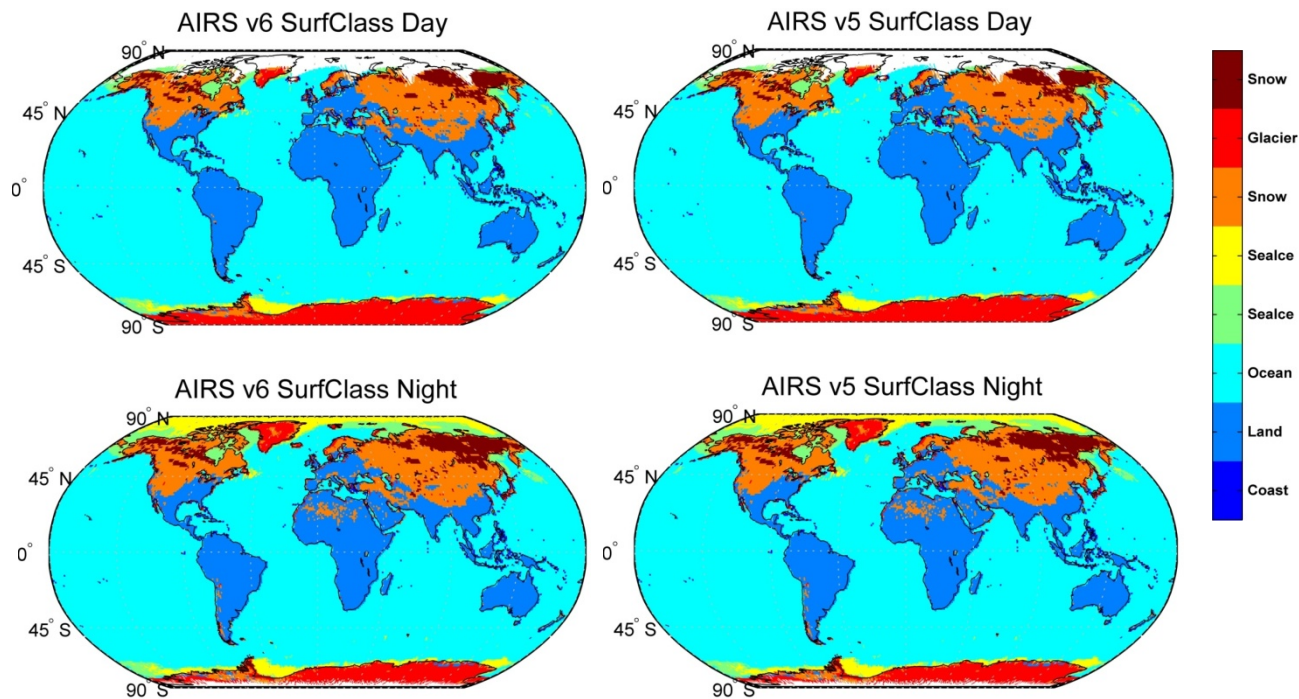


Figure 40. Maximum values of SurfClass from 6-12 Jan. 2007 for AIRS V6 (left) and V5 (right) for daytime (top) and night-time (bottom).

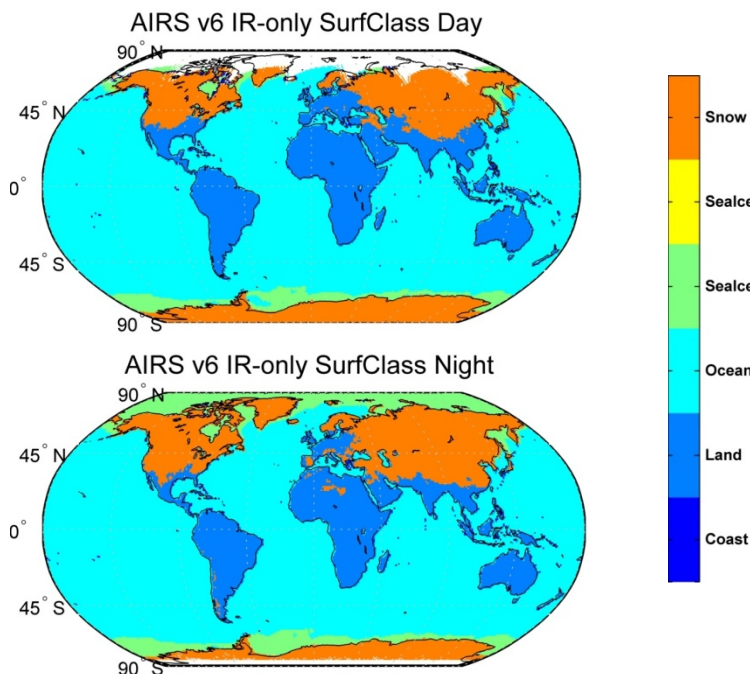


Figure 41. Same as Figure 40 except results are for the AIRS IR-only retrieval.

Version 6 Performance and Test Report

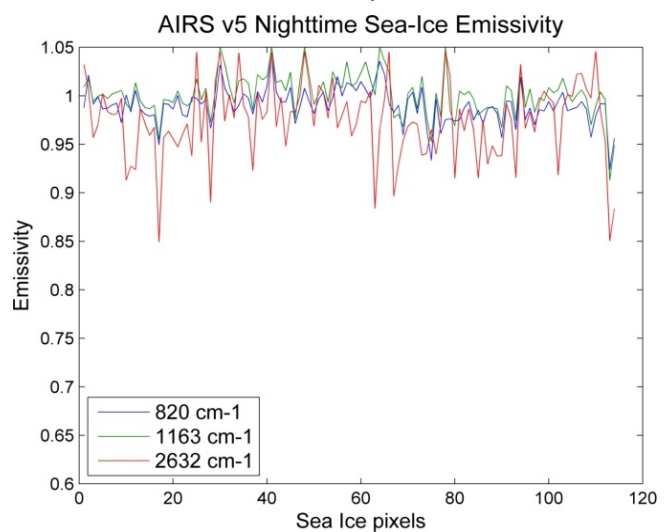
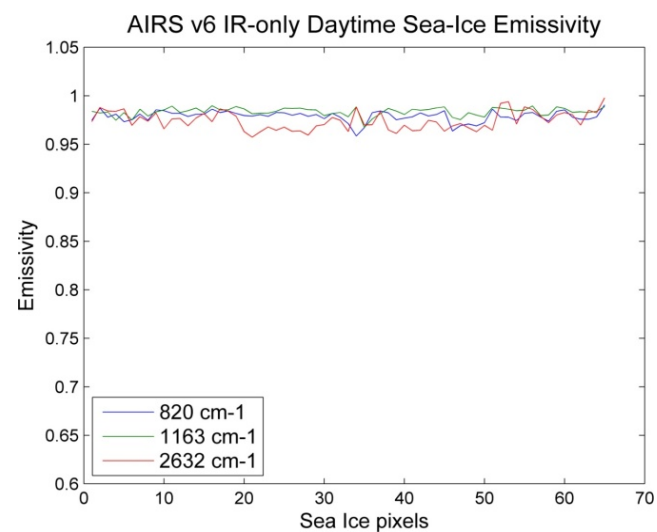
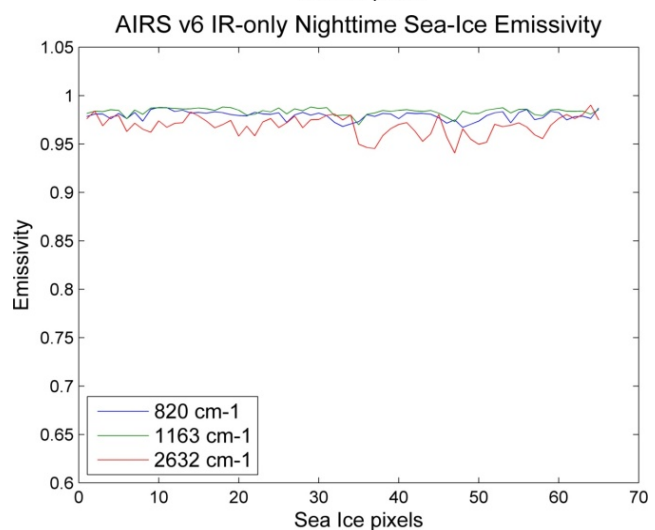
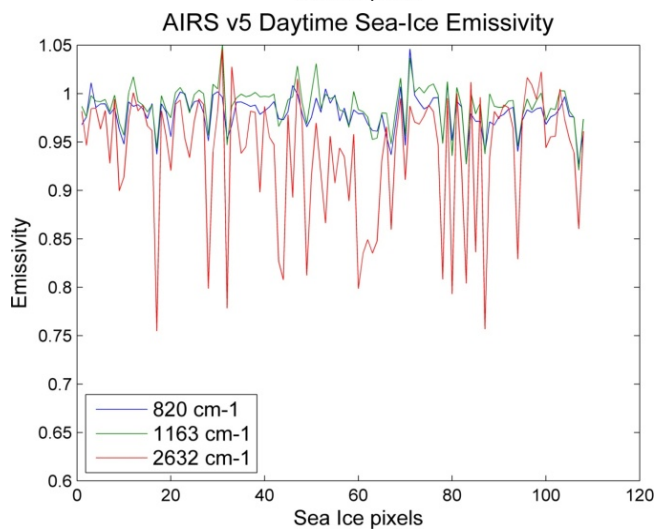
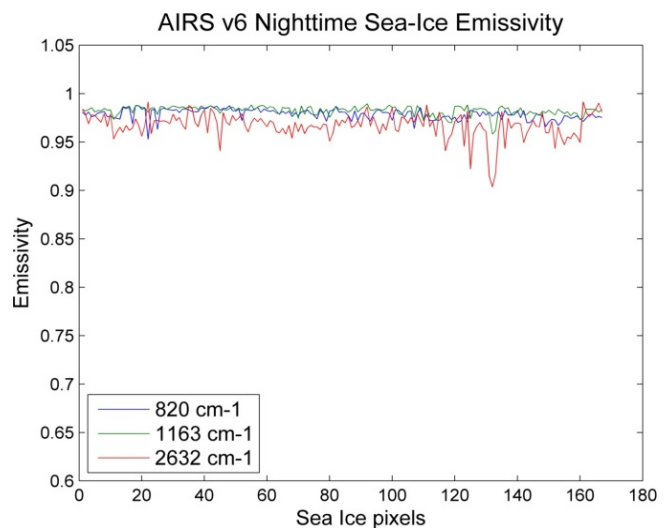
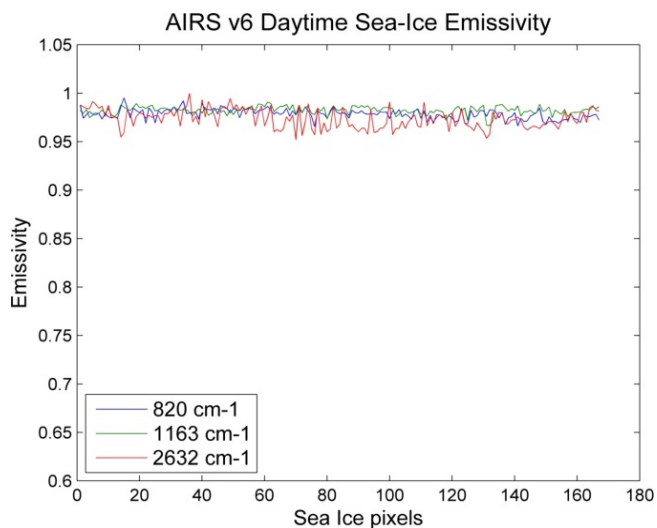
		TSurfStd (K)			
		Max	Min	Mean	SDev
AIRS/AMSU V6	Day	276.8	241.5	256.8	8.4
	Night	273.9	241.1	255.4	7.8
AIRS/AMSU V5	Day	279.3	237.8	258.3	9.4
	Night	271.7	230.4	253.8	8.5
AIRS IR V6	Day	272.9	240.6	256.5	8.2
	Night	272.6	239.7	255.5	7.8

Table 2. *TSurfStd statistics over sea-ice pixels for Jan. 2007 day and night.*

Table 2 shows statistics of the surface temperature product, TSurfStd over sea-ice pixels defined by SurfClass for Jan 2007 day and night data, and for AIRS/AMSU V6 and V5 and AIRS IR-only retrievals. If the classification for sea-ice is correct we expect maximum temperatures of 273 K. For AIRS/AMSU V6 daytime, less than 5 pixels had temperature exceeding 273 K while AIRS/AMSU V5 daytime had 12 pixels >273 K. The higher temperatures for V5 could either be due to misclassification (mixed ocean/ice pixel) or shortwave emissivities that are too low (Figure 42). For the AIRS IR-only V6 retrieval, max temperatures are within normal bounds. All retrievals had mean temperatures in the 255-260 K range with standard deviations of ~8 K.

Figure 42 shows spectral emissivities for a shortwave (2632 cm⁻¹), quartz band (1163 cm⁻¹) and longwave (820 cm⁻¹) channel for all pixels classified as sea-ice in SurfClass. We expect the emissivities to be high (~0.98) and spectrally invariant for ice and in general this is what we observe for the AIRS/AMSU V6 daytime product, except for a few cases in the shortwave that are <0.96 (possible misclassification). For V5 there are several cases where the emissivities drop below 0.95 and also the shortwave is highly variable with many unphysical values <0.9 and >1. For AIRS/AMSU V6 nighttime, several misclassified pixels result in shortwave emissivities below 0.95, but the longer wavelengths are stable, and the retrievals are more stable than in V5. The AIRS V6 IR-only product emissivities are stable and invariant both day and night for all three channels, except for nighttime which is slightly higher variability.

Version 6 Performance and Test Report



Version 6 Performance and Test Report

Figure 42. AIRS/AMSU V6 (top rows), V5 (middle rows), and AIRS V6 IR-only (bottom rows) surface emissivity for three channels (820, 1163, 2632 cm⁻¹) for sea-pixels classified by SurfClass during July 2007 for day and night-time data.

Version 6 Performance and Test Report

3.6 Ocean Surface Temperature and Emissivity

Tester and Point of contact: Joel Susskind

Surface Skin Temperature, T_s , and Surface Spectral Emissivity, ϵ_v

The most significant difference in the retrieval methodology used in Version-6 and in Version-5 is the approach used to determine T_s and ϵ_v . Version-5 simultaneously retrieves T_s , longwave surface emissivity ϵ_{vlw} , and shortwave surface emissivity ϵ_{vsw} using cloud cleared radiances for an ensemble of longwave and shortwave window channels. Following theoretical considerations, Version-6 simultaneously retrieves T_s and ϵ_{vsw} using for an ensemble of channels found only in the shortwave window regions. According to cloud clearing theory, the Version-6 approach allows for the determination of accurate values of T_s under

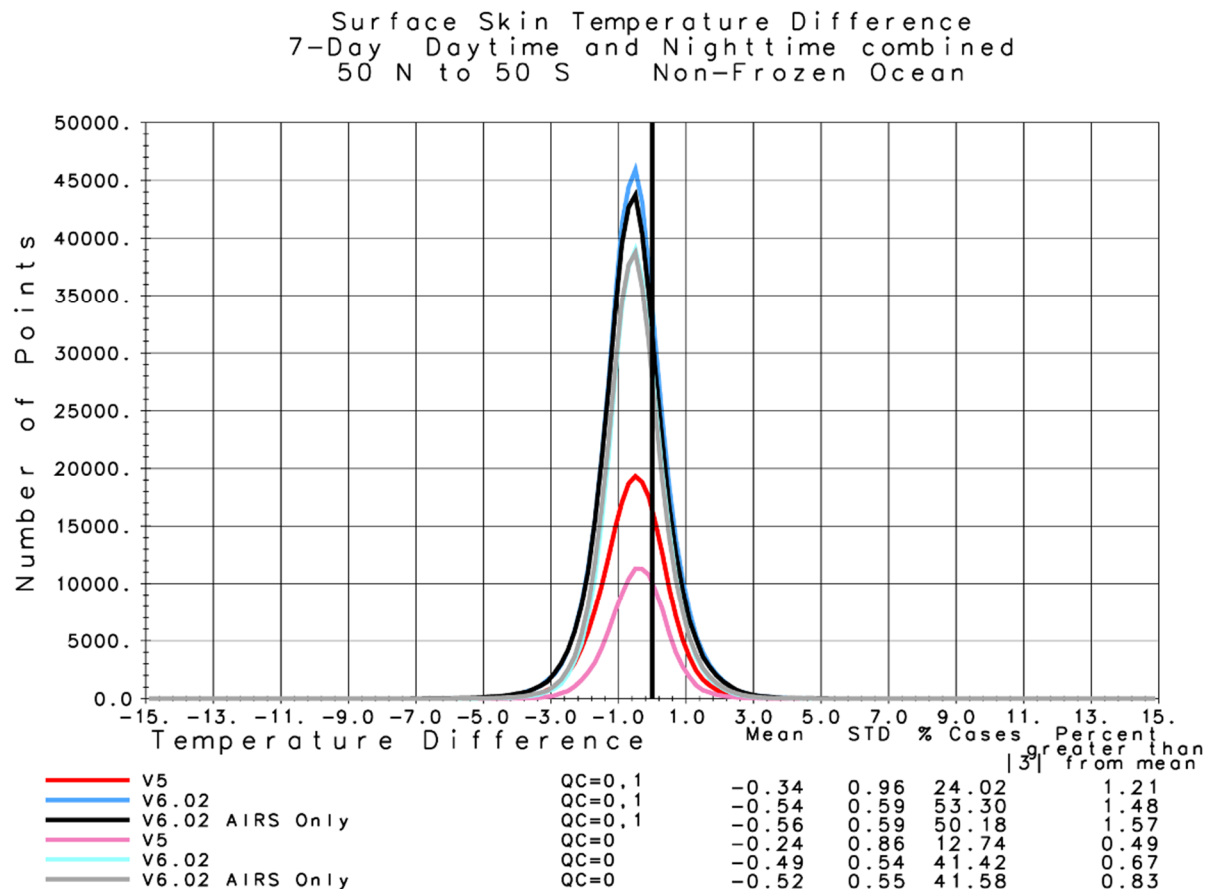


Figure 43 Surface skin temperature difference for seven days with combined night and day time data for 50S to 50N over non-frozen ocean.

Version 6 Performance and Test Report

more stressing cloud conditions than does the Version-5 approach. Longwave surface spectral emissivity is solved for in Version-6 in a subsequent step, using \hat{R}_l in channels found only in the longwave window region, as well as values of T_s , $T(p)$, and $q(p)$ determined in previous steps. Figure 43 shows counts of all Quality Controlled Ocean Surface Skin Temperatures over the latitude range, $50^{\circ}\text{N} - 50^{\circ}\text{S}$, as a function of the difference between T_s and ECMWF “truth” for the 7-day evaluation period. Counts of Version-5 retrievals are shown in red and pink, Version-6.02 retrievals are shown in dark blue and light blue, and Version-6.02 AO retrievals are shown in black and gray. The lighter shade of each color shows counts of best quality T_s retrievals with QC=0 and the darker shade shows counts of both best and good quality T_s retrievals including cases with QC=0 or 1. Ocean T_s retrievals with QC=0 or 1 are the ensemble used to generate the Level-3 Oceanic SST product. Figure 1 also contains statistics for each set of retrievals showing the mean difference from ECMWF, the standard deviation of the ensemble differences, the percentage of all possible cases included in the Quality Controlled ensemble, and percentage of all accepted cases with absolute differences from ECMWF of more than 3K from the mean difference. Such cases are referred to as outliers.

Version-6.02 QC'd retrievals accept considerably more cases than Version-5 and have much lower standard deviations of the errors as well. In both ensembles, the percentage of outliers grows with loosening the QC thresholds as expected. Version-6.02 outliers with QC=0,1 are somewhat larger than Version-5, but the yield is more than twice as large. It is noteworthy that Version-6.02 retrievals with QC=0 have a much smaller percent outliers than does Version-5 retrievals with QC=0,1 along with a substantially higher yield. One point of slight concern in this figure is that the cold mean bias in Version-6.02 retrievals compared to ECMWF is somewhat larger than that of Version-5. Statistics of QC'd Version-6.02 AO retrievals are very similar to those of Version-6.02.

Figure 44 shows the spatial distribution of the seven daily differences of the Level-3 SST products from collocated ECMWF values for both Version-6.02 and Version-5. The values shown in a given grid box are the average values for that grid box of all accepted cases where the SST retrieval was accepted either at 1:30 AM or 1:30 PM. A grid point for which not a single value of QC'd SST was obtained for all 14 possible cases (seven days, twice daily) is shown in gray. Figure 2 represents the spatial coverage and accuracy of “pseudo seven day mean” Level-3 products. The seven days included in the figure are not consecutive, but the figure is very informative nonetheless.

Version 6 Performance and Test Report

The caption under each field indicates the mean difference of the Level-3 SST field from its own collocated ECMWF values, the spatial standard deviation over all grid points of the Level-3 differences, and the % of all possible grid points that have at least one accepted value over the seven day period (i.e., one not gray). The Version-6.02 Level-3 SST product has much better spatial coverage, with 98.35% of all oceanic grid points 60°N-60°S being filled, compared to Version-5 with only 92.24%. Moreover, there are large coherent spatial areas in which no Version-5 retrievals were accepted on any of the seven days. The spatial standard deviation of the Version-6.02 Level-3 SST product errors compared to ECMWF truth is also much smaller than that of Version-5, and the Version-6.02 area mean negative bias is also smaller than that of Version-5.

7-Day Surface Skin Temperature (K) Non-Frozen Ocean Retrieved minus ECMWF AM/PM Average

Version-6.02

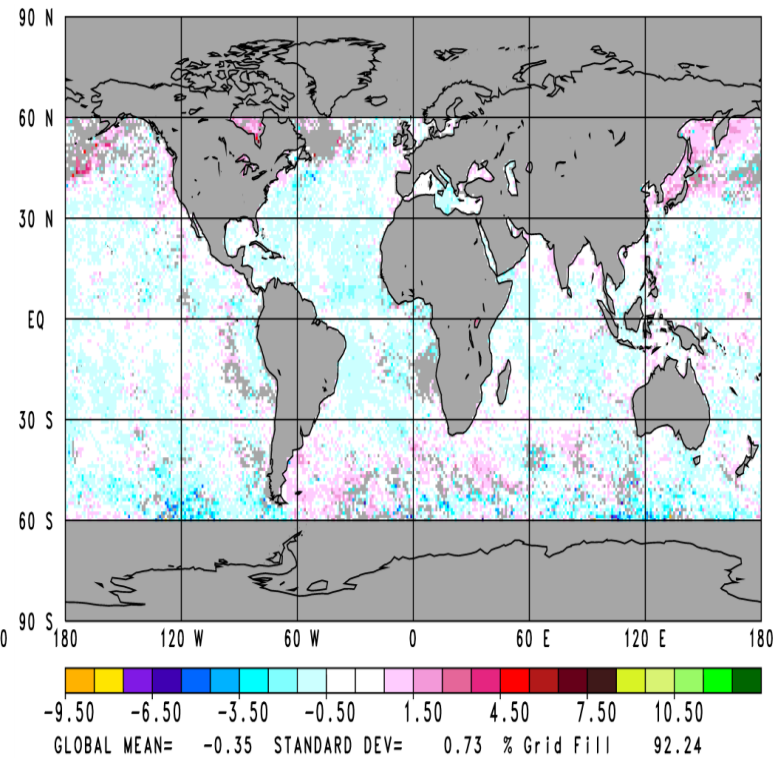
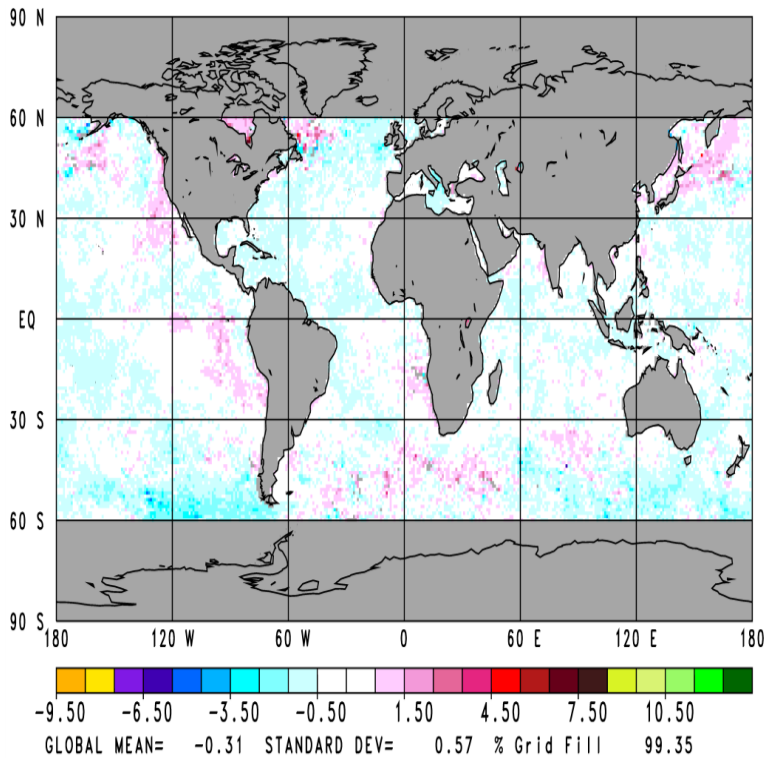


Figure 44 Difference between AIRS and ECMWF surface skin temperature for V5 and V6.

Version 6 Performance and Test Report

Figure 45 to 48 show statistics related to retrieved ocean surface spectral emissivity ε_v as a function of satellite zenith angle for $v = 950 \text{ cm}^{-1}$ and $v = 2400 \text{ cm}^{-1}$. The channels are in the longwave and shortwave window regions respectively. In these figures, statistics are shown separately for AM orbits in dark colors, and PM orbits in light colors. Figure 45 and Figure 46 show the mean differences of retrieved values of ε_v from those values calculated using the Masuda ocean spectral emissivity model, which is taken as truth. In both the longwave and shortwave window regions, Version-6.02 (as well as Version-6.02 AO) retrieved ocean spectral emissivities as a function of satellite zenith angle are very close to the values expected using the Masuda emissivity model. Differences of Version-5 retrieved ε_v from ECMWF truth are much larger than those of Version-6 AO. Version-5 values of ε_v also show a large spurious feature during the day in the vicinity of a satellite zenith angle of -18.24 degrees, which is the viewing angle in which sunglint appears in the field of view. Figure 47 and Figure 48 show the standard deviations of the retrieved values of ε_v from their mean values for the same two frequencies. These standard deviations are much smaller in Version-6.02 as compared to Version-5 indicating that the retrieved values are not only more accurate in Version-6.02 but considerably more stable as well. There is no appreciable difference between Version-6.02 and Version-6.02 AO in results related to ocean values of ε_v .

Surface spectral emissivity over land is not well known nor is it easily modeled. Nevertheless, land surface emissivity is not expected to change significantly from night to day. Therefore, it is useful to examine the characteristics of land surface emissivity determined at night minus those determined during the day. Figure 49 shows the 7-day mean value of the nighttime minus daytime retrieved Quality Controlled surface emissivity over land as a function of satellite zenith angle for 950 cm^{-1} and 2400 cm^{-1} . The (spurious) diurnal signal in Version-6.02 land surface emissivity is much smaller at both frequencies than found in Version-5. This is an indication that Version-6.02 land surface emissivities should be of higher quality than those of Version-6. Figure 50 shows the spatial distribution of the nighttime minus daytime seven-day mean land surface emissivities of 950 cm^{-1} and 2400 cm^{-1} for both Version-6.02 and Version-5. Some spurious day/night differences in land surface emissivity still exist in Version-6.02, particularly over the Sahara desert and Saudi Arabia at 2400 cm^{-1} , but these diurnal differences are much smaller than those found in Version-5.

Version 6 Performance and Test Report

Mean 950 cm^{-1} Emissivity minus Masuda
50 North to 50 South Ocean
7-Day

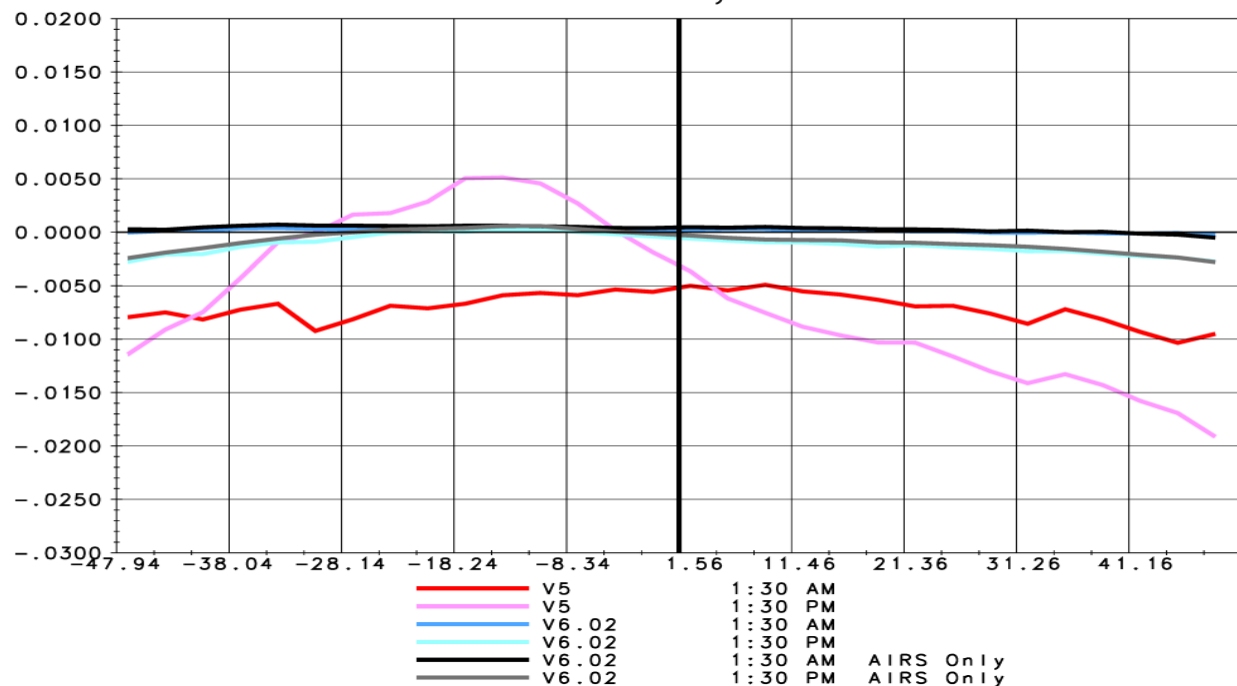


Figure 45 Mean difference between AIRS and Masuda emissivity for 950 cm^{-1} .

Version 6 Performance and Test Report

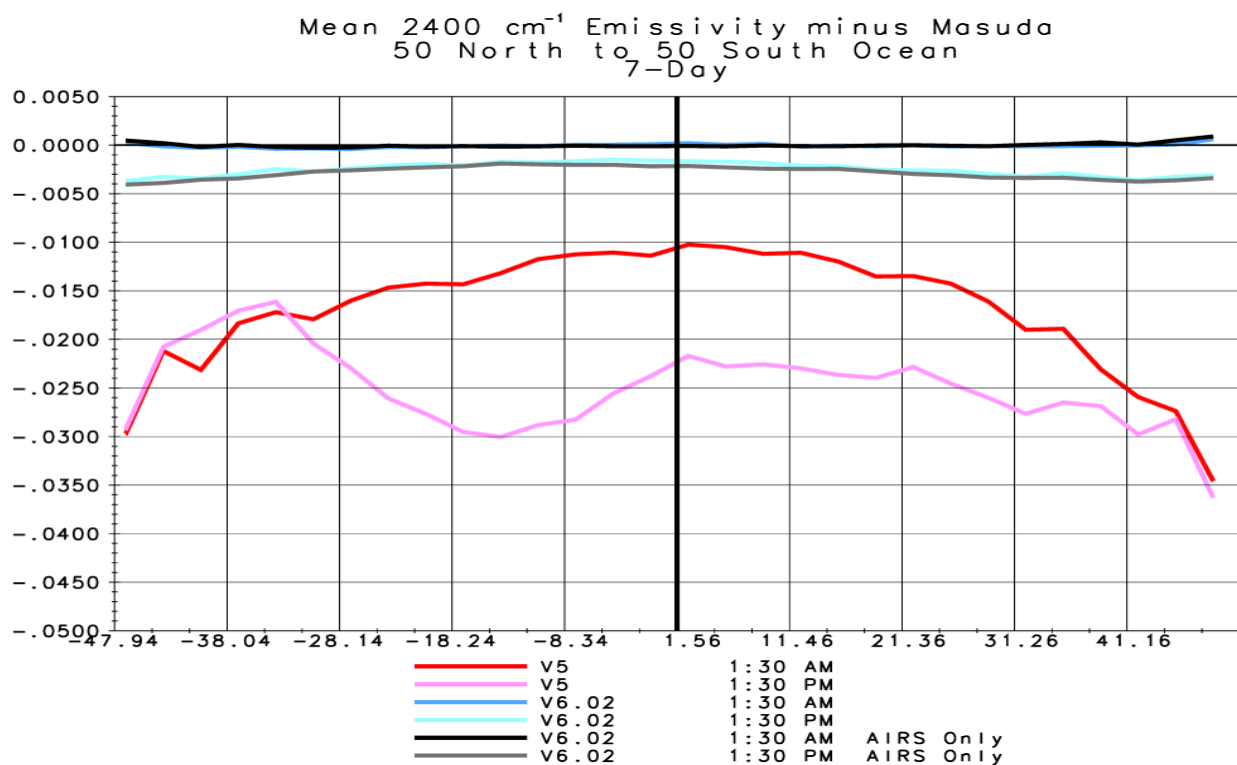


Figure 46 Mean difference between AIRS and Masuda emissivity for 2400 cm^{-1} .

Version 6 Performance and Test Report

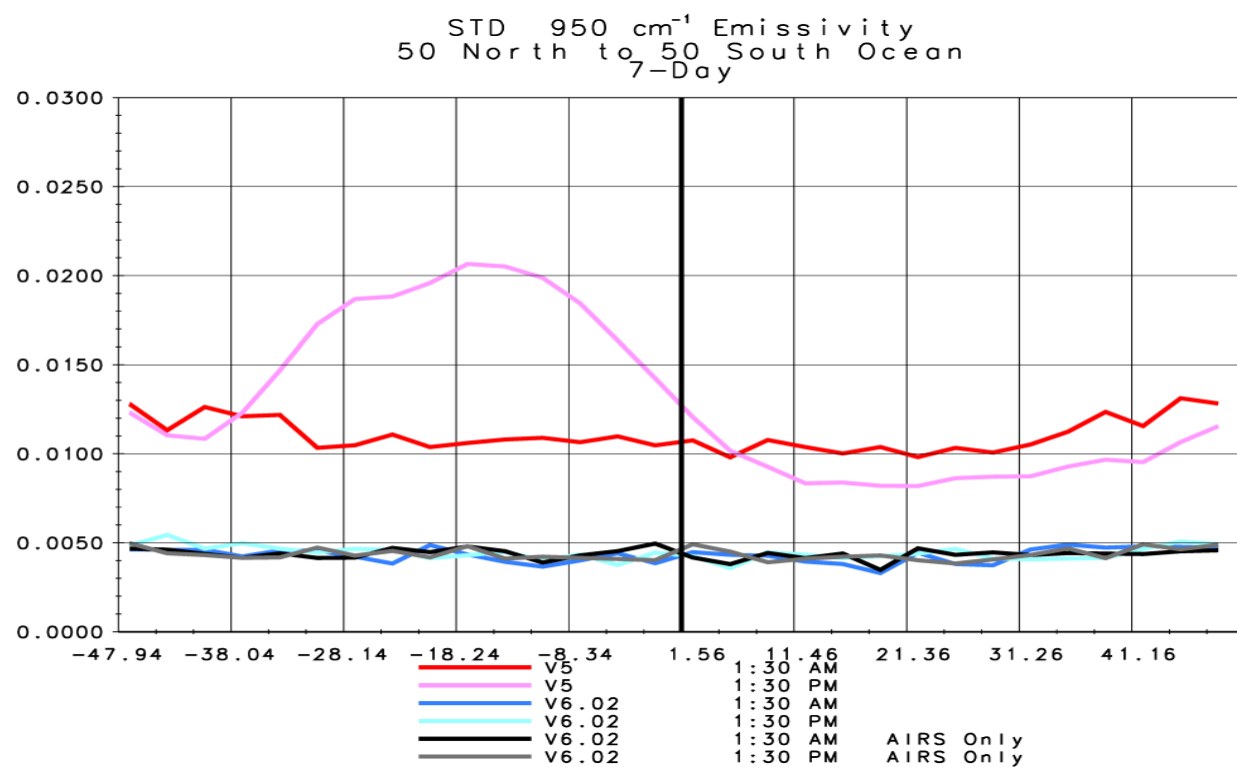


Figure 47 Standard deviation of Emissivity at 950 cm^{-1} .

Version 6 Performance and Test Report

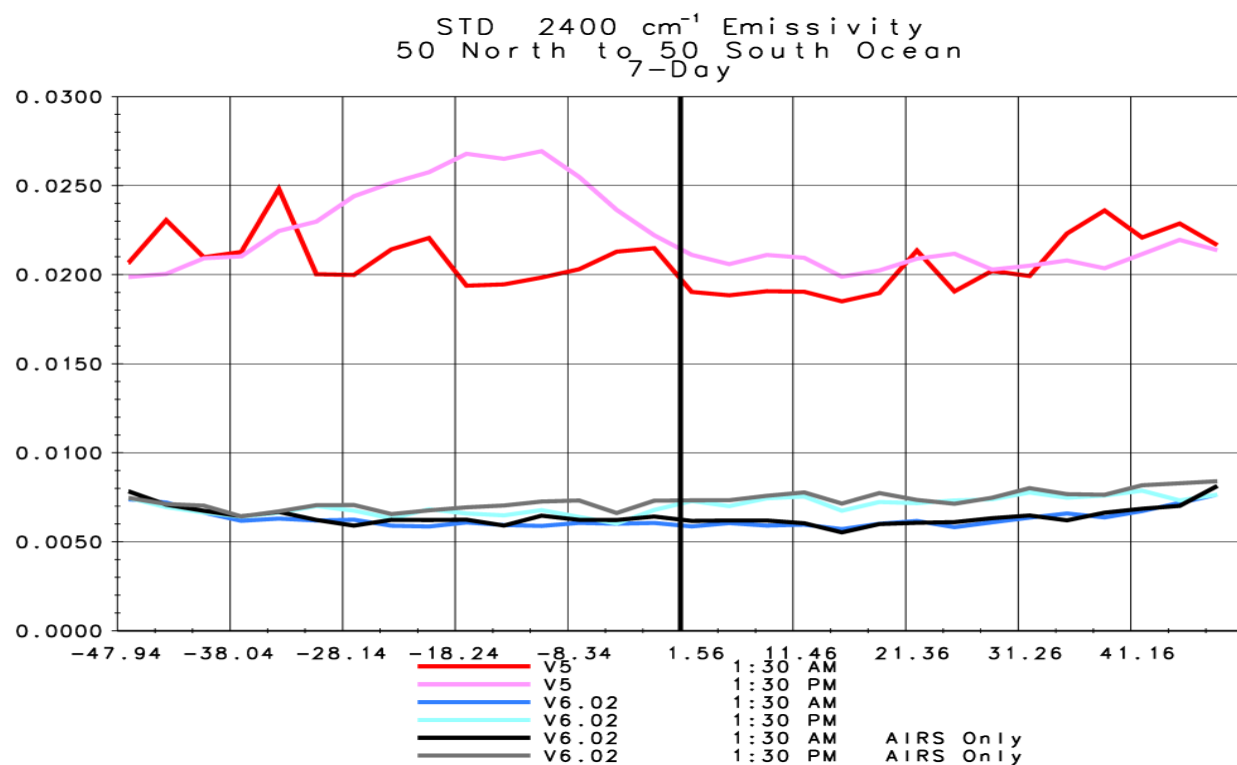


Figure 48 Standard deviation of Emissivity at 2400 cm^{-1} .

Version 6 Performance and Test Report

Mean AM minus PM Emissivity 7-Day Average 50° North to 50° South Land

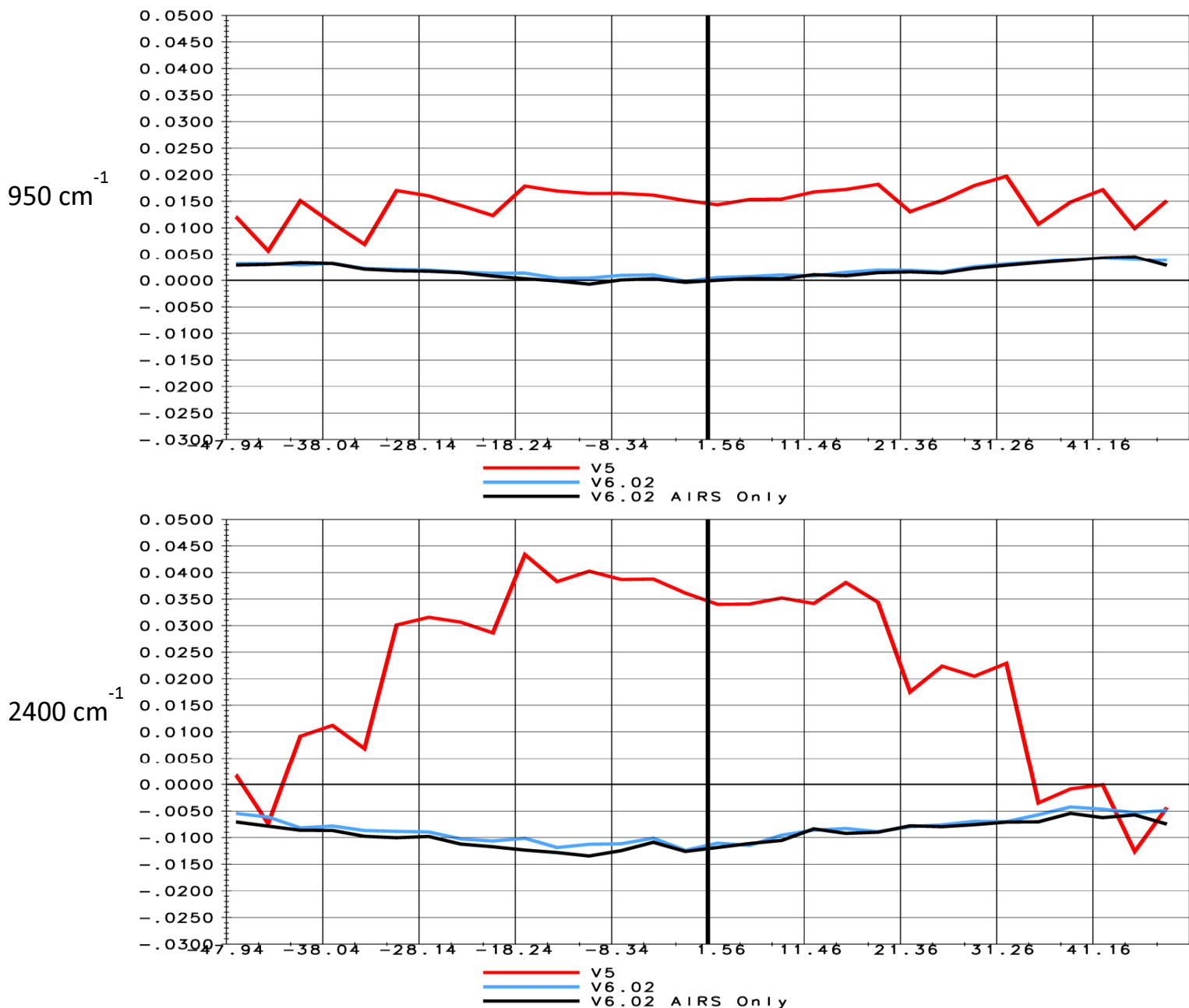


Figure 49 Mean difference between daytime and nighttime emissivities for 950 cm^{-1} and 2400 cm^{-1} .

Version 6 Performance and Test Report

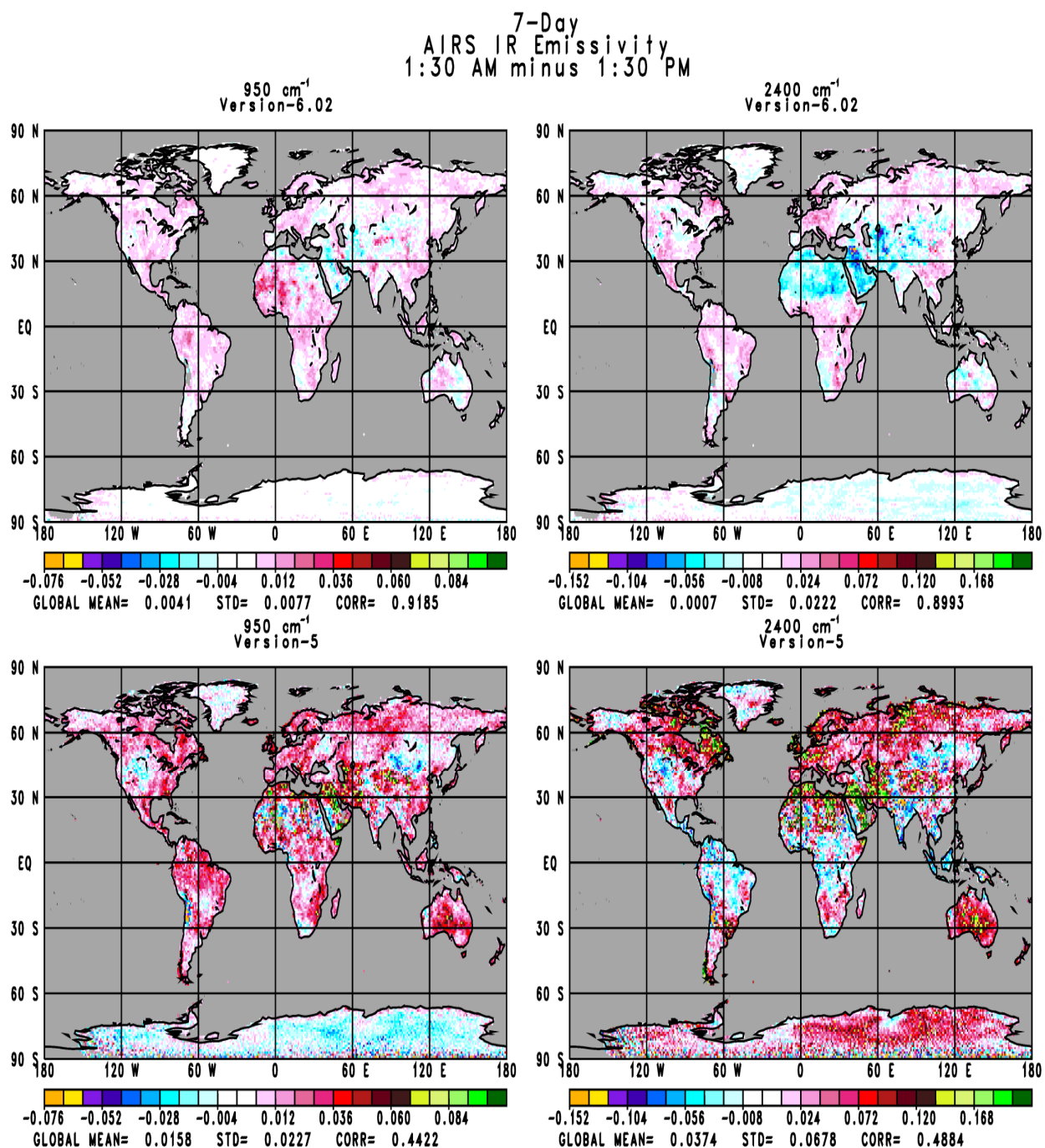


Figure 50 Mean difference in Emissivity between night and day for different AIRS versions.

Version 6 Performance and Test Report

3.7. Microwave Surface Products

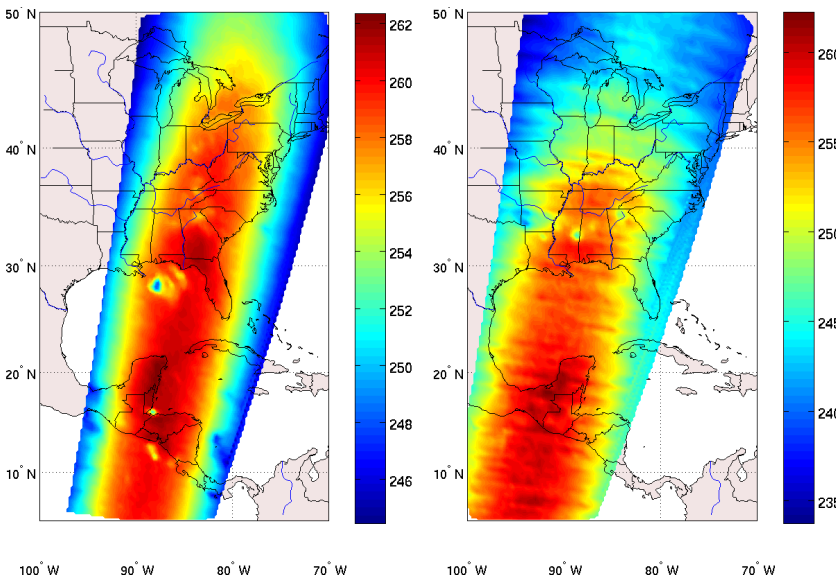
Tester and Point of Contact: Bjorn Lambrightsen

We have done limited testing of MW products to make an assessment of derived surface emissivity as a proxy for all MW-only L2 products. The bottom line is

- The radiometric sensitivity of AMSU-A channel 5 has steadily declined
- This has resulted in noise entering MW-only products
- As a result, MW-only L2 products have also steadily declined
- A decision was made to exclude ch. 5 from V6 processing
- This has resulted in improved performance of MW-only products

Even with the improved performance, users should exercise caution when using MW-only products, since the absence of ch. 5, in addition to ch. 4 (which was excluded from processing some time ago) and ch. 7 (which has been excluded since launch) has resulted in a decline in information content with unknown consequences.

Figure 51 shows ch. 5 brightness temperature for a sample granule in 2002 (left) and 2011 (right). The 2011 image exhibits striping, which is the result of applying noisy calibration coefficients computed per scanline. Such striping will always be present, but the noise amplitude is normally very low and not noticeable, as shown in the 2002 case.



Version 6 Performance and Test Report

Figure 51. AMSU-A channel 5 brightness temperature: 9/14/2002 (left); 4/21/2011 (right)

Figure 52 shows retrieved surface emissivity at 50.3 GHz for the 2011 sample granule processed with V5, which uses ch. 5, and with V6, which does not use ch. 5. It can be seen that the ch. 5 striping noise carries through to the V5 product but is absent from V6 because ch. 5 is no longer used.

Figure 53 also shows retrieved surface emissivity at 50.3 GHz but for the 2002 granule. No striping is apparent in either V5 or V6 because ch. 5 was performing nominally in 2002.

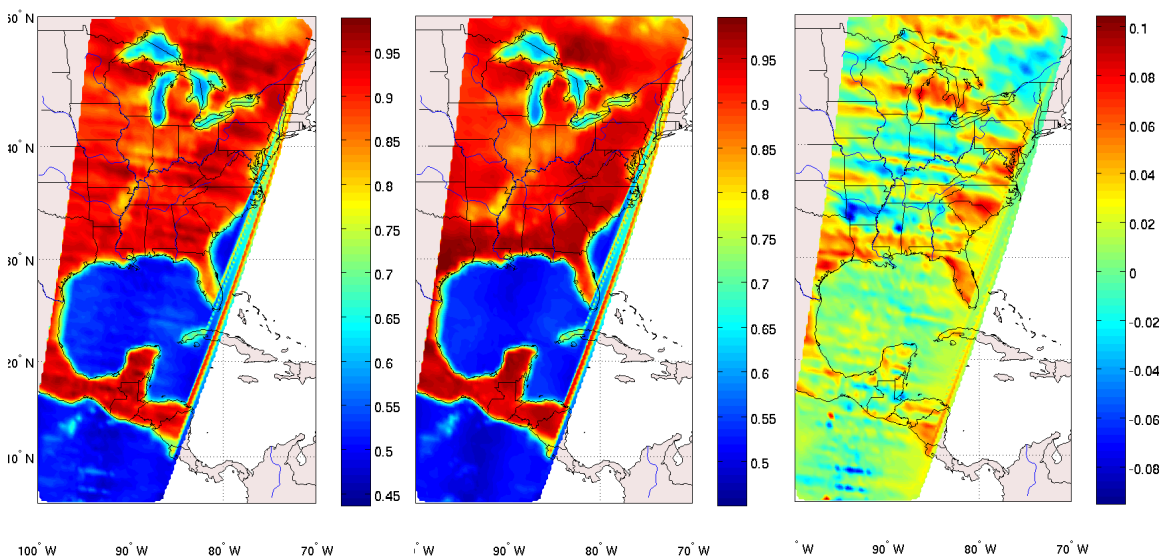


Figure 52. Retrieved surface emissivity at 50.3 GHz, 4/21/2011: V5 (left); V6 (center); V6-V5 (right)

Version 6 Performance and Test Report

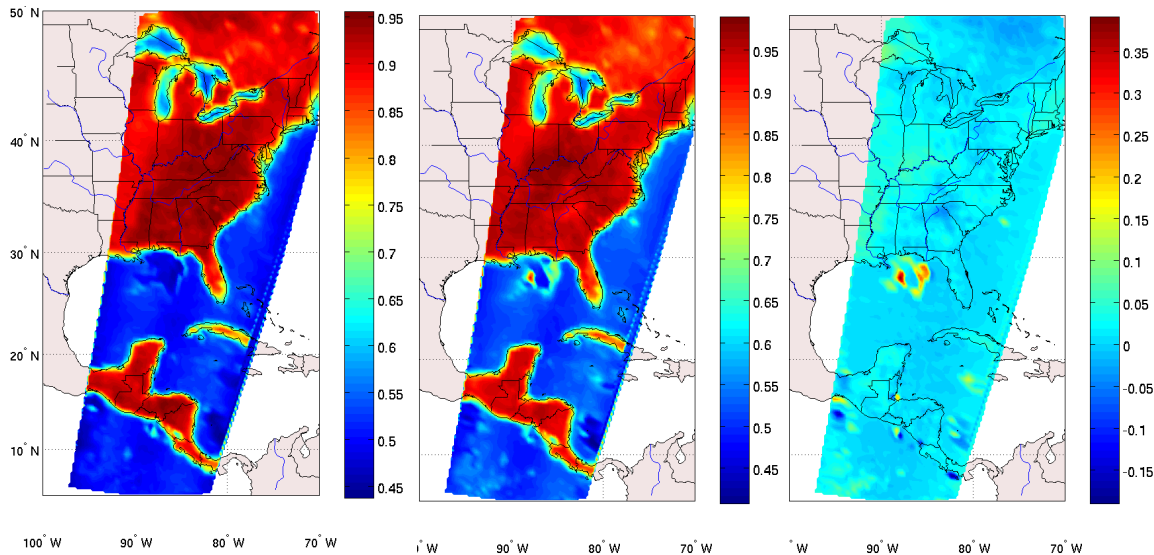


Figure 53. Retrieved surface emissivity at 50.3 GHz, 9/14/2002: V5 (left); V6 (center); V6-V5 (right)

The results shown previously for 50.3 GHz are representative of emissivity at other frequencies. Users can expect similar effects for other retrieved MW L2 products as well and are advised to exercise caution. V5 products from 2010 and later may be suspect. In addition, although V6 does not exhibit the prominent noise striping, V6 MW L2 processing excludes the use of 3 AMSU-A channels (4, 5 and 7) and all HSB channels and MW L2 products can therefore be expected to suffer from reduced information content.

Version 6 Performance and Test Report

3.8. Cloud Top Properties

Tester: H. Van Dang

Data Product	Data Description
CldFrcTot	Total cloud fraction coverage for 15km footprint
CldFrcTot_QC	Quality control of CldFrcTot
CldFrcStd	Maximum two layer cloud fraction coverage for 15km footprint
CldFrcStd_QC	Quality control of CldFrcStd
CldFrcStdErr	Error estimate of CldFrcStd
PCldTop	Pressure of maximum of two layers of clouds within 15km footprint
PCldTop_QC	Quality control of PCldTop
PCldTopErr	Error estimate of PCldTop
TCldTop	Temperature of maximum of two layers of clouds within 15km footprint
TCldTop_QC	Quality control of TCldTop
TCldTopErr	Error estimate of TCldTop

AIRS cloud top properties include cloud top temperature (CTT), cloud top pressure (CTP), and effective cloud fraction (ECF), along with the quality indicators and error estimates associated with each of the three above mentioned data products. AIRS V6 (V6.0.2) cloud products have changed significantly from V5. The V6 cloud top temperature (CTT) and pressure (CTP) are now reported in the 3x3 AIRS field of view (FOV) of about 15km wide rather than the 50 km AMSU FOV of AIRS V5. V6 top layer cloud position does differ dramatically from V5 as shown in the following figures.

Version 6 Performance and Test Report

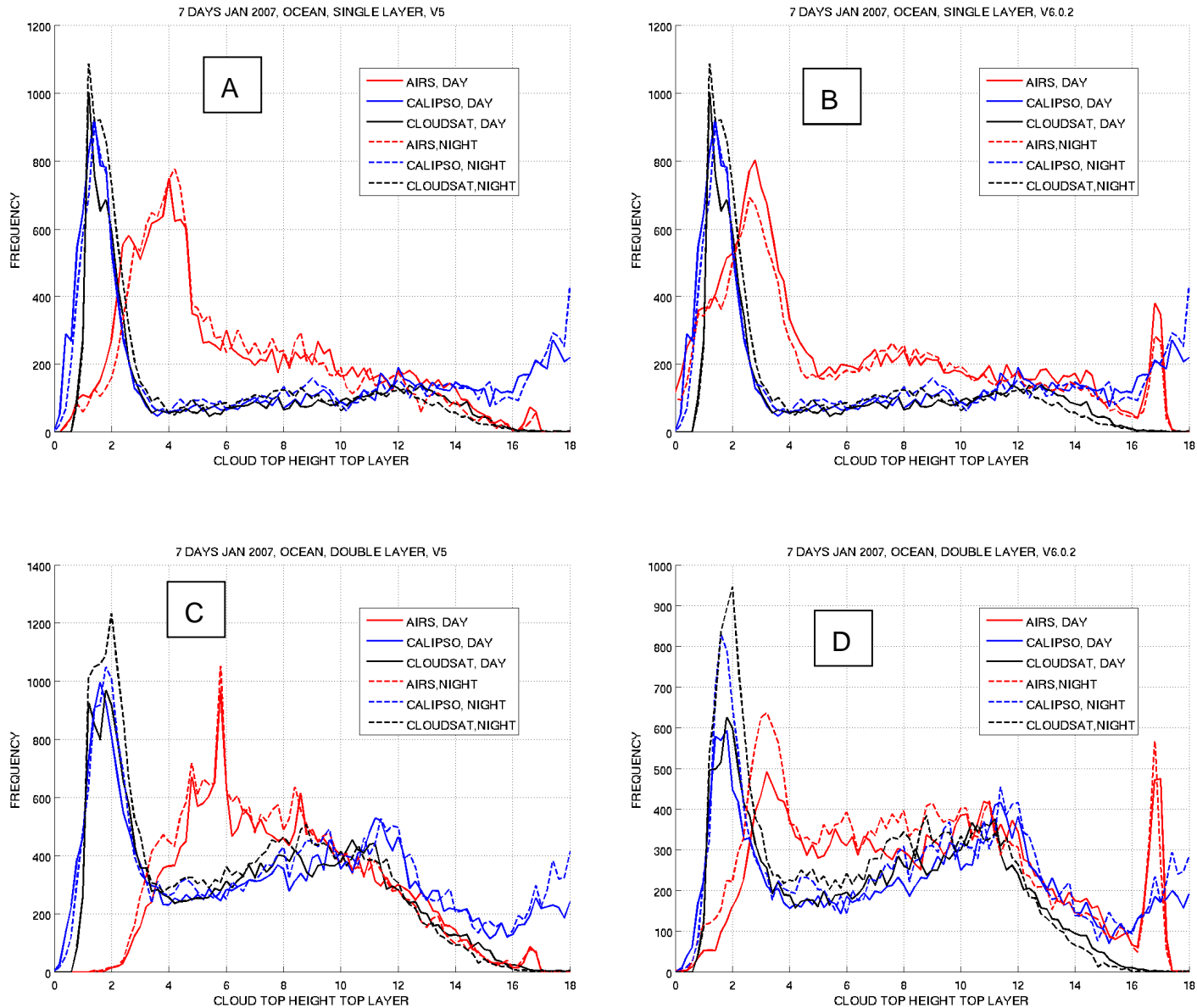
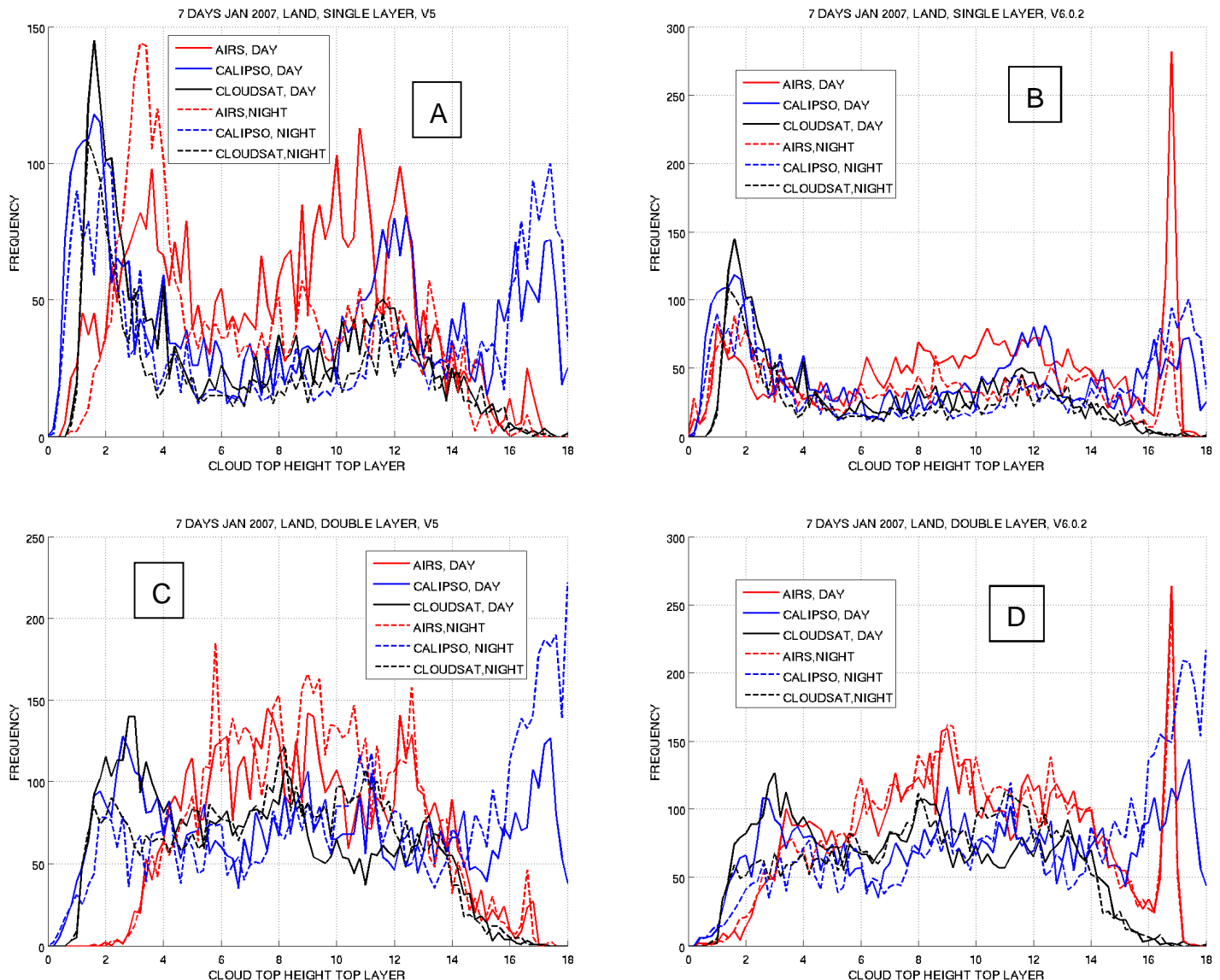


Figure 54. Distributions of Cloud Top Height over ocean for day/night from AIRS, CALIPSO, and CloudSat for V5 and V6 single and double cloud layer as determined by AIRS.

Figure 54 A-D all depict 7 days in January 2007 over ocean of AIRS, averaged CALIPSO (5km Version 3.1), and averaged CloudSat (2B-CLDCLASS version R04) top layer cloud top height (CTH) histograms. CALIPSO and CloudSat have

Version 6 Performance and Test Report

all been collocated and averaged to AIRS 15km FOV and all separated into either day or night scenes and when AIRS reports either a single or a double cloud layer. Figure 54 A and C show the histograms of AIRS V5 CTH that originally is in AMSU FOV of 50 km, but has been replicated 3x3 times to emulate V6's 15 km resolution. The top rows of images are of cases where V5/V6 reports a single layer and the bottom row of images are the double cloud layer cases. Figure 54 B and D show the histogram of AIRS V6 FOV of 15km top layer CTH. One can easily see that the distribution of V6 reported top layer CTH has moved significantly closer to the distribution of Cloudsat and CALIPSO top most layer of CTH for both single and double cloud layer and over day and night.



Version 6 Performance and Test Report

Figure 55. Distribution of Cloud Top Height over Land for AIRS, CALIPSO, and CloudSat during day/night scenes of either single or double cloud layer as determined by AIRS V5/V6.

In Figure 55 B and C over land, V6 has an improved middle and low level Cloud Top Height (CTH) distribution as compared to V5 (Figure 56 A and C), but there is a spike in distribution in high clouds around 17km for V6.

In Figure 56 A for single layered clouds as determined by AIRS V6, the x-axis is the averaged difference between AIRS minus CALIPSO top layer CTH per 10 degree latitude band. For latitude >20 and latitude <-20 degrees, regardless of ocean/land or day/night, V6 is slightly lower than CALIPSO in CTH, but in V5, AIRS CTH is higher than CALIPSO. For latitude bands between +/- 20 degrees over land at night, both V5 and V6 need improvement as they differ from CALIPSO significantly. In that instance, AIRS is too low in comparison to CALIPSO CTH.

In Figure 56 B for double layered clouds as determined by AIRS V6, the x-axis is the averaged difference between AIRS and CALIPSO top layer CTH per 10 degree latitude band. For all latitude bands, AIRS V6 over ocean during day and night compares the best to CALIPSO when scrutinized with V5 for the same conditions.

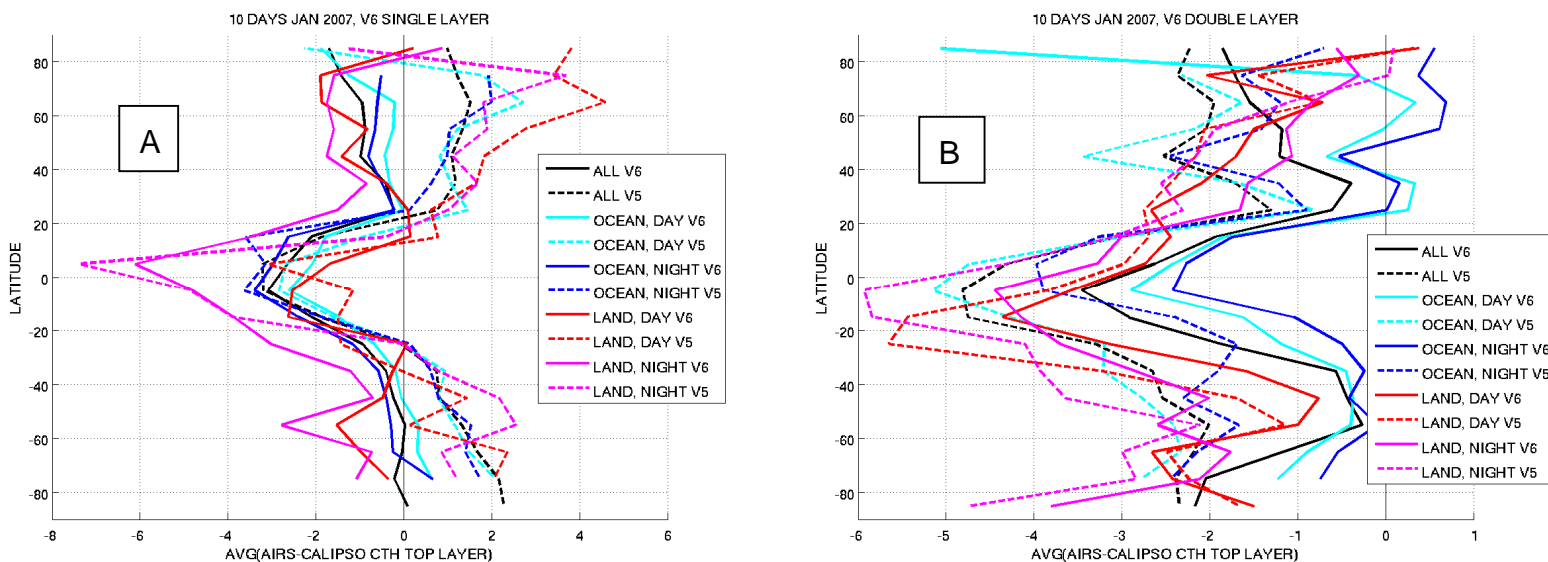


Figure 56. Average AIRS deviation from CALIPSO CTH per 10 degree latitude band for V5/V6 LAND/OCEAN and DAY/NIGHT scenes.

Version 6 Performance and Test Report

Figure 57 A is the histogram of V5 CTT and Figure 57 B is the histogram of V6 CTT. Figure 57 C is the distribution of V5 CTP and Figure 57 D is V6 CTP. The red and blue lines are the top layer and bottom layer respectively. The green line is the weighted layer of either the CTT (WCTT), or the CTP (WCTP).

$$WCTP = f_1 * P_1 + f_2 * P_2; \quad WCTT = f_1 * T_1 + f_2 * T_2,$$

where $f_{1/2}$ is the effective cloud coverage of the top/bottom layer and $P_{1/2}$ is the cloud top pressure of the top/bottom layer. $T_{1/2}$ is the cloud top temperature of the top/bottom layer. In the following figures, one can see that cloud top pressure in V6 does not have the frequency spikes that V5 has. There is also the addition of high clouds around 100 mb (~150k) and low clouds around 1000 mb (~210k) in V6 that V5 did not have that much of.

Version 6 Performance and Test Report

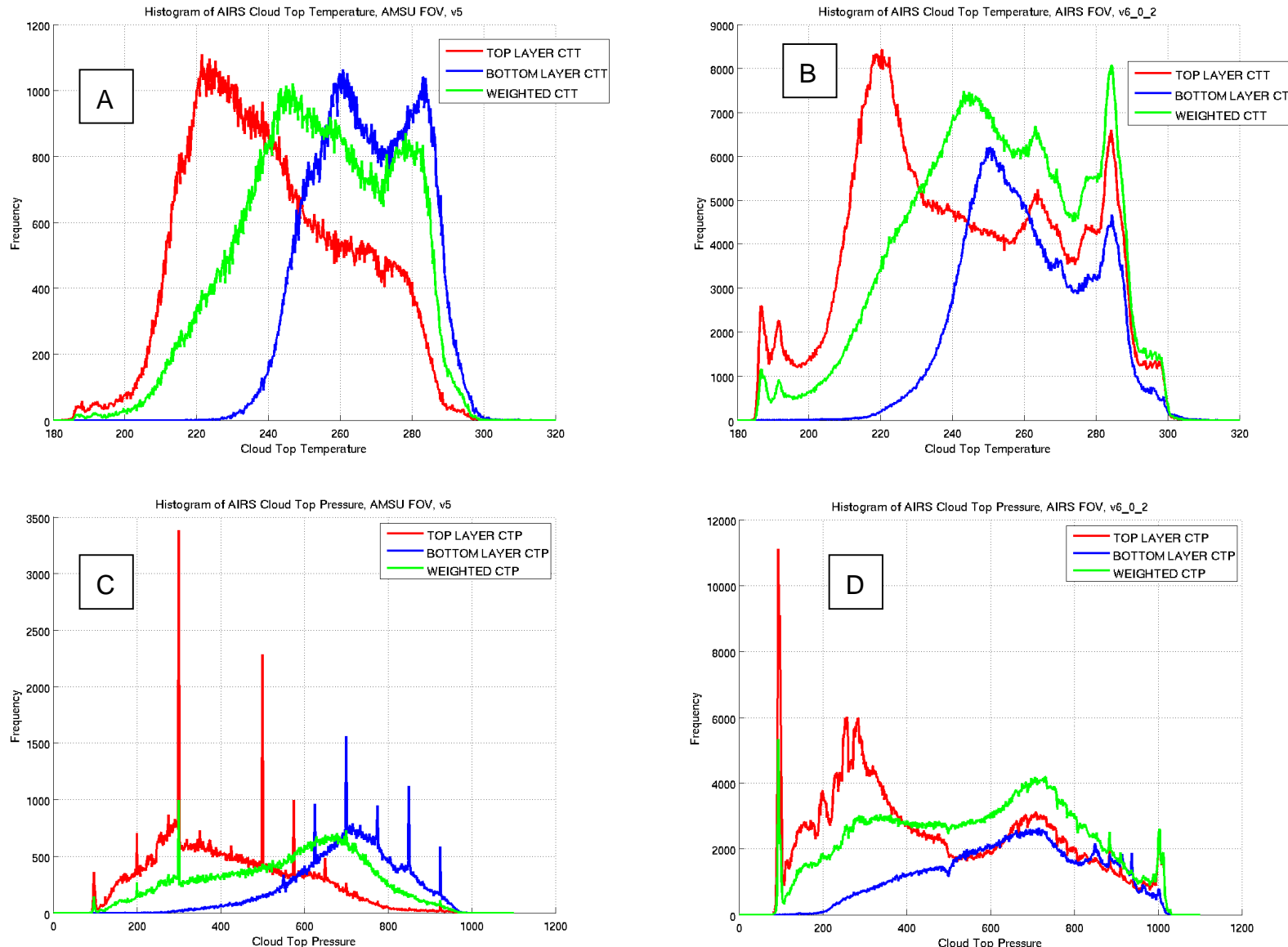


Figure 57. Distribution of V5 and V6 Cloud Top Temperature and Cloud Top Pressure of the top and bottom layer along with the values weighted by the Effective Cloud Fraction.

Version 6 Performance and Test Report

In Figure 58 A and B, the x-axis is V6 minus V5 top layer CTP, and the y-axis is the average result of V6 minus V5 top layer ECF. One can see how the top layer effective cloud fraction (ECF) changes from V5 to V6 by how the top layer of the cloud top pressure changes. If the top layer cloud has decreased in height from V5 to V6, then the ECF should increase in V6 for the top cloud layer. If there is a decrease in height from V5 to V6 for the top cloud layer, then the averaged ECF should decrease in V6 from V5. The trade-off between ECF and CTP is very reasonable in order to maintain radiative consistency between measured radiance and calculated radiance.

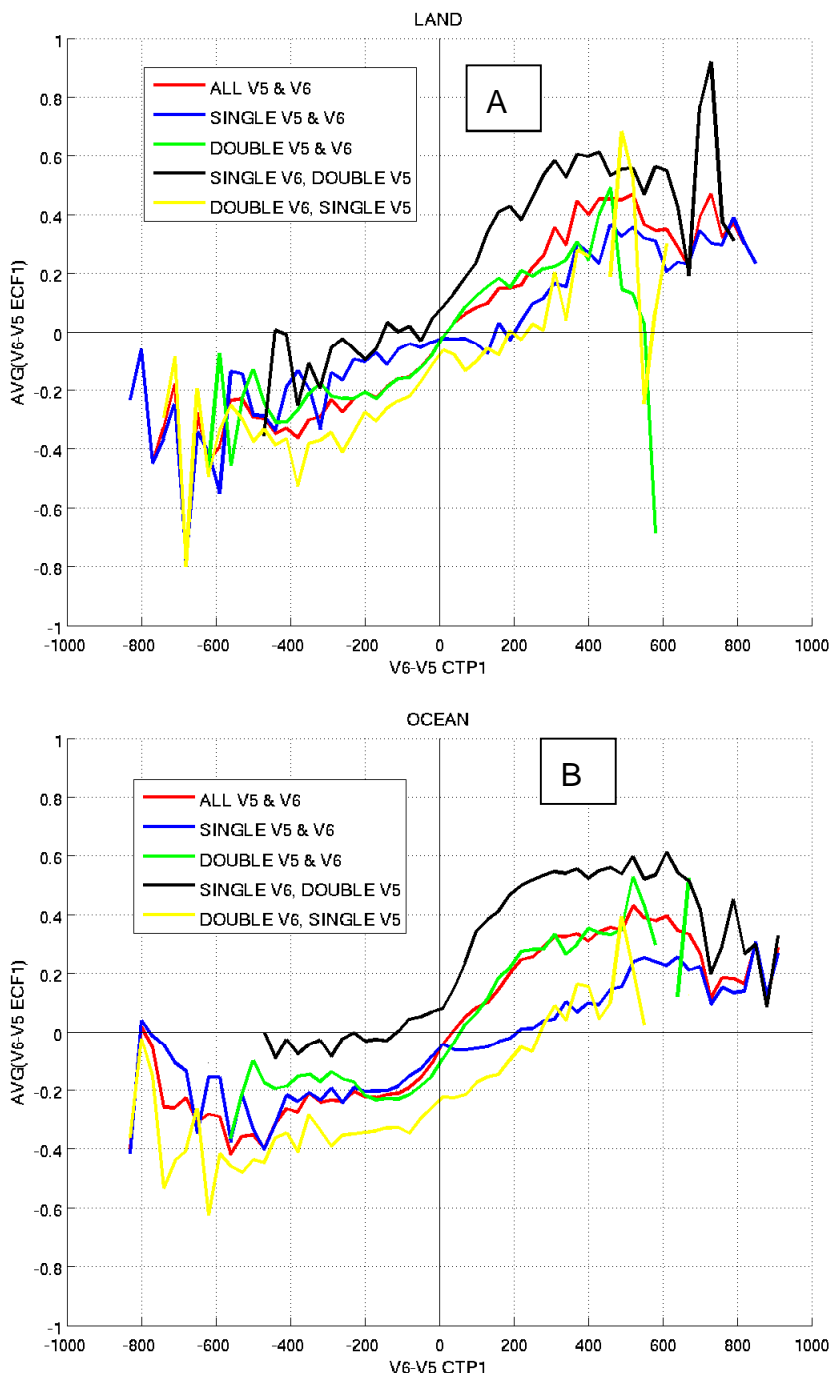


Figure 58. Showing the top layer effective cloud coverage changes from V5 to V6 given the changes in the top layer of cloud top pressure from V5 to V6.

Version 6 Performance and Test Report

In Figure 59, the CTP of the top and the bottom layer is compared between AIRS/AMSU and AIRS-ONLY retrieval. CTP is shown here rather than also including CTT, because they are very similar. In general AIRS/AMSU and AIRS-ONLY retrieval are quite similar, but there are small number of cases with drastic differences. Those cases will be investigated in the validation report.

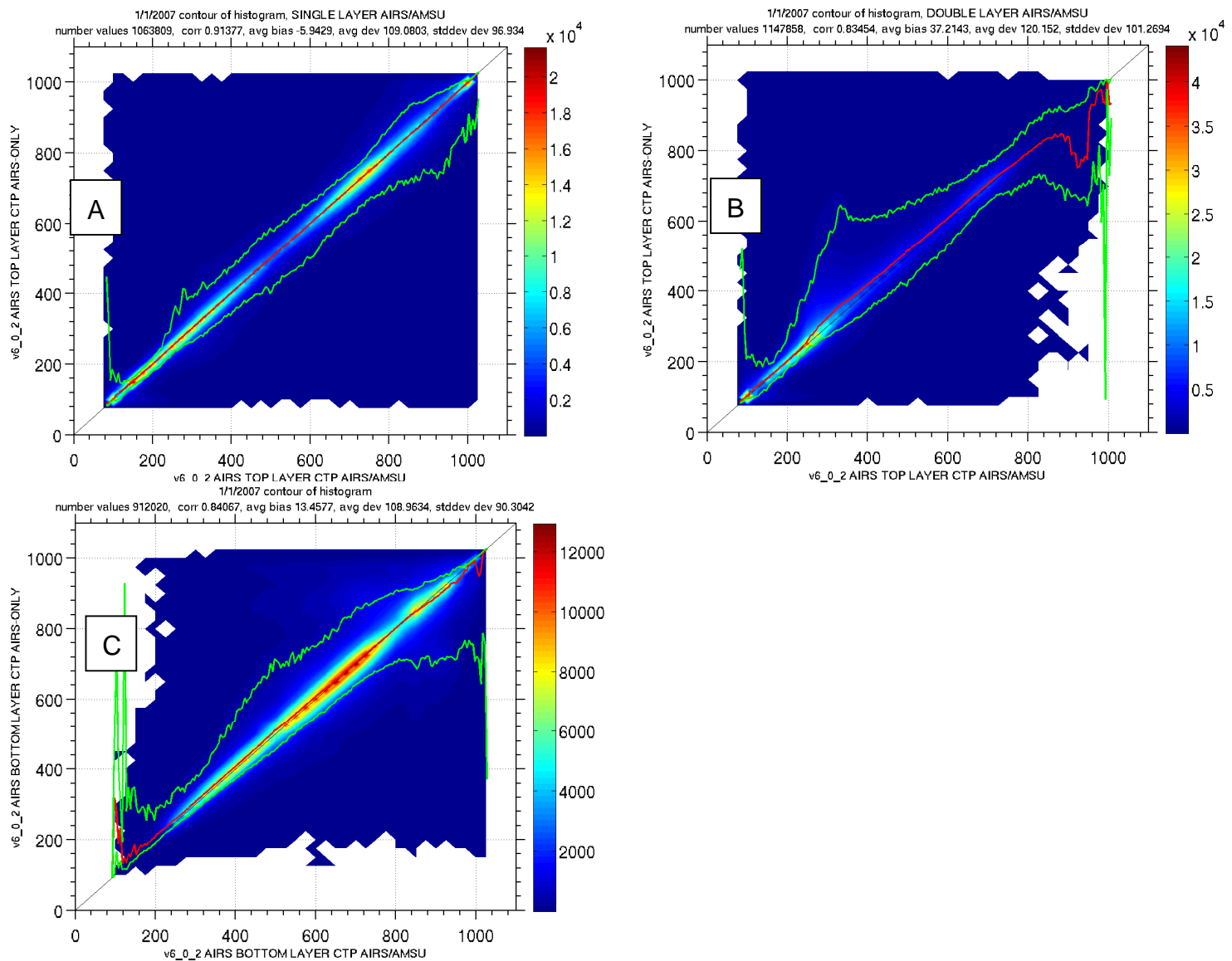


Figure 59 Comparing AIRS/AMSU and AIRS-ONLY CTP retrieval in V6.0.2. A) For single layer as determined by AIRS/AMSU, comparing top layer CTP AIRS/AMSU top layer CTP of AIRS-ONLY B) For double layer as determined by AIRS/AMSU, comparing top layer CTP AIRS/AMSU top layer CTP of AIRS-ONLY. C) Comparing the bottom layer CTP of AIRS/AMSU to AIRS-ONLY

Version 6 Performance and Test Report

In Figure 60, the distribution of CTP top layer, bottom layer, and weighted do not appear to be significantly different.

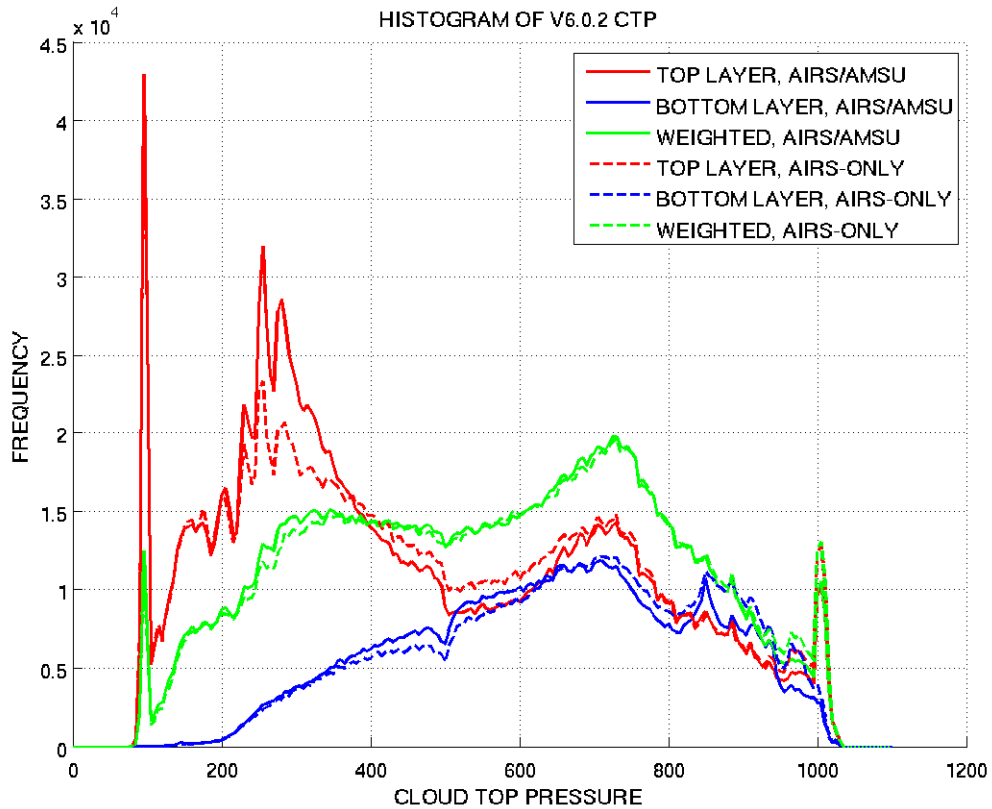


Figure 60 Distribution of the CTP between AIRS/AMSU and AIRS-ONLY retrieval.

Version 6 Performance and Test Report

3.9. Cloud Phase and Ice Cloud properties

Tester and Point of Contact: Brian Kahn

Data Product	Description
cloud_phase_3x3	The final cloud thermodynamic phase (ice, liquid, unknown, or clear sky)
cloud_phase_bits	The individual phase tests organized into bits
ice_cld_opt_dpth	Ice cloud optical depth reported at 0.55 microns
ice_cld_opt_dpth_QC	The quality control for the ice cloud optical depth (0=Best, 1=Good, 2=Do Not Use)
ice_cld_eff_diam	Ice Cloud Effective Diameter reported in microns
ice_cld_eff_diam_QC	The quality control for the ice cloud effective diameter (1=Good, 2=Do Not Use; there is no 0=Best for this variable)
ice_cld_temp_eff	Effective ice cloud top temperature reported in Kelvins
ice_cld_temp_eff_QC	The quality control for the effective ice cloud top temperature (0=Best, 1=Good, 2=Do Not Use)
ice_cld_fit_reduced_chisq	The average over channels of the chi-squared residual fit between the simulated and observed radiances (normalized by the radiance error). $\frac{1}{N_{chan}} \times \sqrt{\sum_i \left[\frac{\Theta_i^{obs} - \Theta_i^{calc}}{\Theta_i^{err}} \right]^2}$
ice_cld_opt_dpth_ave_kern	The scalar averaging kernel for the ice cloud optical depth
ice_cld_eff_diam_ave_kern	The scalar averaging kernel for the ice cloud effective diameter
ice_cld_temp_eff_ave_kern	The scalar averaging kernel for the

Version 6 Performance and Test Report

	effective ice cloud top temperature
ice_cld_opt_dpth_err	The error for the ice cloud optical depth. Do not use. These values may be meaningless.

Data Product	Description
ice_cld_eff_diam_err	The error for the ice cloud effective diameter. Do not use. These values may be meaningless.
ice_cld_temp_eff_err	The error for the effective ice cloud top temperature. Do not use. These values may be meaningless.
log_ice_cld_opt_dpth_prior_var	The covariance prior for the ice cloud optical depth. This is a single fixed value.
log_ice_cld_eff_diam_prior_var	The covariance prior for the ice cloud effective diameter. This is a single fixed value.
ice_cld_temp_eff_prior_var	The covariance prior for the effective ice cloud top temperature. This is a single fixed value.
ice_cld_opt_dpth_first_guess	The first guess prior for the ice cloud optical depth. This is a single fixed value.
ice_cld_eff_diam_first_guess	The first guess for the ice cloud effective diameter. This is a single fixed value.
ice_cld_temp_eff_first_guess	The first guess for the effective ice cloud top temperature. This value is taken from the AIRS Standard L2 upper level cloud top temperature.

The four primary new cloud products found in the Level 2 (L2) Support product are cloud thermodynamic phase (**cloud_phase_3x3**), ice cloud optical thickness (**ice_cld_opt_dpth**), ice cloud effective diameter (**ice_cld_eff_diam**), and effective ice cloud top temperature (**ice_cld_temp_eff**). The cloud

Version 6 Performance and Test Report

thermodynamic phase is based on a series of spectral radiance tests and the presence of cloud, according to the AIRS Standard L2 effective cloud fraction product. The ice cloud optical thickness, ice cloud effective diameter, and effective ice cloud top temperature are retrieved on AIRS FOVs that contain ice, according to the cloud thermodynamic phase product, using an optimal estimation retrieval post-processor after completion of the AIRS Standard L2 retrieval. Details about this retrieval approach are being prepared for a publication led by Brian Kahn (JPL). The remaining new cloud products are either quality control indicators, error estimates on the retrieved quantities, or detailed aspects of the initial guess and information content of the primary retrieval parameters.

The three most important additional parameters are the quality control indicators for ice cloud optical thickness (**ice_cld_opt_dpth_QC**), ice cloud effective diameter (**ice_cld_eff_diam_QC**), and effective ice cloud top temperature (**ice_cld_temp_eff_QC**). For **ice_cld_opt_dpth_QC** and **ice_cld_temp_eff_QC**, the ranges of values are from 0 to 2, where 0 = ‘Best’, 1 = ‘Good’, and 2 = ‘Bad’. We recommend that values of 2 should not be used under any circumstances unless users carefully validate or investigate these values, or consult members of the AIRS Science Team. Values of 0 and 1 are considered ‘usable’, but there are no assurances made that every retrieved value has reasonable error characteristics. For **ice_cld_eff_diam_QC**, only values of 1 and 2 are reported. Since ice cloud effective diameter is the hardest parameter to retrieve, we felt it was necessary to simply report either ‘Good’ or ‘Bad’ values since we have no way of determining whether a given retrieval was differentiable enough to be called ‘Best’. The three retrieval parameters must be used in conjunction with the QC, since we report every retrieval value in the Support product.

The QC indicators are derived from the quality of fit of simulated and observed radiances (**ice_cld_fit_reduced_chisq**) and the scalar averaging kernels (**ice_cld_opt_dpth_ave_kern**, **ice_cld_eff_diam_ave_kern**, and **ice_cld_temp_eff_ave_kern**), which range from 0.0 to 1.0 for the three primary retrieval parameters. The quality control indicators are neither absolute nor quantitative, but should be used as an approximate indicator for more trustworthy values that are determined from good radiance fits and higher values of information content (averaging kernel values closer to 1.0). Furthermore, the QC indicators for these fields are independent of each other. For example, it is possible that one parameter may be ‘Best’, while the other parameters may be either ‘Good’ or ‘Bad’. If the user wants to use the same exact data sample for investigations of the three parameters simultaneously, we recommended that the

Version 6 Performance and Test Report

user restricts data samples to when all three QC parameters report either ‘Best’ or ‘Good’.

The error estimates for the same three parameters (**ice_cld_opt_dpth_err**, **ice_cld_eff_diam_err**, and **ice_cld_temp_eff_err**) are reported, although they are most certainly biased and do not represent the true error of the retrieval parameter. Further research is required to make these useful quantities, so until further notice, do not use these values or expect them to be realistic. Since the retrieval requires a first guess, these are reported in the following variables: **ice_cld_opt_dpth_first_guess**, **ice_cld_eff_diam_first_guess**, and **ice_cld_temp_eff_first_guess**. For **ice_cld_opt_dpth_first_guess**, we assume initially that all clouds have a value of 3.0. We will show evidence of this assumption in the retrieval fields in the figure and its discussion to follow. For **ice_cld_eff_diam_first_guess**, we assume that all retrievals start with an effective radius of 30 microns, regardless of the geophysical context of the scene. Lastly, for **ice_cld_temp_eff_first_guess**, the ice cloud top temperature is initially set to be the upper level cloud top temperature reported in the Standard L2 product. More complex initial guess fields were attempted but ended up leading to poorer retrieval performance (lower yield, large values of **ice_cld_fit_reduced_chisq**, etc.). The covariance between these parameters must be estimated, too, and are reported in **log_ice_cld_opt_dpth_prior_var**, **log_ice_cld_eff_diam_prior_var**, and **ice_cld_temp_eff_prior_var**. All three parameters are fixed to constants, and a more complex assessment of the covariance of geophysical fields is a topic for future research. We expect that these values may be highly variable depending on the cloud and scene type, season, latitude, altitude, and so forth. Lastly, the **cloud_phase_bits** field contains all tests performed in the cloud thermodynamic phase algorithm. There are multiple tests for liquid cloud, ice cloud, warm cloud, and desert surfaces.

Version 6 Performance and Test Report

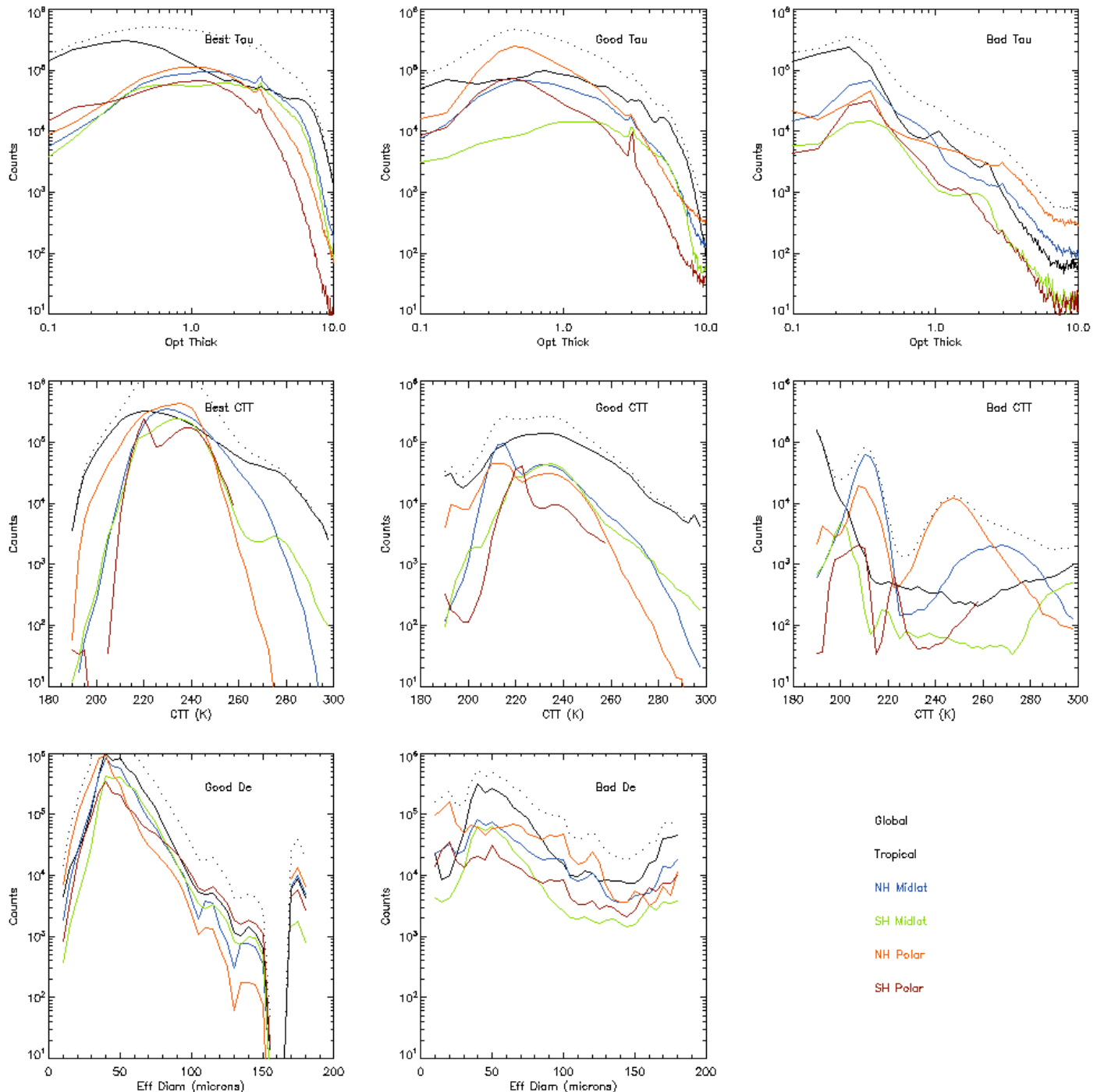


Figure 61 Histogram of new cloud products.

Version 6 Performance and Test Report

The cloud fields have been tested for the month of January 2007 and other selected time periods. We summarize the results for January 2007 in Figure 61. Shown are histograms of **ice_cld_opt_dpth**, **ice_cld_eff_diam**, and **ice_cld_temp_eff** sorted by QC values of ‘Best’, ‘Good’, and ‘Bad’, and broken up by latitude band: Global (all latitudes), Tropical ($\pm 30^\circ$), southern hemisphere mid-latitudes ($30\text{--}60^\circ\text{S}$), northern hemisphere mid-latitudes ($30\text{--}60^\circ\text{N}$), southern hemisphere polar region ($60\text{--}90^\circ\text{S}$), and the northern hemisphere polar region ($60\text{--}90^\circ\text{N}$). For the ice cloud optical thickness, we see that the ‘Best’ and ‘Good’ histograms closely resemble each other in shape and number of counts, and also resemble histograms of optical thickness obtained from other satellite, in situ, and surface-based observations, while the ‘Bad’ histograms are flatter with a larger proportion of values at the highest and lowest ends of the data range. Observe the small spike in the histograms for optical thickness values of 3.0. This shows that in these retrievals, there isn’t enough information for the retrieval parameter to move from the initial guess. It is encouraging that the peak is so small and confined to a small set of bins around 3.0. Thus, we conclude that the a priori guess for optical thickness has little meaningful impact on the broader retrieval results. The relative differences between the latitude bands on the surface seem physically reasonable. For example, the Tropics contain a much higher proportion of thin cirrus clouds compared to other latitudes.

For the effective ice cloud top temperature, again, the histograms for ‘Best’ and ‘Good’ appear realistic and are comparable to the AIRS L2 Standard product and other independent data sources. The Tropics contain the highest proportion of cold clouds, and the polar latitudes contain very few values at unrealistically warm temperatures, except in the case of ‘Bad’ retrievals. This parameter is retrieved (instead of just using the value from the Standard L2 product) because better radiance fits and higher values of averaging kernels are obtained than if only the optical thickness and effective diameter are retrieved alone.

For the effective diameter, the histograms are fairly similar to other data sources. However, there is one glaring issue that requires further investigation, and that is the lack of retrieval values around 160 microns in ‘Good’ retrievals. There are plenty of values in the ‘Bad’ retrieval histograms, and it may be related to the lack of information in the spectra at such large effective diameters (the spectral have little sensitivity at these sizes). Perhaps an adjustment in the QC methodology may be required to include values around these sizes if the information is there, but this is to be determined in future investigations.

Version 6 Performance and Test Report

A few take-home messages:

- Cloud thermodynamic phase and ice cloud properties show patterns that are consistent with expectations from other satellite instruments and in situ observations (to be reported in a future publication), and make physical sense.
- Some pixel-scale comparisons of AIRS to MODIS retrievals show that AIRS is in the ballpark (to be reported in a future publication), but yet are observing a different set of clouds compared to MODIS.
- Pixel-scale match-ups of AIRS to CALIPSO show that AIRS has very good skill in detecting most ice clouds, but detects much fewer liquid water clouds than are actually present. However, when the latter is detected, it is done with very high certainty.

Version 6 Performance and Test Report

3.10. Outgoing Longwave Radiation

Tester and Point of Contact: Joel Susskind

This section compares Version-5 and Version-6.03 monthly mean products for the 12 months in which Version-6.03 was run: January, April, July, and October in each of 2003, 2007, and 2011. The emphasis of the validation is with regard to “trends”, or more importantly the difference in trends of Version-6 and Version-5, where the “trend” is defined as the slope of the linear least squares fit passing through data of all 12 months with a linear time scale. Particular attention will be paid to trends of OLR, clear sky OLR, temperature profile, mid-tropospheric water vapor mixing ratio, total precipitable water, and fractional cloud cover.

Figure 62 is not related to trends but rather shows differences of AIRS global mean monthly mean OLR (green) and Clear Sky OLR (red) values from those generated by the CERES Science Team using CERES observations. Version-5 differences from CERES are shown for each month of the overlap OLR time series, September 2002 through October 2011, and Version-6.03 differences are shown for each of the twelve months for which Version-6.03 was run. The solid lines (green and red) are horizontal lines, passing through the mean differences between AIRS Version-5 and CERES values of OLR and Clear Sky OLR respectively, and the dashed lines (green and red) are horizontal lines passing through the mean differences of AIRS Version-6.03 OLR and Clear Sky OLR from the CERES values of these parameters. Version-5 AIRS OLR and Clear Sky OLR values are significantly biased with regard to those of CERES, with a bias that is essentially constant in time but with a small seasonal cycle. Previous work has shown that the anomaly time series of AIRS and CERES OLR, as well as of AIRS and CERES Clear Sky OLR, are in very close agreement with each other. Nevertheless, the large biases of 8.59 W/m^2 and 7.96 W/m^2 for AIRS OLR and Clear Sky OLR respectively with respect to CERES are somewhat

Version 6 Performance and Test Report

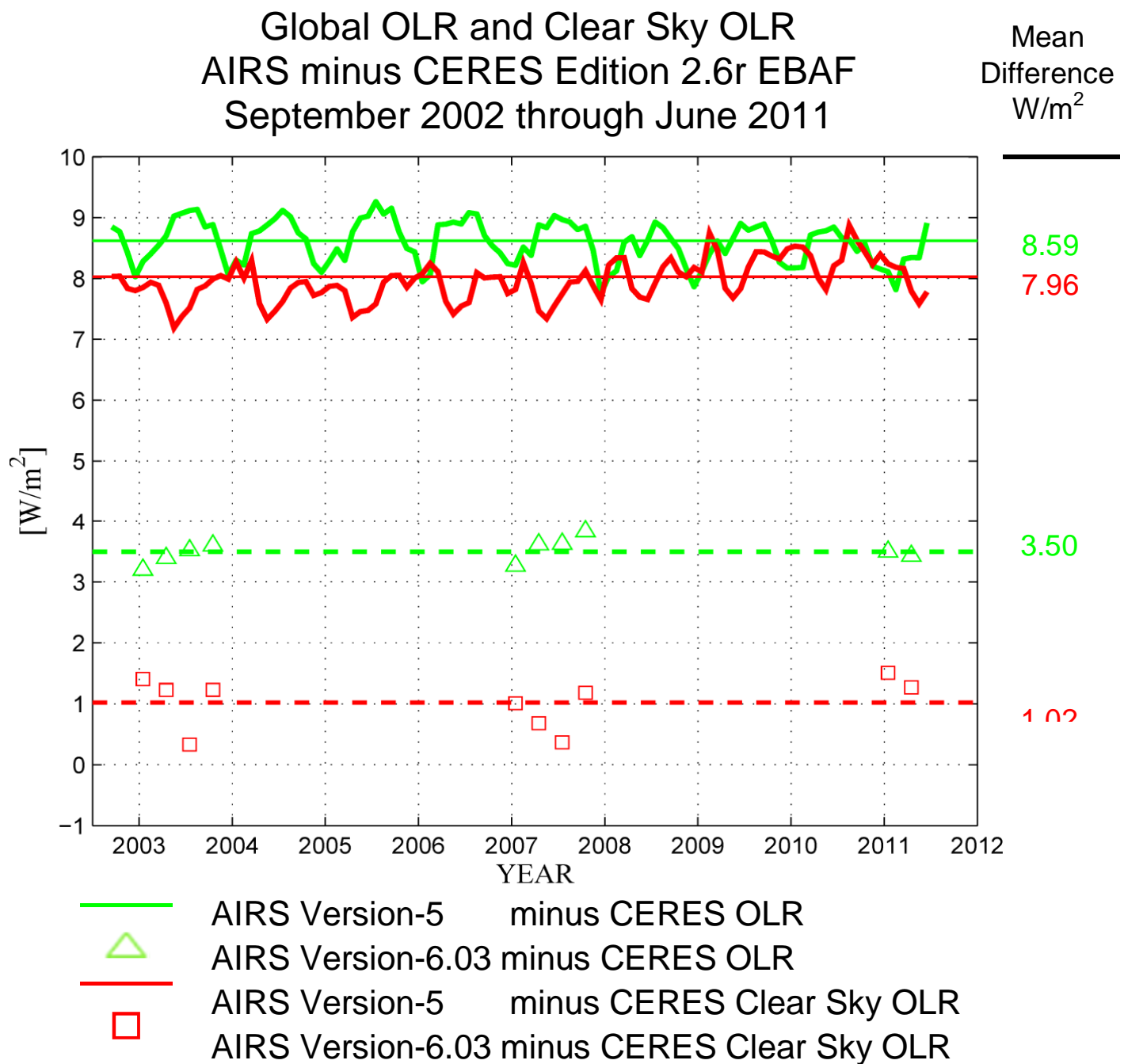


Figure 62 Difference between AIRS and CERES global and clear sky OLR.

Version 6 Performance and Test Report

disconcerting. Figure 62 shows that Version-6.03 OLR and Clear Sky OLR biases compared to CERES will be reduced to much more acceptable values of 3.37 W/m^2 and 1.02 W/m^2 respectively. These differences are generally on the order of the uncertainty of the CERES measurements themselves.

Figure 63 shows values in blue of the global mean time series of six Version-5 products: OLR; Clear Sky OLR; 500 mb temperature; 500 mb water vapor mixing ratio; Total Precipitable Water; and Effective Cloud fraction. Version-5 values for each of the months between January 2003 and October 2011 are given by the dashed blue lines. Version-5 values for the twelve comparison months are also indicated by the blue stars which lie on the dashed blue curve. The solid blue lines show the slopes of the linear least squares fits passing through the 12 blue stars, which we have referred to as “trends”. Figure 63 also shows values of Version-6.03 products for the same 12 months in pink circles, with the straight lines passing those circles given in pink. Finally, the differences between Version-5 products and those of Version-6.03 are shown as black diamonds, and the straight lines passing through those differences, with an offset, are shown in black. The most important part of this figure is the slope of the black lines, which gives estimates of how actual trends of Version-6 products, when evaluated over a long time period, would differ from those of Version-5.

A number of important features are evident from the panels in this figure. While the relative slopes of the Version-5 and Version-6.03 trend lines are generally similar for OLR and Clear Sky OLR, they are considerably different from each other for the remaining geophysical parameters. Values of the slopes of all the lines are given in Table 2. For example, Version-5 500 mb temperature has a negative “trend” of -0.058 K/yr , while the “trend” in Version-6.03 is -0.006 K/yr . These “trends” can be misleading because not only does the time period used contain data from only 12 months in 3 years, but even more significantly, only a portion of the annual cycle is captured. The more significant values are the differences in the two sets of “trends” because these indicate the extent that trends of Version-6 products should differ from those of Version-5 whatever they are. For example, one would expect the trend of Version-6 500 mb temperature to be on the order of 0.052 K/yr more positive (less negative) than that of Version-5. Likewise, the Version-6 trend of 500 mb water vapor mixing ratio is expected to be less negative (or more positive) than that of Version-5 as with Total Precipitable Water. Figure 7 showed that Version-5 tropospheric temperature and water vapor had spurious negative bias trends vs. ECMWF “truth”, based on results for seven days, which were for the most part

Global Time Series January 2003 through October 2011

OLR (W/m^2)

Clear Sky OLR (W/m^2)

a

b

500 mb Temperature (K)

500 mb Mixing Ratio (g/Kg)

Total Precipitable Water (mm)

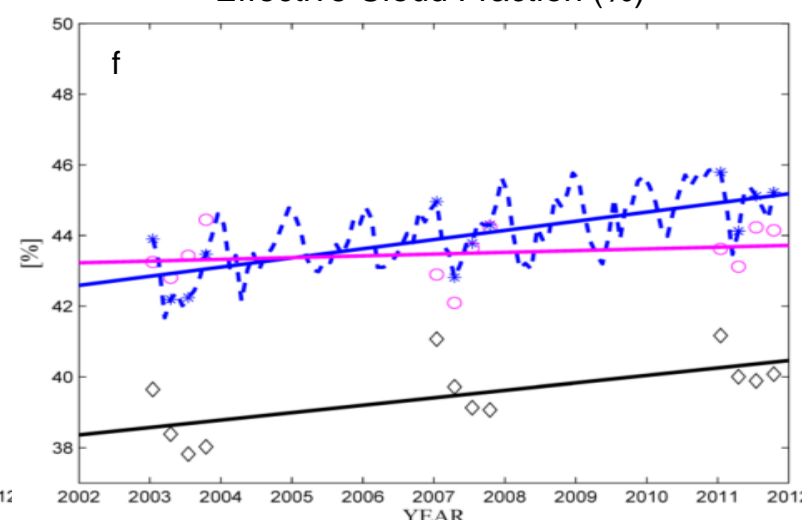
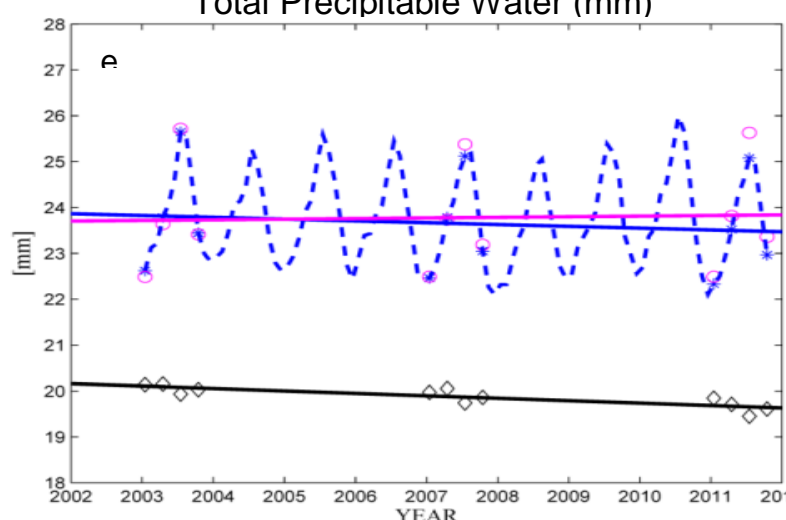
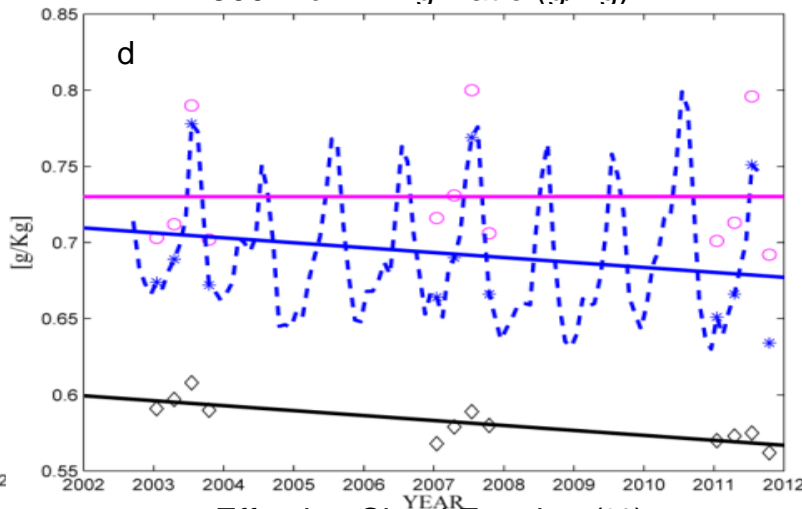
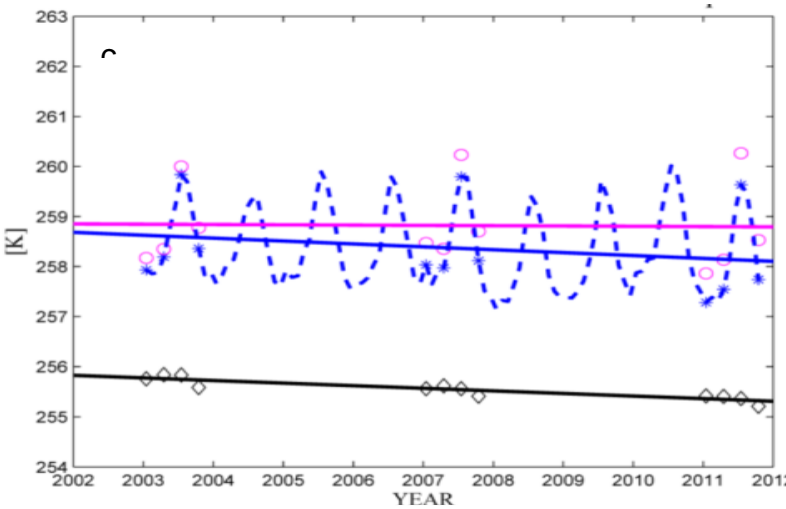
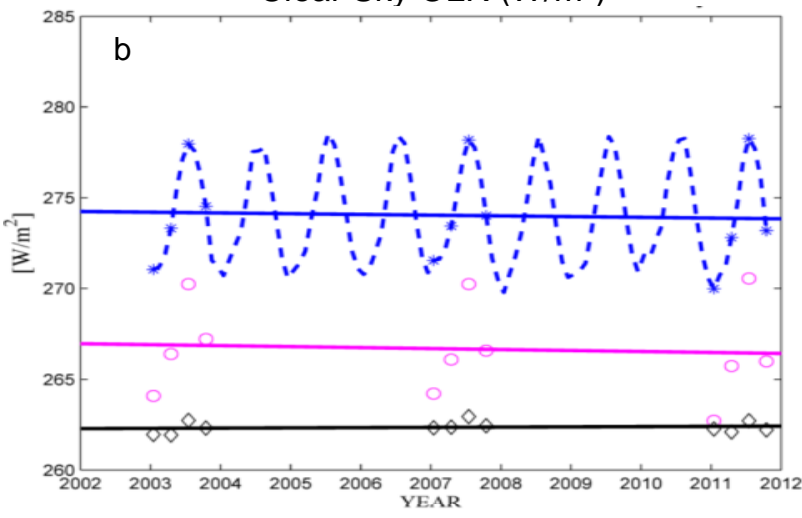
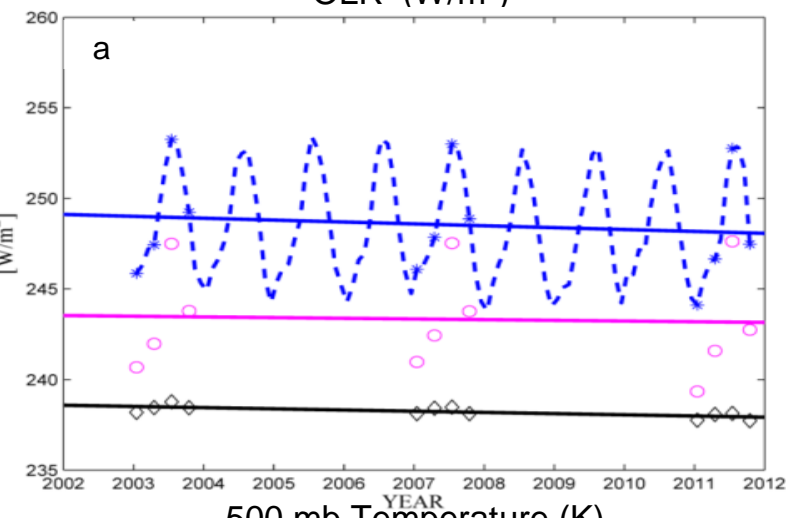
Effective Cloud Fraction (%)

c

d

e

f



— AIRS V5 January 2003 through October 2011

* AIRS V5 12 Months

— Slope

○ AIRS V6.03 Months

◇ AIRS V5 minus AIRS V6.03

— Slope

— Slope

Figure 63 Time series of global and clear sky OLR.

Version 6 Performance and Test Report

Table 3. Annual global trend.

12 Month Global Time Series Slopes (Trends) January 2003 through October 2011

	OLR W/m ² /yr	Clear Sky OLR W/m ² /yr	500 mb Temp K/yr	500 mb Mixing Ratio g/Kg/yr	Total Precipitable Water mm/yr	Cloud Fraction %/yr
*						
AIRS V5	-0.104	-0.040	-0.058	-0.00325	-0.0392	0.260
○						
AIRS V6.03	-0.038	-0.054	-0.006	0.00001	0.0122	0.049
◆						
AIRS V5 minus AIRS V6.03	-0.066	0.014	-0.052	-0.00326	-0.0514	0.211

eliminated in Version-6. Table 3 confirms this result with regard to monthly mean products over different years. Table 3 also shows that Version-5 global mean cloud cover was increasing at a most likely unreasonable rate of 0.26% per year, while Version-6 cloud fraction will increase on the order of 0.21% per year less. As discussed previously, the spurious increase in Version-5 cloud cover over time is consistent with the spurious negative trends of T(p) and q(p) found in Version-5.

Figure 64 shows trends, and trend differences related to Version-5 and Version-6 temperature profiles. The left panel in Figure 64 shows “trends” of Version-5 and Version-6 T(p) computed at different pressure levels as discussed previously, in red and blue respectively, as well the more meaningful statistic, which is the difference in the expected trends of Version-6 temperatures compared to Version-5, shown in green. The appropriate values for 500 mb temperature, given in Table 2, are plotted in Figure 64 at 500 mb. The same green curve is shown in the right panel of Figure 64. Superimposed on the green curve, showing the Version-5 trends minus Version-6 trends, is the dashed red curve which was previously shown in Figure 13. The dashed red curve shows the spurious Version-5 temperature profile bias trends as compared to ECMWF, determined from the seven focus days. To the extent that trends of Version-5 minus Version-6 temperatures match those of Version-5 minus ECMWF, then one would expect Version-6 temperature trends to match those of ECMWF very

Version 6 Performance and Test Report

closely. The green line, aside from being smoother in the vertical, matches the dashed red line very closely in the troposphere. This is a further confirmation that the spurious temperature trends found in Version-5 will be much smaller in Version-6 as desired.

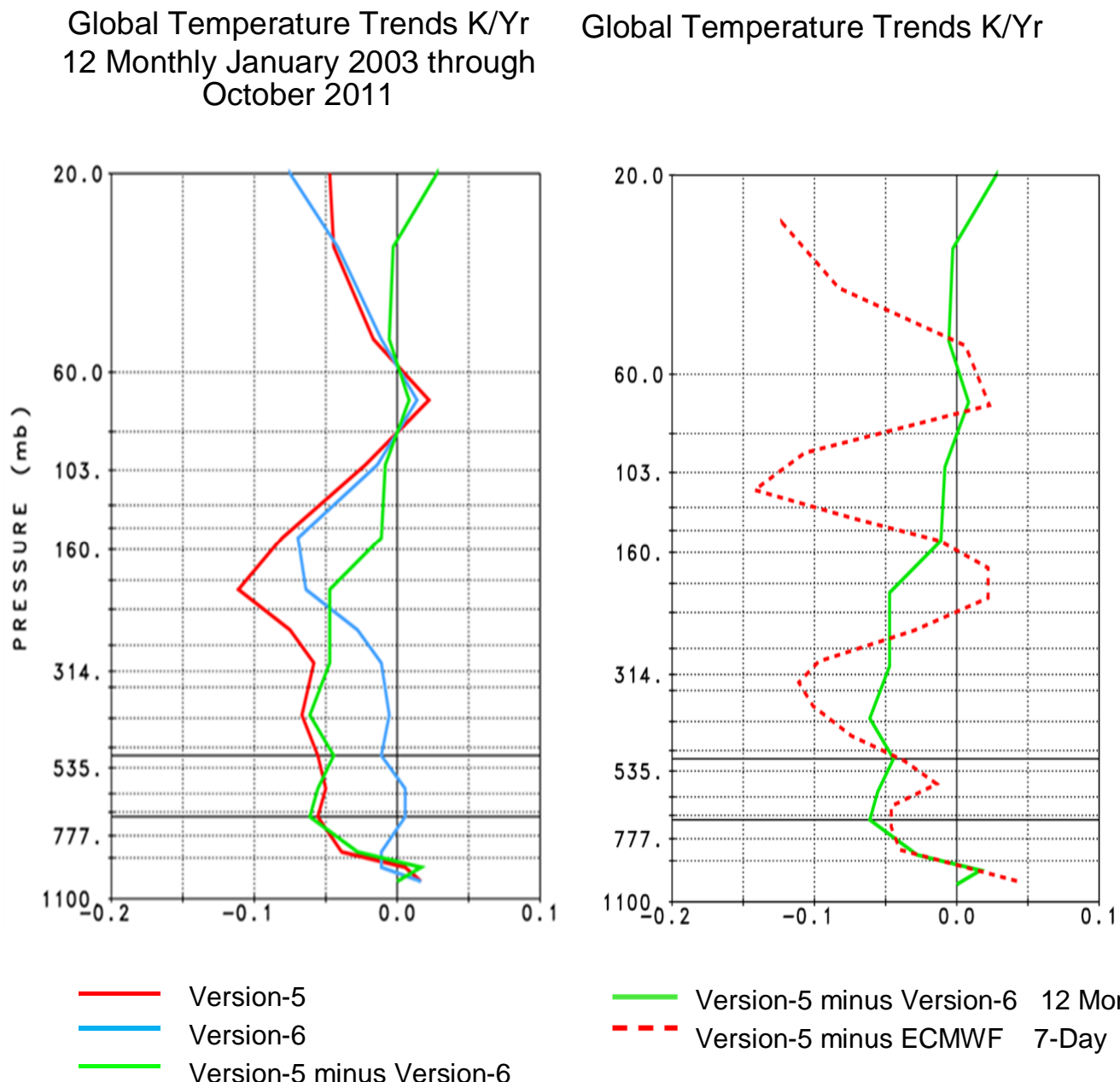


Figure 64 Global temperature trends.

Version 6 Performance and Test Report

3.11. Trace Gases

3.11.1 Methane

Tester and Point of Contact: Xiaozhen Xiong

Data Product	Definition
CH4CDSup	CH4 amount at 100 layers
CH4VMRLevStd	CH4 mixing ratio at 100 levels*
CH4_total_column	CH4 total column amount
CH4_VMR_eff_10func	CH4 mixing ratio at 10 retrieval layers
CH4VMRSurf	CH4 mixing ratio at surface
CH4_ave_kern_10func	CH4 averaging kernels
CH4_eff_press_10func	CH4 mixing ratio at 10 retrieval layers
CH4_verticality_10func	Verticality of CH4 at 10 retrieval layers
CH4_trapezoid_layers_10func	10 retrieval Trapezoid functions
CH4_dof	Degree of freedoms
CH4CDSup_QC	Quality Flag of CH4 at 100 layers
CH VMRSurf_QC	Quality Flag of CH4 at surface
CH4_eff_press_10func_QC	Quality Flag of CH4 at 10 retrieval layers
CH4_total_column_QC	Quality Flag of CH4 total column
CH4VMRLevSup_QC	Quality Flag of CH4 at 100 levels
CH4_Resid_Ratio	Surface skin temperature quality control

Summary of changes in V6 CH4 retrieval methodology

Compared to V5 that used 7 trapezoid functions for retrieval, 10 trapezoid functions (LEVCH4 = 1,21,44,51,56,61,66,72,79,88,100) are used in version 6. Channels were reselected and tuned based on aircraft measurements, in which we removed some channels with strong absorption of HNO3, N2O and SO2. Damping is optimized accordingly by setting CH4wgt = 1.3. First-guess is also optimized with the major changes are at above 200 hPa in the high northern/southern hemisphere. Like AIRS V5, such a “fixed” first guess without any dependence on time and longitude is used in V6.

Version 6 Performance and Test Report

Through comparison with V5 and aircraft measurements from HIPPO (HIAPER Pole-to-Pole Observations) aircraft measurements data, we found some contamination by clouds and slight angular dependence in the tropics at ~200 hPa and above. To resolve these two problems, a lot of efforts have been put to set appropriate quality flags. This is a major change in V6 than in V5.

Test data

Three data (August 5, 2005, Feb 24, 2007, and March 27, 2010) were acquired and tested all the parameters listed in 1.1, except CH4VMRLevStd.

Setting of New Quality Indicators

Compared to version 5 with a simple quality flag, we put more study to set a more strict QC flags to filter out some outliers in order to improve the quality in version 6. Since the CH4 absorption band is within the water vapor absorption band near $7.6\mu\text{m}$, we noticed the CH4 product is highly impacted by the retrieval of water vapor. Under the condition when the $\text{totH2OStd_QC} = 1$, we reset $\text{Qual_CH4} = 1$ if (1) $\text{CH4_Resid_Ratio} \geq 1.0$, or (2) $P_{\text{good}} \leq 610 \text{ hPa}$.

Due to the impact of cloud phase, we found the contamination is mainly impacted by low water cloud, or the cloud is uneven, i.e. in the boundary, of the field of regard (FOR). This setting is also under the condition of $\text{totH2OStd_QC} = 1$.

To reduce the impact of angular dependence in the high altitude in the tropics, PTropopause is used. We noticed that when the tropopause is very high, i.e near 100 hPa, $\text{Qual_CH4} = 2$ is added in the boundary 1-2 FOR in each swash.

With the new QC flags plus all other changes (tuning of two channels and damping), the CH4 peak at 400 hPa, resulting from the cloud contamination, in 60°S disappears (see left panel of Figure 69). From the comparison of CH4 map at 400 hPa (Figure 70, with new QC) with Figure 65, it is obvious that these cloud contaminated pixels have been filtered out using new QC. After applying the new QC flags, the yield drops by 8-10% than before. However, the new yield is still above 60%.

Version 6 Performance and Test Report

Results

Compared to AIRS V5, AIRS V6 has a better sensitivity to CH₄ in the lower troposphere and more information content. A better information content in V6 than V5 can be seen from Figure 65, which shows the map of DOF on March 27, 2010 (ascending). On average, the mean DOFs of V6 is 0.87 ± 0.28 ($Q=0,1$) and 0.93 ± 0.25 ($Q=0$), and for V5 the mean DOFs is 0.80 ± 0.27 ($Q=0,1$) and 0.89 ± 0.24 ($Q=0$). Here V5 and V6 are using their own quality flags and DOFs for V6 are always higher than V5 even using the same quality flags. The number of good pixels with $Q=0$ for V6 is 8.6% higher than V5. From the comparison of the area of averaging kernels (Figure 66), we can see that compared to V5 that are sensitive to CH₄ above 500 hPa , V6 has a better sensitivity to CH₄ towards a lower troposphere at near 700 hPa.

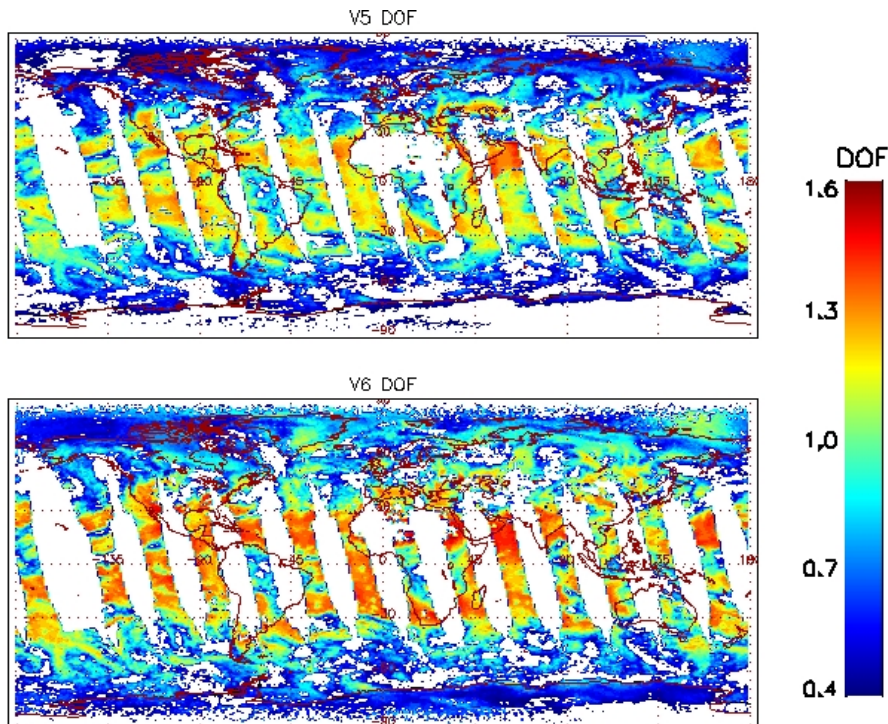


Figure 65 Comparison of DOFs in V6 and V5 for the case on March 27, 2010.

Version 6 Performance and Test Report

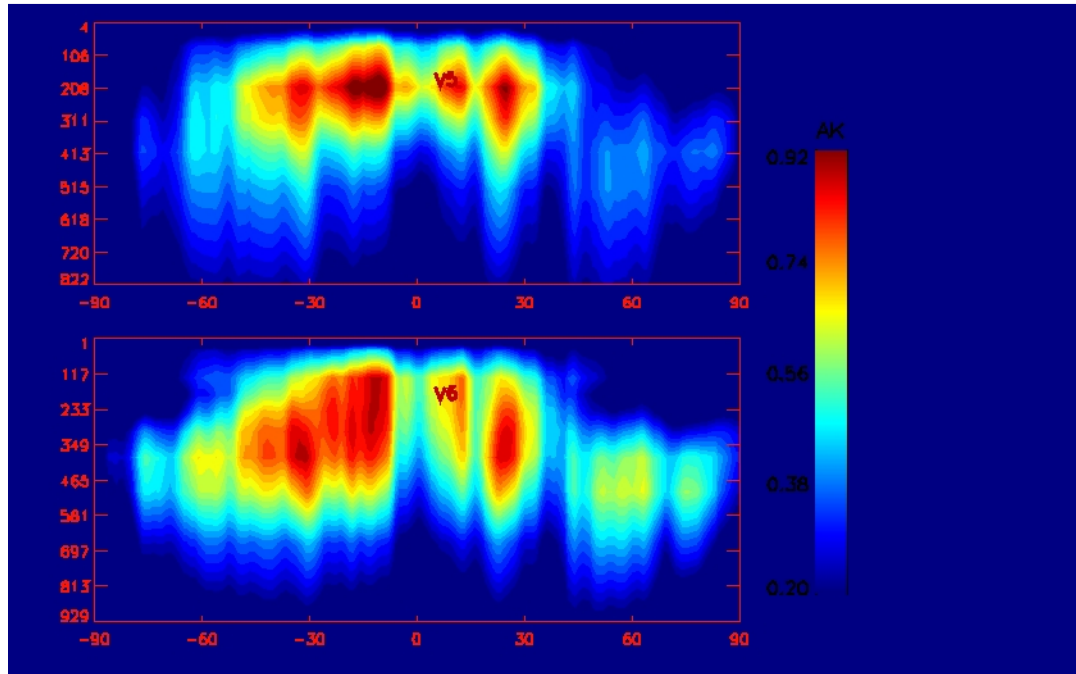


Figure 66 Comparison of the area of averaging kernels function with latitude (upper panel is V5 and the lower panel is for V6) on March 27, 2010.

Figure 67 compares the retrieved total column of CH4 from AIRS V5 and V6 on March 27, 2010, and Figure 68 is the retrieved CH4 at 400 hPa from V5 and V6. The total column in V6 is about 2.7% less than V5 on average, while the difference CH4 at 400 hPa is more obvious from their spatial variation.

Version 6 Performance and Test Report

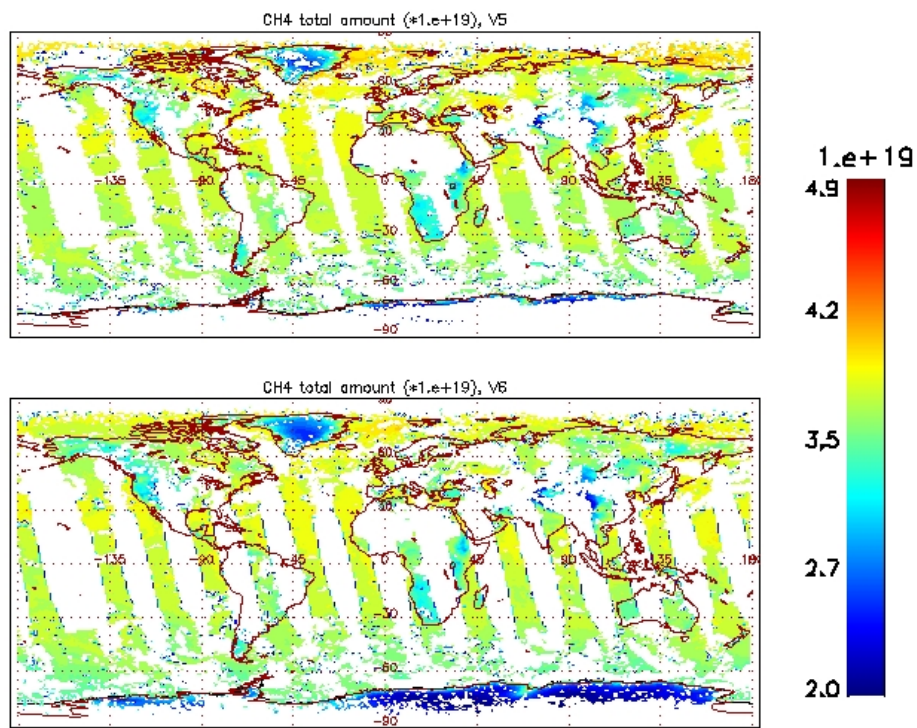


Figure 67 The retrieved total column of CH4 from V6 and V5 on March 27, 2010 (ascending only).

Version 6 Performance and Test Report

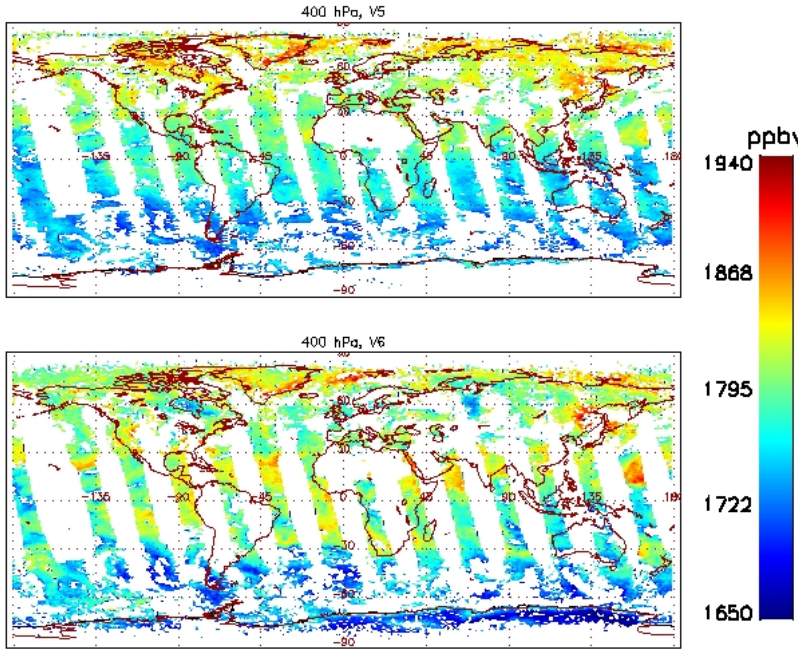


Figure 68 The retrieved CH₄ at 400 hPa from V6 and V5 on March 27, 2010 (ascending only).

Another check is the latitudinal gradient at 400, 800 hPa and a thick layer between 441–575 hPa, as shown in Figure 69. The left two panels, which compare the aircraft measurements in about two months with one day retrieval, can only demonstrate the difference between V5 and V6, while the right panel is the appropriate one to show the difference between AIRS-V6 and aircraft measurements since collocated data are used.

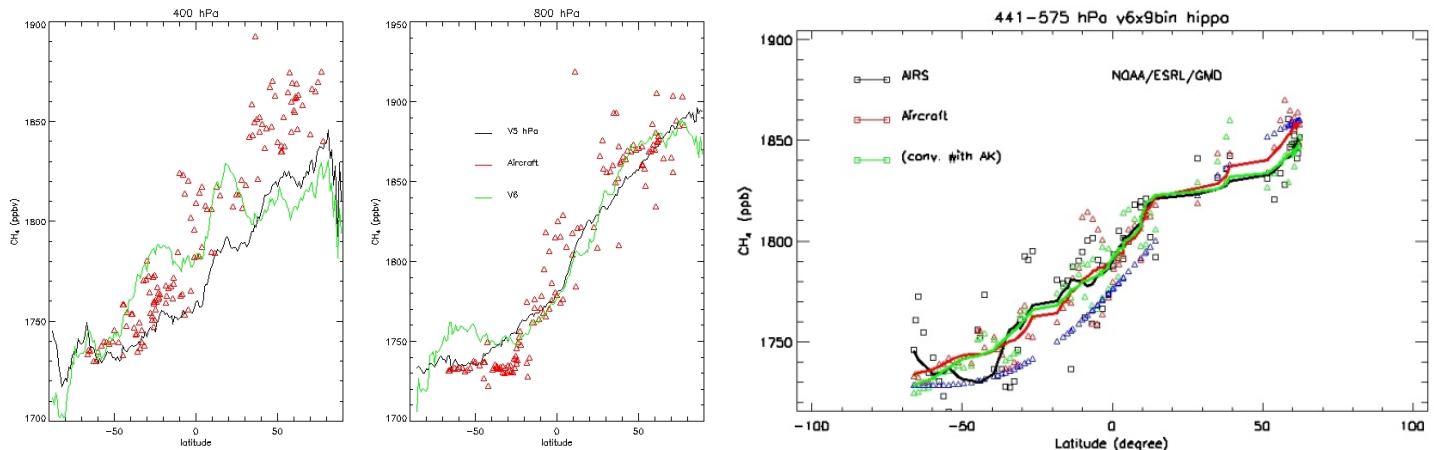


Figure 69 Latitudinal gradient of CH₄ at 400 and 800 hPa from HIPPO-3 aircraft measurement (red triangle) in March/April, 2010, and its comparison with one day retrievals from V5 (black line) and V6 (green line) on March 27, 2010 (left two panels). Right panel is from V6 using all collocated AIRS and HIPPO-1 observations.

Version 6 Performance and Test Report

The most important check to the improvement in AIRS V6 is the validation using more aircraft measurements. Figure 70 and Figure 71 are the validation of AIRS V5 and V6 using HIPPO-1,-2, 3 data. Correlation coefficient increases from 0.78 to 0.91, and the bias decreases from 1% to -0.15%, and rms error decreases from 1.86% to 0.88.

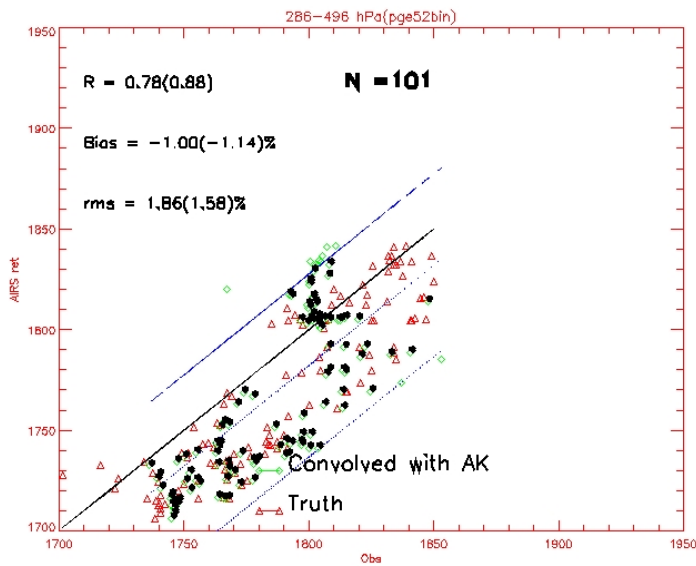


Figure 70 Validation of CH4 retrieval (V5) in layer between 286 – 496 hPa using HIPPO-1,-2,-3 aircraft measurement data. N=101 is the number of data points between the two blue dash lines.

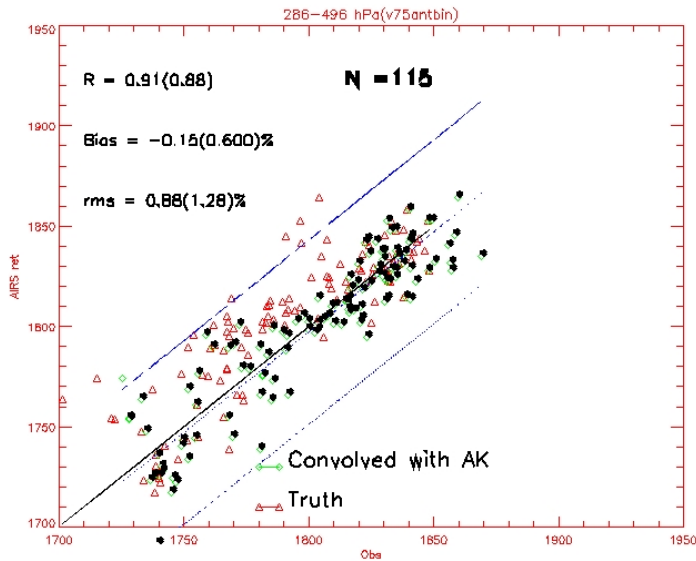


Figure 71 Same as Figure 4a but for AIRS V6. The correlation and bias and RMS error in V6 is much smaller than V5.

Version 6 Performance and Test Report

Moreover, some artificial high CH4 over desert or Antarctic has been removed (not shown).

Caveats and Future work

One caveat is some angular dependence at 200 hPa and above, which usually happens when the tropopause is close to 100 hPa. To resolve, we tuned the two peak CH4 absorption channels at 1304.35 and 1304.93 μm in Q-branch and set new quality flag and mark these pixels with QC=2 in the boundary of the swath. This is a temporal solution, and the factors resulted in this angular dependence are complicated. Further investigation and improvement are required in the future for version 7.

Due to the uncertainty in CH4 absorption spectrum, tuning to CH4 channels in the Q-branch need more investigate. Current tuning for version 6 was based on HIPPO-1,-2,-3 data, but as of now, there are no aircraft data in the summer season. Further improvement can be made with more aircraft measurements.

Version 6 Performance and Test Report

3.11.2 Carbon Monoxide

Tester and Point of Contact: Juying Warner

Parameter	Dimension	Definition
CO_total_column	FLOAT32 size: 30x45	Total column CO (molecules/cm ²)
CO_total_column_QC	UINT16 size: 30x45	Quality Flag for total column CO
COCDSup	FLOAT32 size: 100x30x45	Layer column CO (molecules/cm ²)
COCDSup_QC	UINT16 size: 100x30x45	Quality Flag for layer column CO
COCDSupErr	FLOAT32 size: 100x30x45	Error estimate for COCDSup
COVMRLevSup	FLOAT32 size: 100x30x45	Level CO Volume Mixing Ratios
COVMRLevSup_QC	UINT16 size: 100x30x45	Quality Flag for Level CO VMR
COVMRLevSupErr	FLOAT32 size: 100x30x45	Error for Level CO VMR
COVMRSurf	FLOAT32 size: 30x45	Surface CO Volume Mixing Ratios
COVMRSurf_QC	UINT16 size: 30x45	Quality Flag for Surface CO VMR
COVMRSurfErr	FLOAT32 size: 30x45	Error for Surface CO VMR
num_CO_Func	INT16 size: 30x45	Number of valid entries in each dimension of CO_ave_kern
CO_eff_press	FLOAT32 size: 9x30x45	CO effective pressure for each trapezoid
CO_VMR_eff	FLOAT32 size: 9x30x45	Effective CO VMR for each trapezoid
CO_VMR_eff_QC	UINT16 size: 9x30x45	Quality flag for each effective CO VMR
CO_VMR_eff_err	FLOAT32 size: 9x30x45	Error for each effective CO VMR
CO_verticality	FLOAT32 size: 9x30x45	Sum of the rows of CO_ave_kern
CO_dof	FLOAT32 size: 30x45	CO retrieved degrees of freedom
CO_ave_kern	FLOAT32 size: 9x9x30x45	Average kernel for CO retrievals

Version 6 Performance and Test Report

This section describes the AIRS V6 carbon monoxide (CO) products previously listed, the tests, and the preliminary validation for these products. For testing of the V6 CO product, AIRS dataset from March 4, 2006 is used to compare against *in situ* measurements obtained by the Differential Absorption Carbon Monoxide Measurements (DACOM) (Sachse et al., 1987), which took place as part of NASA's Intercontinental Chemical Transport Experiment (INTEX-B) (Singh et al., 2008) field mission. The V6 CO products are further compared with the V5 products to evaluate improvements. The majority of the testing is done for the AIRS/AMSU retrieval using QC = (0,1), but comparisons are also shown with the AIRS IR-only retrievals. The latest V6 version tested to date is V6.0.2.

Carbon Monoxide Trapezoids and A Priori:

In AIRS V6 CO, we have adapted the same retrieval layers as in V5, which correspond to 9 trapezoidal functions (McMillan et al., 2011). The major differences for the AIRS CO retrievals between AIRS V5 and V6 are primarily due to the use of the prior information or first guess. Two uniform CO profiles are used for the Northern Hemisphere (NH) and the Southern Hemisphere (SH) separately and they are developed using NCAR global MOZART (Model of Ozone and Related Tracers, Brasseur et al., 1998) monthly mean climatology. The MOZART monthly mean climatology was computed from 2.8x2.8 grid point 3D model outputs from 2002-2009, and interpolated to AIRS spatial and temporal resolution before averaging for each month. We have trimmed off the boundary layer high CO amount from the model outputs by extrapolation from the layers above since AIRS sensitivity does not extend to this layer and the high CO values would be entirely from the model. In addition, we add the Air Force Geophysics Laboratory (AFGL) climatology profile, same as used in V5, from 30 to 2 hPa. Figure 72 shows the monthly variation of the CO climatology profiles used as the first guess profiles for the NH (top) and SH (bottom), respectively.

Version 6 Performance and Test Report

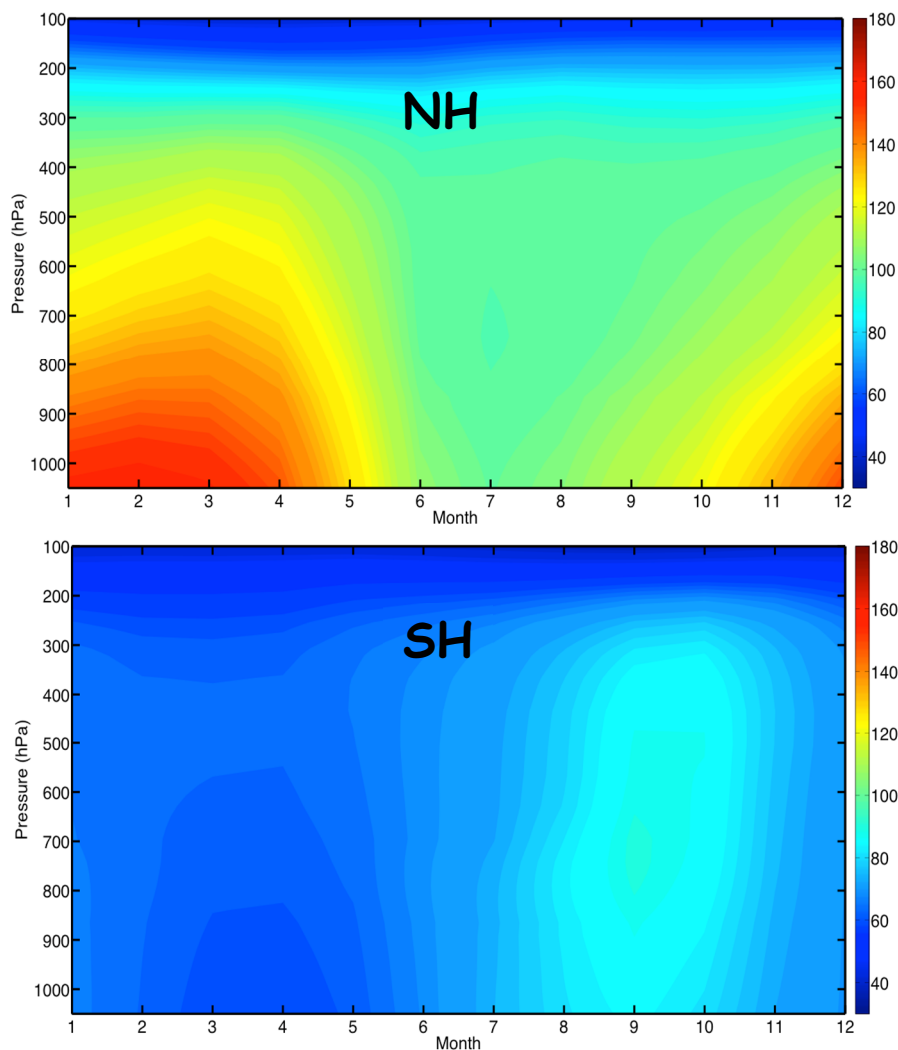


Figure 72 Monthly variation of CO used as the first guess for AIRS retrieval of CO.

Version 6 Performance and Test Report

Quality Indicators:

In V5 **Qual_CO** was used to describe quality indicators for all the CO products for each pixel. In V6, each product has its own quality control, e.g. **CO_total_column_QC**, **COCDSup_QC**, **COVMRLevSup_QC**, **COVMRSurf_QC**, and **CO_VMR_eff_QC**, however, the quality assurance definition is the same as for V5 (i.e. 0=best, 1=good, 2=bad). Figure 73 shows the pie charts that indicate the yields for each quality flag of 0, 1, and 2, and for V5 (left), V6 AIRS/AMSU (middle), and V6 IR-only (right) CO values at 500hPa during daytime (top) and nighttime (bottom), respectively. The yield for good retrievals (QC=0&1) has increased from 68.39% in V5 to 77.71%-76.63% in V6 during daytime and from 69.31% in V5 to 73.1%-72.64% in V6 at nighttime. There is a higher number of QC=0 cases during the day than at night even though the total QC=0&1 cases are about the same in both V5 and V6. The total number of good retrievals for both V6 AIRS/AMSU and IR-only are approximately the same.

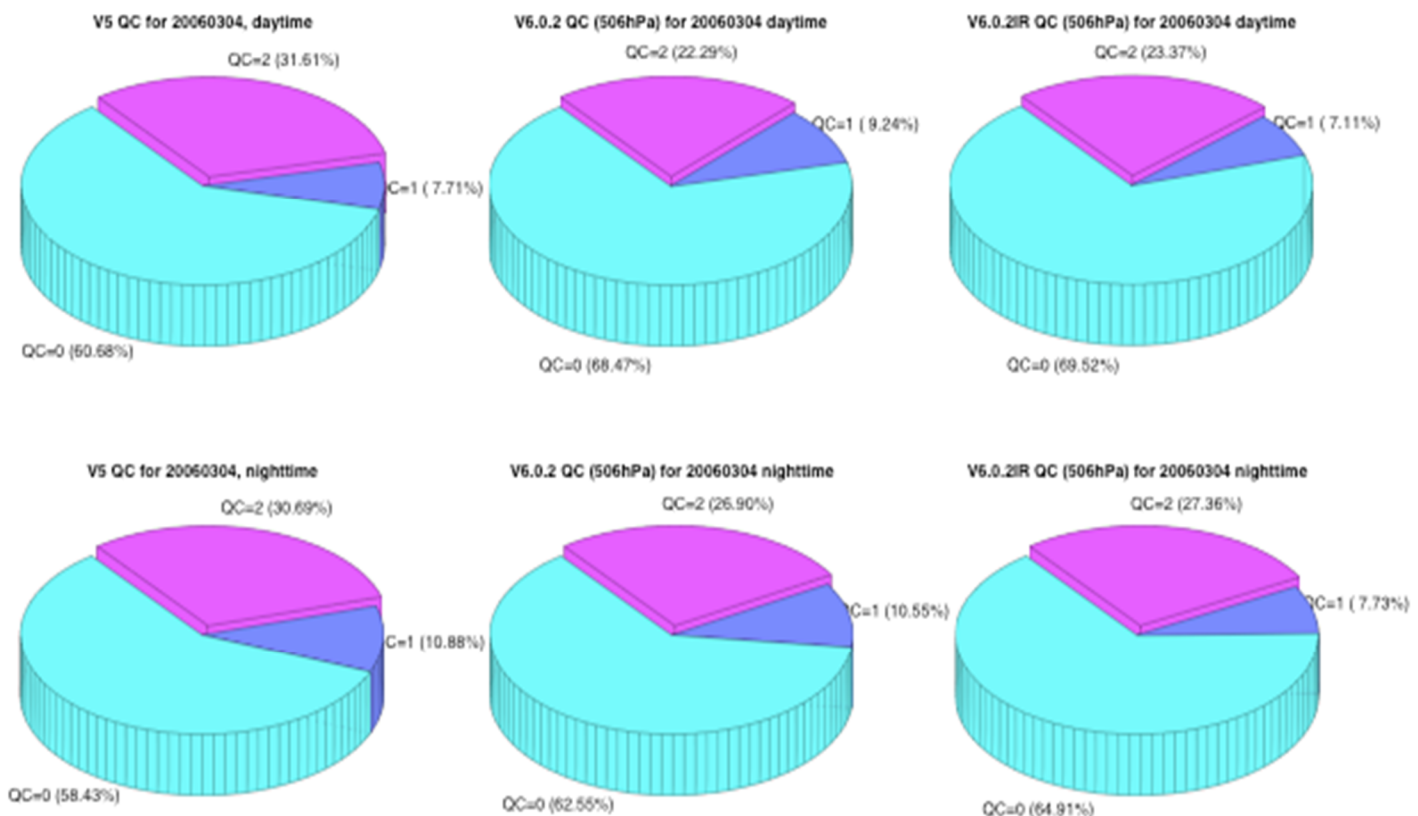


Figure 73 Yields of CO for different quality flags.

Version 6 Performance and Test Report

V6 CO Distributions Compared with V5 CO:

The standard CO VMRs are outputted at 9 levels equivalent to the effective pressure levels of the retrieval trapezoids. Also provided as part of the standard CO products are: the CO total column amounts, the quality control flags for the total columns, the CO effective pressure, the quality flag for each effective CO VMR, the error for each effective CO VMR, the average kernel for CO retrievals, the CO retrieved degrees of freedom, and the sum of the rows of CO averaging kernels referred as CO verticality. In addition, the support product is provided for users with needs to understand the performances of the retrieval processes in more details. The support products offer CO layer column densities in each of the 100 internal forward model layers alone with the quality flags and errors for each value. An added set of quantities for V6 in the support files is the VMRs at the internal forward model grid of 100 levels, as well as the related quality control flags and errors. Figure 74 shows an example of the global CO total column comparison between V5 and V6 for Mar. 4, 2006 for daytime (left panels) and nighttime (right panels), respectively. The top panels show the CO total column amounts from V5 and the middle panels are from V6, while the bottom panels are the differences (V6-V5). The V6 CO total column values are significantly higher in the NH, especially at high latitudes, and are lower in the SH compared to V5, which signifies improvements globally based on previous validations (Warner *et al.*, 2010, McMillan *et al.*, 2011). The improvements range approximately - 50×10^{17} to 50×10^{17} molecules/cm², which is equivalent to approximately 15% of the V6 CO total column values. This improvements in the V6 CO retrievals are primarily due to the upgrade of hemispherical and seasonally varying first guess profiles. The improvements in V6 CO over V5 are more significant over land and at night where the V5 CO was biased low, as shown in the top right panel.

Version 6 Performance and Test Report

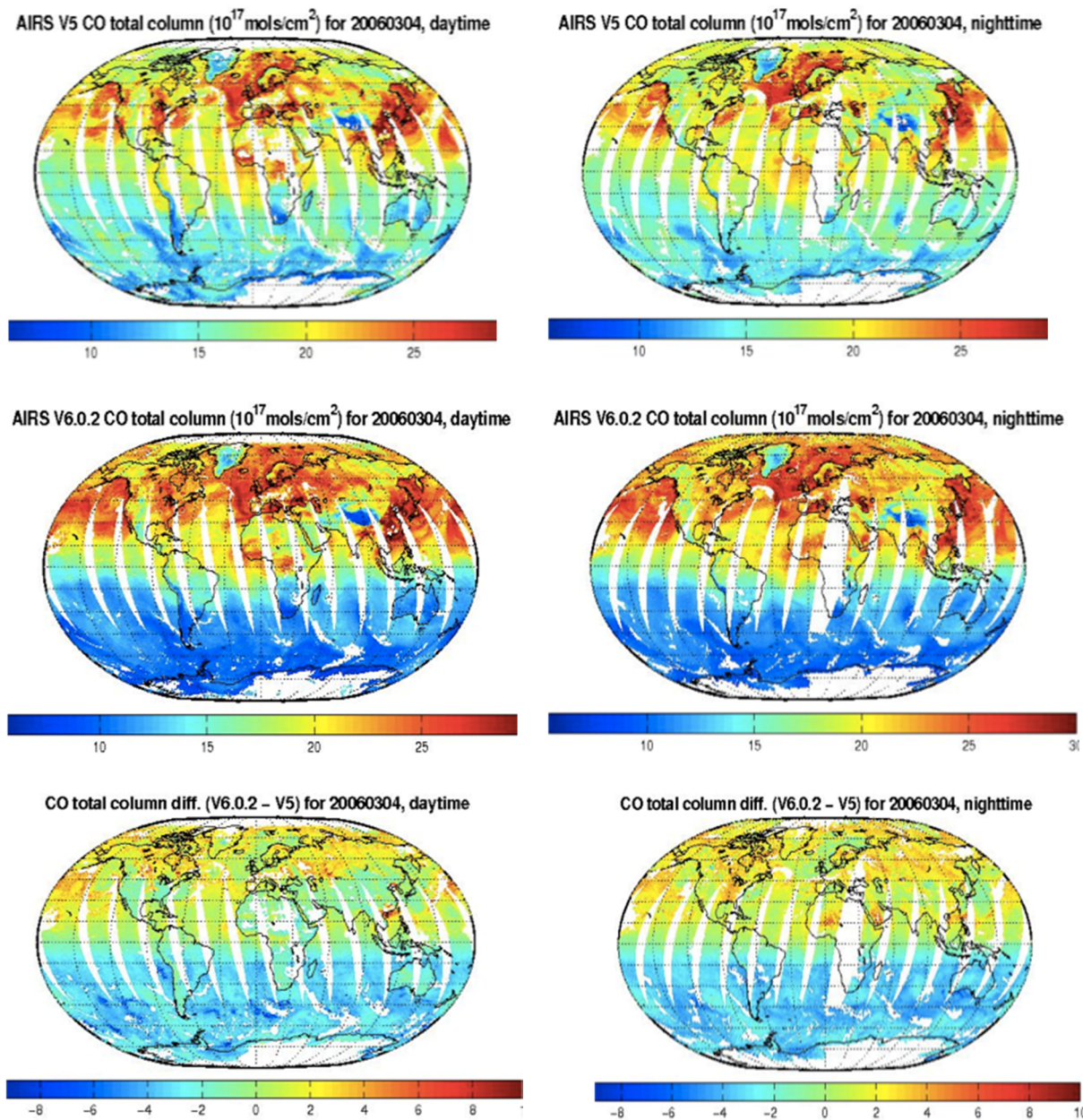


Figure 74 Global total column CO for day and night for V5 and V6 and their differences.

Version 6 Performance and Test Report

The retrieval errors are given for each CO product at each level or layer for V6, i.e., COCDSupErr, COVMRLevSupErr, COVMRSurfErr, CO_VMR_eff_err. These error estimates not only incorporate the uncertainties for the currently retrieved parameter, they also represent an accumulated effect from the previous retrieval steps that affect the current parameter. As an example, the CO retrieval errors at 506hPa for Mar. 4, 2006 are shown in Figure 75 for V5 (left panels), for V6 AIRS/AMSU (middle panels), and for V6 IR-only (right panels), respectively, and the top panels represent the daytime retrievals while the bottom panels are nighttime retrievals. The retrieval errors are at a magnitude of approximately 10ppbv over ocean and approximately less than 30ppbv over land. The errors for V6 IR-only retrievals are slightly higher than the AIRS/AMSU cases by a very small margin, while both V6 cases are better than V5. The true evaluation of the V6 CO retrieval quality should rely on detailed validations, which will be a continued effort.

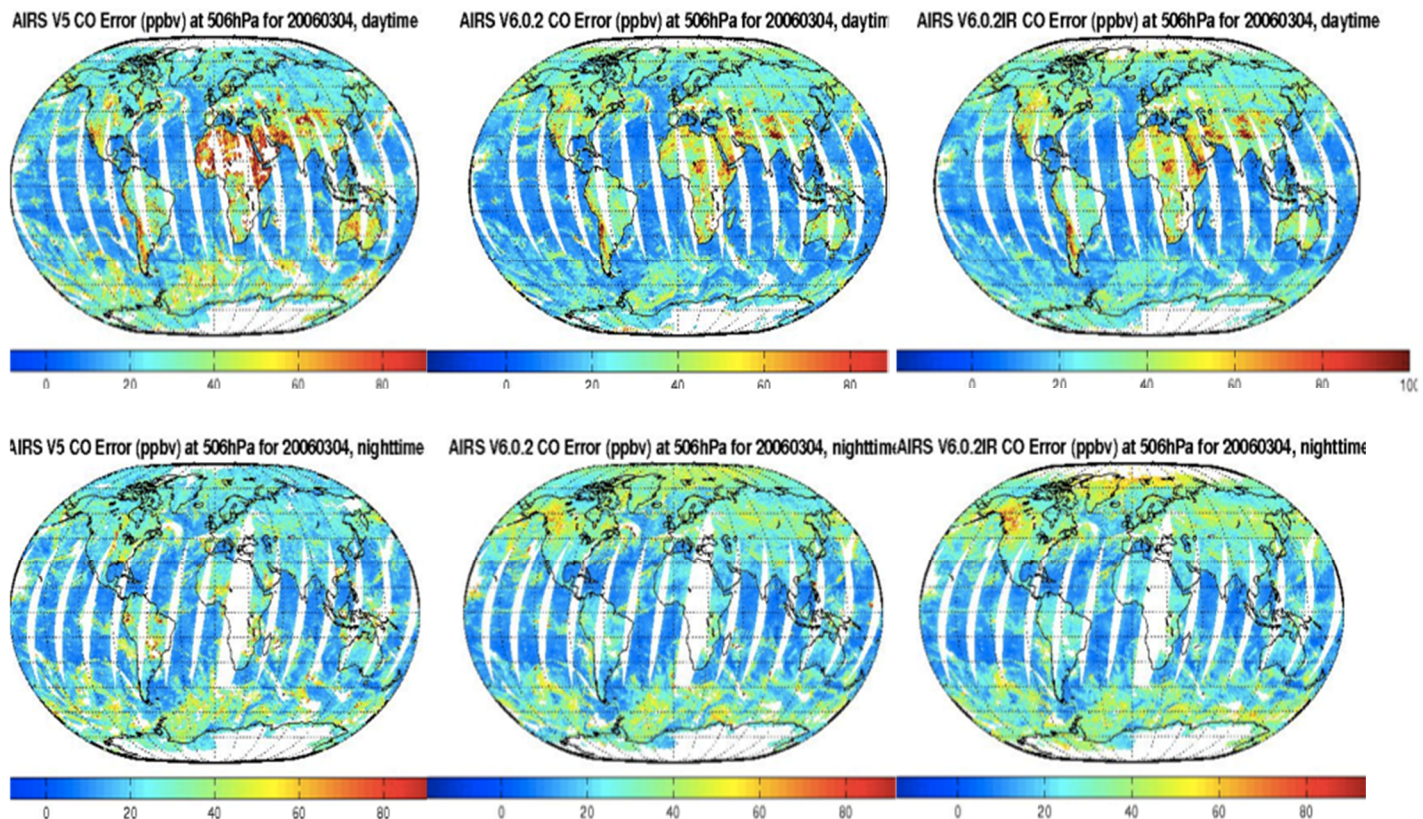


Figure 75 Error estimates CO retrieval at 506 mb for day and night of V5 and V6.

Version 6 Performance and Test Report

Preliminary Validation for V6 CO:

A large amount of *in situ* CO data exists during the lifetime of AIRS mission that will be used for a thorough validation study. The V6 CO is validated against the

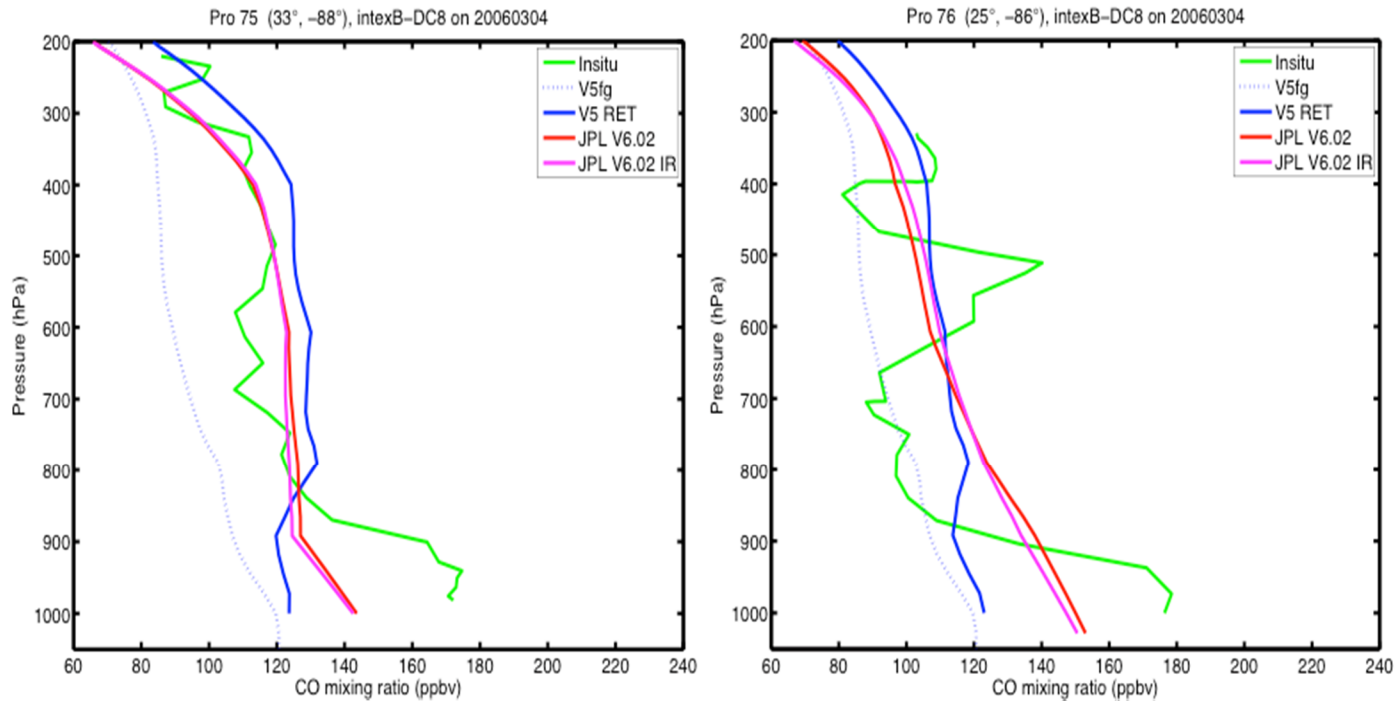


Figure 76 Profiles of CO mixing ratio.

DACOM CO measurements collected during the INTEX-B experiment and two *in situ* profiles on Mar. 4, 2006, at 20:33:37 (left panel) and 18:10:30 UTC time (right panel), are shown in Figure 76 where the *in situ* profiles are depicted by the green curves. This geographical region on that particular day was affected by agricultural fires in the southeast US, which resulted in high CO concentrations in the lower troposphere. The spiral profile on the left panel was collected over the Gulf of Mexico and the one on the right was collected over land to the west of Birmingham, AL, near the fires. The V6 CO shown as in red and magenta curves lead to significantly greater agreement between the retrievals and the *in situ* profiles in the lower troposphere, especially below 800 hPa. The more realistic results for the AIRS V6 CO, compared to the *in situ* profiles, are largely due to the new *a priori* information from the monthly mean climatology.

Version 6 Performance and Test Report

References:

Brasseur, G. P., Hauglustaine, D. A., Walters, S., Rasch, P. J., Muller, J. F., Granier, C. and Tie, X. X.: MOZART, a global chemical transport model for ozone and related chemical tracers 1. Model description, *J. Geophys. Res.-Atmos.*, 103(D21), 28 265–28 289, 1998.

McMillan, W. W., Keith D. Evans, Christopher D. Barnet, Eric S. Maddy, Glen W. Sachse, and Glenn S. Diskin: Validating the AIRS Version 5 CO Retrieval With DACOM *In Situ* Measurements During INTEX-A and –B, *IEEE Trans. on Geosci. Remote Sensing*, 10.1109/TGRS.2011.2106505, 2011

Sachse, G. W., Hill, G. F., Wade, L. O., and Perry, M. G.: Fast-response, high-precision carbon monoxide sensor using a tunable diode laser absorption technique, *J. Geophys. Res.*, 92, 2071–2081, 1987.

Singh, H. B., Brune, W. H., Crawford, J. H., Flocke, F., and Jacob, D. J.: Chemistry and transport of pollution over the Gulf of Mexico and the Pacific: Spring 2006 INTEX-B Campaign overview and first results, *Atmos. Chem. Phys. Discuss.*, 9, 363-409, 2009.

Warner, J. X., Wei, Z., Strow, L. L., Barnet, C. D., Sparling, L. C., Diskin, G., and Sachse, G., 2010: Improved Agreement of AIRS Tropospheric Carbon Monoxide Products with other EOS Sensors Using Optimal Estimation Retrievals, *Atmos. Chem. Phys.*, 10, 9521-9533, doi:10.5194/acp-10-9521-2010.

Version 6 Performance and Test Report

3.11.3 Ozone

Tester and Point of Contact: Frederick (Bill) Irion

Testing of AIRS Versions 5, 6 and 6 AIRS-only¹ total column ozone retrievals were made by comparisons against coincident measurements by the Ozone Monitoring Instrument (OMI). This testing was meant to be a comparison of the total columns between the AIRS versions and to check for pathologies in V6, and not as a rigorous validation of AIRS ozone.

For total column ozone, we tested against one day of OMI data, Feb 24, 2007, using the Version 3 OMI Level 3e product, which has a $0.25^\circ \times 0.25^\circ$ gridding. AIRS and OMI total ozone observations were compared if the geographical center of the AIRS observation was within the OMI grid box. As OMI relies on backscattered UV radiation, only sunlit measurements of AIRS could be used.

Figure 77 below compares the relative difference between V5 and V6 AIRS and OMI total ozone (calculated as $(\text{AIRS}-\text{OMI})/\text{OMI}$ in percent). The general pattern is similar in both versions, with significant regional biases, and that the number of observations has increased in V6. Also, the negative bias over a large region over the interior of Antarctica in Version 5 has shown improvement in Version 6. Table 1 compares V5 and V6 AIRS against OMI, but binned by quality flag². (We note that AIRS V6 has better agreement than Version 5 for an unweighted average. However, if the differing areas of the OMI $0.25^\circ \times 0.25^\circ$ gridding is taken into account by weighting the average by the cosine of the latitude, the V6 agreement is slightly worse than V5.)

A comparison of the bias sensitivity to biases in the ocean skin temperature is shown in Figure 78. Here, we compare AIRS vs OMI ozone against AIRS vs Version 7 Advanced Microwave Scanning Radiometer – EOS (AMSR-E) ocean

¹ AIRS retrievals without using AMSU microwave data.

² Field names are ‘Qual_O3’ in Version 5, and ‘totO3Std_QC’ in Version 6. A quality flag of 0 is ‘best’, 1 is ‘good’, and 2 is ‘poor.’ Note that there are very few AIRS ozone observations with ozone quality flag = 1.

Version 6 Performance and Test Report

skin temperature³. In both AIRS V5 and V6, the relative ozone column bias compared to OMI increases as the AIRS minus AMSR-E temperature difference decrease. (Assuming OMI and AMSR-E as ‘truth,’ if the AIRS ocean skin temperature is too cold, then the retrieved ozone may become too high.) Errors in the ocean skin temperature may have a significant effect on the ozone bias. Taking data with an AIRS ozone quality flag equal to zero (‘best data’), a least-squares fit of the AIRS-OMI relative ozone bias vs. the AIRS-AMSR-E temperature bias (not shown) has a slope of $-0.43 \pm 0.01 \text{ %/K}$ for Version 5, and $-0.30 \pm 0.01 \text{ %/K}$ for Version 6, and $-0.34 \pm 0.01 \text{ %/K}$ for Version 6 AIRS-only.

Finally, we compare AIRS-OMI bias as a function of cloud top pressure and cloud fraction. The upper panel of Figure 79 compares the AIRS Version 5 relative ozone bias against a (linearly) weighted combined cloud-top pressure as retrieved by AIRS, while the lower panel shows the number of observations in each bin. (AIRS retrieves properties for up to two cloud layers.) Figure 80 shows the same for AIRS Version 6, and Figure 81 for Version 6 AIRS-only. Both Version 5 and 6 AIRS ozone show low average bias against OMI as a function of cloud pressure, although in both versions, a low bias is seen for lower pressure, thicker cloud amounts. Also, AIRS Version 6 shows better agreement than Version 5 at zero cloud. With no cloud, the relative bias for V5 AIRS-OMI is $(4.3 \pm 9.9) \text{ %}$ ($N=21611$), while that for V6 is $-(0.9 \pm 8.1) \text{ %}$ ($N=17697$), and for V6-AIRS only is $(0.85 \pm 7.62) \text{ %}$ ($N=16177$).

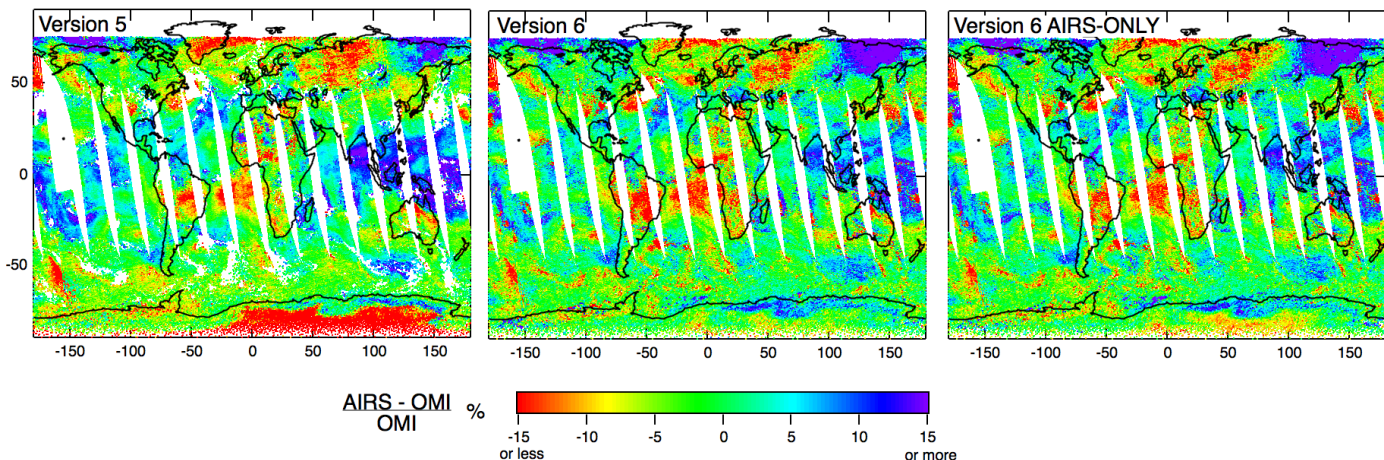


Figure 77 Relative bias of Versions 5, 6, and 6 AIRS-only and Version 3 OMI total ozone for Feb. 24, 2007.

³ AMSR-E data are produced by Remote Sensing Systems and sponsored by the NASA Earth Science MEaSUREs DISCOVER Project and the AMSR-E Science Team. Data are available at www.remss.com.

Version 6 Performance and Test Report

	Quality flag filter	V5 avg bias vs OMI (% $\pm 1\sigma$)	V5 number of comparisons	V6 avg bias vs OMI (% $\pm 1\sigma$)	V6 number of comparisons	V6 AIRS ONLY avg bias vs OMI (% $\pm 1\sigma$)	V6 AIRS ONLY number of comparisons
<i>Unweighted by cos(latitude)</i>	all	1.43 \pm 8.17	127477	0.77 \pm 8.11	148189	0.63 \pm 8.33	148131
	O ₃ qual flag = 0	1.30 \pm 7.89	113628	0.48 \pm 7.06	133098	0.41 \pm 6.91	127583
<i>Weighted by cos(latitude)</i>	all	0.12 \pm 2.70	127477	0.71 \pm 2.42	148189	0.43 \pm 2.49	148131
	O ₃ qual flag = 0	-0.08 \pm 2.40	113628	0.30 \pm 1.98	133098	0.05 \pm 1.82	127583

Table 4. Relative biases of V5, V6, and V6-AIRS only total ozone compared to OMI, filtered by quality flags, for sunlit observations of Feb. 24, 2007. The upper rows are unweighted averages, while the lower rows are averages weighted by cos(latitude).

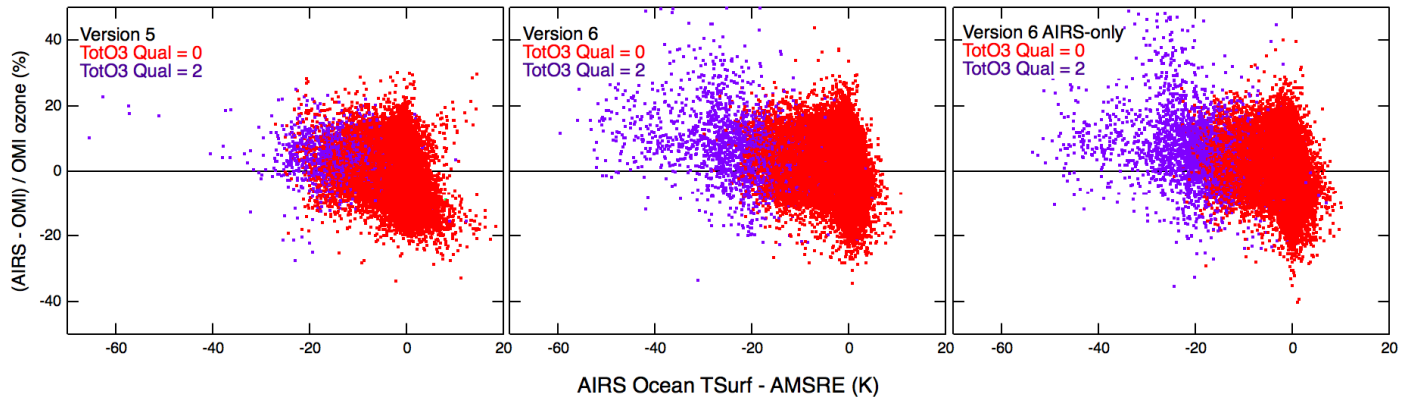


Figure 78 AIRS-OMI relative difference vs AIRS-AMSRe ocean surface temperature difference for Feb. 24, 2007.

Version 6 Performance and Test Report

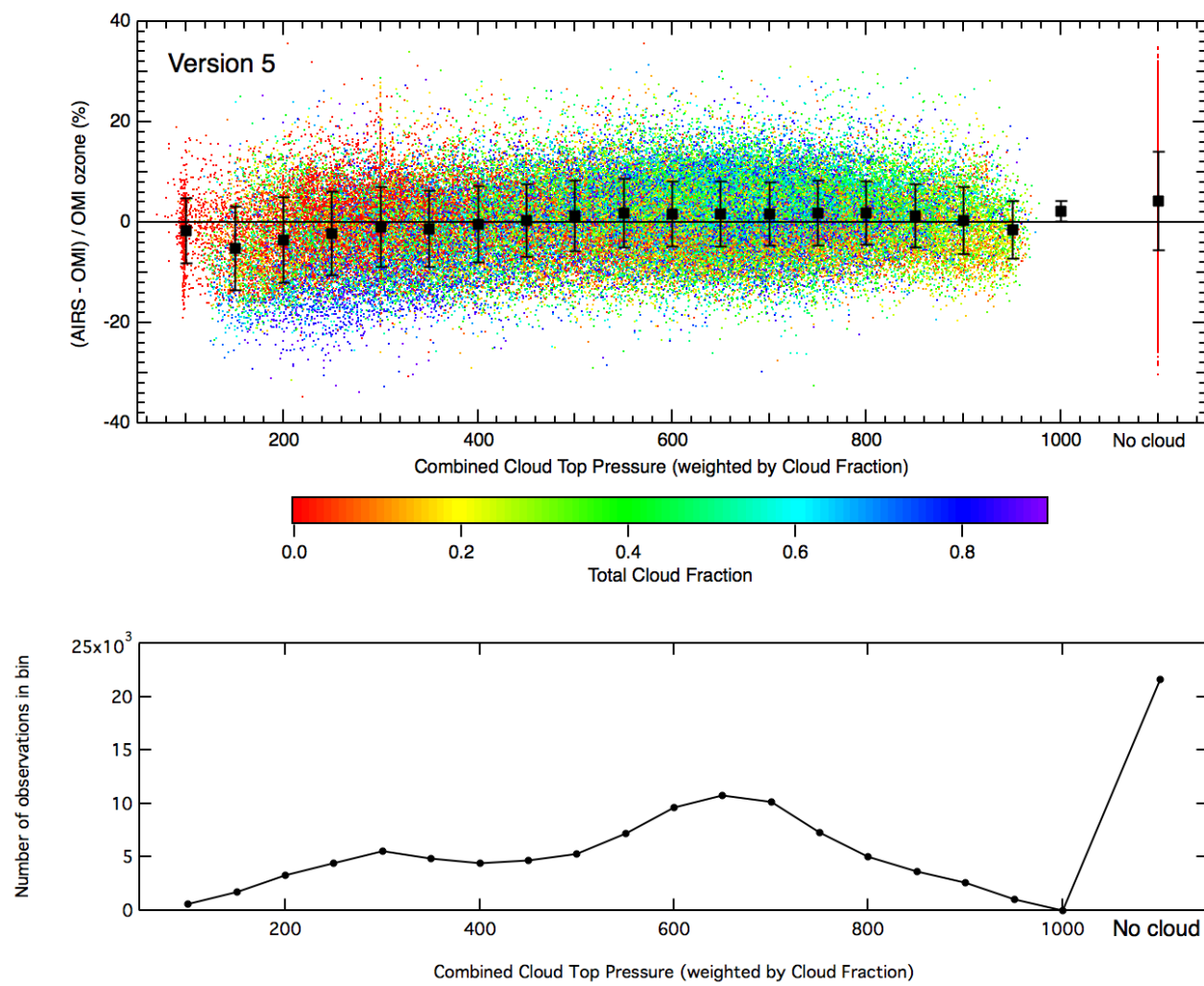


Figure 79 Version 5 AIRS-OMI relative ozone bias vs combined cloud-top pressure (top panel) and number of observations in bin (bottom panel) for sunlit observations of Feb. 24, 2007. Dots are colored by the total cloud fraction. The combined cloud-top pressure is the sum of the retrieved pressures weighted by the cloud fraction in each cloud layer.

Version 6 Performance and Test Report

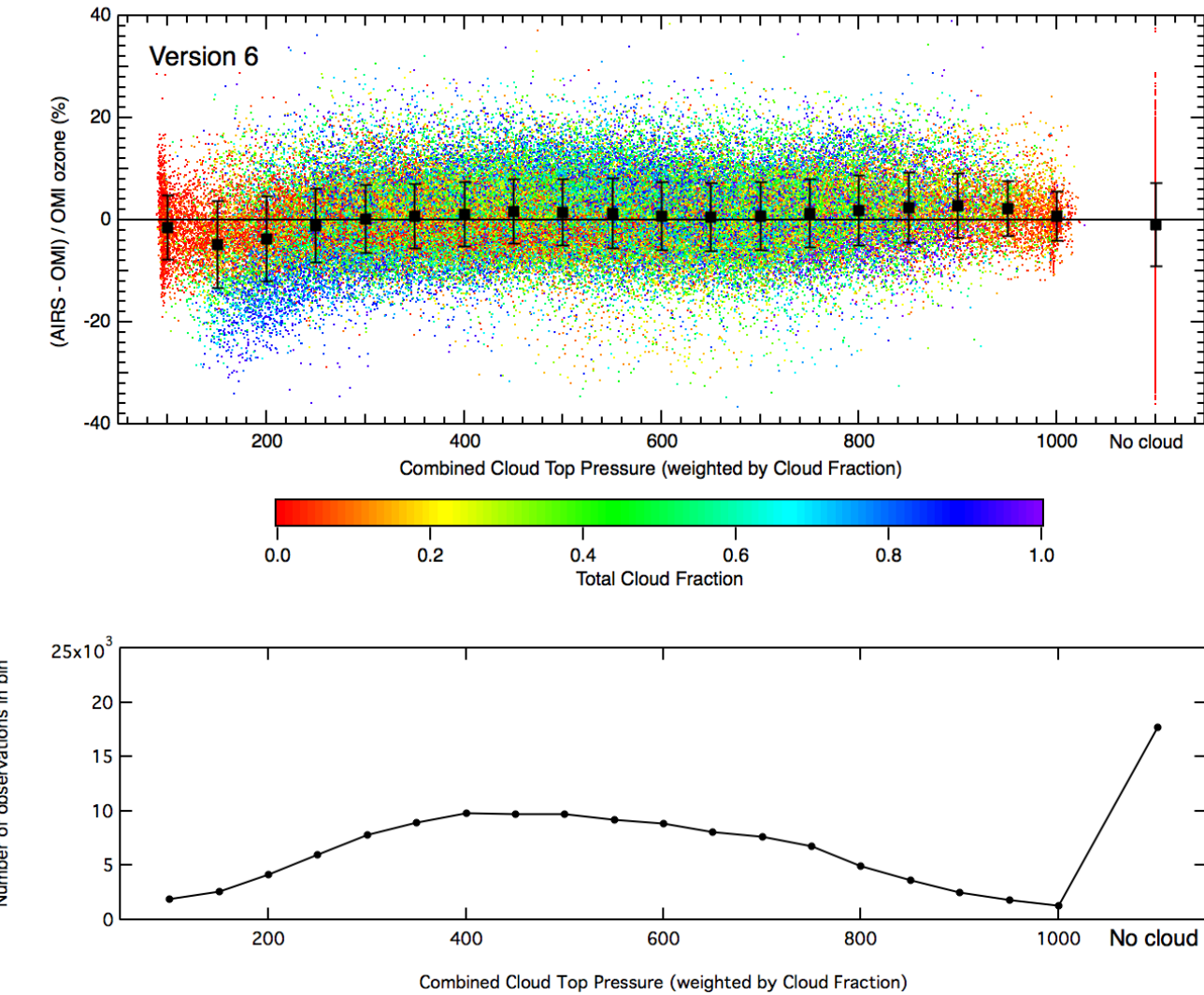


Figure 80 Version 6 AIRS-OMI relative ozone bias vs combined cloud-top pressure (top panel) and number of observations in bin (bottom panel) for sunlit observations of Feb. 24, 2007. Dots are colored by the total cloud fraction. The combined cloud-top pressure is the sum of the retrieved pressures weighted by the cloud fraction in each cloud layer.

Version 6 Performance and Test Report

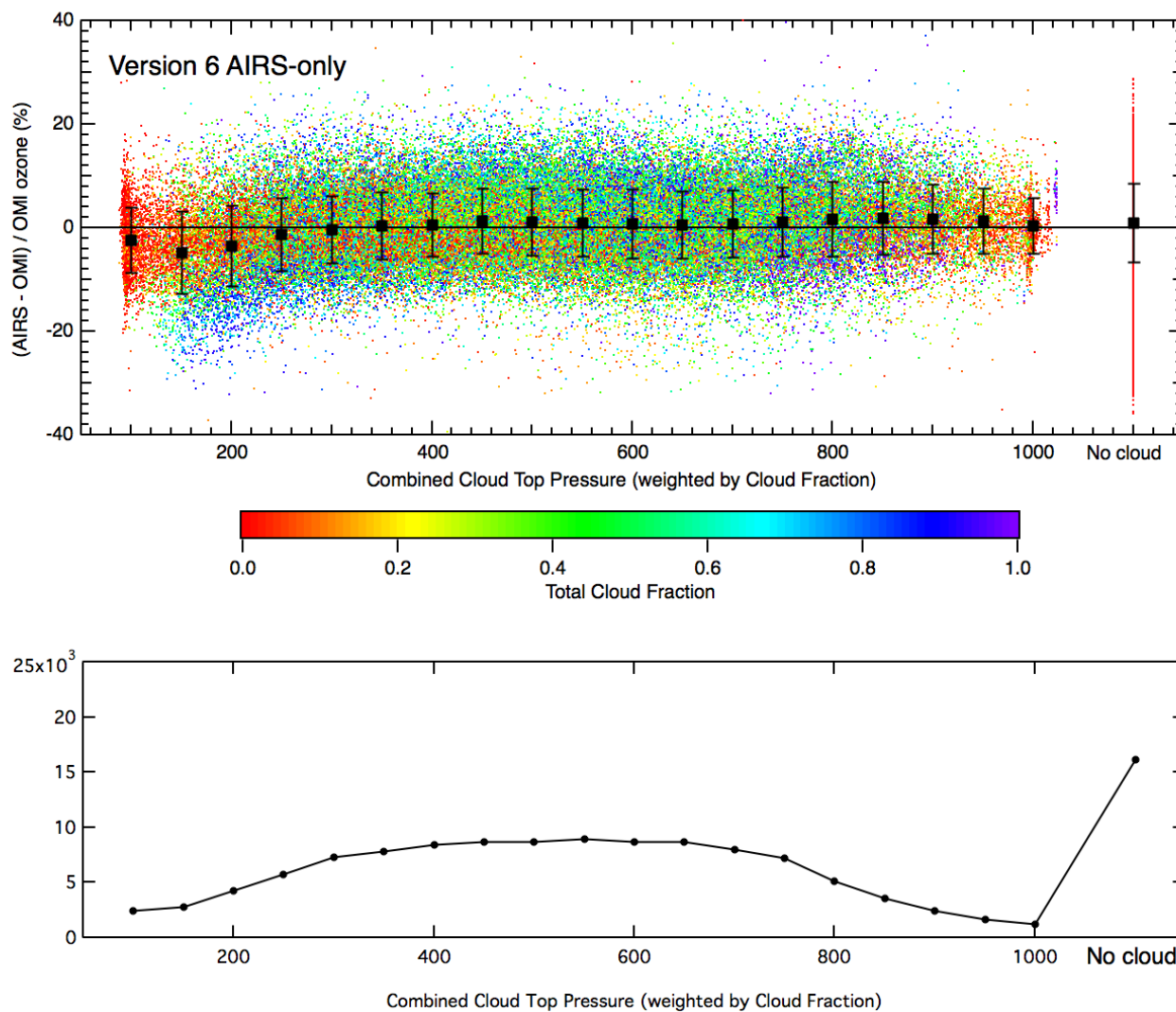


Figure 81 Version 6 AIRS only-OMI relative ozone bias vs combined cloud-top pressure (top panel) and number of observations in bin (bottom panel) for sunlit observations of Feb. 24, 2007. Dots are colored by the total cloud fraction. The combined cloud-top pressure is the sum of the retrieved pressures weighted by the cloud fraction in each cloud layer.

Version 6 Performance and Test Report

3.12. Tropopause Pressure and Height

Tester and Point of Contact: Baijun Tian

Data Products	Description
PTropopause	
PTropopause_QC	
GP_Tropopause	
GP_Tropopause_QC	
T_Tropopause	
T_Tropopause_QC	

In this report, we are reporting the testing results of the AIRS V6.0.2 (V6) L3 tropopause products including tropopause pressure (TropPres), tropopause temperature (TropTemp), and tropopause height (TropHeight). By examining the spatial patterns of the tropopause products for the ascending node of January 1st, 2007, we found that the AIRS V6 tropopause products are reasonable and can capture the general global features of tropopause. For example, the AIRS V6 tropopause products show that tropical tropopause is high in height, low in pressure, and cold in temperature. On the other hand, middle- and high-latitude tropopause is low in height, high in pressure, and warm in temperature. There is a sharp transition in the subtropics between the tropical tropopause and middle- and high-latitude tropopause. The AIRS V6 tropopause products can also capture the wave pattern of the middle-latitude tropopause. Furthermore, comparing the AIRS V5 and V6 tropopause products, we found that the yield is much higher in V6 and the AIRS tropopause products are much better in terms of spatial coverage in V6. Since the AIRS V6 L3 tropopause products are gridded average of the AIRS V6 L2 tropopause products (e.g., PTropopause, T_Tropopause, and GP_Tropopause) with QC applied. This means the AIRS V6 L2 tropopause products are generally reasonable too.

Version 6 Performance and Test Report

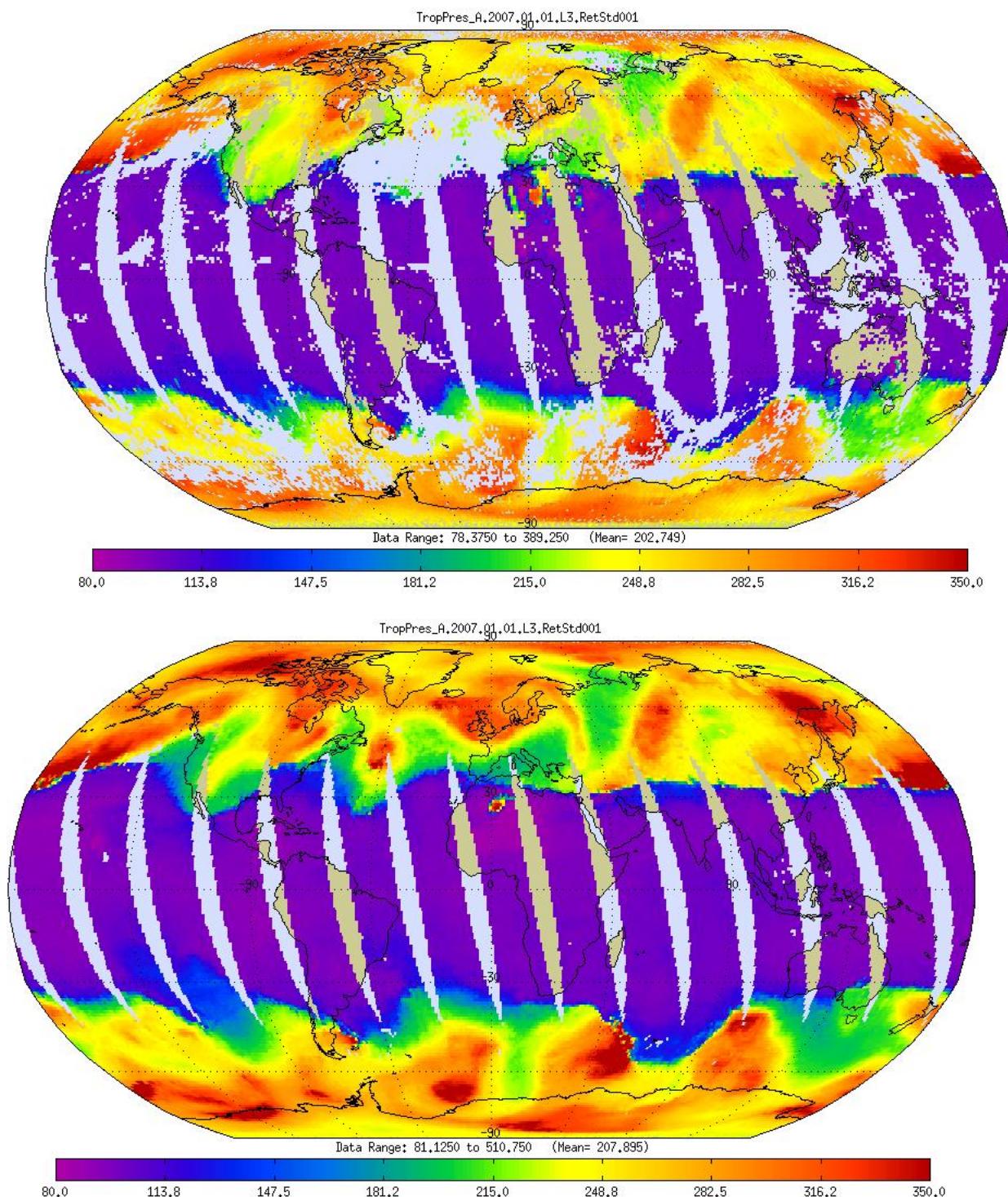


Figure 82. The AIRS tropopause pressure (TropPres) for the ascending node of January 1st, 2007. The upper panel is for V5 and the lower panel is for V6.

Version 6 Performance and Test Report

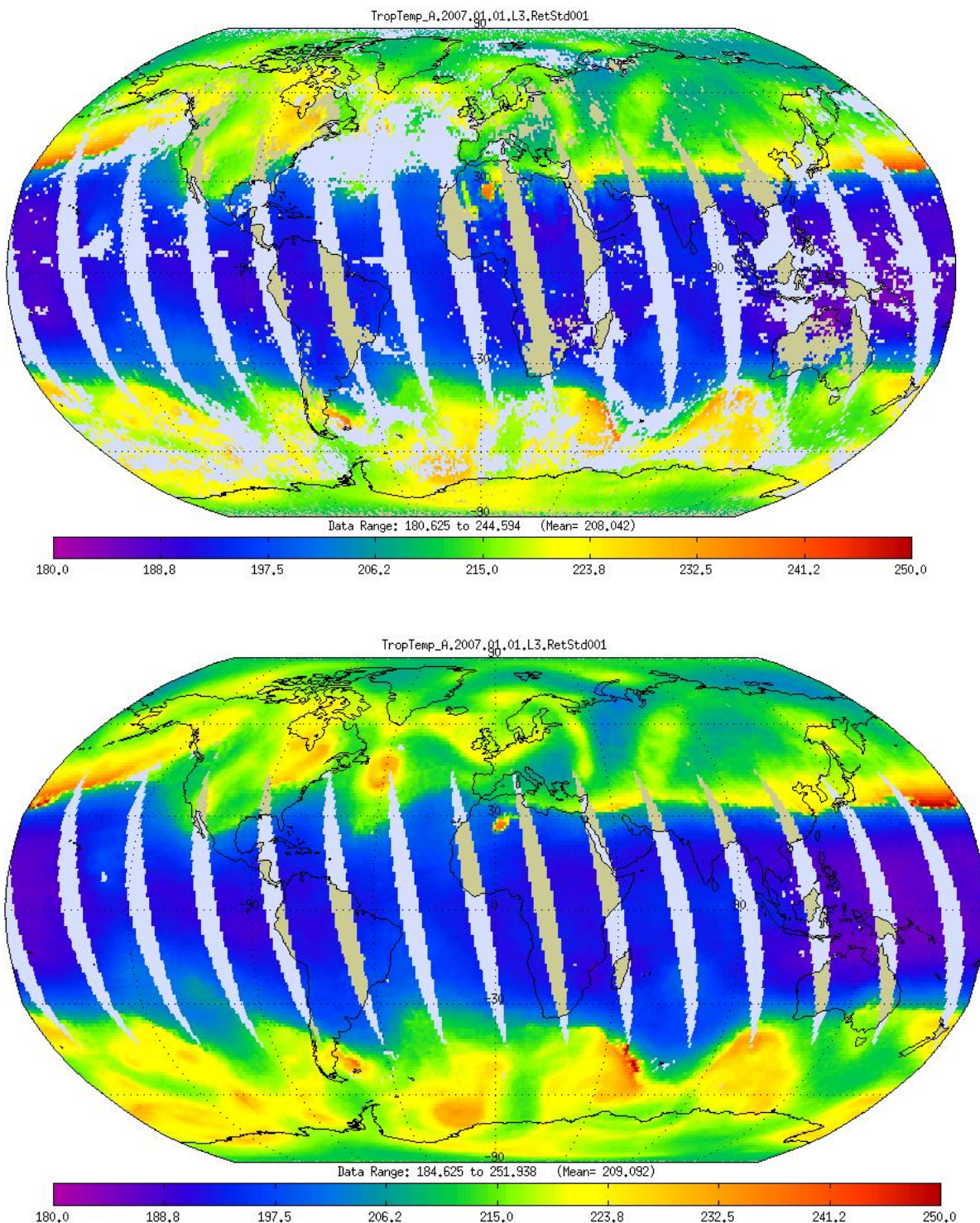


Figure 83. The AIRS tropopause temperature (TropTemp) for the ascending node of January 1st, 2007. The upper panel is for V5 and the lower panel is for V6..

Version 6 Performance and Test Report

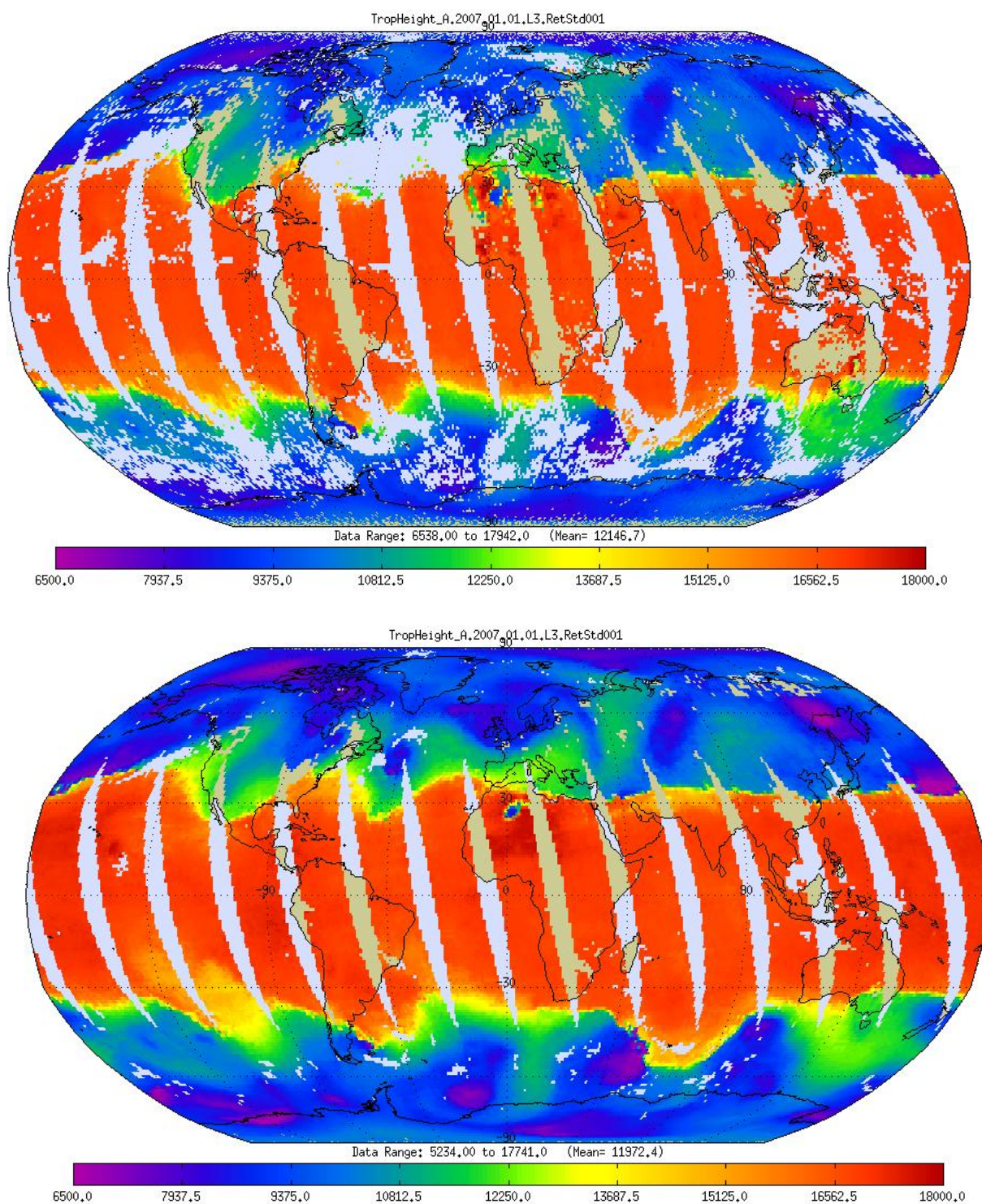


Figure 84. The AIRS tropopause height (TropHeight) for the ascending node of January 1st, 2007. The upper panel is for V5 and the lower panel is for V6.

Version 6 Performance and Test Report

3.13. Height of Top of Boundary Layer

Tester: Brian Kahn Point of Contact: Joao Teixeira

The AIRS V6 planetary boundary layer (PBL) top product (pbl_height) and associated quality control (pbl_height_qc) are reported on the AMSU FOV, since it uses the vertical positioning of thermodynamic profile gradients to locate the top of the PBL. This height is reported in units of pressure (hPa). The QC, as with most of the Standard and Support product fields, are reported in three bins: QC=0 (best), QC=1 (good), and QC=2 (do not use). (Note that FOVs over land have QC=2. Often, the pbl_height values are still reported, but they have not been determined to be of sufficient quality for use at this time. Use any value of pbl_height over land with great caution.)

The following January 2003 monthly map examples for the full AIRS/AMSU retrieval (Figure 85) and the AIRS-only retrieval (Figure 86) are produced with QC=[0,1]. Observe in Figure 85 that the regions dominated by stratocumulus clouds contain significantly lower altitudes (higher pressures) for pbl_height. On a monthly average, there is a smooth transition towards higher altitudes (lower pressures) into the trade cumulus regimes. There are also shallower PBLs noted near south Asia and on the equatorial side of the southern hemisphere storm track. In other months (not shown), these features largely persist, but are found to move geographically and change in magnitude, consistent with expectations and previous research findings. For the AIRS-only retrieval in Figure 86, all of the features found with the AIRS/AMSU retrieval are basically preserved in the AIRS-only system, although in most regions globally, the depth of the PBL appears to be slightly more or less shallow, depending on the particular cloud regime of interest.

Version 6 Performance and Test Report

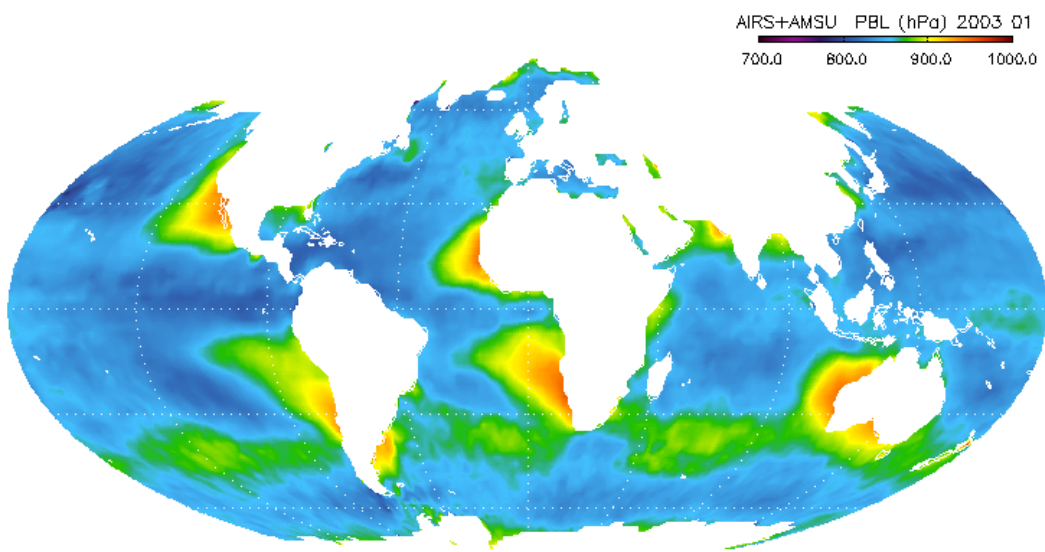


Figure 85 Monthly average (January 2003) PBL height (in pressure, hPa) for the AIRS+AMSU operational version 6 retrieval system.

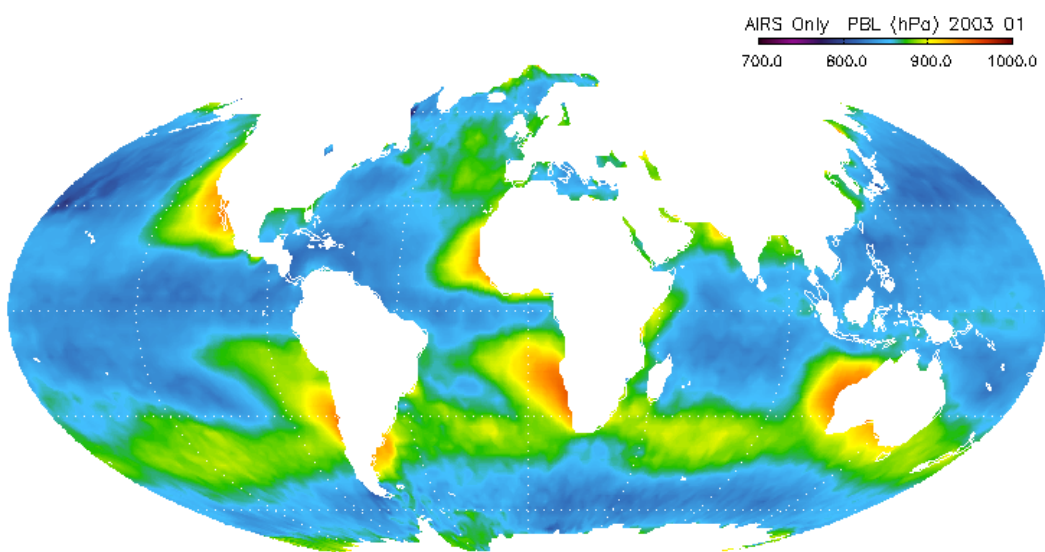


Figure 86 Monthly average (January 2003) PBL height (in pressure, hPa) for the AIRS-only operational version 6 retrieval system.

Version 6 Performance and Test Report

3.14. Cloud Cleared Radiances

Tester and Point of Contact: Larrabee Strow and Scott Hannon

The V6 Level-2 cloud-cleared radiances for Feb. 25, 2012 were evaluated using the known sea-surface temperature (SST) as the truth. The AIRS Calibration Data Set (ACDS) has high skill in finding clear ocean scenes for AIRS, which can be used to compare to the Level-2 cloud-cleared radiances. We concentrate here on the 1231 cm^{-1} , since it has very little atmospheric absorption, and is most sensitive to clouds of all optical depths. The Feb. 15 cloud-cleared radiances, and the ACDS clear scenes, are matched to the ECMWF forecast/analysis fields and the SARTA radiative transfer algorithm is used to compute simulated clear scene radiances. We evaluate the cloud-cleared radiances by comparing PDFs/histograms of the cloud-cleared radiance biases versus the ACDS clear radiance biases for the same day.

With AIRS products it is always difficult to make a coherent quality flag selection. In V6 each channel has its own cloud-cleared radiance quality flag. We decided to select scenes based on summing the radiance_QC metric (over channels). We then deemed spectra with the max of this sum < 400 to be “Best”, spectra with a sum maximum < 1200 as “Better”, and spectra with this sum maximum < 2400 to be “Good”. “Better” scenes are included in “Good”, “Best” scenes in “Better” and so on. For individual channels, 0 = highest quality, 1 = good quality, and 2 = do not use. Figure 87 shows a map of the cloud-cleared radiance quality for this day. “Good” spectra represent about 50% of all observations, removing a large number of North. Hemis. mid-latitude scenes for this winter day. Thus, the results we show here are representative of yields well below 100% even for “Good”. After subsetting all scenes to ± 60 deg ocean, night scenes, we find that the “Better” subset contains 40% of “Good” and “Best” contains about 10% of “Good”. We also matched these data to the Level-2 supplement file to get the estimated cloud-fraction.

Version 6 Performance and Test Report

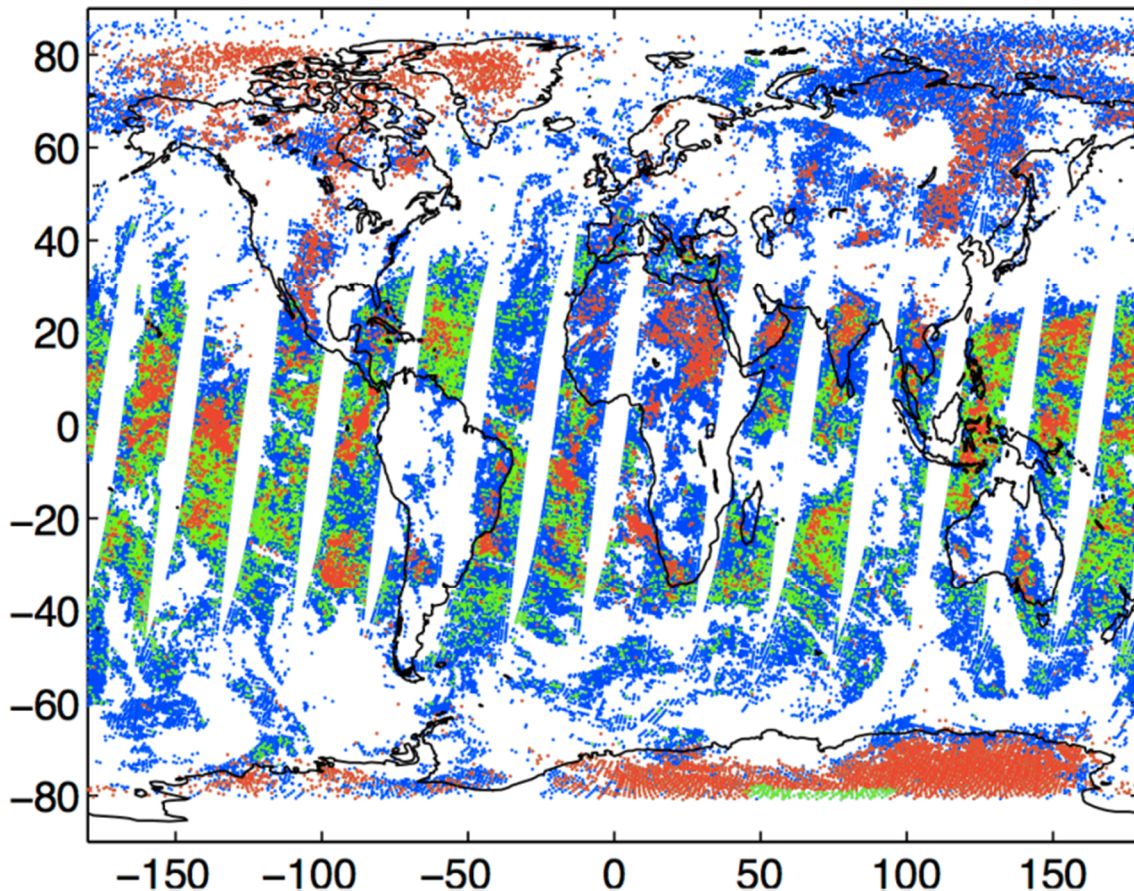


Figure 87 Map of cloud cleared radiance quality for Feb. 25, 2012. Good=blue, Better=green, Best=red.

Figure 88 shows the 1231 cm^{-1} histograms for Good, Better, and Best over ± 60 degree ocean, as well as histograms for the AIRS ACDS clear ocean and for ACDS land-only clear. The ACDS ocean PDF exhibits a width well below 1K, approaching some combination of the AIRS noise and SST model errors. All three cloud-cleared PDFs are wider. The Better and Good PDFs show higher negative wings indicative of cloud-contamination. The width of the Good PDF is about 2K. This is not surprising, and the cloud-cleared radiance product attempts to assign uncertainties to these radiances that are used in the retrieval.

Version 6 Performance and Test Report

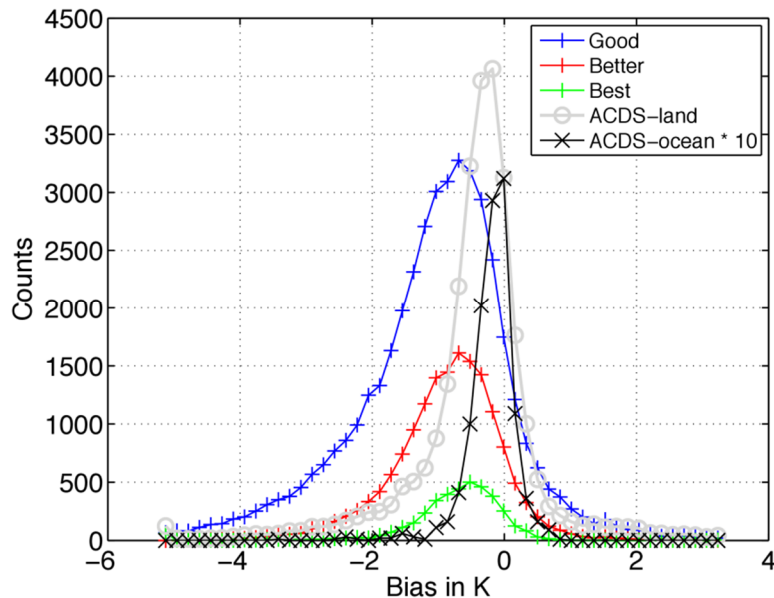


Figure 88 Bias histograms of cloud-cleared versus sea-surface temperature between ± 60 deg latitude. Also shown is the AIRS Calibration Data Set (ACDS) “very” clear bias histogram and the ACDS bias over land (versus ECMWF land surface temperatures).

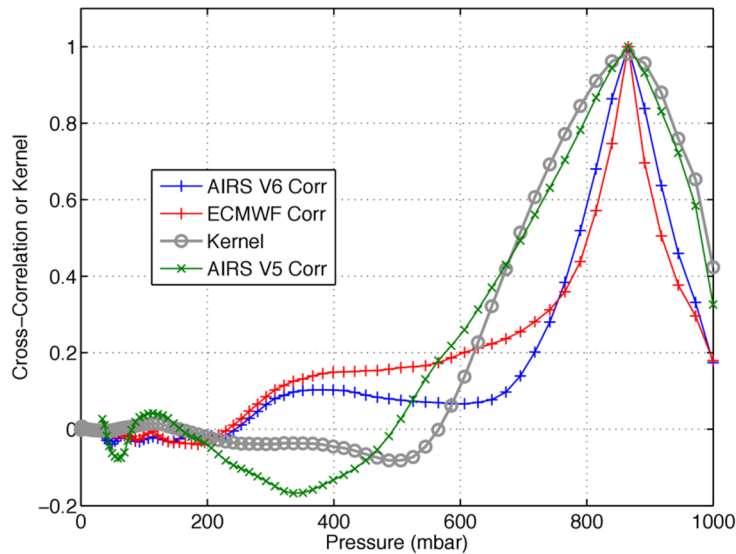


Figure 89 Comparison of widths of AIRS V5 and V6 covariances versus kernel function widths near 850 mbar. Also shown is the ECMWF 850 mbar covariance.

Version 6 Performance and Test Report

A more detailed look at the cloud-cleared radiances in the mid-latitudes remind you that Figure 88 is to some degree dominated by tropical scenes that are relatively easy to handle with cloud-clearing. Figure 90 shows the PDFs of the Good scenes for 30N-60N and 30S-60S ocean. The ACDS clear PDF is shown for comparison. Here we see very significant cloud-contamination, with a very unsymmetrical PDF that has significant population even 4K away from zero bias.

We have concentrated on two topics thus far, guided by the fact that the present CLARREO mission has been cancelled. First, following our proposal, we are examining the utility of using changes in radiance (or brightness temperature) probability distribution functions (PDFs) as a means of monitoring climate change with infrared hyperspectral sensors.

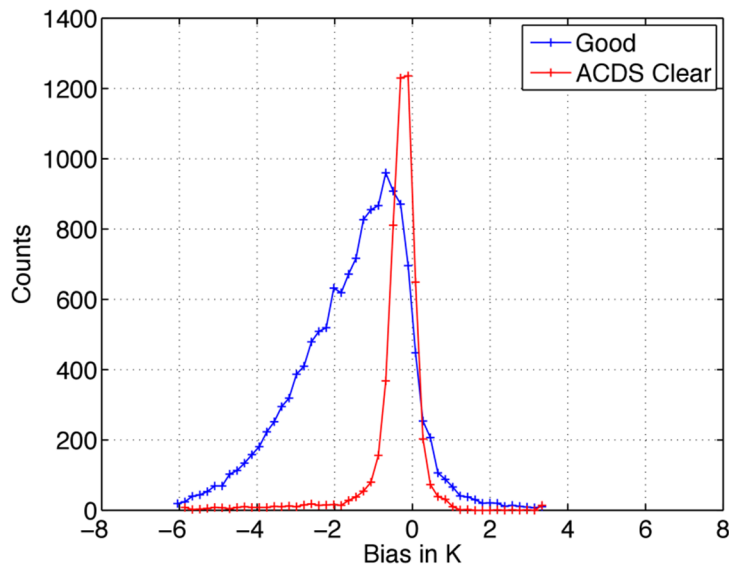


Figure 90 Similar bias histograms as in Figure 88 but now for combined latitudes of 30N-60N and 30S-60S and only for “Good” cloud-cleared radiances. The ACDS clear bias histogram is shown for reference. Clearly the cloud-cleared radiances contain significant cloud contamination.

One question to ask would be, how good is cloud-clearing when the field-of-regard contains a “manageable” cloud fraction. Clearly with high cloud amounts cloud-clearing will not work. To address this we selected all scenes (Good,

Version 6 Performance and Test Report

Better, Best) with 25-50% cloud fraction (according to the L2 Supplement file) for the 30-70 deg N/S latitude range. Figure 91 shows the PDFs for this subset. Here we indeed see a nice peak near zero bias, but with significant wings beyond -5K. In this case we also observed some positive wings that are presumably due to cloud-clearing errors.

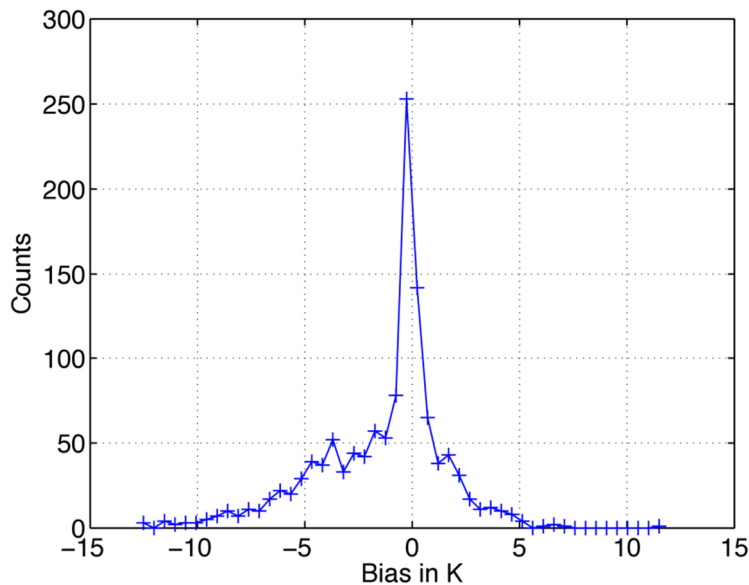


Figure 91 Bias histograms for cloud-cleared ocean radiances for 30-70 deg N/S but subsetted for observations (according to L2 Supplemental product) with cloud fraction ranging from 25-50%.

Since the 1231 cm^{-1} is primarily a surface channel, one expects it to exhibit the larger cloud-clearing errors than for more opaque channels. Thus, this study mostly examines the cloud-clearing errors that would impact the lower altitudes in the retrieval products. However, it must be remembered that in order to get even roughly 50% yield, one is introducing many scenes with several K of cloud contamination into the retrieval process.

Version 6 Performance and Test Report

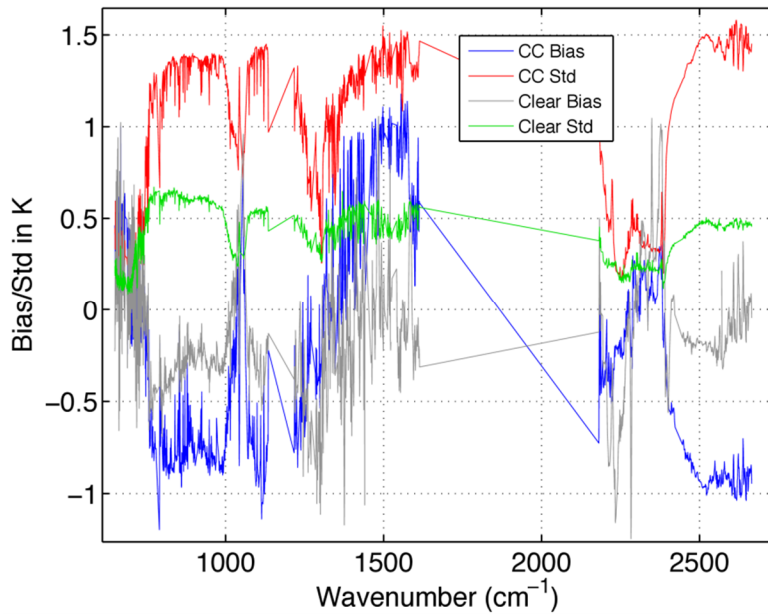


Figure 92: Bias and standard deviations for cloud-cleared and clear scenes for ± 60 degrees, ocean, night.

Bias and standard deviation statistics for “Good” scenes, over ocean, ± 60 deg. latitude, night, are shown in Figure 92 for all channels. Under these observing conditions the spectra computed from ECMWF model fields should be very accurate, with several tenths of a K offset for SST due to diurnal variations and evaporative cooling. Also shown for reference are the bias and standard deviation for the AIRS ACDS clear spectra for this observing subset.

Version 6 Performance and Test Report

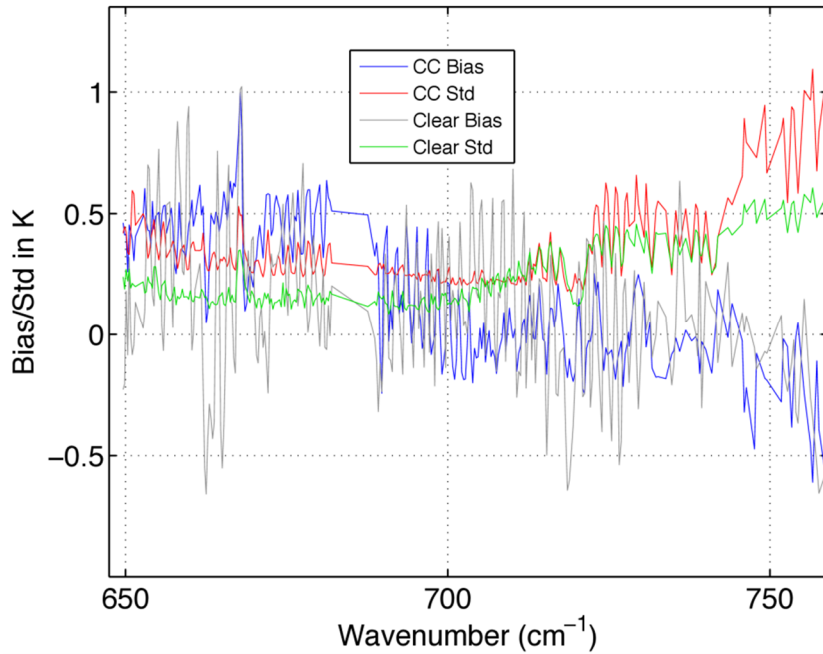


Figure 93: Zoom of Figure 92

These averaged results are quite good in that the cloud-cleared scenes only contain about 0.5K of cloud-contamination in general, with a standard deviation about 2.5 time larger (in window regions). Figure 93 is a zoom of Figure 92 and shows that the cloud-cleared standard deviation for this day approaches the clear standard deviation in the 700-750 cm⁻¹. However, at the longest wavelengths the clear standard deviation is still slightly smaller, where one might expect the cloud-cleared variance to be smaller due to scene averaging. However, these differences (and differences in the biases) are quite small and could easily be due to differential sampling of the cloud-cleared and clear scenes.

Version 6 Performance and Test Report

3.15. SO₂ Brightness Temperature and Flag

Tester: Juying Warner

BT_diff_SO ₂	32-bit floating-point	AIRSTrack (= 3) * AIRSXTrack (= 3)	SO ₂ determined from brightness differences
NumSO2FOVs (per-granule)	16-bit integer	One number per granule	Number of Field-Of-Views with high SO ₂ per granule
BT_diff_SO ₂ _QC	16-bit unsigned integer	AIRSTrack (= 3) * AIRSXTrack (= 3)	Quality Control for SO ₂ products

This section describes the AIRS V6 sulfur dioxide (SO₂) products defined in Table 1, the tests, and the preliminary validation for these products. To test the V6 SO₂ product, the AIRS dataset from May 27-30, 2011 over Iceland is used to compare against the Ozone Monitoring Instrument (OMI) SO₂ measurements, also on the Aqua platform. The V6 SO₂ products are further compared with the V5 products to evaluate any improvements.

AIRS V6 products provide an indicator of SO₂ release from volcanoes using the brightness temperature difference $\Delta\text{Tb}=\text{Tb}(1361.44 \text{ cm}^{-1})-\text{Tb}(1433.06 \text{ cm}^{-1})$. Values under -6K are likely to be associated with volcanic SO₂. A number of fields-of-views (NumSO2FOVs>=1), out of a nominal 1350, with a significant SO₂ concentration based on the value of BT_diff_SO₂ is used to alarm volcanologists for possible volcanic eruptions. The Quality Control codes for BT_diff_SO₂ is similar to other AIRS V6 trace gas products (0: Highest Quality; 1: Good; 2: Do Not Use.)

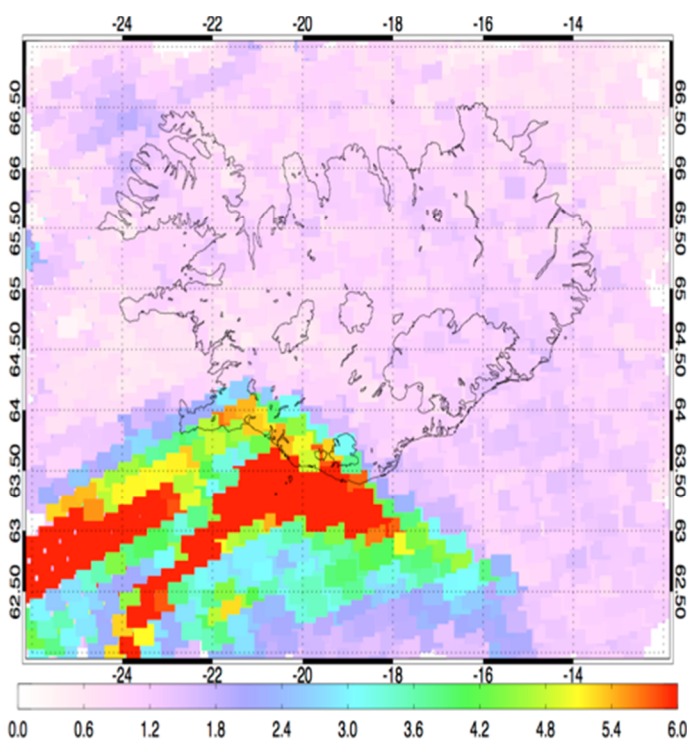
AIRS V6 SO₂ flags are compared with the Aura/OMI SO₂ total columns (in DU) during the Reykjavik, Iceland event on May 27, 2011 (see Figure 1). High SO₂ values (>2 DU) are observed off the Southwest coast of Iceland by OMI, which correlate well with AIRS SO₂ flag of high negative brightness temperature differences (<-3K). Although the volcanologists only receive alerts from the AIRS team when the SO₂ flag reaches -6K, smaller brightness temperature differences (-3 to -6K) indicate elevated SO₂ concentrations.

The differences of the SO₂ flags between AIRS V5 and V6 are minor since the threshold has not been changed with the new release. In addition, there is no difference in the SO₂

Version 6 Performance and Test Report

flags between AIRS retrievals using AMSU in the cloud-clearing process and using AIRS IR-only.

AIRS V6 ABS(Δ Tb) SO₂ flag, May 27/2011



Aura/OMI - 05/27/2011 13:44-13:46 UT
SO₂ mass: 17.363 kt; Area: 73909 km²; SO₂ max: 30.37 DU at lon: -20.18 lat: 63.38 ; 13:45UTC

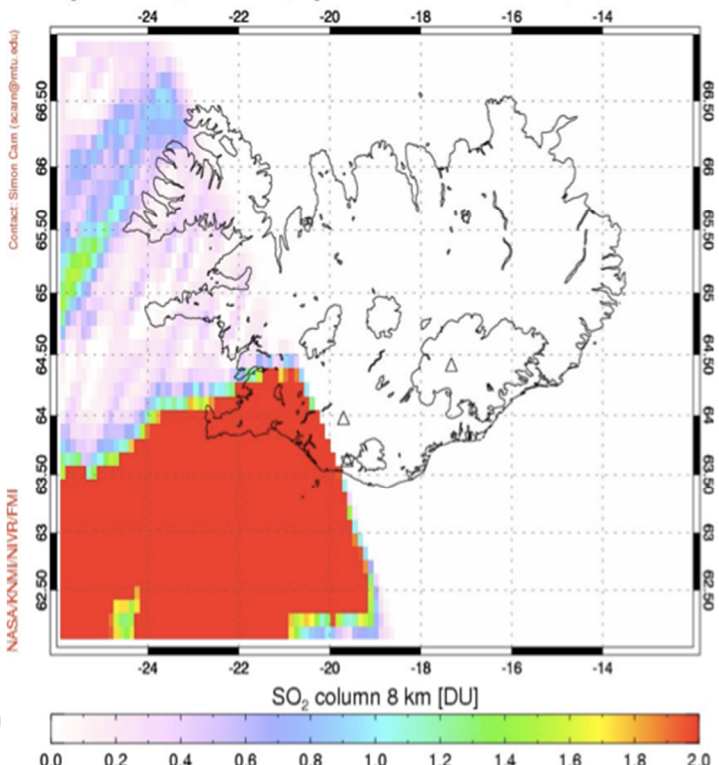


Figure 94. AIRS V6 SO₂ flags (left panel) shown with the absolute values of the brightness temperature differences compared against the Aura/OMI SO₂ total columns (DU) (right panel) over Reykjavik, Iceland on May 27, 2011

Reference:

- Krotkov, N.A., S.A. Carn, A.J. Krueger, P.K. Bhartia, and K. Yang (2006). Band residual difference algorithm for retrieval of SO₂ from the Aura Ozone Monitoring Instrument (OMI). *IEEE Trans. Geosci. Remote Sensing, AURA special issue*, 44(5), 1259-1266, doi:10.1109/TGRS.2005.861932, 2006

Version 6 Performance and Test Report

3.16. *Dust Detection*

There has been no change to the dust algorithm from version 5 to version 6, hence there is not a test report produced for it.

Version 6 Performance and Test Report

3.17. Layer to level transformation

Tester and Point of Contact: Evan Fishbein

AIRS retrieval uses layer mean quantities for water vapor, ozone, carbon monoxide, and methane. Previous versions of AIRS products reported only column totals and layer quantities for these gases, and the previous sections of this test report address only those. V6 products also provide values for gas concentration at specific pressure levels. This section shows how water vapor level values compare to the original layer quantities. Layer vs. level differences for CO₃, CO, and CH₄ are much smaller.

The algorithm used to produce level values is a smoothing cubic spline, designed to preserve the retrieved information content while suppressing vertical structure which exceeds the instrument sensitivity.

Figure 95 shows the mixing ratio of the layer profile in comparison to the level profile of water vapor. AIRS water vapor retrievals lose information at 200-300 hPa and one can see in the image that a sharp transition occurs in that region for the layer profile. This type of structure is statistically improbable and error estimates indicate that this structure is not significant. The leveling algorithm removes the features as shown in the figure. However, the lower tropospheric structure, as depicted in same figure, is statistically significant and is retained, although attenuated. However, in some cases as shown in Figure 96, the smoothing can extend well into the lower stratosphere and lead to large differences with the layer profile. These differences are not important because AIRS is not sensitive to water vapor in this region.

Version 6 Performance and Test Report

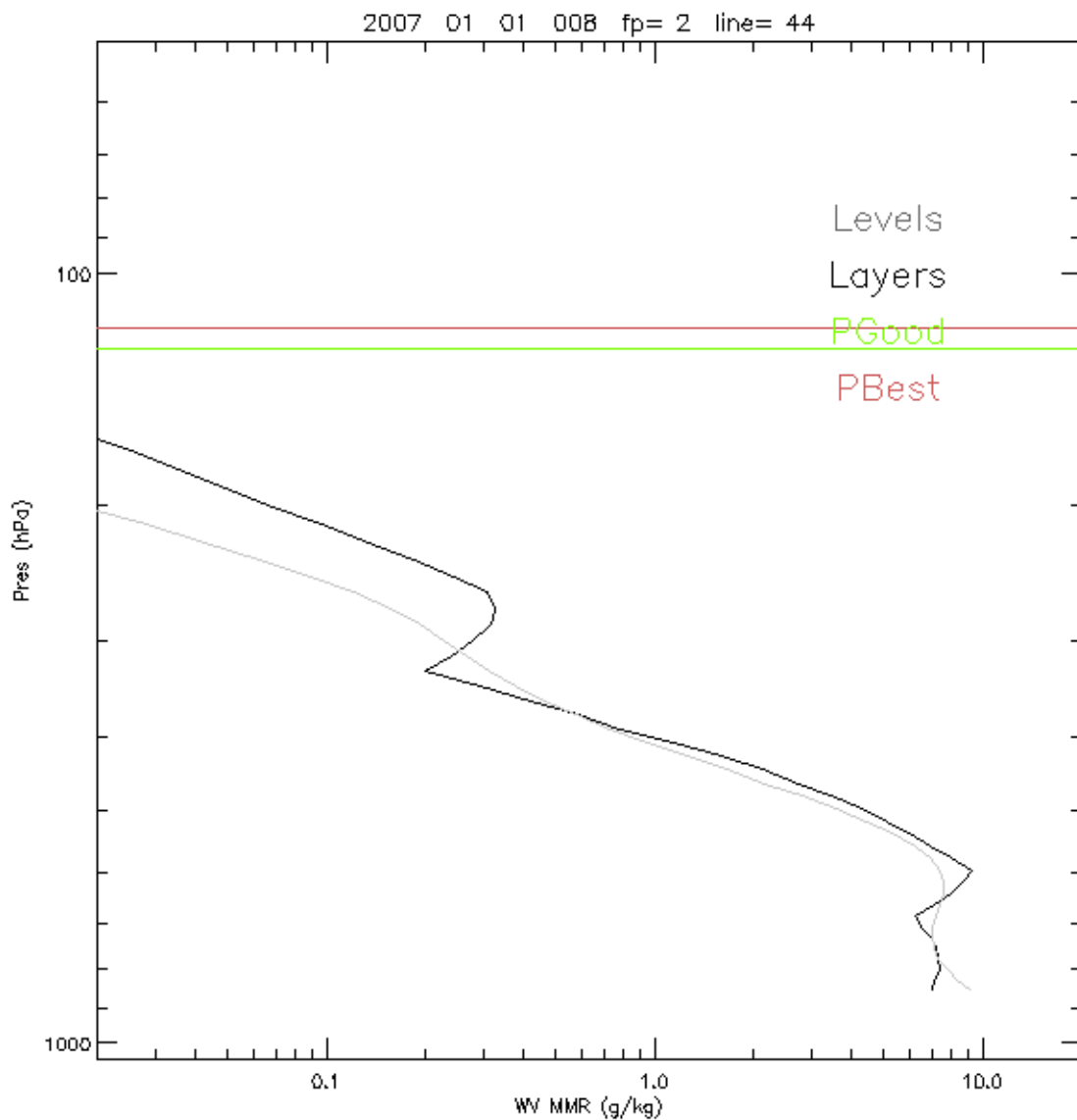


Figure 95 Layer and level profile comparison of water vapor from the support product.

Version 6 Performance and Test Report

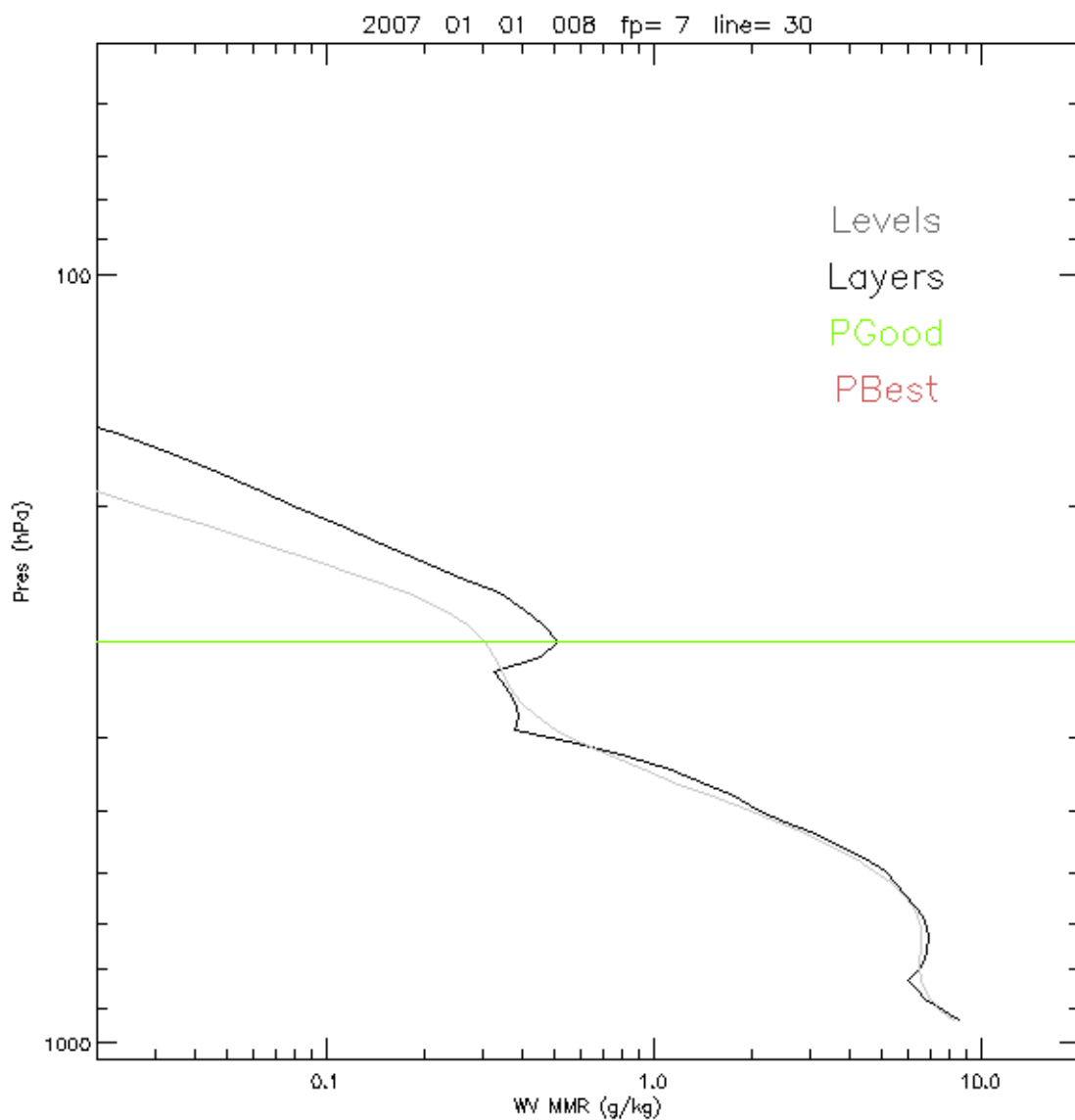


Figure 96 Layer and level profile comparison of water vapor from the support product.

Version 6 Performance and Test Report

4. APPENDIX A: Product tables

4.1. Standard products ('airx2ret')

Fieldname	Qual	NumGood	NumBad	Mean	[Min,	Max]
satheight		10800	0	714.5	[703.7,	730.3]
satroll		10800	0	-0.0004961	[-0.03416,	0.03116]
satpitch		10800	0	-0.02367	[-0.03092,	-0.007053]
satyaw		10800	0	-0.0006888	[-0.03821,	0.03502]
satzen		323907	0	28.08	[1.73,	55.83]
satazi		323907	0	0.02965	[-180,	180]
solzen		323907	0	90.55	[14.77,	165.2]
solazi		172264	151643	-52.04	[-180,	180]
glintlat		5353	5447	7.832	[-65.87,	75.93]
glintlon		5353	5447	-0.7059	[-180,	180]
sun_glint_distance		323907	0	1.554e+04	[0,	3e+04]
nadirTAI		10800	0	3.055e+08	[3.054e+08,	3.055e+08]
sat_lat		10800	0	-1.526	[-81.87,	81.87]
sat_lon		10800	0	-0.4735	[-180,	180]
scan_node_type		10800	0	66.51	[65,	68]
topog		323907	0	343.1	[-82.4,	5805]
topog_err		323907	0	32.41	[0,	1437]
landFrac		323907	0	0.3314	[0,	1]
landFrac_err		323907	0	0.03044	[0,	0.471]
satgeoqa		10800	0	0	[0,	0]
glintgeoqa		10800	0	1.025	[0,	77]
moongeoqa		10800	0	9.259e-05	[0,	1]
latAIRS		2915325	675	-1.529	[-89.89,	89.91]
lonAIRS		2915325	675	-0.5426	[-180,	180]
PSurfStd		323907	0	970.3	[500.6,	1033]
PSurfStd	Q0	323907	0	970.3	[500.6,	1033]
nSurfStd		323907	0	2.703	[2,	7]
PBest		323907	0	485.1	[0,	1033]
PGood		323907	0	912.2	[0,	1033]
nBestStd		323907	0	7.645	[2,	29]
nGoodStd		323907	0	3.329	[2,	29]
TSurfStd		323907	0	278.8	[189.2,	339.8]
TSurfStd	Q0	55085	0	296	[261.8,	305.2]
TSurfStd	Q1	142308	0	274.9	[189.2,	339.8]
TSurfStd	Q2	126514	0	275.6	[189.8,	339.1]
TSurfStdErr		323907	0	3.623	[0.25,	50]
TSurfStdErr	Q0	55085	0	0.7598	[0.25,	1.1]
TSurfStdErr	Q1	142308	0	3.269	[0.7,	7]
TSurfStdErr	Q2	126514	0	5.269	[0.7,	50]
numHingeSurf		323907	0	39	[39,	39]
freqEmis		12636000	19764000	1380	[649.3,	2632]
freqEmis(649)		323907	0	649.3	[649.3,	649.3]
freqEmis(725)		323907	0	724.6	[724.6,	724.6]
freqEmis(909)		323907	0	909.1	[909.1,	909.1]
freqEmis(1163)		323907	0	1163	[1163,	1163]
freqEmis(1205)		323907	0	1205	[1205,	1205]
freqEmis(1639)		323907	0	1639	[1639,	1639]
freqEmis(2174)		323907	0	2174	[2174,	2174]
freqEmis(2381)		323907	0	2381	[2381,	2381]
freqEmis(2500)		323907	0	2500	[2500,	2500]
freqEmis(2632)		323907	0	2632	[2632,	2632]
emisIRStd		12594114	19805886	0.9668	[0.4419,	1]
emisIRStd	Q0	2148315	0	0.9725	[0.8783,	1]
emisIRStd	Q1	5550012	0	0.9644	[0.4419,	1]
emisIRStd	Q2	4895787	19805886	0.9671	[0.4429,	1]
emisIRStd(649)		322926	981	0.9522	[0.7562,	1]
emisIRStd(649)	Q0	55085	0	0.9391	[0.8783,	0.9934]
emisIRStd(649)	Q1	142308	0	0.9637	[0.7569,	1]
emisIRStd(649)	Q2	125533	981	0.9449	[0.7562,	1]
emisIRStd(725)		322926	981	0.9599	[0.8264,	1]
emisIRStd(725)	Q0	55085	0	0.955	[0.8988,	0.9954]
emisIRStd(725)	Q1	142308	0	0.9652	[0.8276,	1]
emisIRStd(725)	Q2	125533	981	0.9561	[0.8264,	1]

Version 6 Performance and Test Report

emisIRStd(909)		322926	981	0.9822	[0.8393,	1]
emisIRStd(909)	Q0	55085	0	0.9879	[0.9566,	1]
emisIRStd(909)	Q1	142308	0	0.977	[0.8711,	1]
emisIRStd(909)	Q2	125533	981	0.9857	[0.8393,	1]
emisIRStd(1163)		322926	981	0.9711	[0.6372,	1]
emisIRStd(1163)	Q0	55085	0	0.9802	[0.9405,	1]
emisIRStd(1163)	Q1	142308	0	0.9636	[0.6372,	1]
emisIRStd(1163)	Q2	125533	981	0.9755	[0.6572,	1]
emisIRStd(1205)		322926	981	0.9671	[0.6371,	1]
emisIRStd(1205)	Q0	55085	0	0.9792	[0.9388,	1]
emisIRStd(1205)	Q1	142308	0	0.9604	[0.6371,	1]
emisIRStd(1205)	Q2	125533	981	0.9693	[0.662,	1]
emisIRStd(1639)		322926	981	0.9677	[0.547,	1]
emisIRStd(1639)	Q0	55085	0	0.9718	[0.9222,	1]
emisIRStd(1639)	Q1	142308	0	0.9694	[0.727,	1]
emisIRStd(1639)	Q2	125533	981	0.9641	[0.547,	1]
emisIRStd(2174)		322926	981	0.9546	[0.5596,	1]
emisIRStd(2174)	Q0	55085	0	0.9728	[0.9323,	0.9978]
emisIRStd(2174)	Q1	142308	0	0.9471	[0.5621,	1]
emisIRStd(2174)	Q2	125533	981	0.9551	[0.5596,	1]
emisIRStd(2381)		322926	981	0.9504	[0.5084,	1]
emisIRStd(2381)	Q0	55085	0	0.9714	[0.9239,	0.9977]
emisIRStd(2381)	Q1	142308	0	0.9411	[0.5084,	1]
emisIRStd(2381)	Q2	125533	981	0.9518	[0.5214,	1]
emisIRStd(2500)		322926	981	0.9579	[0.6,	1]
emisIRStd(2500)	Q0	55085	0	0.9689	[0.9085,	0.9971]
emisIRStd(2500)	Q1	142308	0	0.9473	[0.6,	1]
emisIRStd(2500)	Q2	125533	981	0.9652	[0.6,	1]
emisIRStd(2632)		322926	981	0.9631	[0.6,	1]
emisIRStd(2632)	Q0	55085	0	0.9708	[0.9158,	1]
emisIRStd(2632)	Q1	142308	0	0.9543	[0.6,	1]
emisIRStd(2632)	Q2	125533	981	0.9697	[0.6,	1]
emisIRStdErr		12594114	19805886	0.01477	[0.005,	0.2229]
emisIRStdErr	Q0	2148315	0	0.005114	[0.005,	0.01217]
emisIRStdErr	Q1	5500012	0	0.01489	[0.01,	0.1116]
emisIRStdErr	Q2	4895787	19805886	0.01886	[0.01,	0.2229]
emisIRStdErr(649)		322926	981	0.01717	[0.005,	0.09752]
emisIRStdErr(649)	Q0	55085	0	0.006187	[0.005,	0.01217]
emisIRStdErr(649)	Q1	142308	0	0.01486	[0.01,	0.04862]
emisIRStdErr(649)	Q2	125533	981	0.02461	[0.01205,	0.09752]
emisIRStdErr(725)		322926	981	0.0152	[0.005,	0.06943]
emisIRStdErr(725)	Q0	55085	0	0.005133	[0.005,	0.01012]
emisIRStdErr(725)	Q1	142308	0	0.01446	[0.01,	0.03448]
emisIRStdErr(725)	Q2	125533	981	0.02039	[0.01,	0.06943]
emisIRStdErr(909)		322926	981	0.01353	[0.005,	0.06428]
emisIRStdErr(909)	Q0	55085	0	0.005	[0.005,	0.005]
emisIRStdErr(909)	Q1	142308	0	0.01428	[0.01,	0.02578]
emisIRStdErr(909)	Q2	125533	981	0.01643	[0.01,	0.06428]
emisIRStdErr(1163)		322926	981	0.01429	[0.005,	0.1371]
emisIRStdErr(1163)	Q0	55085	0	0.005001	[0.005,	0.005954]
emisIRStdErr(1163)	Q1	142308	0	0.01536	[0.01,	0.07255]
emisIRStdErr(1163)	Q2	125533	981	0.01716	[0.01,	0.1371]
emisIRStdErr(1205)		322926	981	0.01454	[0.005,	0.1352]
emisIRStdErr(1205)	Q0	55085	0	0.005003	[0.005,	0.006123]
emisIRStdErr(1205)	Q1	142308	0	0.01539	[0.01,	0.07258]
emisIRStdErr(1205)	Q2	125533	981	0.01776	[0.01,	0.1352]
emisIRStdErr(1639)		322926	981	0.01435	[0.005,	0.1812]
emisIRStdErr(1639)	Q0	55085	0	0.005041	[0.005,	0.007779]
emisIRStdErr(1639)	Q1	142308	0	0.01432	[0.01,	0.0546]
emisIRStdErr(1639)	Q2	125533	981	0.01848	[0.01,	0.1812]
emisIRStdErr(2174)		322926	981	0.01598	[0.005,	0.1761]
emisIRStdErr(2174)	Q0	55085	0	0.005022	[0.005,	0.006771]
emisIRStdErr(2174)	Q1	142308	0	0.0156	[0.01,	0.08758]
emisIRStdErr(2174)	Q2	125533	981	0.02122	[0.01,	0.1761]
emisIRStdErr(2381)		322926	981	0.01686	[0.005,	0.1915]
emisIRStdErr(2381)	Q0	55085	0	0.005032	[0.005,	0.007611]
emisIRStdErr(2381)	Q1	142308	0	0.01656	[0.01,	0.09831]
emisIRStdErr(2381)	Q2	125533	981	0.02238	[0.01,	0.1915]
emisIRStdErr(2500)		322926	981	0.01521	[0.005,	0.16]
emisIRStdErr(2500)	Q0	55085	0	0.005068	[0.005,	0.009147]
emisIRStdErr(2500)	Q1	142308	0	0.01571	[0.01,	0.08]
emisIRStdErr(2500)	Q2	125533	981	0.0191	[0.01,	0.16]
emisIRStdErr(2632)		322926	981	0.01496	[0.005,	0.16]

Version 6 Performance and Test Report

emisIRStdErr(2632)	Q0	55085	0	0.005058	[0.005,	0.008423]
emisIRStdErr(2632)	Q1	142308	0	0.0156	[0.01,	0.08]
emisIRStdErr(2632)	Q2	125533	981	0.01858	[0.01,	0.16]
TAirStd		8517674	554326	240	[180,	315.8]
TAirStd	Q0	6788301	0	235.3	[182.1,	312.7]
TAirStd	Q1	1502634	0	258.9	[182.5,	315.8]
TAirStd	Q2	226739	554326	254.5	[180,	313.3]
TAirStd(1000hPa)		186287	137620	287.1	[232.6,	315.8]
TAirStd(1000hPa)	Q0	40801	0	293.9	[254.8,	308.3]
TAirStd(1000hPa)	Q1	126779	0	286.4	[235.3,	315.8]
TAirStd(1000hPa)	Q2	18707	137620	276.9	[232.6,	313.3]
TAirStd(400hPa)		323907	0	243.1	[208.6,	270.3]
TAirStd(400hPa)	Q0	183900	0	247.4	[214.3,	264.6]
TAirStd(400hPa)	Q1	127401	0	236.8	[212.3,	269.4]
TAirStd(400hPa)	Q2	12606	0	245.2	[208.6,	270.3]
TAirStd(70hPa)		323907	0	209.4	[182.2,	232.2]
TAirStd(70hPa)	Q0	317523	0	209.5	[183.3,	232.2]
TAirStd(70hPa)	Q1	2761	0	206	[183.4,	232.1]
TAirStd(70hPa)	Q2	3623	0	206.5	[182.2,	231.7]
TAirStd(7.0hPa)		323907	0	232.6	[212.2,	253.7]
TAirStd(7.0hPa)	Q0	322921	0	232.6	[212.2,	253.7]
TAirStd(7.0hPa)	Q2	986	0	231.6	[216.8,	246.9]
TAirStd(0.5hPa)		323907	0	263.7	[243.7,	286]
TAirStd(0.5hPa)	Q0	322921	0	263.7	[243.7,	286]
TAirStd(0.5hPa)	Q2	986	0	263.6	[250,	283.7]
TAirStdErr		8517674	554326	1.945	[0.3,	50]
TAirStdErr	Q0	6788301	0	1.859	[0.3,	50]
TAirStdErr	Q1	1502634	0	1.269	[0.3,	8.525]
TAirStdErr	Q2	226739	554326	9.018	[0.3,	50]
TAirStdErr(1000hPa)		186287	137620	1.896	[0.3,	50]
TAirStdErr(1000hPa)	Q0	40801	0	0.8043	[0.3,	1.427]
TAirStdErr(1000hPa)	Q1	126779	0	1.635	[0.3,	5.52]
TAirStdErr(1000hPa)	Q2	18707	137620	6.042	[1.5,	50]
TAirStdErr(400hPa)		323907	0	0.9768	[0.3,	50]
TAirStdErr(400hPa)	Q0	183900	0	0.563	[0.3,	0.9072]
TAirStdErr(400hPa)	Q1	127401	0	1.039	[0.3,	2.988]
TAirStdErr(400hPa)	Q2	12606	0	6.383	[0.6315,	50]
TAirStdErr(70hPa)		323907	0	1.094	[0.3,	50]
TAirStdErr(70hPa)	Q0	317523	0	0.9055	[0.3,	3.906]
TAirStdErr(70hPa)	Q1	2761	0	2.531	[1.422,	4.19]
TAirStdErr(70hPa)	Q2	3623	0	16.54	[1.5,	50]
TAirStdErr(7.0hPa)		323907	0	1.708	[0.3,	50]
TAirStdErr(7.0hPa)	Q0	322921	0	1.561	[0.3,	29.74]
TAirStdErr(7.0hPa)	Q2	986	0	49.76	[1.713,	50]
TAirStdErr(0.5hPa)		323907	0	4.11	[0.3,	50]
TAirStdErr(0.5hPa)	Q0	322921	0	3.97	[0.3,	49.27]
TAirStdErr(0.5hPa)	Q2	986	0	49.78	[3.824,	50]
TSurfAir		323907	0	280.7	[203.8,	318.1]
TSurfAir	Q0	50324	0	290.6	[205.5,	313.9]
TSurfAir	Q1	229687	0	280.2	[203.8,	318.1]
TSurfAir	Q2	43896	0	272.2	[205.5,	316.7]
TSurfAirErr		323907	0	2.236	[0.3,	50]
TSurfAirErr	Q0	50324	0	0.9164	[0.3,	2.622]
TSurfAirErr	Q1	229687	0	1.864	[0.3,	8.627]
TSurfAirErr	Q2	43896	0	5.69	[1.5,	50]
Temp_dof		322926	981	6.245	[2.567,	8.847]
H20MMRSat		3982976	553024	2.614	[0.0003225,	48.66]
H20MMRSat	Q0	2273117	0	1.436	[0.0005606,	42.23]
H20MMRSat	Q1	1500647	0	4.363	[0.0005449,	48.66]
H20MMRSat	Q2	209212	553024	2.871	[0.0003225,	45.38]
H20MMRSat(1000hPa)		186287	137620	11.22	[0.343,	48.66]
H20MMRSat(1000hPa)	Q0	40801	0	14.94	[0.8252,	32.37]
H20MMRSat(1000hPa)	Q1	126779	0	10.77	[0.3948,	48.66]
H20MMRSat(1000hPa)	Q2	18707	137620	6.136	[0.343,	43.14]
H20MMRSat(700hPa)		310829	13078	5.036	[0.001378,	21.7]
H20MMRSat(700hPa)	Q0	81429	0	6.715	[0.06746,	14.34]
H20MMRSat(700hPa)	Q1	203263	0	4.635	[0.05527,	14.52]
H20MMRSat(700hPa)	Q2	26137	13078	2.919	[0.001378,	21.7]
H20MMRSat(400hPa)		323907	0	0.6425	[0.006669,	5.653]
H20MMRSat(400hPa)	Q0	183900	0	0.7965	[0.01188,	2.838]
H20MMRSat(400hPa)	Q1	127401	0	0.4078	[0.00903,	4.884]
H20MMRSat(400hPa)	Q2	12606	0	0.7671	[0.006669,	5.653]
H20MMRSat(200hPa)		323907	0	0.08934	[0.0003225,	0.5914]

Version 6 Performance and Test Report

H2OMMRSat(200hPa)	Q0	271961	0	0.08823	[0.0006641, 0.5914]
H2OMMRSat(200hPa)	Q1	44558	0	0.09829	[0.0005824, 0.5803]
H2OMMRSat(200hPa)	Q2	7388	0	0.07621	[0.0003225, 0.5128]
H2OMMRSat(70hPa)		323907	0	0.1636	[0.0008504, 1.128]
H2OMMRSat(70hPa)	Q0	317523	0	0.1644	[0.0009429, 1.128]
H2OMMRSat(70hPa)	Q1	2761	0	0.123	[0.001006, 1.058]
H2OMMRSat(70hPa)	Q2	3623	0	0.1208	[0.0008504, 1.035]
H2OMMRSatLevStd		4306883	553117	2.865	[0.0002223, 61.37]
H2OMMRSatLevStd	Q0	2592570	0	1.537	[0.0005064, 55.41]
H2OMMRSatLevStd	Q1	1502100	0	5.099	[0.0004817, 61.37]
H2OMMRSatLevStd	Q2	212213	553117	3.272	[0.0002223, 54.06]
H2OMMRSatLevStd(1000hPa)		186287	137620	12.72	[0.07497, 61.37]
H2OMMRSatLevStd(1000hPa)	Q0	40801	0	17.09	[0.755, 38.97]
H2OMMRSatLevStd(1000hPa)	Q1	126779	0	12.15	[0.1023, 61.37]
H2OMMRSatLevStd(1000hPa)	Q2	18707	137620	7.039	[0.07497, 52.57]
H2OMMRSatLevStd(700hPa)		310829	13078	6.007	[0.001242, 28.52]
H2OMMRSatLevStd(700hPa)	Q0	81429	0	8.03	[0.0106, 19.69]
H2OMMRSatLevStd(700hPa)	Q1	203263	0	5.539	[0.008932, 19.92]
H2OMMRSatLevStd(700hPa)	Q2	26137	13078	3.34	[0.001242, 28.52]
H2OMMRSatLevStd(400hPa)		323907	0	1.072	[0.009006, 7.671]
H2OMMRSatLevStd(400hPa)	Q0	183900	0	1.331	[0.01967, 4.665]
H2OMMRSatLevStd(400hPa)	Q1	127401	0	0.682	[0.015, 7.064]
H2OMMRSatLevStd(400hPa)	Q2	12606	0	1.234	[0.009006, 7.671]
H2OMMRSatLevStd(200hPa)		323907	0	0.095	[0.0003849, 0.5764]
H2OMMRSatLevStd(200hPa)	Q0	271961	0	0.09549	[0.0008853, 0.5764]
H2OMMRSatLevStd(200hPa)	Q1	44558	0	0.09304	[0.0008679, 0.5605]
H2OMMRSatLevStd(200hPa)	Q2	7388	0	0.08854	[0.0003849, 0.4869]
H2OMMRSatLevStd(70hPa)		323907	0	0.1357	[0.000721, 1.032]
H2OMMRSatLevStd(70hPa)	Q0	317523	0	0.1365	[0.0008834, 1.032]
H2OMMRSatLevStd(70hPa)	Q1	2761	0	0.09787	[0.0009072, 1.014]
H2OMMRSatLevStd(70hPa)	Q2	3623	0	0.09594	[0.000721, 0.9648]
H2OMMRSatSurf		323907	0	11.21	[0.00296, 66.82]
H2OMMRSatSurf	Q0	50324	0	16.37	[0.003684, 54.22]
H2OMMRSatSurf	Q1	229687	0	11.08	[0.00296, 66.82]
H2OMMRSatSurf	Q2	43896	0	5.962	[0.003978, 62.1]
H2OMMRSat_liquid		3982976	553024	2.716	[0.0006581, 48.66]
H2OMMRSat_liquid	Q0	2273117	0	1.531	[0.001141, 42.23]
H2OMMRSat_liquid	Q1	1500647	0	4.472	[0.00111, 48.66]
H2OMMRSat_liquid	Q2	209212	553024	3.003	[0.0006581, 45.38]
H2OMMRSat_liquid(1000hPa)		186287	137620	11.24	[0.4405, 48.66]
H2OMMRSat_liquid(1000hPa)	Q0	40801	0	14.94	[0.9812, 32.37]
H2OMMRSat_liquid(1000hPa)	Q1	126779	0	10.79	[0.5044, 48.66]
H2OMMRSat_liquid(1000hPa)	Q2	18707	137620	6.198	[0.4405, 43.14]
H2OMMRSat_liquid(700hPa)		310829	13078	5.15	[0.002563, 21.7]
H2OMMRSat_liquid(700hPa)	Q0	81429	0	6.787	[0.1037, 14.34]
H2OMMRSat_liquid(700hPa)	Q1	203263	0	4.76	[0.08606, 14.52]
H2OMMRSat_liquid(700hPa)	Q2	26137	13078	3.084	[0.002563, 21.7]
H2OMMRSat_liquid(400hPa)		323907	0	0.8216	[0.01201, 6.097]
H2OMMRSat_liquid(400hPa)	Q0	183900	0	1.014	[0.02081, 3.276]
H2OMMRSat_liquid(400hPa)	Q1	127401	0	0.53	[0.01601, 5.329]
H2OMMRSat_liquid(400hPa)	Q2	12606	0	0.9655	[0.01201, 6.097]
H2OMMRSat_liquid(200hPa)		323907	0	0.1427	[0.0006581, 0.8532]
H2OMMRSat_liquid(200hPa)	Q0	271961	0	0.1412	[0.001329, 0.8532]
H2OMMRSat_liquid(200hPa)	Q1	44558	0	0.1553	[0.00117, 0.8385]
H2OMMRSat_liquid(200hPa)	Q2	7388	0	0.1223	[0.0006581, 0.7486]
H2OMMRSat_liquid(70hPa)		323907	0	0.268	[0.001748, 1.686]
H2OMMRSat_liquid(70hPa)	Q0	317523	0	0.2693	[0.001932, 1.686]
H2OMMRSat_liquid(70hPa)	Q1	2761	0	0.2033	[0.002058, 1.589]
H2OMMRSat_liquid(70hPa)	Q2	3623	0	0.2006	[0.001748, 1.556]
H2OMMRSatLevStd_liquid		4306883	553117	2.967	[0.000463, 61.37]
H2OMMRSatLevStd_liquid	Q0	2592570	0	1.638	[0.001028, 55.41]
H2OMMRSatLevStd_liquid	Q1	1502100	0	5.199	[0.000979, 61.37]
H2OMMRSatLevStd_liquid	Q2	212213	553117	3.397	[0.000463, 54.06]
H2OMMRSatLevStd_liquid(1000hPa)		186287	137620	12.74	[0.111, 61.37]
H2OMMRSatLevStd_liquid(1000hPa)	Q0	40801	0	17.09	[0.9031, 38.97]
H2OMMRSatLevStd_liquid(1000hPa)	Q1	126779	0	12.17	[0.1476, 61.37]
H2OMMRSatLevStd_liquid(1000hPa)	Q2	18707	137620	7.086	[0.111, 52.57]
H2OMMRSatLevStd_liquid(700hPa)		310829	13078	6.103	[0.002324, 28.52]
H2OMMRSatLevStd_liquid(700hPa)	Q0	81429	0	8.075	[0.01818, 19.69]
H2OMMRSatLevStd_liquid(700hPa)	Q1	203263	0	5.649	[0.01544, 19.92]
H2OMMRSatLevStd_liquid(700hPa)	Q2	26137	13078	3.49	[0.002324, 28.52]
H2OMMRSatLevStd_liquid(400hPa)		323907	0	1.3	[0.01596, 7.888]
H2OMMRSatLevStd_liquid(400hPa)	Q0	183900	0	1.605	[0.03363, 5.073]

Version 6 Performance and Test Report

H2OMMRSatLevStd_liquid(400hPa)	Q1	127401	0	0.8418	[0.02599,	7.333]
H2OMMRSatLevStd_liquid(400hPa)	Q2	12606	0	1.48	[0.01596,	7.888]
H2OMMRSatLevStd_liquid(200hPa)		323907	0	0.1515	[0.0007806,	0.824]
H2OMMRSatLevStd_liquid(200hPa)	Q0	271961	0	0.1525	[0.001748,	0.824]
H2OMMRSatLevStd_liquid(200hPa)	Q1	44558	0	0.1468	[0.001715,	0.8031]
H2OMMRSatLevStd_liquid(200hPa)	Q2	7388	0	0.1414	[0.0007806,	0.706]
H2OMMRSatLevStd_liquid(70hPa)		323907	0	0.2209	[0.001482,	1.534]
H2OMMRSatLevStd_liquid(70hPa)	Q0	317523	0	0.2221	[0.001804,	1.534]
H2OMMRSatLevStd_liquid(70hPa)	Q1	2761	0	0.1608	[0.001851,	1.51]
H2OMMRSatLevStd_liquid(70hPa)	Q2	3623	0	0.1582	[0.001482,	1.442]
H2OMMRSatSurf_liquid		323907	0	11.24	[0.005394,	66.82]
H2OMMRSatSurf_liquid	Q0	50324	0	16.37	[0.006649,	54.22]
H2OMMRSatSurf_liquid	Q1	229687	0	11.11	[0.005394,	66.82]
H2OMMRSatSurf_liquid	Q2	43896	0	6.021	[0.007177,	62.1]
PTropopause		323907	0	191.9	[88.87,	515.7]
PTropopause	Q0	247480	0	175.7	[88.87,	391.9]
PTropopause	Q1	69356	0	250.3	[92.73,	464.6]
PTropopause	Q2	7071	0	187.3	[94.62,	515.7]
T_Tropopause		323907	0	207.4	[182.7,	264.3]
T_Tropopause	Q0	247480	0	206.1	[185,	236.4]
T_Tropopause	Q1	69356	0	212.1	[183.2,	245.4]
T_Tropopause	Q2	7071	0	206.7	[182.7,	264.3]
totH20Std		323907	0	19.65	[0.06554,	205.3]
totH20Std	Q0	50324	0	28.78	[0.06554,	66.35]
totH20Std	Q1	229670	0	18.54	[0.0656,	78.73]
totH20Std	Q2	43913	0	14.99	[0.09213,	205.3]
totH20StdErr		323907	0	2.977	[0.01113,	317.8]
totH20StdErr	Q0	50324	0	1.935	[0.01119,	8.047]
totH20StdErr	Q1	229670	0	2.302	[0.01113,	60.2]
totH20StdErr	Q2	43913	0	7.704	[0.03505,	317.8]
H20MMRStd		3982976	553024	1.51	[0.0001485,	63]
H20MMRStd	Q0	2273117	0	0.7583	[0.0002009,	21.16]
H20MMRStd	Q1	1500647	0	2.505	[0.0001485,	23.61]
H20MMRStd	Q2	209212	553024	2.541	[0.0002912,	63]
H20MMRStd(1000hPa)		186287	137620	8.783	[0.1437,	52.65]
H20MMRStd(1000hPa)	Q0	40801	0	11.78	[0.5054,	21.16]
H20MMRStd(1000hPa)	Q1	126779	0	8.299	[0.2288,	23.61]
H20MMRStd(1000hPa)	Q2	18707	137620	5.527	[0.1437,	52.65]
H20MMRStd(700hPa)		310829	13078	2.336	[0.01981,	58.22]
H20MMRStd(700hPa)	Q0	81429	0	2.86	[0.03477,	9.822]
H20MMRStd(700hPa)	Q1	203263	0	2.032	[0.02107,	15.83]
H20MMRStd(700hPa)	Q2	26137	13078	3.068	[0.01981,	58.22]
H20MMRStd(400hPa)		323907	0	0.2287	[0.001705,	6.077]
H20MMRStd(400hPa)	Q0	183900	0	0.2473	[0.002778,	1.964]
H20MMRStd(400hPa)	Q1	127401	0	0.1758	[0.001705,	2.863]
H20MMRStd(400hPa)	Q2	12606	0	0.4936	[0.002297,	6.077]
H20MMRStd(200hPa)		323907	0	0.009601	[0.0002912,	0.09659]
H20MMRStd(200hPa)	Q0	271961	0	0.01002	[0.0003678,	0.07684]
H20MMRStd(200hPa)	Q1	44558	0	0.006687	[0.0002982,	0.07715]
H20MMRStd(200hPa)	Q2	7388	0	0.01186	[0.0002912,	0.09659]
H20MMRStd(70hPa)		323907	0	0.002078	[0.0002009,	0.00646]
H20MMRStd(70hPa)	Q0	317523	0	0.002077	[0.0002009,	0.006286]
H20MMRStd(70hPa)	Q1	2761	0	0.002114	[0.0005683,	0.006399]
H20MMRStd(70hPa)	Q2	3623	0	0.002089	[0.0003806,	0.00646]
H20MMRStdErr		3982976	553024	0.3762	[0.0001643,	207.5]
H20MMRStdErr	Q0	2273117	0	0.111	[0.0001643,	4.339]
H20MMRStdErr	Q1	1500647	0	0.5567	[0.0001648,	18.73]
H20MMRStdErr	Q2	209212	553024	1.962	[0.0002181,	207.5]
H20MMRStdErr(1000hPa)		186287	137620	1.25	[0.04512,	101.1]
H20MMRStdErr(1000hPa)	Q0	40801	0	0.8862	[0.06541,	3.065]
H20MMRStdErr(1000hPa)	Q1	126779	0	1.136	[0.04512,	17.84]
H20MMRStdErr(1000hPa)	Q2	18707	137620	2.821	[0.08262,	101.1]
H20MMRStdErr(700hPa)		310829	13078	0.8953	[0.00728,	207.5]
H20MMRStdErr(700hPa)	Q0	81429	0	0.6293	[0.01064,	2.824]
H20MMRStdErr(700hPa)	Q1	203263	0	0.7048	[0.008602,	14.32]
H20MMRStdErr(700hPa)	Q2	26137	13078	3.206	[0.00728,	207.5]
H20MMRStdErr(400hPa)		323907	0	0.08652	[0.0004828,	17.67]
H20MMRStdErr(400hPa)	Q0	183900	0	0.06278	[0.0005744,	0.6259]
H20MMRStdErr(400hPa)	Q1	127401	0	0.07311	[0.0004828,	2.462]
H20MMRStdErr(400hPa)	Q2	12606	0	0.5683	[0.001136,	17.67]
H20MMRStdErr(200hPa)		323907	0	0.003403	[0.0001648,	0.129]
H20MMRStdErr(200hPa)	Q0	271961	0	0.00303	[0.0001764,	0.03996]
H20MMRStdErr(200hPa)	Q1	44558	0	0.004035	[0.0001648,	0.08493]

Version 6 Performance and Test Report

H2OMMRStdErr(200hPa)	Q2	7388	0	0.01332	[0.0002327, 0.129]
H2OMMRStdErr(70hPa)		323907	0	0.0003661	[0.000238, 0.006876]
H2OMMRStdErr(70hPa)	Q0	317523	0	0.0003483	[0.000238, 0.006006]
H2OMMRStdErr(70hPa)	Q1	2761	0	0.001023	[0.0002495, 0.003789]
H2OMMRStdErr(70hPa)	Q2	3623	0	0.001426	[0.0002497, 0.006876]
H2OMMRLevStd		4306882	553118	1.678	[0.0001277, 73.17]
H2OMMRLevStd	Q0	2592570	0	0.8172	[0.0001417, 22.55]
H2OMMRLevStd	Q1	1502100	0	2.995	[0.0001277, 25.43]
H2OMMRLevStd	Q2	212212	553118	2.874	[0.0002553, 73.17]
H2OMMRLevStd(1000hPa)		186287	137620	9.572	[0.03316, 73.17]
H2OMMRLevStd(1000hPa)	Q0	40801	0	12.65	[0.6211, 22.55]
H2OMMRLevStd(1000hPa)	Q1	126779	0	9.078	[0.2027, 25.43]
H2OMMRLevStd(1000hPa)	Q2	18707	137620	6.206	[0.03316, 73.17]
H2OMMRLevStd(700hPa)		310829	13078	2.871	[0.02704, 59.99]
H2OMMRLevStd(700hPa)	Q0	81429	0	3.587	[0.02997, 12.93]
H2OMMRLevStd(700hPa)	Q1	203263	0	2.517	[0.02867, 16.5]
H2OMMRLevStd(700hPa)	Q2	26137	13078	3.395	[0.02704, 59.99]
H2OMMRLevStd(400hPa)		323907	0	0.3704	[0.001591, 10.27]
H2OMMRLevStd(400hPa)	Q0	183900	0	0.3993	[0.002912, 3.27]
H2OMMRLevStd(400hPa)	Q1	127401	0	0.2869	[0.001591, 3.597]
H2OMMRLevStd(400hPa)	Q2	12606	0	0.7923	[0.002674, 10.27]
H2OMMRLevStd(200hPa)		323907	0	0.0134	[0.0003187, 0.1062]
H2OMMRLevStd(200hPa)	Q0	271961	0	0.01443	[0.0004206, 0.1062]
H2OMMRLevStd(200hPa)	Q1	44558	0	0.007597	[0.0003742, 0.09021]
H2OMMRLevStd(200hPa)	Q2	7388	0	0.0106	[0.0003187, 0.09966]
H2OMMRLevStd(70hPa)		323907	0	0.00204	[0.0001417, 0.006436]
H2OMMRLevStd(70hPa)	Q0	317523	0	0.002043	[0.0001417, 0.006436]
H2OMMRLevStd(70hPa)	Q1	2761	0	0.001948	[0.0004787, 0.005736]
H2OMMRLevStd(70hPa)	Q2	3623	0	0.001838	[0.0003299, 0.005885]
H2OMMRLevStdErr		4306882	553118	0.1973	[5.897e-05, 41.68]
H2OMMRLevStdErr	Q0	2592570	0	0.07029	[5.897e-05, 3.134]
H2OMMRLevStdErr	Q1	1502100	0	0.3424	[6.399e-05, 9.864]
H2OMMRLevStdErr	Q2	212212	553118	0.7228	[8.413e-05, 41.68]
H2OMMRLevStdErr(1000hPa)		186287	137620	1.06	[0.05076, 41.68]
H2OMMRLevStdErr(1000hPa)	Q0	40801	0	0.8785	[0.07853, 2.989]
H2OMMRLevStdErr(1000hPa)	Q1	126779	0	0.9882	[0.05076, 9.864]
H2OMMRLevStdErr(1000hPa)	Q2	18707	137620	1.94	[0.06236, 41.68]
H2OMMRLevStdErr(700hPa)		310829	13078	0.4386	[0.004573, 17.07]
H2OMMRLevStdErr(700hPa)	Q0	81429	0	0.4122	[0.005813, 2.371]
H2OMMRLevStdErr(700hPa)	Q1	203263	0	0.3905	[0.004789, 4.274]
H2OMMRLevStdErr(700hPa)	Q2	26137	13078	0.8951	[0.004573, 17.07]
H2OMMRLevStdErr(400hPa)		323907	0	0.06349	[0.000503, 4.334]
H2OMMRLevStdErr(400hPa)	Q0	183900	0	0.05558	[0.000503, 0.4936]
H2OMMRLevStdErr(400hPa)	Q1	127401	0	0.05587	[0.0005122, 1.085]
H2OMMRLevStdErr(400hPa)	Q2	12606	0	0.2559	[0.0006342, 4.334]
H2OMMRLevStdErr(200hPa)		323907	0	0.002086	[0.0001206, 0.02714]
H2OMMRLevStdErr(200hPa)	Q0	271961	0	0.002065	[0.0001209, 0.01884]
H2OMMRLevStdErr(200hPa)	Q1	44558	0	0.001924	[0.0001206, 0.02184]
H2OMMRLevStdErr(200hPa)	Q2	7388	0	0.000386	[0.0001384, 0.02714]
H2OMMRLevStdErr(70hPa)		323907	0	0.0001462	[6.109e-05, 0.001704]
H2OMMRLevStdErr(70hPa)	Q0	317523	0	0.0001416	[6.109e-05, 0.00142]
H2OMMRLevStdErr(70hPa)	Q1	2761	0	0.0003192	[8.903e-05, 0.00122]
H2OMMRLevStdErr(70hPa)	Q2	3623	0	0.0004142	[9.254e-05, 0.001704]
H2OMMRSurf		323906	1	7.667	[0.01135, 74.87]
H2OMMRSurf	Q0	50324	0	11.51	[0.01796, 22.69]
H2OMMRSurf	Q1	229687	0	7.36	[0.01666, 25.83]
H2OMMRSurf	Q2	43895	1	4.857	[0.01135, 74.87]
H2OMMRSurfErr		323906	1	1.211	[0.008688, 45.62]
H2OMMRSurfErr	Q0	50324	0	1.184	[0.009439, 3.704]
H2OMMRSurfErr	Q1	229687	0	1.13	[0.008688, 10.94]
H2OMMRSurfErr	Q2	43895	1	1.666	[0.009893, 45.62]
num_H2O_Func		323907	0	10.77	[0, 11]
H2O_verticality		3488238	75762	0.6979	[-0.4047, 1.625]
H2O_dof		322926	981	3.314	[0.3766, 5.399]
RelHum		4306882	553118	40.93	[0.02539, 1.876e+05]
RelHum	Q0	2592570	0	28.63	[0.02539, 945.6]
RelHum	Q1	1502100	0	55.59	[0.05083, 988.3]
RelHum	Q2	212212	553118	87.32	[0.06864, 1.876e+05]
RelHum(1000hPa)		186287	137620	78.48	[1.573, 1260]
RelHum(1000hPa)	Q0	40801	0	73.35	[16.29, 134]
RelHum(1000hPa)	Q1	126779	0	77.98	[6.504, 385.8]
RelHum(1000hPa)	Q2	18707	137620	93	[1.573, 1260]
RelHum(700hPa)		310829	13078	56.07	[0.6696, 1.292e+05]

Version 6 Performance and Test Report

RelHum(700hPa)	Q0	81429	0	45.18	[1.295,	442.8]
RelHum(700hPa)	Q1	203263	0	50.4	[0.6696,	736.4]
RelHum(700hPa)	Q2	26137	13078	134.1	[0.9509,	1.292e+05]
RelHum(400hPa)		323907	0	45.63	[0.5735,	1196]
RelHum(400hPa)	Q0	183900	0	38.04	[0.5735,	177]
RelHum(400hPa)	Q1	127401	0	54.72	[0.6316,	224.8]
RelHum(400hPa)	Q2	12606	0	64.41	[1.747,	1196]
RelHum(200hPa)		323907	0	26.23	[0.1141,	2124]
RelHum(200hPa)	Q0	271961	0	25.3	[0.1141,	545.1]
RelHum(200hPa)	Q1	44558	0	31.03	[0.1305,	564.8]
RelHum(200hPa)	Q2	7388	0	31.42	[0.1933,	2124]
RelHum(70hPa)		323907	0	9.143	[0.03062,	233.7]
RelHum(70hPa)	Q0	317523	0	9.04	[0.03062,	233.7]
RelHum(70hPa)	Q1	2761	0	15.94	[0.08859,	196.6]
RelHum(70hPa)	Q2	3623	0	12.94	[0.09074,	211.8]
RelHumSurf		323906	1	93.32	[0.1714,	3368]
RelHumSurf	Q0	50324	0	86.34	[5.763,	1915]
RelHumSurf	Q1	229687	0	94.75	[4.183,	3368]
RelHumSurf	Q2	43895	1	93.84	[0.1714,	2352]
RelHum_liquid		4306882	553118	32.75	[0.01694,	1.119e+05]
RelHum_liquid	Q0	2592570	0	20.29	[0.01694,	554]
RelHum_liquid	Q1	1502100	0	48.2	[0.03172,	578.3]
RelHum_liquid	Q2	212212	553118	75.58	[0.04533,	1.119e+05]
RelHum_liquid(1000hPa)		186287	137620	77.52	[1.566,	1260]
RelHum_liquid(1000hPa)	Q0	40801	0	73.31	[16.29,	127.5]
RelHum_liquid(1000hPa)	Q1	126779	0	77.14	[6.504,	273.5]
RelHum_liquid(1000hPa)	Q2	18707	137620	89.25	[1.566,	1260]
RelHum_liquid(700hPa)		310829	13078	51.25	[0.6696,	7.859e+04]
RelHum_liquid(700hPa)	Q0	81429	0	44.17	[1.295,	266]
RelHum_liquid(700hPa)	Q1	203263	0	46.08	[0.6696,	452.8]
RelHum_liquid(700hPa)	Q2	26137	13078	113.5	[0.9509,	7.859e+04]
RelHum_liquid(400hPa)		323907	0	33.21	[0.4949,	853.9]
RelHum_liquid(400hPa)	Q0	183900	0	28.79	[0.4949,	112]
RelHum_liquid(400hPa)	Q1	127401	0	38	[0.54,	135]
RelHum_liquid(400hPa)	Q2	12606	0	49.36	[1.164,	853.9]
RelHum_liquid(200hPa)		323907	0	15.18	[0.07827,	1065]
RelHum_liquid(200hPa)	Q0	271961	0	14.81	[0.07827,	284.8]
RelHum_liquid(200hPa)	Q1	44558	0	17	[0.08814,	291.1]
RelHum_liquid(200hPa)	Q2	7388	0	17.55	[0.129,	1065]
RelHum_liquid(70hPa)		323907	0	4.884	[0.02045,	114.5]
RelHum_liquid(70hPa)	Q0	317523	0	4.833	[0.02045,	114.5]
RelHum_liquid(70hPa)	Q1	2761	0	8.283	[0.05895,	96.62]
RelHum_liquid(70hPa)	Q2	3623	0	6.759	[0.05666,	103]
RelHumSurf_liquid		323906	1	82.95	[0.1714,	1848]
RelHumSurf_liquid	Q0	50324	0	78.44	[5.763,	1068]
RelHumSurf_liquid	Q1	229687	0	83.34	[4.183,	1848]
RelHumSurf_liquid	Q2	43895	1	86.11	[0.1714,	1304]
GP_Tropopause		323907	0	1.256e+04	[5033,	1.717e+04]
GP_Tropopause	Q0	50324	0	1.424e+04	[6916,	1.715e+04]
GP_Tropopause	Q1	229687	0	1.244e+04	[5597,	1.717e+04]
GP_Tropopause	Q2	43896	0	1.126e+04	[5033,	1.706e+04]
GP_Height		8517674	554326	2.463e+04	[0.4608,	6.558e+04]
GP_Height	Q0	1336295	0	2.466e+04	[0.6214,	6.553e+04]
GP_Height	Q1	6028754	0	2.467e+04	[0.5011,	6.558e+04]
GP_Height	Q2	1152625	554326	2.436e+04	[0.4608,	6.553e+04]
GP_Height(1000hPa)		186287	137620	115	[0.4608,	279]
GP_Height(1000hPa)	Q0	40801	0	131.8	[0.6214,	279]
GP_Height(1000hPa)	Q1	126779	0	113.2	[0.5011,	277.6]
GP_Height(1000hPa)	Q2	18707	137620	90.55	[0.4608,	252.5]
GP_Height(400hPa)		323907	0	7175	[5887,	7736]
GP_Height(400hPa)	Q0	50324	0	7424	[6102,	7684]
GP_Height(400hPa)	Q1	229687	0	7163	[6089,	7718]
GP_Height(400hPa)	Q2	43896	0	6953	[5887,	7736]
GP_Height(70hPa)		323907	0	1.827e+04	[1.572e+04,	1.902e+04]
GP_Height(70hPa)	Q0	50324	0	1.854e+04	[1.638e+04,	1.89e+04]
GP_Height(70hPa)	Q1	229687	0	1.827e+04	[1.636e+04,	1.902e+04]
GP_Height(70hPa)	Q2	43896	0	1.797e+04	[1.572e+04,	1.901e+04]
GP_Height(7.0hPa)		323907	0	3.308e+04	[2.874e+04,	3.424e+04]
GP_Height(7.0hPa)	Q0	50324	0	3.337e+04	[2.98e+04,	3.421e+04]
GP_Height(7.0hPa)	Q1	229687	0	3.309e+04	[2.977e+04,	3.424e+04]
GP_Height(7.0hPa)	Q2	43896	0	3.269e+04	[2.874e+04,	3.423e+04]
GP_Height(0.5hPa)		323907	0	5.262e+04	[4.856e+04,	5.376e+04]
GP_Height(0.5hPa)	Q0	50324	0	5.303e+04	[4.965e+04,	5.373e+04]

Version 6 Performance and Test Report

GP_Height(0.5hPa)	Q1	229687	0	5.263e+04	[4.953e+04, 5.376e+04]
GP_Height(0.5hPa)	Q2	43896	0	5.213e+04	[4.856e+04, 5.376e+04]
GP_Surface		323907	0	343.3	[-82.29, 5794]
GP_Surface	Q0	50324	0	297.7	[-28.05, 5506]
GP_Surface	Q1	229687	0	375.2	[-82.29, 5794]
GP_Surface	Q2	43896	0	228.9	[-53.83, 5597]
CldFrcTot		323907	0	0.4574	[0, 1]
CldFrcTot	Q0	322926	0	0.4559	[0, 1]
CldFrcTot	Q1	658	0	0.9681	[0, 1]
CldFrcTot	Q2	323	0	0.9387	[0, 1]
CldFrcStd		5830344	1656	0.2287	[0, 1]
CldFrcStd	Q0	5812668	0	0.2279	[0, 1]
CldFrcStd	Q1	11862	0	0.4836	[0, 1]
CldFrcStd	Q2	5814	1656	0.471	[0, 1]
CldFrcStdErr		3491244	2340756	0.07321	[0.01139, 0.3]
CldFrcStdErr	Q0	3475854	2336814	0.07321	[0.01139, 0.3] ***
CldFrcStdErr	Q1	10305	1557	0.07173	[0.01846, 0.2417] ***
CldFrcStdErr	Q2	5085	2385	0.07124	[0.01709, 0.1911]
PCldTop		3491244	2340756	537.9	[89.33, 1023]
PCldTop	Q0	3475854	0	538.3	[89.33, 1023]
PCldTop	Q1	10305	0	449.2	[123.1, 1001]
PCldTop	Q2	5085	2340756	441.6	[108.8, 953.8]
PCldTopErr		3491244	2340756	47.86	[10, 250]
PCldTopErr	Q0	3475854	0	47.83	[10, 250]
PCldTopErr	Q1	10305	0	54.21	[11.09, 236.2]
PCldTopErr	Q2	5085	2340756	56.29	[10.58, 247.6]
TCldTop		3491244	2340756	250.7	[183.3, 316.1]
TCldTop	Q0	3475854	0	250.8	[183.3, 316.1]
TCldTop	Q1	10305	0	241.1	[189.7, 301.4]
TCldTop	Q2	5085	2340756	240	[189.7, 298.5]
TCldTopErr		3491244	2340756	5.776	[0.2553, 72.74]
TCldTopErr	Q0	3475854	0	5.557	[0.2553, 48.49]
TCldTopErr	Q1	10305	0	55.09	[50.04, 72.38]
TCldTopErr	Q2	5085	2340756	55.31	[50.07, 72.74]
nCld		2916000	0	1.197	[0, 2]
tot03Std		322926	981	289.3	[94.73, 704.1]
tot03Std	Q0	279758	0	288.6	[119, 544]
tot03Std	Q1	236	0	135.5	[105.7, 438]
tot03Std	Q2	42932	981	294.7	[94.73, 704.1]
tot03StdErr		322926	981	32.86	[11.9, 140.8]
tot03StdErr	Q0	279758	0	28.86	[11.9, 54.4]
tot03StdErr	Q1	236	0	20.32	[15.86, 65.7]
tot03StdErr	Q2	42932	981	58.94	[18.95, 140.8]
O3VMRStd		8491700	580300	2.384e-06	[1.004e-08, 2.687e-05]
O3VMRStd	Q0	7358319	0	2.395e-06	[1.004e-08, 1.795e-05]
O3VMRStd	Q1	6287	0	8.951e-07	[1.143e-08, 6.762e-06]
O3VMRStd	Q2	1127094	580300	2.325e-06	[1.838e-08, 2.687e-05]
O3VMRStd(1000hPa)		185716	138191	3.162e-08	[1.77e-08, 5.596e-08]
O3VMRStd(1000hPa)	Q0	167428	0	3.169e-08	[1.77e-08, 5.469e-08]
O3VMRStd(1000hPa)	Q1	151	0	2.919e-08	[2.472e-08, 3.298e-08]
O3VMRStd(1000hPa)	Q2	18137	138191	3.106e-08	[1.838e-08, 5.596e-08]
O3VMRStd(400hPa)		322926	981	6.615e-08	[1.237e-08, 1.665e-07]
O3VMRStd(400hPa)	Q0	279758	0	6.597e-08	[1.237e-08, 1.665e-07]
O3VMRStd(400hPa)	Q1	236	0	3.573e-08	[1.592e-08, 1.045e-07]
O3VMRStd(400hPa)	Q2	42932	981	6.747e-08	[2.162e-08, 1.559e-07]
O3VMRStd(70hPa)		322926	981	1.713e-06	[2.544e-07, 4.647e-06]
O3VMRStd(70hPa)	Q0	279758	0	1.691e-06	[3.968e-07, 4.45e-06]
O3VMRStd(70hPa)	Q1	236	0	9.066e-07	[4.679e-07, 3.439e-06]
O3VMRStd(70hPa)	Q2	42932	981	1.859e-06	[2.544e-07, 4.647e-06]
O3VMRStd(7.0hPa)		322926	981	6.885e-06	[1.305e-06, 2.479e-05]
O3VMRStd(7.0hPa)	Q0	279758	0	6.954e-06	[2.087e-06, 1.602e-05]
O3VMRStd(7.0hPa)	Q1	236	0	2.151e-06	[1.584e-06, 6.762e-06]
O3VMRStd(7.0hPa)	Q2	42932	981	6.464e-06	[1.305e-06, 2.479e-05]
O3VMRStd(0.5hPa)		322926	981	1.441e-06	[3.428e-07, 3.832e-06]
O3VMRStd(0.5hPa)	Q0	279758	0	1.438e-06	[4.29e-07, 2.374e-06]
O3VMRStd(0.5hPa)	Q1	236	0	8.018e-07	[4.143e-07, 1.522e-06]
O3VMRStd(0.5hPa)	Q2	42932	981	1.466e-06	[3.428e-07, 3.832e-06]
O3VMRStdErr		8491700	580300	5.054e-07	[3.011e-09, 8.062e-06]
O3VMRStdErr	Q0	7358319	0	4.753e-07	[3.011e-09, 3.591e-06]
O3VMRStdErr	Q1	6287	0	2.246e-07	[5.144e-09, 1.691e-06]
O3VMRStdErr	Q2	1127094	580300	7.032e-07	[9.506e-09, 8.062e-06]
O3VMRStdErr(1000hPa)		185716	138191	1.04e-08	[5.311e-09, 3.358e-08]
O3VMRStdErr(1000hPa)	Q0	167428	0	9.506e-09	[5.311e-09, 1.641e-08]

Version 6 Performance and Test Report

O3VMRStdErr(1000hPa)	Q1	151	0	1.314e-08	[1.113e-08, 1.484e-08]
O3VMRStdErr(1000hPa)	Q2	18137	138191	1.864e-08	[1.103e-08, 3.358e-08]
O3VMRStdErr(400hPa)		322926	981	2.254e-08	[3.711e-09, 9.352e-08]
O3VMRStdErr(400hPa)	Q0	279758	0	1.979e-08	[3.711e-09, 4.994e-08]
O3VMRStdErr(400hPa)	Q1	236	0	1.608e-08	[7.162e-09, 4.704e-08]
O3VMRStdErr(400hPa)	Q2	42932	981	4.048e-08	[1.297e-08, 9.352e-08]
O3VMRStdErr(70hPa)		322926	981	2.94e-07	[5.952e-08, 1.394e-06]
O3VMRStdErr(70hPa)	Q0	279758	0	2.536e-07	[5.952e-08, 6.675e-07]
O3VMRStdErr(70hPa)	Q1	236	0	2.085e-07	[1.076e-07, 7.909e-07]
O3VMRStdErr(70hPa)	Q2	42932	981	5.577e-07	[7.632e-08, 1.394e-06]
O3VMRStdErr(7.0hPa)		322926	981	1.463e-06	[3.915e-07, 7.437e-06]
O3VMRStdErr(7.0hPa)	Q0	279758	0	1.391e-06	[4.173e-07, 3.204e-06]
O3VMRStdErr(7.0hPa)	Q1	236	0	5.377e-07	[3.959e-07, 1.691e-06]
O3VMRStdErr(7.0hPa)	Q2	42932	981	1.938e-06	[3.915e-07, 7.437e-06]
O3VMRStdErr(0.5hPa)		322926	981	3.078e-07	[8.58e-08, 1.149e-06]
O3VMRStdErr(0.5hPa)	Q0	279758	0	2.877e-07	[8.58e-08, 4.748e-07]
O3VMRStdErr(0.5hPa)	Q1	236	0	2.005e-07	[1.036e-07, 3.806e-07]
O3VMRStdErr(0.5hPa)	Q2	42932	981	4.397e-07	[1.029e-07, 1.149e-06]
O3VMRLevStd		8517674	554326	2.355e-06	[1.068e-08, 3.103e-05]
O3VMRLevStd	Q0	7358319	0	2.366e-06	[1.068e-08, 1.905e-05]
O3VMRLevStd	Q1	6287	0	8.727e-07	[1.192e-08, 6.59e-06]
O3VMRLevStd	Q2	1153068	554326	2.289e-06	[1.884e-08, 3.103e-05]
O3VMRLevStd(1000hPa)		186287	137620	3.132e-08	[1.816e-08, 5.637e-08]
O3VMRLevStd(1000hPa)	Q0	167428	0	3.136e-08	[1.816e-08, 5.468e-08]
O3VMRLevStd(1000hPa)	Q1	151	0	3.043e-08	[2.677e-08, 3.414e-08]
O3VMRLevStd(1000hPa)	Q2	18708	137620	3.102e-08	[1.884e-08, 5.637e-08]
O3VMRLevStd(400hPa)		323907	0	5.989e-08	[1.132e-08, 1.495e-07]
O3VMRLevStd(400hPa)	Q0	279758	0	6.001e-08	[1.132e-08, 1.493e-07]
O3VMRLevStd(400hPa)	Q1	236	0	3.252e-08	[1.429e-08, 8.693e-08]
O3VMRLevStd(400hPa)	Q2	43913	0	5.925e-08	[2.057e-08, 1.495e-07]
O3VMRLevStd(70hPa)		323907	0	1.254e-06	[1.68e-07, 3.79e-06]
O3VMRLevStd(70hPa)	Q0	279758	0	1.226e-06	[2.616e-07, 3.275e-06]
O3VMRLevStd(70hPa)	Q1	236	0	7.872e-07	[4.65e-07, 2.83e-06]
O3VMRLevStd(70hPa)	Q2	43913	0	1.437e-06	[1.68e-07, 3.79e-06]
O3VMRLevStd(7.0hPa)		323907	0	6.966e-06	[1.313e-06, 2.888e-05]
O3VMRLevStd(7.0hPa)	Q0	279758	0	7.045e-06	[2.064e-06, 1.784e-05]
O3VMRLevStd(7.0hPa)	Q1	236	0	2.08e-06	[1.582e-06, 6.59e-06]
O3VMRLevStd(7.0hPa)	Q2	43913	0	6.486e-06	[1.313e-06, 2.888e-05]
O3VMRLevStd(0.5hPa)		323907	0	1.826e-06	[4.258e-07, 4.853e-06]
O3VMRLevStd(0.5hPa)	Q0	279758	0	1.819e-06	[5.487e-07, 2.987e-06]
O3VMRLevStd(0.5hPa)	Q1	236	0	9.71e-07	[5.343e-07, 1.948e-06]
O3VMRLevStd(0.5hPa)	Q2	43913	0	1.88e-06	[4.258e-07, 4.853e-06]
O3VMRLevStdErr		8517674	554326	2.427e-07	[1.101e-09, 2.353e-06]
O3VMRLevStdErr	Q0	7358319	0	2.413e-07	[1.101e-09, 1.389e-06]
O3VMRLevStdErr	Q1	6287	0	1.046e-07	[1.305e-09, 7.639e-07]
O3VMRLevStdErr	Q2	1153068	554326	2.522e-07	[1.845e-09, 2.353e-06]
O3VMRLevStdErr(1000hPa)		186287	137620	5.104e-09	[2.796e-09, 1.735e-08]
O3VMRLevStdErr(1000hPa)	Q0	167428	0	5.078e-09	[2.796e-09, 9.367e-09]
O3VMRLevStdErr(1000hPa)	Q1	151	0	4.59e-09	[3.719e-09, 5.22e-09]
O3VMRLevStdErr(1000hPa)	Q2	18708	137620	5.338e-09	[2.966e-09, 1.735e-08]
O3VMRLevStdErr(400hPa)		323907	0	6.536e-09	[1.306e-09, 1.725e-08]
O3VMRLevStdErr(400hPa)	Q0	279758	0	6.525e-09	[1.306e-09, 1.537e-08]
O3VMRLevStdErr(400hPa)	Q1	236	0	3.591e-09	[1.628e-09, 9.152e-09]
O3VMRLevStdErr(400hPa)	Q2	43913	0	6.622e-09	[2.352e-09, 1.725e-08]
O3VMRLevStdErr(70hPa)		323907	0	1.198e-07	[1.787e-08, 3.67e-07]
O3VMRLevStdErr(70hPa)	Q0	279758	0	1.168e-07	[2.696e-08, 3.052e-07]
O3VMRLevStdErr(70hPa)	Q1	236	0	7.236e-08	[4.643e-08, 2.507e-07]
O3VMRLevStdErr(70hPa)	Q2	43913	0	1.394e-07	[1.787e-08, 3.67e-07]
O3VMRLevStdErr(7.0hPa)		323907	0	6.678e-07	[1.51e-07, 2.302e-06]
O3VMRLevStdErr(7.0hPa)	Q0	279758	0	6.687e-07	[2.34e-07, 1.378e-06]
O3VMRLevStdErr(7.0hPa)	Q1	236	0	2.355e-07	[1.785e-07, 7.368e-07]
O3VMRLevStdErr(7.0hPa)	Q2	43913	0	6.642e-07	[1.51e-07, 2.302e-06]
O3VMRLevStdErr(0.5hPa)		323907	0	2.805e-07	[7.027e-08, 7.705e-07]
O3VMRLevStdErr(0.5hPa)	Q0	279758	0	2.775e-07	[8.732e-08, 4.574e-07]
O3VMRLevStdErr(0.5hPa)	Q1	236	0	1.565e-07	[8.533e-08, 3.009e-07]
O3VMRLevStdErr(0.5hPa)	Q2	43913	0	3.003e-07	[7.027e-08, 7.705e-07]
num_O3_Func		323907	0	8.952	[0, 9]
O3_verticality		2899672	16328	0.7559	[-0.5106, 1.736]
O3_dof		322926	981	1.554	[0.1303, 2.746]
CO_total_column		323907	0	1.734e+18	[6.379e+17, 1.065e+19]
CO_total_column	Q0	242781	0	1.799e+18	[7.297e+17, 7.324e+18]
CO_total_column	Q1	16789	0	1.508e+18	[7.939e+17, 2.411e+18]
CO_total_column	Q2	64337	0	1.545e+18	[6.379e+17, 1.065e+19]

Version 6 Performance and Test Report

COVMRLevStd		8517667	554333	6.177e-08	[1.664e-09, 9.201e-07]
COVMRLevStd	Q0	6438414	0	6.242e-08	[1.386e-08, 5.096e-07]
COVMRLevStd	Q1	432264	0	5.858e-08	[1.518e-08, 2.848e-07]
COVMRLevStd	Q2	1646989	554333	6.007e-08	[1.664e-09, 9.201e-07]
COVMRLevStd(1000hPa)		186287	137620	1.115e-07	[5.676e-08, 4.795e-07]
COVMRLevStd(1000hPa)	Q0	158618	0	1.096e-07	[6.391e-08, 2.547e-07]
COVMRLevStd(1000hPa)	Q1	6468	0	1.139e-07	[7.326e-08, 1.601e-07]
COVMRLevStd(1000hPa)	Q2	21201	137620	1.254e-07	[5.676e-08, 4.795e-07]
COVMRLevStd(400hPa)		323907	0	9.006e-08	[4.109e-08, 5.34e-07]
COVMRLevStd(400hPa)	Q0	242781	0	9.33e-08	[5.144e-08, 5.012e-07]
COVMRLevStd(400hPa)	Q1	16789	0	7.943e-08	[4.959e-08, 1.431e-07]
COVMRLevStd(400hPa)	Q2	64337	0	8.06e-08	[4.109e-08, 5.34e-07]
COVMRLevStd(70hPa)		323907	0	2.935e-08	[1.479e-08, 1.149e-07]
COVMRLevStd(70hPa)	Q0	242781	0	2.921e-08	[1.968e-08, 5.588e-08]
COVMRLevStd(70hPa)	Q1	16789	0	2.945e-08	[2.243e-08, 3.811e-08]
COVMRLevStd(70hPa)	Q2	64337	0	2.985e-08	[1.479e-08, 1.149e-07]
COVMRLevStd(7.0hPa)		323907	0	2.269e-08	[4.527e-09, 6.121e-08]
COVMRLevStd(7.0hPa)	Q0	242781	0	2.205e-08	[1.574e-08, 4.993e-08]
COVMRLevStd(7.0hPa)	Q1	16789	0	2.388e-08	[1.688e-08, 4.423e-08]
COVMRLevStd(7.0hPa)	Q2	64337	0	2.482e-08	[4.527e-09, 6.121e-08]
COVMRLevStd(0.5hPa)		323906	1	6.219e-08	[5.585e-09, 1.409e-07]
COVMRLevStd(0.5hPa)	Q0	242781	0	6.147e-08	[5.145e-08, 1.112e-07]
COVMRLevStd(0.5hPa)	Q1	16789	0	6.275e-08	[5.145e-08, 9.699e-08]
COVMRLevStd(0.5hPa)	Q2	64336	1	6.477e-08	[5.585e-09, 1.409e-07]
COVMRLevStdErr		8517667	554333	8.152e-09	[1.348e-09, 1.203e-07]
COVMRLevStdErr	Q0	6438414	0	7.318e-09	[1.348e-09, 6.985e-08]
COVMRLevStdErr	Q1	432264	0	9.052e-09	[1.945e-09, 6.09e-08]
COVMRLevStdErr	Q2	1646989	554333	1.117e-08	[1.878e-09, 1.203e-07]
COVMRLevStdErr(1000hPa)		186287	137620	1.46e-08	[6.853e-09, 1.203e-07]
COVMRLevStdErr(1000hPa)	Q0	158618	0	1.328e-08	[6.853e-09, 4.862e-08]
COVMRLevStdErr(1000hPa)	Q1	6468	0	1.838e-08	[1.052e-08, 3.208e-08]
COVMRLevStdErr(1000hPa)	Q2	21201	137620	2.328e-08	[1.1e-08, 1.203e-07]
COVMRLevStdErr(400hPa)		323907	0	7.749e-09	[2.647e-09, 7.349e-08]
COVMRLevStdErr(400hPa)	Q0	242781	0	7.148e-09	[2.647e-09, 2.407e-08]
COVMRLevStdErr(400hPa)	Q1	16789	0	8.406e-09	[3.719e-09, 1.645e-08]
COVMRLevStdErr(400hPa)	Q2	64337	0	9.842e-09	[3.055e-09, 7.349e-08]
COVMRLevStdErr(70hPa)		323907	0	4.253e-09	[1.506e-09, 4.163e-08]
COVMRLevStdErr(70hPa)	Q0	242781	0	3.504e-09	[1.506e-09, 2.805e-08]
COVMRLevStdErr(70hPa)	Q1	16789	0	5.048e-09	[2.139e-09, 1.982e-08]
COVMRLevStdErr(70hPa)	Q2	64337	0	6.872e-09	[2.091e-09, 4.163e-08]
COVMRLevStdErr(7.0hPa)		323907	0	4.775e-09	[2.083e-09, 3.801e-08]
COVMRLevStdErr(7.0hPa)	Q0	242781	0	4.025e-09	[2.083e-09, 2.933e-08]
COVMRLevStdErr(7.0hPa)	Q1	16789	0	5.607e-09	[2.889e-09, 2.371e-08]
COVMRLevStdErr(7.0hPa)	Q2	64337	0	7.39e-09	[3.052e-09, 3.801e-08]
COVMRLevStdErr(0.5hPa)		323906	1	1.155e-08	[8.143e-09, 6.42e-08]
COVMRLevStdErr(0.5hPa)	Q0	242781	0	1.042e-08	[8.199e-09, 4.727e-08]
COVMRLevStdErr(0.5hPa)	Q1	16789	0	1.261e-08	[8.143e-09, 3.893e-08]
COVMRLevStdErr(0.5hPa)	Q2	64336	1	1.553e-08	[8.701e-09, 6.42e-08]
num_CO_Func		323907	0	8.709	[0, 9]
CO_verticality		2820791	95209	0.4131	[-0.3166, 1.546]
CO_dof		322923	984	0.7243	[0, 1.454]
CH4_total_column		323907	0	3.56e+19	[1.85e+19, 6.911e+19]
CH4_total_column	Q0	212097	0	3.565e+19	[1.912e+19, 4.046e+19]
CH4_total_column	Q1	9454	0	3.487e+19	[2.025e+19, 3.98e+19]
CH4_total_column	Q2	102356	0	3.555e+19	[1.85e+19, 6.911e+19]
CH4VMRLevStd		8517674	554326	1.221e-06	[1.237e-07, 4.767e-06]
CH4VMRLevStd	Q0	5583048	0	1.235e-06	[1.409e-07, 2.102e-06]
CH4VMRLevStd	Q1	247305	0	1.121e-06	[1.43e-07, 2.025e-06]
CH4VMRLevStd	Q2	2687321	554326	1.201e-06	[1.237e-07, 4.767e-06]
CH4VMRLevStd(1000hPa)		186287	137620	1.819e-06	[7.804e-07, 2.72e-06]
CH4VMRLevStd(1000hPa)	Q0	129474	0	1.818e-06	[1.543e-06, 2.102e-06]
CH4VMRLevStd(1000hPa)	Q1	4798	0	1.833e-06	[1.65e-06, 2.025e-06]
CH4VMRLevStd(1000hPa)	Q2	52015	137620	1.821e-06	[7.804e-07, 2.72e-06]
CH4VMRLevStd(400hPa)		323907	0	1.771e-06	[1.471e-06, 3.467e-06]
CH4VMRLevStd(400hPa)	Q0	212097	0	1.772e-06	[1.599e-06, 1.961e-06]
CH4VMRLevStd(400hPa)	Q1	9454	0	1.764e-06	[1.633e-06, 1.933e-06]
CH4VMRLevStd(400hPa)	Q2	102356	0	1.771e-06	[1.471e-06, 3.467e-06]
CH4VMRLevStd(70hPa)		323907	0	1.552e-06	[8.784e-07, 2.522e-06]
CH4VMRLevStd(70hPa)	Q0	212097	0	1.563e-06	[1.269e-06, 1.78e-06]
CH4VMRLevStd(70hPa)	Q1	9454	0	1.494e-06	[1.321e-06, 1.75e-06]
CH4VMRLevStd(70hPa)	Q2	102356	0	1.537e-06	[8.784e-07, 2.522e-06]
CH4VMRLevStd(7.0hPa)		323907	0	7.486e-07	[3.787e-07, 1.467e-06]
CH4VMRLevStd(7.0hPa)	Q0	212097	0	7.73e-07	[3.787e-07, 1.294e-06]

Version 6 Performance and Test Report

CH4VMRLevStd(7.0hPa)	Q1	9454	0	5.687e-07	[3.856e-07, 1.248e-06]
CH4VMRLevStd(7.0hPa)	Q2	102356	0	7.146e-07	[3.793e-07, 1.467e-06]
CH4VMRLevStd(0.5hPa)		323907	0	4.851e-07	[1.414e-07, 1.209e-06]
CH4VMRLevStd(0.5hPa)	Q0	212097	0	5.116e-07	[1.414e-07, 1.091e-06]
CH4VMRLevStd(0.5hPa)	Q1	9454	0	2.926e-07	[1.435e-07, 1.061e-06]
CH4VMRLevStd(0.5hPa)	Q2	102356	0	4.479e-07	[1.418e-07, 1.209e-06]
CH4VMRLevStdErr		8517674	554326	3.725e-08	[8.112e-09, 9.487e-07]
CH4VMRLevStdErr	Q0	5583048	0	3.726e-08	[8.112e-09, 8.77e-08]
CH4VMRLevStdErr	Q1	247305	0	3.131e-08	[8.203e-09, 7.998e-08]
CH4VMRLevStdErr	Q2	2687321	554326	3.775e-08	[8.21e-09, 9.487e-07]
CH4VMRLevStdErr(1000hPa)		186287	137620	4.916e-08	[3.471e-08, 2.647e-07]
CH4VMRLevStdErr(1000hPa)	Q0	129474	0	4.853e-08	[4.329e-08, 5.489e-08]
CH4VMRLevStdErr(1000hPa)	Q1	4798	0	4.913e-08	[4.41e-08, 5.488e-08]
CH4VMRLevStdErr(1000hPa)	Q2	52015	137620	5.074e-08	[3.471e-08, 2.647e-07]
CH4VMRLevStdErr(400hPa)		323907	0	2.68e-08	[1.558e-08, 1.515e-07]
CH4VMRLevStdErr(400hPa)	Q0	212097	0	2.667e-08	[1.558e-08, 3.131e-08]
CH4VMRLevStdErr(400hPa)	Q1	9454	0	2.635e-08	[1.603e-08, 3.051e-08]
CH4VMRLevStdErr(400hPa)	Q2	102356	0	2.712e-08	[1.577e-08, 1.515e-07]
CH4VMRLevStdErr(70hPa)		323907	0	4.994e-08	[3.125e-08, 4.087e-07]
CH4VMRLevStdErr(70hPa)	Q0	212097	0	4.928e-08	[3.911e-08, 5.72e-08]
CH4VMRLevStdErr(70hPa)	Q1	9454	0	4.716e-08	[4.098e-08, 5.512e-08]
CH4VMRLevStdErr(70hPa)	Q2	102356	0	5.156e-08	[3.125e-08, 4.087e-07]
CH4VMRLevStdErr(7.0hPa)		323907	0	4.086e-08	[1.946e-08, 5.465e-07]
CH4VMRLevStdErr(7.0hPa)	Q0	212097	0	4.126e-08	[1.946e-08, 7.354e-08]
CH4VMRLevStdErr(7.0hPa)	Q1	9454	0	3.019e-08	[1.978e-08, 6.708e-08]
CH4VMRLevStdErr(7.0hPa)	Q2	102356	0	4.101e-08	[1.947e-08, 5.465e-07]
CH4VMRLevStdErr(0.5hPa)		323907	0	3.234e-08	[8.112e-09, 7.404e-07]
CH4VMRLevStdErr(0.5hPa)	Q0	212097	0	3.322e-08	[8.112e-09, 7.596e-08]
CH4VMRLevStdErr(0.5hPa)	Q1	9454	0	1.88e-08	[8.203e-09, 7.03e-08]
CH4VMRLevStdErr(0.5hPa)	Q2	102356	0	3.176e-08	[8.21e-09, 7.404e-07]
num_CH4_Func		323907	0	9.873	[0, 10]
CH4_verticality_10func		3198016	41984	0.5266	[-0.3359, 1.514]
CH4_dof		322923	984	0.8974	[0, 1.75]
olr		323907	0	230.8	[80.24, 392.3]
olr	Q0	322926	0	231	[80.24, 392.3]
olr	Q1	658	0	163.3	[89.4, 297]
olr	Q2	323	0	161.4	[81.83, 264.5]
olr3x3		2915172	828	230.8	[78.97, 392.4]
olr3x3	Q0	2906334	0	231	[78.97, 392.4]
olr3x3	Q1	5931	0	163.5	[89.4, 297]
olr3x3	Q2	2907	828	161.4	[81.83, 264.5]
olr_err		323907	0	5.006	[5, 7]
olr_err	Q0	322926	0	5	[5, 5]
olr_err	Q1	658	0	7	[7, 7]
olr_err	Q2	323	0	7	[7, 7]
clrolr		323907	0	251	[88.43, 392.4]
clrolr	Q0	280015	0	255.1	[88.43, 392.4]
clrolr	Q2	43892	0	224.8	[90.37, 385.6]
clrolr_err		323907	0	12.71	[10, 30]
clrolr_err	Q0	280015	0	10	[10, 10]
clrolr_err	Q2	43892	0	30	[30, 30]
ftpgeoqa		323907	0	0	[0, 0]
zengeoqa		323907	0	0	[0, 0]
demgeoqa		323907	0	0.01092	[0, 4]
dust_flag		2916000	0	-1.794	[-4, 1]
all_spots_avg		323907	0	0.074	[0, 1]
retrieval_type		324000	0	0.1096	[0, 100]
SurfClass		323907	0	2.224	[0, 7]
TAirMWOnlyStd		8261788	810212	240	[181.6, 313.5]
TAirMWOnlyStd	Q0	8261788	0	240	[181.6, 313.5]
TAirMWOnlyStd	Q2	0	810212	nan	[0, 0]
TAirMWOnlyStd(1000hPa)		182070	141837	287.1	[237.6, 313.5]
TAirMWOnlyStd(1000hPa)	Q0	182070	0	287.1	[237.6, 313.5]
TAirMWOnlyStd(1000hPa)	Q2	0	141837	nan	[0, 0]
TAirMWOnlyStd(400hPa)		314141	9766	242.9	[210.7, 265.7]
TAirMWOnlyStd(400hPa)	Q0	314141	0	242.9	[210.7, 265.7]
TAirMWOnlyStd(400hPa)	Q2	0	9766	nan	[0, 0]
TAirMWOnlyStd(70hPa)		314141	9766	209.4	[181.9, 232.7]
TAirMWOnlyStd(70hPa)	Q0	314141	0	209.4	[181.9, 232.7]
TAirMWOnlyStd(70hPa)	Q2	0	9766	nan	[0, 0]
TAirMWOnlyStd(7.0hPa)		314141	9766	232	[209.3, 251.1]
TAirMWOnlyStd(7.0hPa)	Q0	314141	0	232	[209.3, 251.1]
TAirMWOnlyStd(7.0hPa)	Q2	0	9766	nan	[0, 0]

Version 6 Performance and Test Report

TAirMWOnlyStd(0.5hPa)		314141	9766	263.9	[235.2,	292]
TAirMWOnlyStd(0.5hPa)	Q0	314141	0	263.9	[235.2,	292]
TAirMWOnlyStd(0.5hPa)	Q2	0	9766	nan	[0,	0]
MWSurfClass		323907	0	2.224	[0,	7]
sfcTbMWStd		1619540	648460	193.1	[75.15,	347.6]
sfcTbMWStd	Q0	1256568	0	191.1	[75.15,	313.2]
sfcTbMWStd	Q2	362972	648460	200	[82.83,	347.6]
EmisMWStd		1619540	648460	0.6913	[0.2751,	1.161]
EmisMWStd	Q0	1570710	0	0.6876	[0.2814,	1]
EmisMWStd	Q2	48830	648460	0.8115	[0.2751,	1.161]
EmisMWStdErr		1619540	648460	0.04861	[0.015,	1]
EmisMWStdErr	Q0	1570710	0	0.01903	[0.015,	1]
EmisMWStdErr	Q2	48830	648460	1	[1,	1]
totH2OMWOnlyStd		323907	0	19.66	[0.06155,	94.35]
totH2OMWOnlyStd	Q1	176898	0	25.13	[1.948,	72.35]
totH2OMWOnlyStd	Q2	147009	0	13.08	[0.06155,	94.35]
GP_Height_MWOnly		8261788	810212	2.462e+04	[0.6974,	6.625e+04]
GP_Height_MWOnly	Q1	4753102	0	2.429e+04	[0.6974,	6.619e+04]
GP_Height_MWOnly	Q2	3508686	810212	2.506e+04	[0.7326,	6.625e+04]
GP_Height_MWOnly(1000hPa)		182070	141837	115.6	[0.6974,	278.7]
GP_Height_MWOnly(1000hPa)	Q1	153838	0	122.7	[0.6974,	278.7]
GP_Height_MWOnly(1000hPa)	Q2	28232	141837	77.06	[0.7326,	234.7]
GP_Height_MWOnly(400hPa)		314141	9766	7165	[6060,	7749]
GP_Height_MWOnly(400hPa)	Q1	176898	0	7300	[6259,	7699]
GP_Height_MWOnly(400hPa)	Q2	137243	9766	6991	[6060,	7749]
GP_Height_MWOnly(70hPa)		314141	9766	1.826e+04	[1.634e+04,	1.897e+04]
GP_Height_MWOnly(70hPa)	Q1	176898	0	1.847e+04	[1.671e+04,	1.892e+04]
GP_Height_MWOnly(70hPa)	Q2	137243	9766	1.8e+04	[1.634e+04,	1.897e+04]
GP_Height_MWOnly(7.0hPa)		314141	9766	3.307e+04	[2.981e+04,	3.425e+04]
GP_Height_MWOnly(7.0hPa)	Q1	176898	0	3.332e+04	[3.001e+04,	3.425e+04]
GP_Height_MWOnly(7.0hPa)	Q2	137243	9766	3.273e+04	[2.981e+04,	3.411e+04]
GP_Height_MWOnly(0.5hPa)		314141	9766	5.262e+04	[4.952e+04,	5.389e+04]
GP_Height_MWOnly(0.5hPa)	Q1	176898	0	5.284e+04	[4.952e+04,	5.389e+04]
GP_Height_MWOnly(0.5hPa)	Q2	137243	9766	5.232e+04	[4.958e+04,	5.389e+04]
MW_ret_used		323907	0	0.003029	[0,	1]
totCldH20Std		323907	0	0.03035	[0,	15.67]
totCldH20Std	Q1	176897	0	0.03017	[5.963e-08,	0.4997]
totCldH20Std	Q2	147010	0	0.03057	[0,	15.67]
totCldH20StdErr		299257	24650	0.0162	[0.0005,	15.67]
totCldH20StdErr	Q1	176897	0	0.00179	[0.0005,	0.04648]
totCldH20StdErr	Q2	122360	24650	0.03702	[0.0005,	15.67]

4.2. Support products ('airx2sup')

Fieldname	Qual	NumGood	NumBad	Mean	[Min,	Max]
satheight		10800	0	714.5	[703.7,	730.3]
satroll		10800	0	-0.0004961	[-0.03416,	0.03116]
satpitch		10800	0	-0.02367	[-0.03092,	-0.007053]
satyaw		10800	0	-0.0006888	[-0.03821,	0.03502]
satzen		323907	0	28.08	[1.73,	55.83]
satazi		323907	0	0.02965	[-180,	180]
solzen		323907	0	90.55	[14.77,	165.2]
solazi		172264	151643	-52.04	[-180,	180]
glintlat		5353	5447	7.832	[-65.87,	75.93]
glintlon		5353	5447	-0.7059	[-180,	180]
sun_glint_distance		323907	0	1.554e+04	[0,	3e+04]
nadirTAI		10800	0	3.055e+08	[3.054e+08,	3.055e+08]
sat_lat		10800	0	-1.526	[-81.87,	81.87]
sat_lon		10800	0	-0.4735	[-180,	180]
scan_node_type		10800	0	66.51	[65,	68]
topog		323907	0	343.1	[-82.4,	5805]
topog_err		323907	0	32.41	[0,	1437]

Version 6 Performance and Test Report

landFrac	323907	0	0.3314	[0,	1]	
landFrac_err	323907	0	0.03044	[0,	0.471]	
satgeoqa	10800	0	0	[0,	0]	
glintgeoqa	10800	0	1.025	[0,	77]	
moongeoqa	10800	0	9.259e-05	[0,	1]	
latAIRS	2915325	675	-1.529	[-89.89,	89.91]	
lonAIRS	2915325	675	-0.5426	[-180,	180]	
pressSupp	24000	0	294.4	[0.0161,	1100]	
pressStd	6720	0	260.4	[0.1,	1100]	
PSurfStd	323907	0	970.3	[500.6,	1033]	
PSurfStd	Q0	323907	0	970.3	[500.6,	1033]
nSurfSup	323907	0	95.62	[75,	98]	
nSurfStd	323907	0	2.703	[2,	7]	
dust_flag	2916000	0	-1.794	[-4,	1]	
dust_score	2916000	0	78.4	[0,	511]	
BT_diff_SO2	2915323	677	-1.438	[-5.104,	4.674]	
BT_diff_SO2	Q0	2915172	0	-1.438	[-5.104,	4.674]
BT_diff_SO2	Q2	151	677	-1.144	[-3.025,	1.923]
cloud_phase_3x3	2281756	634244	0.4358	[-2,	4]	
cloud_phase_bits	2916000	0	286.2	[0,	902]	
PBest	323907	0	485.1	[0,	1033]	
PGood	323907	0	912.2	[0,	1033]	
nBestSup	323907	0	71.31	[0,	98]	
nGoodSup	323907	0	92.6	[0,	98]	
nBestStd	323907	0	7.645	[2,	29]	
nGoodStd	323907	0	3.329	[2,	29]	
TSurfStd	323907	0	278.8	[189.2,	339.8]	
TSurfStd	Q0	55085	0	296	[261.8,	305.2]
TSurfStd	Q1	142308	0	274.9	[189.2,	339.8]
TSurfStd	Q2	126514	0	275.6	[189.8,	339.1]
TSurfStdErr	323907	0	3.623	[0.25,	50]	
TSurfStdErr	Q0	55085	0	0.7598	[0.25,	1.1]
TSurfStdErr	Q1	142308	0	3.269	[0.7,	7]
TSurfStdErr	Q2	126514	0	5.269	[0.7,	50]
numHingeSurf	323907	0	39	[39,	39]	
freqEmis	12636000	19764000	1380	[649.3,	2632]	
freqEmis(649)	323907	0	649.3	[649.3,	649.3]	
freqEmis(725)	323907	0	724.6	[724.6,	724.6]	
freqEmis(909)	323907	0	909.1	[909.1,	909.1]	
freqEmis(1163)	323907	0	1163	[1163,	1163]	
freqEmis(1205)	323907	0	1205	[1205,	1205]	
freqEmis(1639)	323907	0	1639	[1639,	1639]	
freqEmis(2174)	323907	0	2174	[2174,	2174]	
freqEmis(2381)	323907	0	2381	[2381,	2381]	
freqEmis(2500)	323907	0	2500	[2500,	2500]	
freqEmis(2632)	323907	0	2632	[2632,	2632]	
emisIRStd	12594114	19805886	0.9668	[0.4419,	1]	
emisIRStd	Q0	2148315	0	0.9725	[0.8783,	1]
emisIRStd	Q1	5550012	0	0.9644	[0.4419,	1]
emisIRStd	Q2	4895787	19805886	0.9671	[0.4429,	1]
emisIRStd(649)	322926	981	0.9522	[0.7562,	1]	
emisIRStd(649)	Q0	55085	0	0.9391	[0.8783,	0.9934]
emisIRStd(649)	Q1	142308	0	0.9637	[0.7569,	1]

Version 6 Performance and Test Report

emisIRStd(649)	Q2	125533	981	0.9449	[0.7562,	1]
emisIRStd(725)		322926	981	0.9599	[0.8264,	1]
emisIRStd(725)	Q0	55085	0	0.955	[0.8988,	0.9954]
emisIRStd(725)	Q1	142308	0	0.9652	[0.8276,	1]
emisIRStd(725)	Q2	125533	981	0.9561	[0.8264,	1]
emisIRStd(909)		322926	981	0.9822	[0.8393,	1]
emisIRStd(909)	Q0	55085	0	0.9879	[0.9566,	1]
emisIRStd(909)	Q1	142308	0	0.977	[0.8711,	1]
emisIRStd(909)	Q2	125533	981	0.9857	[0.8393,	1]
emisIRStd(1163)		322926	981	0.9711	[0.6372,	1]
emisIRStd(1163)	Q0	55085	0	0.9802	[0.9405,	1]
emisIRStd(1163)	Q1	142308	0	0.9636	[0.6372,	1]
emisIRStd(1163)	Q2	125533	981	0.9755	[0.6572,	1]
emisIRStd(1205)		322926	981	0.9671	[0.6371,	1]
emisIRStd(1205)	Q0	55085	0	0.9792	[0.9388,	1]
emisIRStd(1205)	Q1	142308	0	0.9604	[0.6371,	1]
emisIRStd(1205)	Q2	125533	981	0.9693	[0.662,	1]
emisIRStd(1639)		322926	981	0.9677	[0.547,	1]
emisIRStd(1639)	Q0	55085	0	0.9718	[0.9222,	1]
emisIRStd(1639)	Q1	142308	0	0.9694	[0.727,	1]
emisIRStd(1639)	Q2	125533	981	0.9641	[0.547,	1]
emisIRStd(2174)		322926	981	0.9546	[0.5596,	1]
emisIRStd(2174)	Q0	55085	0	0.9728	[0.9323,	0.9978]
emisIRStd(2174)	Q1	142308	0	0.9471	[0.5621,	1]
emisIRStd(2174)	Q2	125533	981	0.9551	[0.5596,	1]
emisIRStd(2381)		322926	981	0.9504	[0.5084,	1]
emisIRStd(2381)	Q0	55085	0	0.9714	[0.9239,	0.9977]
emisIRStd(2381)	Q1	142308	0	0.9411	[0.5084,	1]
emisIRStd(2381)	Q2	125533	981	0.9518	[0.5214,	1]
emisIRStd(2500)		322926	981	0.9579	[0.6,	1]
emisIRStd(2500)	Q0	55085	0	0.9689	[0.9085,	0.9971]
emisIRStd(2500)	Q1	142308	0	0.9473	[0.6,	1]
emisIRStd(2500)	Q2	125533	981	0.9652	[0.6,	1]
emisIRStd(2632)		322926	981	0.9631	[0.6,	1]
emisIRStd(2632)	Q0	55085	0	0.9708	[0.9158,	1]
emisIRStd(2632)	Q1	142308	0	0.9543	[0.6,	1]
emisIRStd(2632)	Q2	125533	981	0.9697	[0.6,	1]
emisIRStdErr		12594114	19805886	0.01477	[0.005,	0.2229]
emisIRStdErr	Q0	2148315	0	0.005114	[0.005,	0.01217]
emisIRStdErr	Q1	5550012	0	0.01489	[0.01,	0.1116]
emisIRStdErr	Q2	4895787	19805886	0.01886	[0.01,	0.2229]
emisIRStdErr(649)		322926	981	0.01717	[0.005,	0.09752]
emisIRStdErr(649)	Q0	55085	0	0.006187	[0.005,	0.01217]
emisIRStdErr(649)	Q1	142308	0	0.01486	[0.01,	0.04862]
emisIRStdErr(649)	Q2	125533	981	0.02461	[0.01205,	0.09752]
emisIRStdErr(725)		322926	981	0.0152	[0.005,	0.06943]
emisIRStdErr(725)	Q0	55085	0	0.005313	[0.005,	0.01012]
emisIRStdErr(725)	Q1	142308	0	0.01446	[0.01,	0.03448]
emisIRStdErr(725)	Q2	125533	981	0.02039	[0.01,	0.06943]
emisIRStdErr(909)		322926	981	0.01353	[0.005,	0.06428]
emisIRStdErr(909)	Q0	55085	0	0.005	[0.005,	0.005]
emisIRStdErr(909)	Q1	142308	0	0.01428	[0.01,	0.02578]
emisIRStdErr(909)	Q2	125533	981	0.01643	[0.01,	0.06428]

Version 6 Performance and Test Report

emisIRStdErr(1163)		322926	981	0.01429	[0.005,	0.1371]
emisIRStdErr(1163)	Q0	55085	0	0.005001	[0.005,	0.005954]
emisIRStdErr(1163)	Q1	142308	0	0.01536	[0.01,	0.07255]
emisIRStdErr(1163)	Q2	125533	981	0.01716	[0.01,	0.1371]
emisIRStdErr(1205)		322926	981	0.01454	[0.005,	0.1352]
emisIRStdErr(1205)	Q0	55085	0	0.005003	[0.005,	0.006123]
emisIRStdErr(1205)	Q1	142308	0	0.01539	[0.01,	0.07258]
emisIRStdErr(1205)	Q2	125533	981	0.01776	[0.01,	0.1352]
emisIRStdErr(1639)		322926	981	0.01435	[0.005,	0.1812]
emisIRStdErr(1639)	Q0	55085	0	0.005041	[0.005,	0.007779]
emisIRStdErr(1639)	Q1	142308	0	0.01432	[0.01,	0.0546]
emisIRStdErr(1639)	Q2	125533	981	0.01848	[0.01,	0.1812]
emisIRStdErr(2174)		322926	981	0.01598	[0.005,	0.1761]
emisIRStdErr(2174)	Q0	55085	0	0.005022	[0.005,	0.006771]
emisIRStdErr(2174)	Q1	142308	0	0.0156	[0.01,	0.08758]
emisIRStdErr(2174)	Q2	125533	981	0.02122	[0.01,	0.1761]
emisIRStdErr(2381)		322926	981	0.01686	[0.005,	0.1915]
emisIRStdErr(2381)	Q0	55085	0	0.005032	[0.005,	0.007611]
emisIRStdErr(2381)	Q1	142308	0	0.01656	[0.01,	0.09831]
emisIRStdErr(2381)	Q2	125533	981	0.02238	[0.01,	0.1915]
emisIRStdErr(2500)		322926	981	0.01521	[0.005,	0.16]
emisIRStdErr(2500)	Q0	55085	0	0.005068	[0.005,	0.009147]
emisIRStdErr(2500)	Q1	142308	0	0.01571	[0.01,	0.08]
emisIRStdErr(2500)	Q2	125533	981	0.0191	[0.01,	0.16]
emisIRStdErr(2632)		322926	981	0.01496	[0.005,	0.16]
emisIRStdErr(2632)	Q0	55085	0	0.005058	[0.005,	0.008423]
emisIRStdErr(2632)	Q1	142308	0	0.0156	[0.01,	0.08]
emisIRStdErr(2632)	Q2	125533	981	0.01858	[0.01,	0.16]
Effective_Solar_Reflectance		12594114	19805886	0.01083	[9.966e-08,	1]
Effective_Solar_Reflectance	Q0	2148315	0	0.008537	[9.996e-08,	0.2538]
Effective_Solar_Reflectance	Q1	5550012	0	0.01108	[9.966e-08,	0.5156]
Effective_Solar_Reflectance	Q2	4895787	19805886	0.01156	[9.966e-08,	1]
Effective_Solar_Reflectance(649)		322926	981	0.0166	[1e-07,	0.9332]
Effective_Solar_Reflectance(649)	Q0	55085	0	0.01825	[1e-07,	0.2538]
Effective_Solar_Reflectance(649)	Q1	142308	0	0.01215	[1e-07,	0.4398]
Effective_Solar_Reflectance(649)	Q2	125533	981	0.02091	[1e-07,	0.9332]
Effective_Solar_Reflectance(725)		322926	981	0.01417	[1e-07,	1]
Effective_Solar_Reflectance(725)	Q0	55085	0	0.01336	[1e-07,	0.1981]
Effective_Solar_Reflectance(725)	Q1	142308	0	0.01209	[1e-07,	0.4997]
Effective_Solar_Reflectance(725)	Q2	125533	981	0.0169	[1e-07,	1]
Effective_Solar_Reflectance(909)		322926	981	0.006265	[1e-07,	0.3381]
Effective_Solar_Reflectance(909)	Q0	55085	0	0.00335	[1e-07,	0.05894]
Effective_Solar_Reflectance(909)	Q1	142308	0	0.007858	[1e-07,	0.1593]
Effective_Solar_Reflectance(909)	Q2	125533	981	0.005739	[1e-07,	0.3381]
Effective_Solar_Reflectance(1163)		322926	981	0.009837	[1e-07,	0.3053]
Effective_Solar_Reflectance(1163)	Q0	55085	0	0.0064	[1e-07,	0.09856]
Effective_Solar_Reflectance(1163)	Q1	142308	0	0.01173	[1e-07,	0.1959]
Effective_Solar_Reflectance(1163)	Q2	125533	981	0.009198	[1e-07,	0.3053]
Effective_Solar_Reflectance(1205)		322926	981	0.01014	[1e-07,	0.341]
Effective_Solar_Reflectance(1205)	Q0	55085	0	0.006701	[1e-07,	0.1024]
Effective_Solar_Reflectance(1205)	Q1	142308	0	0.01198	[1e-07,	0.1959]
Effective_Solar_Reflectance(1205)	Q2	125533	981	0.009577	[1e-07,	0.341]
Effective_Solar_Reflectance(1639)		322926	981	0.009654	[1e-07,	0.4638]

Version 6 Performance and Test Report

Effective_Solar_Reflectance(1639)	Q0	55085	0	0.009142	[1e-07,	0.133]
Effective_Solar_Reflectance(1639)	Q1	142308	0	0.008404	[1e-07,	0.2186]
Effective_Solar_Reflectance(1639)	Q2	125533	981	0.0113	[1e-07,	0.4638]
Effective_Solar_Reflectance(2174)		322926	981	0.01261	[1e-07,	0.5204]
Effective_Solar_Reflectance(2174)	Q0	55085	0	0.008414	[1e-07,	0.1228]
Effective_Solar_Reflectance(2174)	Q1	142308	0	0.01439	[1e-07,	0.2453]
Effective_Solar_Reflectance(2174)	Q2	125533	981	0.01243	[1e-07,	0.5204]
Effective_Solar_Reflectance(2381)		322926	981	0.01376	[1e-07,	0.4791]
Effective_Solar_Reflectance(2381)	Q0	55085	0	0.008881	[1e-07,	0.1282]
Effective_Solar_Reflectance(2381)	Q1	142308	0	0.01611	[1e-07,	0.2472]
Effective_Solar_Reflectance(2381)	Q2	125533	981	0.01325	[1e-07,	0.4791]
Effective_Solar_Reflectance(2500)		322926	981	0.01319	[1e-07,	0.5279]
Effective_Solar_Reflectance(2500)	Q0	55085	0	0.009231	[1e-07,	0.1324]
Effective_Solar_Reflectance(2500)	Q1	142308	0	0.01497	[1e-07,	0.2488]
Effective_Solar_Reflectance(2500)	Q2	125533	981	0.01292	[1e-07,	0.5279]
Effective_Solar_Reflectance(2632)		322926	981	0.01375	[9.966e-08,	0.5029]
Effective_Solar_Reflectance(2632)	Q0	55085	0	0.01009	[9.966e-08,	0.1345]
Effective_Solar_Reflectance(2632)	Q1	142308	0	0.01465	[9.966e-08,	0.2371]
Effective_Solar_Reflectance(2632)	Q2	125533	981	0.01433	[9.966e-08,	0.5029]
TAirSup		30972691	1427309	236.7	[156.1,	322.9]
TAirSup	Q0	23063291	0	230.1	[181.7,	313.6]
TAirSup	Q1	6707720	0	255.6	[182.4,	316.4]
TAirSup	Q2	1201680	1427309	258.3	[156.1,	322.9]
TAirSup(0.1hPa)		323907	0	239.4	[229.1,	264]
TAirSup(0.1hPa)	Q0	322921	0	239.4	[229.1,	264]
TAirSup(0.1hPa)	Q2	986	0	240.6	[229.9,	262.3]
TAirSup(3.3hPa)		323907	0	243.8	[224.4,	264.4]
TAirSup(3.3hPa)	Q0	322921	0	243.8	[224.4,	264.4]
TAirSup(3.3hPa)	Q2	986	0	243.9	[229.4,	256.8]
TAirSup(16hPa)		323907	0	222.1	[193.7,	240.3]
TAirSup(16hPa)	Q0	322921	0	222.1	[193.8,	240.3]
TAirSup(16hPa)	Q2	986	0	220.6	[193.7,	236]
TAirSup(47hPa)		323907	0	212.6	[181.9,	232.2]
TAirSup(47hPa)	Q0	319829	0	212.7	[181.9,	232.2]
TAirSup(47hPa)	Q1	1196	0	208.6	[182.5,	231]
TAirSup(47hPa)	Q2	2882	0	210	[182,	231.2]
TAirSup(103hPa)		323907	0	207.1	[181.8,	233]
TAirSup(103hPa)	Q0	299596	0	207.3	[182.7,	232.9]
TAirSup(103hPa)	Q1	19631	0	205.1	[182.9,	233]
TAirSup(103hPa)	Q2	4680	0	204.7	[181.8,	232.6]
TAirSup(190hPa)		323907	0	217	[183.7,	236.2]
TAirSup(190hPa)	Q0	273818	0	217.4	[187.8,	236.2]
TAirSup(190hPa)	Q1	42839	0	215	[187.5,	236]
TAirSup(190hPa)	Q2	7250	0	215.4	[183.7,	234.8]
TAirSup(314hPa)		323907	0	231.3	[203,	262.4]
TAirSup(314hPa)	Q0	239485	0	233.4	[204.1,	253]
TAirSup(314hPa)	Q1	74887	0	224.1	[203.1,	258.5]
TAirSup(314hPa)	Q2	9535	0	234.2	[203,	262.4]
TAirSup(478hPa)		323907	0	252.1	[214.3,	276.8]
TAirSup(478hPa)	Q0	112423	0	257.5	[222,	272.8]
TAirSup(478hPa)	Q1	196878	0	249	[219.8,	275.3]
TAirSup(478hPa)	Q2	14606	0	253.1	[214.3,	276.8]
TAirSup(684hPa)		314518	9389	268.9	[178.6,	296.7]

Version 6 Performance and Test Report

TAirSup(684hPa)	Q0	82563	0	275.6	[211.8,	290.5]
TAirSup(684hPa)	Q1	205785	0	267.3	[210,	290]
TAirSup(684hPa)	Q2	26170	9389	259.3	[178.6,	296.7]
TAirSup(932hPa)		281825	42082	281.3	[216,	316.9]
TAirSup(932hPa)	Q0	44841	0	289.4	[248.9,	311.7]
TAirSup(932hPa)	Q1	192490	0	281.4	[231.3,	313.9]
TAirSup(932hPa)	Q2	44494	42082	272.4	[216,	316.9]
TAirSupErr		30972691	1427309	1.666	[0.25,	50]
TAirSupErr	Q0	23063291	0	1.522	[0.25,	50]
TAirSupErr	Q1	6707720	0	1.221	[0.25,	8.262]
TAirSupErr	Q2	1201680	1427309	6.916	[0.25,	50]
TAirSupErr(0.1hPa)		323907	0	4.189	[0.25,	50]
TAirSupErr(0.1hPa)	Q0	322921	0	4.049	[0.25,	50]
TAirSupErr(0.1hPa)	Q2	986	0	49.79	[4.328,	50]
TAirSupErr(3.3hPa)		323907	0	2.643	[0.25,	50]
TAirSupErr(3.3hPa)	Q0	322921	0	2.499	[0.25,	42.93]
TAirSupErr(3.3hPa)	Q2	986	0	49.76	[2.842,	50]
TAirSupErr(16hPa)		323907	0	1.527	[0.25,	50]
TAirSupErr(16hPa)	Q0	322921	0	1.38	[0.25,	25.53]
TAirSupErr(16hPa)	Q2	986	0	49.76	[1.604,	50]
TAirSupErr(47hPa)		323907	0	1.103	[0.25,	50]
TAirSupErr(47hPa)	Q0	319829	0	0.9236	[0.25,	5.439]
TAirSupErr(47hPa)	Q1	1196	0	3.074	[2.534,	5.576]
TAirSupErr(47hPa)	Q2	2882	0	20.18	[1.174,	50]
TAirSupErr(103hPa)		323907	0	1.216	[0.25,	50]
TAirSupErr(103hPa)	Q0	299596	0	1.002	[0.25,	6.215]
TAirSupErr(103hPa)	Q1	19631	0	1.51	[0.25,	5.817]
TAirSupErr(103hPa)	Q2	4680	0	13.68	[0.2817,	50]
TAirSupErr(190hPa)		323907	0	1.097	[0.25,	50]
TAirSupErr(190hPa)	Q0	273818	0	0.7819	[0.25,	2.771]
TAirSupErr(190hPa)	Q1	42839	0	1.609	[0.25,	3.788]
TAirSupErr(190hPa)	Q2	7250	0	9.981	[0.25,	50]
TAirSupErr(314hPa)		323907	0	0.9764	[0.25,	50]
TAirSupErr(314hPa)	Q0	239485	0	0.6356	[0.25,	1.173]
TAirSupErr(314hPa)	Q1	74887	0	1.211	[0.25,	3.319]
TAirSupErr(314hPa)	Q2	9535	0	7.693	[0.25,	50]
TAirSupErr(478hPa)		323907	0	1.028	[0.25,	50]
TAirSupErr(478hPa)	Q0	112423	0	0.5307	[0.25,	0.9027]
TAirSupErr(478hPa)	Q1	196878	0	0.9589	[0.25,	3.013]
TAirSupErr(478hPa)	Q2	14606	0	5.792	[0.25,	50]
TAirSupErr(684hPa)		314518	9389	1.33	[0.25,	50]
TAirSupErr(684hPa)	Q0	82563	0	0.6006	[0.25,	1.61]
TAirSupErr(684hPa)	Q1	205785	0	1.149	[0.25,	8.262]
TAirSupErr(684hPa)	Q2	26170	9389	5.046	[0.25,	50]
TAirSupErr(932hPa)		281825	42082	2.053	[0.25,	50]
TAirSupErr(932hPa)	Q0	44841	0	0.7013	[0.25,	1.64]
TAirSupErr(932hPa)	Q1	192490	0	1.629	[0.25,	4.773]
TAirSupErr(932hPa)	Q2	44494	42082	5.253	[0.577,	50]
TSurfAir		323907	0	280.7	[203.8,	318.1]
TSurfAir	Q0	50324	0	290.6	[205.5,	313.9]
TSurfAir	Q1	229687	0	280.2	[203.8,	318.1]
TSurfAir	Q2	43896	0	272.2	[205.5,	316.7]
TSurfAirErr		323907	0	2.236	[0.3,	50]

Version 6 Performance and Test Report

TSurfAirErr	Q0	50324	0	0.9164	[0.3,	2.622]
TSurfAirErr	Q1	229687	0	1.864	[0.3,	8.627]
TSurfAirErr	Q2	43896	0	5.69	[1.5,	50]
num_Temp_Func		323907	0	22.66	[0,	23]
Temp_ave_kern		171396000	0	0.03986	[-0.1921,	0.7845]
Temp_verticality		7340370	111630	0.93	[-0.1889,	1.472]
Temp_dof		322926	981	6.245	[2.567,	8.847]
H2OMMRSatLevSup		28233024	4166976	598	[0.0001838,	9.629e+09]
H2OMMRSatLevSup	Q0	20592533	0	817.6	[0.0004838,	9.629e+09]
H2OMMRSatLevSup	Q1	6707720	0	4.202	[0.000478,	60.8]
H2OMMRSatLevSup	Q2	932771	4166976	20.68	[0.0001838,	1.44e+06]
H2OMMRSatLevSup(0.1hPa)		42023	281884	3.704e+04	[899,	1.157e+08]
H2OMMRSatLevSup(0.1hPa)	Q0	41931	0	3.705e+04	[899,	1.157e+08]
H2OMMRSatLevSup(0.1hPa)	Q2	92	281884	3.351e+04	[1116,	1.386e+06]
H2OMMRSatLevSup(3.3hPa)		323907	0	98.48	[8.711,	4165]
H2OMMRSatLevSup(3.3hPa)	Q0	322921	0	98.49	[8.711,	4165]
H2OMMRSatLevSup(3.3hPa)	Q2	986	0	97.19	[15.91,	485.1]
H2OMMRSatLevSup(16hPa)		323907	0	1.677	[0.02281,	10.86]
H2OMMRSatLevSup(16hPa)	Q0	322921	0	1.677	[0.02307,	10.86]
H2OMMRSatLevSup(16hPa)	Q2	986	0	1.511	[0.02281,	6.752]
H2OMMRSatLevSup(47hPa)		323907	0	0.2259	[0.001014,	1.516]
H2OMMRSatLevSup(47hPa)	Q0	319829	0	0.2265	[0.001014,	1.516]
H2OMMRSatLevSup(47hPa)	Q1	1196	0	0.174	[0.001129,	1.331]
H2OMMRSatLevSup(47hPa)	Q2	2882	0	0.1786	[0.00104,	1.355]
H2OMMRSatLevSup(103hPa)		323907	0	0.09012	[0.0004577,	0.7649]
H2OMMRSatLevSup(103hPa)	Q0	299596	0	0.09046	[0.0005343,	0.7589]
H2OMMRSatLevSup(103hPa)	Q1	19631	0	0.08854	[0.0005632,	0.7649]
H2OMMRSatLevSup(103hPa)	Q2	4680	0	0.07504	[0.0004577,	0.7314]
H2OMMRSatLevSup(190hPa)		323907	0	0.09231	[0.0003503,	0.5918]
H2OMMRSatLevSup(190hPa)	Q0	273818	0	0.09199	[0.0007296,	0.5918]
H2OMMRSatLevSup(190hPa)	Q1	42839	0	0.09599	[0.0006898,	0.5783]
H2OMMRSatLevSup(190hPa)	Q2	7250	0	0.08286	[0.0003503,	0.5033]
H2OMMRSatLevSup(314hPa)		323907	0	0.3808	[0.005101,	4.837]
H2OMMRSatLevSup(314hPa)	Q0	239485	0	0.4297	[0.005934,	2.018]
H2OMMRSatLevSup(314hPa)	Q1	74887	0	0.2058	[0.005171,	3.397]
H2OMMRSatLevSup(314hPa)	Q2	9535	0	0.5255	[0.005101,	4.837]
H2OMMRSatLevSup(478hPa)		323907	0	2.079	[0.01648,	10.53]
H2OMMRSatLevSup(478hPa)	Q0	112423	0	2.707	[0.0443,	7.828]
H2OMMRSatLevSup(478hPa)	Q1	196878	0	1.723	[0.03369,	9.416]
H2OMMRSatLevSup(478hPa)	Q2	14606	0	2.039	[0.01648,	10.53]
H2OMMRSatLevSup(684hPa)		312713	11194	5.628	[0.0009345,	27.68]
H2OMMRSatLevSup(684hPa)	Q0	82563	0	7.537	[0.00821,	18.52]
H2OMMRSatLevSup(684hPa)	Q1	205785	0	5.142	[0.006359,	17.95]
H2OMMRSatLevSup(684hPa)	Q2	24365	11194	3.256	[0.0009345,	27.68]
H2OMMRSatLevSup(932hPa)		275886	48021	9.848	[0.05955,	56]
H2OMMRSatLevSup(932hPa)	Q0	44841	0	13.69	[0.4548,	49.14]
H2OMMRSatLevSup(932hPa)	Q1	192490	0	9.947	[0.06985,	56]
H2OMMRSatLevSup(932hPa)	Q2	38555	48021	4.886	[0.05955,	52.63]
H2OMMRSatSurf		323907	0	11.21	[0.00296,	66.82]
H2OMMRSatSurf	Q0	50324	0	16.37	[0.003684,	54.22]
H2OMMRSatSurf	Q1	229687	0	11.08	[0.00296,	66.82]
H2OMMRSatSurf	Q2	43896	0	5.962	[0.003978,	62.1]
H2OMMRSatLevSup_liquid		28019609	4380391	209.1	[0.0003843,	5.777e+08]

Version 6 Performance and Test Report

H2OMMRSatLevSup_liquid	Q0	20379780	0	285.2	[0.0009792, 5.777e+08]
H2OMMRSatLevSup_liquid	Q1	6707720	0	4.313	[0.0009715, 60.8]
H2OMMRSatLevSup_liquid	Q2	932109	4380391	18.5	[0.0003843, 3.713e+06]
H2OMMRSatLevSup_liquid(0.1hPa)		38	323869	8.162e+04	[5718, 1.039e+06]
H2OMMRSatLevSup_liquid(0.1hPa)	Q0	37	0	8.32e+04	[5718, 1.039e+06]
H2OMMRSatLevSup_liquid(0.1hPa)	Q2	1	323869	2.313e+04	[2.313e+04, 2.313e+04]
H2OMMRSatLevSup_liquid(3.3hPa)		323907	0	136.5	[13.94, 1.117e+04]
H2OMMRSatLevSup_liquid(3.3hPa)	Q0	322921	0	136.5	[13.94, 1.117e+04]
H2OMMRSatLevSup_liquid(3.3hPa)	Q2	986	0	134.6	[24.55, 657.1]
H2OMMRSatLevSup_liquid(16hPa)		323907	0	2.638	[0.04394, 15.05]
H2OMMRSatLevSup_liquid(16hPa)	Q0	322921	0	2.638	[0.04443, 15.05]
H2OMMRSatLevSup_liquid(16hPa)	Q2	986	0	2.393	[0.04394, 9.731]
H2OMMRSatLevSup_liquid(47hPa)		323907	0	0.3713	[0.002087, 2.255]
H2OMMRSatLevSup_liquid(47hPa)	Q0	319829	0	0.3723	[0.002087, 2.255]
H2OMMRSatLevSup_liquid(47hPa)	Q1	1196	0	0.2882	[0.002317, 2]
H2OMMRSatLevSup_liquid(47hPa)	Q2	2882	0	0.2968	[0.002139, 2.033]
H2OMMRSatLevSup_liquid(103hPa)		323907	0	0.1455	[0.000943, 1.128]
H2OMMRSatLevSup_liquid(103hPa)	Q0	299596	0	0.1461	[0.001095, 1.12]
H2OMMRSatLevSup_liquid(103hPa)	Q1	19631	0	0.1418	[0.001153, 1.128]
H2OMMRSatLevSup_liquid(103hPa)	Q2	4680	0	0.1213	[0.000943, 1.083]
H2OMMRSatLevSup_liquid(190hPa)		323907	0	0.1473	[0.0007138, 0.8474]
H2OMMRSatLevSup_liquid(190hPa)	Q0	273818	0	0.1471	[0.001452, 0.8474]
H2OMMRSatLevSup_liquid(190hPa)	Q1	42839	0	0.1514	[0.001375, 0.8298]
H2OMMRSatLevSup_liquid(190hPa)	Q2	7250	0	0.1327	[0.0007138, 0.7305]
H2OMMRSatLevSup_liquid(314hPa)		323907	0	0.5202	[0.009335, 5.377]
H2OMMRSatLevSup_liquid(314hPa)	Q0	239485	0	0.5859	[0.0108, 2.458]
H2OMMRSatLevSup_liquid(314hPa)	Q1	74887	0	0.2877	[0.009458, 3.922]
H2OMMRSatLevSup_liquid(314hPa)	Q2	9535	0	0.6977	[0.009335, 5.377]
H2OMMRSatLevSup_liquid(478hPa)		323907	0	2.318	[0.02818, 10.53]
H2OMMRSatLevSup_liquid(478hPa)	Q0	112423	0	2.992	[0.0717, 7.855]
H2OMMRSatLevSup_liquid(478hPa)	Q1	196878	0	1.935	[0.05544, 9.416]
H2OMMRSatLevSup_liquid(478hPa)	Q2	14606	0	2.29	[0.02818, 10.53]
H2OMMRSatLevSup_liquid(684hPa)		312713	11194	5.728	[0.001768, 27.68]
H2OMMRSatLevSup_liquid(684hPa)	Q0	82563	0	7.588	[0.01426, 18.52]
H2OMMRSatLevSup_liquid(684hPa)	Q1	205785	0	5.257	[0.01118, 17.95]
H2OMMRSatLevSup_liquid(684hPa)	Q2	24365	11194	3.41	[0.001768, 27.68]
H2OMMRSatLevSup_liquid(932hPa)		275886	48021	9.886	[0.09022, 56]
H2OMMRSatLevSup_liquid(932hPa)	Q0	44841	0	13.69	[0.5765, 49.14]
H2OMMRSatLevSup_liquid(932hPa)	Q1	192490	0	9.984	[0.1045, 56]
H2OMMRSatLevSup_liquid(932hPa)	Q2	38555	48021	4.972	[0.09022, 52.63]
H2OMMRSatSurf_liquid		323907	0	11.21	[0.00296, 66.82]
H2OMMRSatSurf_liquid	Q0	50324	0	16.37	[0.003684, 54.22]
H2OMMRSatSurf_liquid	Q1	229687	0	11.08	[0.00296, 66.82]
H2OMMRSatSurf_liquid	Q2	43896	0	5.962	[0.003978, 62.1]
PTropopause		323907	0	191.9	[88.87, 515.7]
PTropopause	Q0	247480	0	175.7	[88.87, 391.9]
PTropopause	Q1	69356	0	250.3	[92.73, 464.6]
PTropopause	Q2	7071	0	187.3	[94.62, 515.7]
T_Tropopause		323907	0	207.4	[182.7, 264.3]
T_Tropopause	Q0	247480	0	206.1	[185, 236.4]
T_Tropopause	Q1	69356	0	212.1	[183.2, 245.4]
T_Tropopause	Q2	7071	0	206.7	[182.7, 264.3]
totH2OStd		323907	0	19.65	[0.06554, 205.3]

Version 6 Performance and Test Report

totH2OStd	Q0	50324	0	28.78	[0.06554, 66.35]
totH2OStd	Q1	229670	0	18.54	[0.0656, 78.73]
totH2OStd	Q2	43913	0	14.99	[0.09213, 205.3]
totH2OStdErr		323907	0	2.977	[0.01113, 317.8]
totH2OStdErr	Q0	50324	0	1.935	[0.01119, 8.047]
totH2OStdErr	Q1	229670	0	2.302	[0.01113, 60.2]
totH2OStdErr	Q2	43913	0	7.704	[0.03505, 317.8]
H2OCDSup		30972691	1427309	7.051e+20	[3.611e+14, 5.649e+22]
H2OCDSup	Q0	23063291	0	2.603e+20	[3.611e+14, 1.977e+22]
H2OCDSup	Q1	6707720	0	1.828e+21	[3.832e+16, 2.181e+22]
H2OCDSup	Q2	1201680	1427309	2.974e+21	[3.983e+14, 5.649e+22]
H2OCDSup(0.1hPa)		323907	0	5.316e+15	[1.424e+15, 1.715e+16]
H2OCDSup(0.1hPa)	Q0	322921	0	5.317e+15	[1.424e+15, 1.715e+16]
H2OCDSup(0.1hPa)	Q2	986	0	5.243e+15	[1.893e+15, 1.251e+16]
H2OCDSup(3.3hPa)		323907	0	5.091e+16	[1.089e+16, 1.423e+17]
H2OCDSup(3.3hPa)	Q0	322921	0	5.091e+16	[1.089e+16, 1.423e+17]
H2OCDSup(3.3hPa)	Q2	986	0	5.206e+16	[1.579e+16, 1.05e+17]
H2OCDSup(16hPa)		323907	0	1.417e+17	[2.019e+16, 4.267e+17]
H2OCDSup(16hPa)	Q0	322921	0	1.417e+17	[2.019e+16, 4.267e+17]
H2OCDSup(16hPa)	Q2	986	0	1.416e+17	[4.806e+16, 3.192e+17]
H2OCDSup(47hPa)		323907	0	2.895e+17	[3.081e+16, 8.986e+17]
H2OCDSup(47hPa)	Q0	319829	0	2.896e+17	[3.081e+16, 8.727e+17]
H2OCDSup(47hPa)	Q1	1196	0	2.755e+17	[8.334e+16, 8.886e+17]
H2OCDSup(47hPa)	Q2	2882	0	2.888e+17	[5.697e+16, 8.986e+17]
H2OCDSup(103hPa)		323907	0	5.227e+17	[3.832e+16, 1.854e+18]
H2OCDSup(103hPa)	Q0	299596	0	5.324e+17	[7.701e+16, 1.854e+18]
H2OCDSup(103hPa)	Q1	19631	0	3.848e+17	[3.832e+16, 1.486e+18]
H2OCDSup(103hPa)	Q2	4680	0	4.799e+17	[8.542e+16, 1.662e+18]
H2OCDSup(190hPa)		323907	0	4.13e+18	[9.435e+16, 4.308e+19]
H2OCDSup(190hPa)	Q0	273818	0	4.308e+18	[1.369e+17, 3.4e+19]
H2OCDSup(190hPa)	Q1	42839	0	2.836e+18	[1.004e+17, 3.506e+19]
H2OCDSup(190hPa)	Q2	7250	0	5.069e+18	[9.435e+16, 4.308e+19]
H2OCDSup(314hPa)		323907	0	6.243e+19	[4.67e+17, 2.621e+21]
H2OCDSup(314hPa)	Q0	239485	0	6.605e+19	[5.303e+17, 8.392e+20]
H2OCDSup(314hPa)	Q1	74887	0	4.468e+19	[4.67e+17, 1.121e+21]
H2OCDSup(314hPa)	Q2	9535	0	1.109e+20	[5.739e+17, 2.621e+21]
H2OCDSup(478hPa)		323907	0	4.381e+20	[2.246e+18, 1.077e+22]
H2OCDSup(478hPa)	Q0	112423	0	4.873e+20	[3.77e+18, 3.579e+21]
H2OCDSup(478hPa)	Q1	196878	0	3.645e+20	[2.246e+18, 4.399e+21]
H2OCDSup(478hPa)	Q2	14606	0	1.05e+21	[2.465e+18, 1.077e+22]
H2OCDSup(684hPa)		314518	9389	1.948e+21	[8.253e+18, 4.54e+22]
H2OCDSup(684hPa)	Q0	82563	0	2.416e+21	[1.766e+19, 8.237e+21]
H2OCDSup(684hPa)	Q1	205785	0	1.698e+21	[1.255e+19, 1.39e+22]
H2OCDSup(684hPa)	Q2	26170	9389	2.435e+21	[8.253e+18, 4.54e+22]
H2OCDSup(932hPa)		281825	42082	6.181e+21	[4.277e+19, 5.171e+22]
H2OCDSup(932hPa)	Q0	44841	0	9.26e+21	[2.207e+20, 1.773e+22]
H2OCDSup(932hPa)	Q1	192490	0	5.985e+21	[5.804e+19, 1.992e+22]
H2OCDSup(932hPa)	Q2	44494	42082	3.924e+21	[4.277e+19, 5.171e+22]
H2OCDSupErr		30972691	1427309	1.9e+20	[9.666e+13, 1.749e+23]
H2OCDSupErr	Q0	23063291	0	4.485e+19	[9.666e+13, 4.715e+21]
H2OCDSupErr	Q1	6707720	0	4.613e+20	[2.699e+16, 1.789e+22]
H2OCDSupErr	Q2	1201680	1427309	1.46e+21	[1.992e+14, 1.749e+23]
H2OCDSupErr(0.1hPa)		323907	0	1.995e+15	[5.207e+14, 5.019e+16]

Version 6 Performance and Test Report

H2OCDSupErr(0.1hPa)	Q0	322921	0	1.993e+15	[5.207e+14, 5.019e+16]
H2OCDSupErr(0.1hPa)	Q2	986	0	2.623e+15	[9.466e+14, 6.254e+15]
H2OCDSupErr(3.3hPa)		323907	0	1.791e+16	[5.493e+15, 3.912e+17]
H2OCDSupErr(3.3hPa)	Q0	322921	0	1.789e+16	[5.493e+15, 3.912e+17]
H2OCDSupErr(3.3hPa)	Q2	986	0	2.605e+16	[7.894e+15, 5.248e+16]
H2OCDSupErr(16hPa)		323907	0	3.912e+16	[1.693e+16, 1.264e+18]
H2OCDSupErr(16hPa)	Q0	322921	0	3.903e+16	[1.693e+16, 1.264e+18]
H2OCDSupErr(16hPa)	Q2	986	0	7.077e+16	[2.403e+16, 1.596e+17]
H2OCDSupErr(47hPa)		323907	0	4.897e+16	[3.496e+16, 8.247e+17]
H2OCDSupErr(47hPa)	Q0	319829	0	4.734e+16	[3.496e+16, 7.076e+17]
H2OCDSupErr(47hPa)	Q1	1196	0	1.397e+17	[3.496e+16, 5.897e+17]
H2OCDSupErr(47hPa)	Q2	2882	0	1.92e+17	[3.496e+16, 8.247e+17]
H2OCDSupErr(103hPa)		323907	0	1.157e+17	[5.895e+16, 2.17e+18]
H2OCDSupErr(103hPa)	Q0	299596	0	1.102e+17	[5.895e+16, 1.518e+18]
H2OCDSupErr(103hPa)	Q1	19631	0	1.452e+17	[5.895e+16, 1.297e+18]
H2OCDSupErr(103hPa)	Q2	4680	0	3.46e+17	[5.895e+16, 2.17e+18]
H2OCDSupErr(190hPa)		323907	0	1.453e+18	[8.786e+16, 5.523e+19]
H2OCDSupErr(190hPa)	Q0	273818	0	1.297e+18	[8.786e+16, 1.728e+19]
H2OCDSupErr(190hPa)	Q1	42839	0	1.725e+18	[8.786e+16, 3.765e+19]
H2OCDSupErr(190hPa)	Q2	7250	0	5.764e+18	[8.786e+16, 5.523e+19]
H2OCDSupErr(314hPa)		323907	0	2.235e+19	[4.279e+17, 7.766e+21]
H2OCDSupErr(314hPa)	Q0	239485	0	1.789e+19	[4.279e+17, 3.519e+20]
H2OCDSupErr(314hPa)	Q1	74887	0	2.175e+19	[4.279e+17, 7.449e+20]
H2OCDSupErr(314hPa)	Q2	9535	0	1.391e+20	[4.279e+17, 7.766e+21]
H2OCDSupErr(478hPa)		323907	0	1.778e+20	[1.11e+18, 3.953e+22]
H2OCDSupErr(478hPa)	Q0	112423	0	1.175e+20	[1.137e+18, 1.254e+21]
H2OCDSupErr(478hPa)	Q1	196878	0	1.371e+20	[1.11e+18, 3.399e+21]
H2OCDSupErr(478hPa)	Q2	14606	0	1.191e+21	[1.559e+18, 3.953e+22]
H2OCDSupErr(684hPa)		314518	9389	7.31e+20	[9.811e+18, 1.58e+23]
H2OCDSupErr(684hPa)	Q0	82563	0	5.306e+20	[9.811e+18, 2.479e+21]
H2OCDSupErr(684hPa)	Q1	205785	0	5.88e+20	[9.811e+18, 1.297e+22]
H2OCDSupErr(684hPa)	Q2	26170	9389	2.489e+21	[9.811e+18, 1.58e+23]
H2OCDSupErr(932hPa)		281825	42082	1.169e+21	[2.9e+19, 1.067e+23]
H2OCDSupErr(932hPa)	Q0	44841	0	9.469e+20	[2.9e+19, 2.923e+21]
H2OCDSupErr(932hPa)	Q1	192490	0	1.03e+21	[2.9e+19, 1.679e+22]
H2OCDSupErr(932hPa)	Q2	44494	42082	1.992e+21	[2.9e+19, 1.067e+23]
H2OMMRLevSup		30711463	1688537	0.8368	[0.000127, 69.49]
H2OMMRLevSup	Q0	23063291	0	0.3456	[0.000127, 21.94]
H2OMMRLevSup	Q1	6707720	0	2.303	[0.0001286, 24.92]
H2OMMRLevSup	Q2	940452	1688537	2.423	[0.0002341, 69.49]
H2OMMRLevSup(0.1hPa)		323907	0	0.002386	[0.0007447, 0.008983]
H2OMMRLevSup(0.1hPa)	Q0	322921	0	0.002386	[0.0007447, 0.008983]
H2OMMRLevSup(0.1hPa)	Q2	986	0	0.002431	[0.0007835, 0.005307]
H2OMMRLevSup(3.3hPa)		323907	0	0.002506	[0.0005587, 0.009555]
H2OMMRLevSup(3.3hPa)	Q0	322921	0	0.002506	[0.0005587, 0.009555]
H2OMMRLevSup(3.3hPa)	Q2	986	0	0.002645	[0.0008516, 0.005691]
H2OMMRLevSup(16hPa)		323907	0	0.002209	[0.0003497, 0.007962]
H2OMMRLevSup(16hPa)	Q0	322921	0	0.002208	[0.0003497, 0.007962]
H2OMMRLevSup(16hPa)	Q2	986	0	0.002244	[0.0007438, 0.004907]
H2OMMRLevSup(47hPa)		323907	0	0.001999	[0.0001884, 0.006299]
H2OMMRLevSup(47hPa)	Q0	319829	0	0.002	[0.0001884, 0.006038]
H2OMMRLevSup(47hPa)	Q1	1196	0	0.001886	[0.000556, 0.005892]
H2OMMRLevSup(47hPa)	Q2	2882	0	0.001925	[0.0003964, 0.006299]

Version 6 Performance and Test Report

H2OMMRLevSup(103hPa)		323907	0	0.002264	[0.0001286, 0.008263]
H2OMMRLevSup(103hPa)	Q0	299596	0	0.002312	[0.0002672, 0.008263]
H2OMMRLevSup(103hPa)	Q1	19631	0	0.001605	[0.0001286, 0.006407]
H2OMMRLevSup(103hPa)	Q2	4680	0	0.001915	[0.000249, 0.006368]
H2OMMRLevSup(190hPa)		323907	0	0.01042	[0.0003199, 0.07931]
H2OMMRLevSup(190hPa)	Q0	273818	0	0.0112	[0.0004002, 0.07931]
H2OMMRLevSup(190hPa)	Q1	42839	0	0.005853	[0.0003475, 0.06698]
H2OMMRLevSup(190hPa)	Q2	7250	0	0.007766	[0.0003199, 0.07324]
H2OMMRLevSup(314hPa)		323907	0	0.1334	[0.001486, 1.765]
H2OMMRLevSup(314hPa)	Q0	239485	0	0.1435	[0.001647, 1.55]
H2OMMRLevSup(314hPa)	Q1	74887	0	0.09209	[0.00155, 1.684]
H2OMMRLevSup(314hPa)	Q2	9535	0	0.2029	[0.001486, 1.765]
H2OMMRLevSup(478hPa)		323907	0	0.7638	[0.004281, 18.09]
H2OMMRLevSup(478hPa)	Q0	112423	0	0.8477	[0.007311, 5.708]
H2OMMRLevSup(478hPa)	Q1	196878	0	0.6361	[0.004281, 7.791]
H2OMMRLevSup(478hPa)	Q2	14606	0	1.838	[0.004497, 18.09]
H2OMMRLevSup(684hPa)		312713	11194	2.669	[0.02157, 60.15]
H2OMMRLevSup(684hPa)	Q0	82563	0	3.314	[0.02442, 11.83]
H2OMMRLevSup(684hPa)	Q1	205785	0	2.318	[0.02157, 19.65]
H2OMMRLevSup(684hPa)	Q2	24365	11194	3.451	[0.02519, 60.15]
H2OMMRLevSup(932hPa)		275885	48022	7.096	[0.008383, 56.77]
H2OMMRLevSup(932hPa)	Q0	44841	0	10.69	[0.3011, 20.29]
H2OMMRLevSup(932hPa)	Q1	192490	0	6.849	[0.0782, 22.89]
H2OMMRLevSup(932hPa)	Q2	38554	48022	4.154	[0.008383, 56.77]
H2OMMRLevSupErr		30711463	1688537	0.1027	[5.208e-05, 36.1]
H2OMMRLevSupErr	Q0	23063291	0	0.03206	[5.208e-05, 3.547]
H2OMMRLevSupErr	Q1	6707720	0	0.2756	[6.438e-05, 8.037]
H2OMMRLevSupErr	Q2	940452	1688537	0.6006	[7.914e-05, 36.1]
H2OMMRLevSupErr(0.1hPa)		323907	0	0.0003206	[0.0001069, 0.005541]
H2OMMRLevSupErr(0.1hPa)	Q0	322921	0	0.0003201	[0.0001069, 0.005541]
H2OMMRLevSupErr(0.1hPa)	Q2	986	0	0.0004702	[0.0001599, 0.001068]
H2OMMRLevSupErr(3.3hPa)		323907	0	0.0001937	[6.742e-05, 0.002857]
H2OMMRLevSupErr(3.3hPa)	Q0	322921	0	0.0001934	[6.742e-05, 0.002857]
H2OMMRLevSupErr(3.3hPa)	Q2	986	0	0.0002773	[8.828e-05, 0.0005923]
H2OMMRLevSupErr(16hPa)		323907	0	0.0001336	[5.217e-05, 0.001769]
H2OMMRLevSupErr(16hPa)	Q0	322921	0	0.0001333	[5.217e-05, 0.001769]
H2OMMRLevSupErr(16hPa)	Q2	986	0	0.0002449	[8.247e-05, 0.0005455]
H2OMMRLevSupErr(47hPa)		323907	0	0.0001258	[5.858e-05, 0.001584]
H2OMMRLevSupErr(47hPa)	Q0	319829	0	0.0001228	[5.858e-05, 0.001425]
H2OMMRLevSupErr(47hPa)	Q1	1196	0	0.0003052	[9.322e-05, 0.001158]
H2OMMRLevSupErr(47hPa)	Q2	2882	0	0.0003897	[8.793e-05, 0.001584]
H2OMMRLevSupErr(103hPa)		323907	0	0.0002139	[6.438e-05, 0.002112]
H2OMMRLevSupErr(103hPa)	Q0	299596	0	0.0002083	[7.659e-05, 0.001506]
H2OMMRLevSupErr(103hPa)	Q1	19631	0	0.000234	[6.438e-05, 0.001536]
H2OMMRLevSupErr(103hPa)	Q2	4680	0	0.000485	[8.533e-05, 0.002112]
H2OMMRLevSupErr(190hPa)		323907	0	0.001652	[0.0001097, 0.0196]
H2OMMRLevSupErr(190hPa)	Q0	273818	0	0.001644	[0.0001128, 0.01436]
H2OMMRLevSupErr(190hPa)	Q1	42839	0	0.001493	[0.0001097, 0.01568]
H2OMMRLevSupErr(190hPa)	Q2	7250	0	0.002896	[0.000125, 0.0196]
H2OMMRLevSupErr(314hPa)		323907	0	0.02058	[0.0003606, 0.8908]
H2OMMRLevSupErr(314hPa)	Q0	239485	0	0.01943	[0.0003606, 0.303]
H2OMMRLevSupErr(314hPa)	Q1	74887	0	0.01931	[0.0003613, 0.4972]
H2OMMRLevSupErr(314hPa)	Q2	9535	0	0.05932	[0.0004192, 0.8908]

Version 6 Performance and Test Report

H2OMMRLevSupErr(478hPa)		323907	0	0.1335	[0.001129,	7.827]
H2OMMRLevSupErr(478hPa)	Q0	112423	0	0.1094	[0.001338,	0.8729]
H2OMMRLevSupErr(478hPa)	Q1	196878	0	0.1138	[0.001129,	2.126]
H2OMMRLevSupErr(478hPa)	Q2	14606	0	0.584	[0.001479,	7.827]
H2OMMRLevSupErr(684hPa)		312713	11194	0.4117	[0.004055,	16.95]
H2OMMRLevSupErr(684hPa)	Q0	82563	0	0.381	[0.005787,	2.246]
H2OMMRLevSupErr(684hPa)	Q1	205785	0	0.3639	[0.004563,	4.19]
H2OMMRLevSupErr(684hPa)	Q2	24365	11194	0.9192	[0.004055,	16.95]
H2OMMRLevSupErr(932hPa)		275885	48022	0.6219	[0.01186,	32.16]
H2OMMRLevSupErr(932hPa)	Q0	44841	0	0.6064	[0.01943,	2.649]
H2OMMRLevSupErr(932hPa)	Q1	192490	0	0.5795	[0.01186,	4.556]
H2OMMRLevSupErr(932hPa)	Q2	38554	48022	0.8515	[0.01433,	32.16]
H2OMMSurf		323906	1	7.667	[0.01135,	74.87]
H2OMMSurf	Q0	50324	0	11.51	[0.01796,	22.69]
H2OMMSurf	Q1	229687	0	7.36	[0.01666,	25.83]
H2OMMSurf	Q2	43895	1	4.857	[0.01135,	74.87]
H2OMMSurfErr		323906	1	1.211	[0.008688,	45.62]
H2OMMSurfErr	Q0	50324	0	1.184	[0.009439,	3.704]
H2OMMSurfErr	Q1	229687	0	1.13	[0.008688,	10.94]
H2OMMSurfErr	Q2	43895	1	1.666	[0.009893,	45.62]
num_H2O_Func		323907	0	10.77	[0,	11]
H2O_eff_press		3493141	70859	421.7	[7.476,	939.9]
H2O_VMR_eff		3498978	65022	0.002251	[2.531e-07,	0.09727]
H2O_VMR_eff	Q0	1997774	0	0.001229	[4.318e-07,	0.03231]
H2O_VMR_eff	Q1	1330872	0	0.003536	[2.531e-07,	0.03617]
H2O_VMR_eff	Q2	170332	65022	0.004205	[5.854e-07,	0.09727]
H2O_VMR_eff_err		3498978	65022	0.0006481	[3.997e-07,	0.3382]
H2O_VMR_eff_err	Q0	1997774	0	0.0002245	[3.997e-07,	0.007416]
H2O_VMR_eff_err	Q1	1330872	0	0.0009163	[4.004e-07,	0.03053]
H2O_VMR_eff_err	Q2	170332	65022	0.00352	[4.016e-07,	0.3382]
H2O_trapezoid_layers		2640	0	62.36	[1,	91]
H2O_verticality		3488238	75762	0.6979	[-0.4047,	1.625]
H2O_dof		322926	981	3.314	[0.3766,	5.399]
H2O_ave_kern		39204000	0	0.0621	[-0.3182,	0.9408]
RelHum		4306882	553118	40.93	[0.02539,	1.876e+05]
RelHum	Q0	2592570	0	28.63	[0.02539,	945.6]
RelHum	Q1	1502100	0	55.59	[0.05083,	988.3]
RelHum	Q2	212212	553118	87.32	[0.06864,	1.876e+05]
RelHum(1000hPa)		186287	137620	78.48	[1.573,	1260]
RelHum(1000hPa)	Q0	40801	0	73.35	[16.29,	134]
RelHum(1000hPa)	Q1	126779	0	77.98	[6.504,	385.8]
RelHum(1000hPa)	Q2	18707	137620	93	[1.573,	1260]
RelHum(700hPa)		310829	13078	56.07	[0.6696,	1.292e+05]
RelHum(700hPa)	Q0	81429	0	45.18	[1.295,	442.8]
RelHum(700hPa)	Q1	203263	0	50.4	[0.6696,	736.4]
RelHum(700hPa)	Q2	26137	13078	134.1	[0.9509,	1.292e+05]
RelHum(400hPa)		323907	0	45.63	[0.5735,	1196]
RelHum(400hPa)	Q0	183900	0	38.04	[0.5735,	177]
RelHum(400hPa)	Q1	127401	0	54.72	[0.6316,	224.8]
RelHum(400hPa)	Q2	12606	0	64.41	[1.747,	1196]
RelHum(200hPa)		323907	0	26.23	[0.1141,	2124]
RelHum(200hPa)	Q0	271961	0	25.3	[0.1141,	545.1]
RelHum(200hPa)	Q1	44558	0	31.03	[0.1305,	564.8]

Version 6 Performance and Test Report

RelHum(200hPa)	Q2	7388	0	31.42	[0.1933,	2124]
RelHum(70hPa)		323907	0	9.143	[0.03062,	233.7]
RelHum(70hPa)	Q0	317523	0	9.04	[0.03062,	233.7]
RelHum(70hPa)	Q1	2761	0	15.94	[0.08859,	196.6]
RelHum(70hPa)	Q2	3623	0	12.94	[0.09074,	211.8]
RelHumSurf		323906	1	93.32	[0.1714,	3368]
RelHumSurf	Q0	50324	0	86.34	[5.763,	1915]
RelHumSurf	Q1	229687	0	94.75	[4.183,	3368]
RelHumSurf	Q2	43895	1	93.84	[0.1714,	2352]
RelHum_liquid		4306882	553118	32.75	[0.01694, 1.119e+05]	
RelHum_liquid	Q0	2592570	0	20.29	[0.01694,	554]
RelHum_liquid	Q1	1502100	0	48.2	[0.03172,	578.3]
RelHum_liquid	Q2	212212	553118	75.58	[0.04533, 1.119e+05]	
RelHum_liquid(1000hPa)		186287	137620	77.52	[1.566,	1260]
RelHum_liquid(1000hPa)	Q0	40801	0	73.31	[16.29,	127.5]
RelHum_liquid(1000hPa)	Q1	126779	0	77.14	[6.504,	273.5]
RelHum_liquid(1000hPa)	Q2	18707	137620	89.25	[1.566,	1260]
RelHum_liquid(700hPa)		310829	13078	51.25	[0.6696, 7.859e+04]	
RelHum_liquid(700hPa)	Q0	81429	0	44.17	[1.295,	266]
RelHum_liquid(700hPa)	Q1	203263	0	46.08	[0.6696,	452.8]
RelHum_liquid(700hPa)	Q2	26137	13078	113.5	[0.9509, 7.859e+04]	
RelHum_liquid(400hPa)		323907	0	33.21	[0.4949,	853.9]
RelHum_liquid(400hPa)	Q0	183900	0	28.79	[0.4949,	112]
RelHum_liquid(400hPa)	Q1	127401	0	38	[0.54,	135]
RelHum_liquid(400hPa)	Q2	12606	0	49.36	[1.164,	853.9]
RelHum_liquid(200hPa)		323907	0	15.18	[0.07827,	1065]
RelHum_liquid(200hPa)	Q0	271961	0	14.81	[0.07827,	284.8]
RelHum_liquid(200hPa)	Q1	44558	0	17	[0.08814,	291.1]
RelHum_liquid(200hPa)	Q2	7388	0	17.55	[0.129,	1065]
RelHum_liquid(70hPa)		323907	0	4.884	[0.02045,	114.5]
RelHum_liquid(70hPa)	Q0	317523	0	4.833	[0.02045,	114.5]
RelHum_liquid(70hPa)	Q1	2761	0	8.283	[0.05895,	96.62]
RelHum_liquid(70hPa)	Q2	3623	0	6.759	[0.05666,	103]
RelHumSurf_liquid		323906	1	82.95	[0.1714,	1848]
RelHumSurf_liquid	Q0	50324	0	78.44	[5.763,	1068]
RelHumSurf_liquid	Q1	229687	0	83.34	[4.183,	1848]
RelHumSurf_liquid	Q2	43895	1	86.11	[0.1714,	1304]
bndry_lyr_top		307596	16311	839.9	[706.6,	986.1]
bndry_lyr_top	Q0	39953	0	840.8	[706.6,	986.1]
bndry_lyr_top	Q1	113167	0	848.2	[706.6,	986.1]
bndry_lyr_top	Q2	154476	16311	833.6	[706.6,	986.1]
GP_Tropopause		323907	0	1.256e+04	[5033, 1.717e+04]	
GP_Tropopause	Q0	50324	0	1.424e+04	[6916, 1.715e+04]	
GP_Tropopause	Q1	229687	0	1.244e+04	[5597, 1.717e+04]	
GP_Tropopause	Q2	43896	0	1.126e+04	[5033, 1.706e+04]	
GP_HeightSup		30711466	1688534	1.969e+04	[-1.5, 8.467e+04]	
GP_HeightSup	Q0	4792260	0	1.987e+04	[15.97, 8.455e+04]	
GP_HeightSup	Q1	21742332	0	1.972e+04	[-1.5, 8.458e+04]	
GP_HeightSup	Q2	4176874	1688534	1.931e+04	[36.42, 8.467e+04]	
GP_HeightSup(0.1hPa)		323907	0	6.294e+04	[5.875e+04, 6.719e+04]	
GP_HeightSup(0.1hPa)	Q0	50324	0	6.333e+04	[5.992e+04, 6.719e+04]	
GP_HeightSup(0.1hPa)	Q1	229687	0	6.295e+04	[5.967e+04, 6.719e+04]	
GP_HeightSup(0.1hPa)	Q2	43896	0	6.239e+04	[5.875e+04, 6.716e+04]	

Version 6 Performance and Test Report

GP_HeightSup(3.3hPa)		323907	0	3.852e+04	[3.381e+04, 4.081e+04]
GP_HeightSup(3.3hPa)	Q0	50324	0	3.883e+04	[3.488e+04, 4.074e+04]
GP_HeightSup(3.3hPa)	Q1	229687	0	3.854e+04	[3.486e+04, 4.079e+04]
GP_HeightSup(3.3hPa)	Q2	43896	0	3.805e+04	[3.381e+04, 4.081e+04]
GP_HeightSup(16hPa)		323907	0	2.755e+04	[2.363e+04, 2.92e+04]
GP_HeightSup(16hPa)	Q0	50324	0	2.783e+04	[2.459e+04, 2.918e+04]
GP_HeightSup(16hPa)	Q1	229687	0	2.756e+04	[2.458e+04, 2.92e+04]
GP_HeightSup(16hPa)	Q2	43896	0	2.717e+04	[2.363e+04, 2.918e+04]
GP_HeightSup(47hPa)		323907	0	2.08e+04	[1.781e+04, 2.189e+04]
GP_HeightSup(47hPa)	Q0	50324	0	2.106e+04	[1.857e+04, 2.187e+04]
GP_HeightSup(47hPa)	Q1	229687	0	2.08e+04	[1.855e+04, 2.189e+04]
GP_HeightSup(47hPa)	Q2	43896	0	2.048e+04	[1.781e+04, 2.189e+04]
GP_HeightSup(103hPa)		323907	0	1.598e+04	[1.366e+04, 1.705e+04]
GP_HeightSup(103hPa)	Q0	50324	0	1.63e+04	[1.419e+04, 1.701e+04]
GP_HeightSup(103hPa)	Q1	229687	0	1.598e+04	[1.417e+04, 1.703e+04]
GP_HeightSup(103hPa)	Q2	43896	0	1.566e+04	[1.366e+04, 1.705e+04]
GP_HeightSup(190hPa)		323907	0	1.218e+04	[1.031e+04, 1.325e+04]
GP_HeightSup(190hPa)	Q0	50324	0	1.253e+04	[1.066e+04, 1.323e+04]
GP_HeightSup(190hPa)	Q1	229687	0	1.216e+04	[1.065e+04, 1.325e+04]
GP_HeightSup(190hPa)	Q2	43896	0	1.185e+04	[1.031e+04, 1.323e+04]
GP_HeightSup(314hPa)		323907	0	8899	[7439, 9796]
GP_HeightSup(314hPa)	Q0	50324	0	9196	[7616, 9766]
GP_HeightSup(314hPa)	Q1	229687	0	8885	[7609, 9796]
GP_HeightSup(314hPa)	Q2	43896	0	8631	[7439, 9779]
GP_HeightSup(478hPa)		323907	0	5926	[4645, 6638]
GP_HeightSup(478hPa)	Q0	50324	0	6140	[4950, 6612]
GP_HeightSup(478hPa)	Q1	229687	0	5918	[4933, 6638]
GP_HeightSup(478hPa)	Q2	43896	0	5724	[4645, 6587]
GP_HeightSup(684hPa)		312713	11194	3204	[2315, 3733]
GP_HeightSup(684hPa)	Q0	48195	0	3349	[2581, 3727]
GP_HeightSup(684hPa)	Q1	220782	0	3203	[2530, 3733]
GP_HeightSup(684hPa)	Q2	43736	11194	3054	[2315, 3680]
GP_HeightSup(932hPa)		275886	48021	712.5	[207.2, 1069]
GP_HeightSup(932hPa)	Q0	43887	0	781.2	[305.9, 1058]
GP_HeightSup(932hPa)	Q1	193372	0	712.2	[209.2, 1069]
GP_HeightSup(932hPa)	Q2	38627	48021	636	[207.2, 1063]
GP_Surface		323907	0	343.3	[-82.29, 5794]
GP_Surface	Q0	50324	0	297.7	[-28.05, 5506]
GP_Surface	Q1	229687	0	375.2	[-82.29, 5794]
GP_Surface	Q2	43896	0	228.9	[-53.83, 5597]
CldFrcTot		323907	0	0.4574	[0, 1]
CldFrcTot	Q0	322926	0	0.4559	[0, 1]
CldFrcTot	Q1	658	0	0.9681	[0, 1]
CldFrcTot	Q2	323	0	0.9387	[0, 1]
CldFrcStd		5830344	1656	0.2287	[0, 1]
CldFrcStd	Q0	5812668	0	0.2279	[0, 1]
CldFrcStd	Q1	11862	0	0.4836	[0, 1]
CldFrcStd	Q2	5814	1656	0.471	[0, 1]
CldFrcStdErr		3491244	2340756	0.07321	[0.01139, 0.3]
CldFrcStdErr	Q0	3475854	2336814	0.07321	[0.01139, 0.3] ***
CldFrcStdErr	Q1	10305	1557	0.07173	[0.01846, 0.2417] ***
CldFrcStdErr	Q2	5085	2385	0.07124	[0.01709, 0.1911]
PCldTop		3491244	2340756	537.9	[89.33, 1023]

Version 6 Performance and Test Report

PCldTop	Q0	3475854	0	538.3	[89.33,	1023]
PCldTop	Q1	10305	0	449.2	[123.1,	1001]
PCldTop	Q2	5085	2340756	441.6	[108.8,	953.8]
PCldTopErr		3491244	2340756	47.86	[10,	250]
PCldTopErr	Q0	3475854	0	47.83	[10,	250]
PCldTopErr	Q1	10305	0	54.21	[11.09,	236.2]
PCldTopErr	Q2	5085	2340756	56.29	[10.58,	247.6]
TCldTop		3491244	2340756	250.7	[183.3,	316.1]
TCldTop	Q0	3475854	0	250.8	[183.3,	316.1]
TCldTop	Q1	10305	0	241.1	[189.7,	301.4]
TCldTop	Q2	5085	2340756	240	[189.7,	298.5]
TCldTopErr		3491244	2340756	5.776	[0.2553,	72.74]
TCldTopErr	Q0	3475854	0	5.557	[0.2553,	48.49]
TCldTopErr	Q1	10305	0	55.09	[50.04,	72.38]
TCldTopErr	Q2	5085	2340756	55.31	[50.07,	72.74]
nCld		2916000	0	1.197	[0,	2]
PCldTopStd		516498	131502	552.9	[89.33,	1022]
PCldTopStd	Q0	514604	0	553.4	[89.33,	1022]
PCldTopStd	Q1	1145	0	449.2	[123.1,	1001]
PCldTopStd	Q2	749	131502	357.7	[100,	953.8]
PCldTopStdErr		516314	131686	47.19	[10,	232.3]
PCldTopStdErr	Q0	514604	0	47.17	[10,	232.3]
PCldTopStdErr	Q1	1145	0	53.75	[11.09,	210.3]
PCldTopStdErr	Q2	565	131686	55.4	[10.58,	219.5]
TCldTopStd		516314	131686	253	[184.5,	316.1]
TCldTopStd	Q0	514604	0	253.1	[184.5,	316.1]
TCldTopStd	Q1	1145	0	241.1	[189.7,	301.4]
TCldTopStd	Q2	565	131686	240	[189.7,	298.5]
TCldTopStdErr		516314	131686	5.608	[0.2553,	66.47]
TCldTopStdErr	Q0	514604	0	5.443	[0.2553,	41.57]
TCldTopStdErr	Q1	1145	0	55.04	[50.04,	66.47]
TCldTopStdErr	Q2	565	131686	55.24	[50.14,	66.47]
numCloud		323907	0	1.594	[0,	2]
numHingeCloud		323907	0	2	[2,	2]
cldFreq		4536000	0	2386	[500,	2700]
CldEmis		3615486	920514	1	[1,	1]
CldEmis	Q1	3614198	0	1	[1,	1]
CldEmis	Q2	1288	920514	1	[1,	1]
CldEmisErr		3614198	921802	0	[0,	0]
CldEmisErr	Q1	3614198	0	0	[0,	0]
CldEmisErr	Q2	0	921802	nan	[0,	0]
CldRho		3614198	921802	0	[0,	0]
CldRho	Q1	3614198	0	0	[0,	0]
CldRho	Q2	0	921802	nan	[0,	0]
CldRhoErr		3614198	921802	0	[0,	0]
CldRhoErr	Q1	3614198	0	0	[0,	0]
CldRhoErr	Q2	0	921802	nan	[0,	0]
ice_cld_opt_dpth		788491	2127509	8.126	[0.0001295,	4.291e+06]
ice_cld_opt_dpth	Q0	477604	0	2.346	[0.01094,	16.67]
ice_cld_opt_dpth	Q1	231420	0	1.848	[0.003079,	19.96]
ice_cld_opt_dpth	Q2	79467	2127509	61.15	[0.0001295,	4.291e+06]
ice_cld_eff_diam		788491	2127509	3.413e+06	[0.001692,	1.47e+12]
ice_cld_eff_diam	Q1	491408	0	48.35	[10,	180]

Version 6 Performance and Test Report

ice_cld_eff_diam	Q2	297083	2127509	9.059e+06	[0.001692, 1.47e+12]
ice_cld_temp_eff		788491	2127509	229.6	[-1628, 3492]
ice_cld_temp_eff	Q0	541033	0	231.5	[185.3, 316]
ice_cld_temp_eff	Q1	194862	0	232.3	[150.8, 327.4]
ice_cld_temp_eff	Q2	52596	2127509	200.8	[-1628, 3492]
ice_cld_fit_reduced_chisq		788491	2127509	47.33	[0, 4.073e+06]
ice_cld_opt_dpth_ave_kern		788472	2127528	0.8791	[0, 1]
ice_cld_eff_diam_ave_kern		788472	2127528	0.934	[2.26e-07, 1]
ice_cld_temp_eff_ave_kern		788472	2127528	0.8967	[0, 1]
ice_cld_opt_dpth_err		788472	2127528	0.07644	[2.465e-05, 0.3333]
ice_cld_opt_dpth_err	Q0	477604	0	0.03683	[0.0006466, 0.1491]
ice_cld_opt_dpth_err	Q1	231420	0	0.1067	[2.465e-05, 0.3333]
ice_cld_opt_dpth_err	Q2	79448	2127528	0.2264	[0.1491, 0.3333]
ice_cld_eff_diam_err		788472	2127528	0.0575	[0.0003051, 0.4]
ice_cld_eff_diam_err	Q1	491408	0	0.04132	[0.001092, 0.1789]
ice_cld_eff_diam_err	Q2	297064	2127528	0.08427	[0.0003051, 0.4]
ice_cld_temp_eff_err		788472	2127528	2.4	[0.0169, 15]
ice_cld_temp_eff_err	Q0	541033	0	1.078	[0.01692, 6.707]
ice_cld_temp_eff_err	Q1	194862	0	2.696	[0.0169, 15]
ice_cld_temp_eff_err	Q2	52577	2127528	14.9	[6.708, 15]
log_ice_cld_opt_dpth_prior_var		788491	2127509	0.1111	[0.1111, 0.1111]
log_ice_cld_eff_diam_prior_var		788491	2127509	0.16	[0.16, 0.16]
ice_cld_temp_eff_prior_var		788491	2127509	225	[225, 225]
ice_cld_opt_dpth_first_guess		788491	2127509	3	[3, 3]
ice_cld_eff_diam_first_guess		788491	2127509	50	[50, 50]
ice_cld_temp_eff_first_guess		788491	2127509	221	[184.5, 314.2]
totO3Std		322926	981	289.3	[94.73, 704.1]
totO3Std	Q0	279758	0	288.6	[119, 544]
totO3Std	Q1	236	0	135.5	[105.7, 438]
totO3Std	Q2	42932	981	294.7	[94.73, 704.1]
totO3StdErr		322926	981	32.86	[11.9, 140.8]
totO3StdErr	Q0	279758	0	28.86	[11.9, 54.4]
totO3StdErr	Q1	236	0	20.32	[15.86, 65.7]
totO3StdErr	Q2	42932	981	58.94	[18.95, 140.8]
O3CDSup		30972691	1427309	8.136e+16	[1.743e+14, 1.076e+18]
O3CDSup	Q0	26734234	0	8.12e+16	[1.877e+14, 6.937e+17]
O3CDSup	Q1	22878	0	3.76e+16	[1.963e+14, 3.689e+17]
O3CDSup	Q2	4215579	1427309	8.259e+16	[1.743e+14, 1.076e+18]
O3CDSup(0.1hPa)		323907	0	1.162e+15	[3.083e+14, 2.998e+15]
O3CDSup(0.1hPa)	Q0	279758	0	1.159e+15	[3.193e+14, 1.873e+15]
O3CDSup(0.1hPa)	Q1	236	0	7.769e+14	[3.12e+14, 1.181e+15]
O3CDSup(0.1hPa)	Q2	43913	0	1.182e+15	[3.083e+14, 2.998e+15]
O3CDSup(3.3hPa)		323907	0	8.046e+16	[1.807e+16, 2.478e+17]
O3CDSup(3.3hPa)	Q0	279758	0	8.051e+16	[2.599e+16, 1.503e+17]
O3CDSup(3.3hPa)	Q1	236	0	3.052e+16	[2.082e+16, 8.58e+16]
O3CDSup(3.3hPa)	Q2	43913	0	8.036e+16	[1.807e+16, 2.478e+17]
O3CDSup(16hPa)		323907	0	2.595e+17	[4.355e+16, 1.058e+18]
O3CDSup(16hPa)	Q0	279758	0	2.633e+17	[7.427e+16, 6.911e+17]
O3CDSup(16hPa)	Q1	236	0	6.978e+16	[5.276e+16, 2.407e+17]
O3CDSup(16hPa)	Q2	43913	0	2.359e+17	[4.355e+16, 1.058e+18]
O3CDSup(47hPa)		323907	0	2.176e+17	[3.808e+16, 6.241e+17]
O3CDSup(47hPa)	Q0	279758	0	2.169e+17	[4.375e+16, 5.579e+17]
O3CDSup(47hPa)	Q1	236	0	1.016e+17	[4.591e+16, 3.675e+17]

Version 6 Performance and Test Report

O3CDSup(47hPa)	Q2	43913	0	2.229e+17	[3.808e+16, 6.241e+17]
O3CDSup(103hPa)		323907	0	9.234e+16	[1.156e+16, 2.963e+17]
O3CDSup(103hPa)	Q0	279758	0	8.902e+16	[1.374e+16, 2.55e+17]
O3CDSup(103hPa)	Q1	236	0	8.276e+16	[4.086e+16, 2.33e+17]
O3CDSup(103hPa)	Q2	43913	0	1.136e+17	[1.156e+16, 2.963e+17]
O3CDSup(190hPa)		323907	0	4.891e+16	[6.648e+15, 1.519e+17]
O3CDSup(190hPa)	Q0	279758	0	4.681e+16	[6.648e+15, 1.519e+17]
O3CDSup(190hPa)	Q1	236	0	3.497e+16	[2.213e+16, 1.251e+17]
O3CDSup(190hPa)	Q2	43913	0	6.235e+16	[6.68e+15, 1.519e+17]
O3CDSup(314hPa)		323907	0	2.3e+16	[3.75e+15, 6.915e+16]
O3CDSup(314hPa)	Q0	279758	0	2.28e+16	[3.75e+15, 6.915e+16]
O3CDSup(314hPa)	Q1	236	0	1.26e+16	[5.734e+15, 4.08e+16]
O3CDSup(314hPa)	Q2	43913	0	2.434e+16	[7.049e+15, 5.86e+16]
O3CDSup(478hPa)		323907	0	2.138e+16	[4.46e+15, 5.949e+16]
O3CDSup(478hPa)	Q0	279758	0	2.148e+16	[4.46e+15, 5.307e+16]
O3CDSup(478hPa)	Q1	236	0	1.234e+16	[4.919e+15, 2.908e+16]
O3CDSup(478hPa)	Q2	43913	0	2.077e+16	[8.373e+15, 5.949e+16]
O3CDSup(684hPa)		314518	9389	2.159e+16	[4.676e+15, 5.795e+16]
O3CDSup(684hPa)	Q0	270508	0	2.175e+16	[4.676e+15, 4.783e+16]
O3CDSup(684hPa)	Q1	236	0	1.517e+16	[7.318e+15, 2.711e+16]
O3CDSup(684hPa)	Q2	43774	9389	2.064e+16	[1.058e+16, 5.795e+16]
O3CDSup(932hPa)		281825	42082	1.871e+16	[7.595e+15, 4.201e+16]
O3CDSup(932hPa)	Q0	241886	0	1.881e+16	[7.595e+15, 3.466e+16]
O3CDSup(932hPa)	Q1	236	0	1.662e+16	[1.243e+16, 2.17e+16]
O3CDSup(932hPa)	Q2	39703	42082	1.814e+16	[1.03e+16, 4.201e+16]
O3CDSupErr		30972691	1427309	1.298e+16	[2.902e+13, 1.939e+17]
O3CDSupErr	Q0	26734234	0	1.282e+16	[3.086e+13, 1.141e+17]
O3CDSupErr	Q1	22878	0	6.119e+15	[3.325e+13, 5.476e+16]
O3CDSupErr	Q2	4215579	1427309	1.399e+16	[2.902e+13, 1.939e+17]
O3CDSupErr(0.1hPa)		323907	0	1.915e+14	[5.194e+13, 6.439e+14]
O3CDSupErr(0.1hPa)	Q0	279758	0	1.89e+14	[5.322e+13, 3.05e+14]
O3CDSupErr(0.1hPa)	Q1	236	0	1.329e+14	[5.353e+13, 1.988e+14]
O3CDSupErr(0.1hPa)	Q2	43913	0	2.076e+14	[5.194e+13, 6.439e+14]
O3CDSupErr(3.3hPa)		323907	0	1.405e+16	[3.38e+15, 4.846e+16]
O3CDSupErr(3.3hPa)	Q0	279758	0	1.39e+16	[4.708e+15, 2.537e+16]
O3CDSupErr(3.3hPa)	Q1	236	0	5.64e+15	[3.872e+15, 1.535e+16]
O3CDSupErr(3.3hPa)	Q2	43913	0	1.506e+16	[3.38e+15, 4.846e+16]
O3CDSupErr(16hPa)		323907	0	4.453e+16	[8.356e+15, 1.925e+17]
O3CDSupErr(16hPa)	Q0	279758	0	4.465e+16	[1.356e+16, 1.141e+17]
O3CDSupErr(16hPa)	Q1	236	0	1.292e+16	[1.015e+16, 4.27e+16]
O3CDSupErr(16hPa)	Q2	43913	0	4.397e+16	[8.356e+15, 1.925e+17]
O3CDSupErr(47hPa)		323907	0	3.21e+16	[6.072e+15, 1.599e+17]
O3CDSupErr(47hPa)	Q0	279758	0	3.153e+16	[7.156e+15, 8.585e+16]
O3CDSupErr(47hPa)	Q1	236	0	1.61e+16	[7.554e+15, 5.473e+16]
O3CDSupErr(47hPa)	Q2	43913	0	3.584e+16	[6.072e+15, 1.599e+17]
O3CDSupErr(103hPa)		323907	0	1.396e+16	[1.871e+15, 7.723e+16]
O3CDSupErr(103hPa)	Q0	279758	0	1.336e+16	[2.192e+15, 3.803e+16]
O3CDSupErr(103hPa)	Q1	236	0	1.255e+16	[6.439e+15, 3.434e+16]
O3CDSupErr(103hPa)	Q2	43913	0	1.776e+16	[1.871e+15, 7.723e+16]
O3CDSupErr(190hPa)		323907	0	7.244e+15	[1.021e+15, 3.846e+16]
O3CDSupErr(190hPa)	Q0	279758	0	6.884e+15	[1.021e+15, 2.195e+16]
O3CDSupErr(190hPa)	Q1	236	0	5.266e+15	[3.367e+15, 1.796e+16]
O3CDSupErr(190hPa)	Q2	43913	0	9.549e+15	[1.031e+15, 3.846e+16]

Version 6 Performance and Test Report

O3CDSupErr(314hPa)		323907	0	3.953e+15	[6.428e+14, 1.694e+16]
O3CDSupErr(314hPa)	Q0	279758	0	3.899e+15	[6.428e+14, 1.101e+16]
O3CDSupErr(314hPa)	Q1	236	0	2.152e+15	[9.867e+14, 6.689e+15]
O3CDSupErr(314hPa)	Q2	43913	0	4.311e+15	[1.214e+15, 1.694e+16]
O3CDSupErr(478hPa)		323907	0	3.81e+15	[7.78e+14, 1.184e+16]
O3CDSupErr(478hPa)	Q0	279758	0	3.81e+15	[7.78e+14, 8.965e+15]
O3CDSupErr(478hPa)	Q1	236	0	2.155e+15	[8.525e+14, 4.942e+15]
O3CDSupErr(478hPa)	Q2	43913	0	3.821e+15	[1.442e+15, 1.184e+16]
O3CDSupErr(684hPa)		314518	9389	3.883e+15	[8.916e+14, 1.265e+16]
O3CDSupErr(684hPa)	Q0	270508	0	3.888e+15	[8.916e+14, 8.392e+15]
O3CDSupErr(684hPa)	Q1	236	0	2.667e+15	[1.276e+15, 4.656e+15]
O3CDSupErr(684hPa)	Q2	43774	9389	3.857e+15	[1.802e+15, 1.265e+16]
O3CDSupErr(932hPa)		281825	42082	3.113e+15	[1.342e+15, 1.22e+16]
O3CDSupErr(932hPa)	Q0	241886	0	3.105e+15	[1.342e+15, 5.836e+15]
O3CDSupErr(932hPa)	Q1	236	0	2.689e+15	[1.995e+15, 3.448e+15]
O3CDSupErr(932hPa)	Q2	39703	42082	3.165e+15	[1.686e+15, 1.22e+16]
O3VMRLevSup		30711466	1688534	1.699e-06	[1.056e-08, 3.107e-05]
O3VMRLevSup	Q0	26510300	0	1.707e-06	[1.056e-08, 1.901e-05]
O3VMRLevSup	Q1	22661	0	6.543e-07	[1.192e-08, 6.591e-06]
O3VMRLevSup	Q2	4178505	1688534	1.654e-06	[1.891e-08, 3.107e-05]
O3VMRLevSup(0.1hPa)		323907	0	9.043e-07	[2.394e-07, 2.357e-06]
O3VMRLevSup(0.1hPa)	Q0	279758	0	9.015e-07	[2.584e-07, 1.466e-06]
O3VMRLevSup(0.1hPa)	Q1	236	0	5.826e-07	[2.548e-07, 9.299e-07]
O3VMRLevSup(0.1hPa)	Q2	43913	0	9.238e-07	[2.394e-07, 2.357e-06]
O3VMRLevSup(3.3hPa)		323907	0	5.823e-06	[1.261e-06, 1.987e-05]
O3VMRLevSup(3.3hPa)	Q0	279758	0	5.843e-06	[1.801e-06, 1.209e-05]
O3VMRLevSup(3.3hPa)	Q1	236	0	2.117e-06	[1.478e-06, 5.974e-06]
O3VMRLevSup(3.3hPa)	Q2	43913	0	5.712e-06	[1.261e-06, 1.987e-05]
O3VMRLevSup(16hPa)		323907	0	6.063e-06	[1.023e-06, 2.772e-05]
O3VMRLevSup(16hPa)	Q0	279758	0	6.155e-06	[1.726e-06, 1.62e-05]
O3VMRLevSup(16hPa)	Q1	236	0	1.693e-06	[1.256e-06, 5.849e-06]
O3VMRLevSup(16hPa)	Q2	43913	0	5.507e-06	[1.023e-06, 2.772e-05]
O3VMRLevSup(47hPa)		323907	0	2.333e-06	[4.083e-07, 6.46e-06]
O3VMRLevSup(47hPa)	Q0	279758	0	2.32e-06	[4.993e-07, 5.946e-06]
O3VMRLevSup(47hPa)	Q1	236	0	1.121e-06	[5.396e-07, 4.139e-06]
O3VMRLevSup(47hPa)	Q2	43913	0	2.423e-06	[4.083e-07, 6.46e-06]
O3VMRLevSup(103hPa)		323907	0	6.049e-07	[6.801e-08, 1.898e-06]
O3VMRLevSup(103hPa)	Q0	279758	0	5.822e-07	[9.159e-08, 1.725e-06]
O3VMRLevSup(103hPa)	Q1	236	0	4.864e-07	[2.738e-07, 1.526e-06]
O3VMRLevSup(103hPa)	Q2	43913	0	7.503e-07	[6.801e-08, 1.898e-06]
O3VMRLevSup(190hPa)		323907	0	2.034e-07	[2.707e-08, 6.154e-07]
O3VMRLevSup(190hPa)	Q0	279758	0	1.951e-07	[2.707e-08, 6.154e-07]
O3VMRLevSup(190hPa)	Q1	236	0	1.433e-07	[9.173e-08, 5.165e-07]
O3VMRLevSup(190hPa)	Q2	43913	0	2.56e-07	[2.931e-08, 6.105e-07]
O3VMRLevSup(314hPa)		323907	0	7.641e-08	[1.235e-08, 2.191e-07]
O3VMRLevSup(314hPa)	Q0	279758	0	7.572e-08	[1.235e-08, 2.191e-07]
O3VMRLevSup(314hPa)	Q1	236	0	4.217e-08	[1.951e-08, 1.342e-07]
O3VMRLevSup(314hPa)	Q2	43913	0	8.101e-08	[2.418e-08, 1.864e-07]
O3VMRLevSup(478hPa)		323907	0	5.419e-08	[1.1e-08, 1.563e-07]
O3VMRLevSup(478hPa)	Q0	279758	0	5.449e-08	[1.1e-08, 1.363e-07]
O3VMRLevSup(478hPa)	Q1	236	0	3.131e-08	[1.207e-08, 7.338e-08]
O3VMRLevSup(478hPa)	Q2	43913	0	5.246e-08	[2.102e-08, 1.563e-07]
O3VMRLevSup(684hPa)		312713	11194	4.389e-08	[1.061e-08, 1.236e-07]

Version 6 Performance and Test Report

O3VMRLevSup(684hPa)	Q0	268724	0	4.423e-08	[1.061e-08, 9.633e-08]
O3VMRLevSup(684hPa)	Q1	236	0	3.115e-08	[1.506e-08, 5.461e-08]
O3VMRLevSup(684hPa)	Q2	43753	11194	4.189e-08	[2.2e-08, 1.236e-07]
O3VMRLevSup(932hPa)		275886	48021	3.346e-08	[1.841e-08, 7.757e-08]
O3VMRLevSup(932hPa)	Q0	237006	0	3.361e-08	[1.841e-08, 6.127e-08]
O3VMRLevSup(932hPa)	Q1	236	0	3.019e-08	[2.258e-08, 3.838e-08]
O3VMRLevSup(932hPa)	Q2	38644	48021	3.25e-08	[1.926e-08, 7.757e-08]
O3VMRLevSupErr		30711466	1688534	1.695e-07	[1.1e-09, 2.353e-06]
O3VMRLevSupErr	Q0	26510300	0	1.686e-07	[1.1e-09, 1.389e-06]
O3VMRLevSupErr	Q1	22661	0	7.587e-08	[1.272e-09, 7.644e-07]
O3VMRLevSupErr	Q2	4178505	1688534	1.762e-07	[1.843e-09, 2.353e-06]
O3VMRLevSupErr(0.1hPa)		323907	0	1.761e-07	[4.892e-08, 5.006e-07]
O3VMRLevSupErr(0.1hPa)	Q0	279758	0	1.742e-07	[5.199e-08, 2.821e-07]
O3VMRLevSupErr(0.1hPa)	Q1	236	0	1.191e-07	[5.24e-08, 1.852e-07]
O3VMRLevSupErr(0.1hPa)	Q2	43913	0	1.887e-07	[4.892e-08, 5.006e-07]
O3VMRLevSupErr(3.3hPa)		323907	0	6.627e-07	[1.578e-07, 2.1e-06]
O3VMRLevSupErr(3.3hPa)	Q0	279758	0	6.597e-07	[2.238e-07, 1.233e-06]
O3VMRLevSupErr(3.3hPa)	Q1	236	0	2.609e-07	[1.802e-07, 7.206e-07]
O3VMRLevSupErr(3.3hPa)	Q2	43913	0	6.839e-07	[1.578e-07, 2.1e-06]
O3VMRLevSupErr(16hPa)		323907	0	4.53e-07	[1.095e-07, 1.367e-06]
O3VMRLevSupErr(16hPa)	Q0	279758	0	4.528e-07	[1.64e-07, 8.747e-07]
O3VMRLevSupErr(16hPa)	Q1	236	0	1.683e-07	[1.277e-07, 5.653e-07]
O3VMRLevSupErr(16hPa)	Q2	43913	0	4.557e-07	[1.095e-07, 1.367e-06]
O3VMRLevSupErr(47hPa)		323907	0	2.081e-07	[4.576e-08, 5.964e-07]
O3VMRLevSupErr(47hPa)	Q0	279758	0	2.058e-07	[5.4443e-08, 4.974e-07]
O3VMRLevSupErr(47hPa)	Q1	236	0	1.03e-07	[5.872e-08, 3.556e-07]
O3VMRLevSupErr(47hPa)	Q2	43913	0	2.23e-07	[4.576e-08, 5.964e-07]
O3VMRLevSupErr(103hPa)		323907	0	6.057e-08	[8.085e-09, 2.125e-07]
O3VMRLevSupErr(103hPa)	Q0	279758	0	5.813e-08	[1.007e-08, 1.611e-07]
O3VMRLevSupErr(103hPa)	Q1	236	0	4.801e-08	[3.074e-08, 1.478e-07]
O3VMRLevSupErr(103hPa)	Q2	43913	0	7.62e-08	[8.085e-09, 2.125e-07]
O3VMRLevSupErr(190hPa)		323907	0	2.18e-08	[3.085e-09, 7.904e-08]
O3VMRLevSupErr(190hPa)	Q0	279758	0	2.088e-08	[3.085e-09, 6.27e-08]
O3VMRLevSupErr(190hPa)	Q1	236	0	1.517e-08	[9.915e-09, 5.293e-08]
O3VMRLevSupErr(190hPa)	Q2	43913	0	2.773e-08	[3.413e-09, 7.904e-08]
O3VMRLevSupErr(314hPa)		323907	0	8.489e-09	[1.432e-09, 2.687e-08]
O3VMRLevSupErr(314hPa)	Q0	279758	0	8.389e-09	[1.432e-09, 2.242e-08]
O3VMRLevSupErr(314hPa)	Q1	236	0	4.702e-09	[2.196e-09, 1.425e-08]
O3VMRLevSupErr(314hPa)	Q2	43913	0	9.143e-09	[2.78e-09, 2.687e-08]
O3VMRLevSupErr(478hPa)		323907	0	5.825e-09	[1.209e-09, 1.592e-08]
O3VMRLevSupErr(478hPa)	Q0	279758	0	5.831e-09	[1.209e-09, 1.376e-08]
O3VMRLevSupErr(478hPa)	Q1	236	0	3.374e-09	[1.364e-09, 7.65e-09]
O3VMRLevSupErr(478hPa)	Q2	43913	0	5.799e-09	[2.279e-09, 1.592e-08]
O3VMRLevSupErr(684hPa)		312713	11194	4.481e-09	[1.1e-09, 1.623e-08]
O3VMRLevSupErr(684hPa)	Q0	268724	0	4.499e-09	[1.1e-09, 1.21e-08]
O3VMRLevSupErr(684hPa)	Q1	236	0	3.054e-09	[1.484e-09, 5.352e-09]
O3VMRLevSupErr(684hPa)	Q2	43753	11194	4.378e-09	[2.094e-09, 1.623e-08]
O3VMRLevSupErr(932hPa)		275886	48021	4.084e-09	[2.094e-09, 1.758e-08]
O3VMRLevSupErr(932hPa)	Q0	237006	0	4.06e-09	[2.094e-09, 1.022e-08]
O3VMRLevSupErr(932hPa)	Q1	236	0	3.447e-09	[2.467e-09, 4.438e-09]
O3VMRLevSupErr(932hPa)	Q2	38644	48021	4.241e-09	[2.226e-09, 1.758e-08]
O3VMRSurf		323907	0	3.224e-08	[1.298e-08, 7.656e-08]
O3VMRSurf	Q0	279758	0	3.235e-08	[1.298e-08, 6.849e-08]

Version 6 Performance and Test Report

O3VMRSurf	Q1	236	0	3.02e-08	[2.459e-08, 3.543e-08]
O3VMRSurf	Q2	43913	0	3.154e-08	[1.88e-08, 7.656e-08]
O3VMRSurfErr		323907	0	5.629e-09	[2.177e-09, 2.393e-08]
O3VMRSurfErr	Q0	279758	0	5.631e-09	[2.177e-09, 1.343e-08]
O3VMRSurfErr	Q1	236	0	4.641e-09	[3.291e-09, 5.801e-09]
O3VMRSurfErr	Q2	43913	0	5.627e-09	[3.058e-09, 2.393e-08]
num_O3_Func		323907	0	8.952	[0, 9]
O3_trapezoid_layers		2160	0	43.67	[1, 80]
O3_eff_press		2899672	16328	213.9	[2.508, 794.6]
O3_VMR_eff		2908499	7501	1.418e-06	[1.146e-08, 2.257e-05]
O3_VMR_eff	Q0	2511265	0	1.419e-06	[1.146e-08, 1.465e-05]
O3_VMR_eff	Q1	2124	0	5.9e-07	[1.437e-08, 5.794e-06]
O3_VMR_eff	Q2	395110	7501	1.416e-06	[2.062e-08, 2.257e-05]
O3_VMR_eff_err		2908499	7501	2.272e-07	[1.995e-09, 4.15e-06]
O3_VMR_eff_err	Q0	2511265	0	2.249e-07	[1.995e-09, 2.458e-06]
O3_VMR_eff_err	Q1	2124	0	9.705e-08	[2.488e-09, 1.038e-06]
O3_VMR_eff_err	Q2	395110	7501	2.425e-07	[3.526e-09, 4.15e-06]
O3_verticality		2899672	16328	0.7559	[-0.5106, 1.736]
O3_dof		322926	981	1.554	[0.1303, 2.746]
O3_ave_kern		26244000	0	0.08352	[-0.226, 0.6636]
CO_total_column		323907	0	1.734e+18	[6.379e+17, 1.065e+19]
CO_total_column	Q0	242781	0	1.799e+18	[7.297e+17, 7.324e+18]
CO_total_column	Q1	16789	0	1.508e+18	[7.939e+17, 2.411e+18]
CO_total_column	Q2	64337	0	1.545e+18	[6.379e+17, 1.065e+19]
COCDSup		30972691	1427309	1.83e+16	[4.85e+13, 4.639e+17]
COCDSup	Q0	23388667	0	1.884e+16	[1.933e+14, 2.221e+17]
COCDSup	Q1	1577374	0	1.623e+16	[1.957e+14, 9.374e+16]
COCDSup	Q2	6006650	1427309	1.672e+16	[4.85e+13, 4.639e+17]
COCDSup(0.1hPa)		323907	0	2.528e+14	[5.156e+13, 4.349e+14]
COCDSup(0.1hPa)	Q0	242781	0	2.521e+14	[2.095e+14, 4.349e+14]
COCDSup(0.1hPa)	Q1	16789	0	2.534e+14	[2.143e+14, 3.86e+14]
COCDSup(0.1hPa)	Q2	64337	0	2.553e+14	[5.156e+13, 4.151e+14]
COCDSup(3.3hPa)		323907	0	3.388e+14	[7.071e+13, 7.473e+14]
COCDSup(3.3hPa)	Q0	242781	0	3.372e+14	[2.735e+14, 6.413e+14]
COCDSup(3.3hPa)	Q1	16789	0	3.406e+14	[2.732e+14, 5.644e+14]
COCDSup(3.3hPa)	Q2	64337	0	3.445e+14	[7.071e+13, 7.473e+14]
COCDSup(16hPa)		323907	0	1.164e+15	[1.86e+14, 3.223e+15]
COCDSup(16hPa)	Q0	242781	0	1.109e+15	[5.722e+14, 2.798e+15]
COCDSup(16hPa)	Q1	16789	0	1.306e+15	[6.737e+14, 2.478e+15]
COCDSup(16hPa)	Q2	64337	0	1.336e+15	[1.86e+14, 3.223e+15]
COCDSup(47hPa)		323907	0	1.628e+15	[3.381e+14, 5.442e+15]
COCDSup(47hPa)	Q0	242781	0	1.632e+15	[1.175e+15, 2.692e+15]
COCDSup(47hPa)	Q1	16789	0	1.593e+15	[1.305e+15, 2.103e+15]
COCDSup(47hPa)	Q2	64337	0	1.621e+15	[3.381e+14, 5.442e+15]
COCDSup(103hPa)		323907	0	5.964e+15	[1.213e+15, 2.378e+16]
COCDSup(103hPa)	Q0	242781	0	6.011e+15	[3.958e+15, 1.115e+16]
COCDSup(103hPa)	Q1	16789	0	5.734e+15	[4.283e+15, 7.874e+15]
COCDSup(103hPa)	Q2	64337	0	5.849e+15	[1.213e+15, 2.378e+16]
COCDSup(190hPa)		323907	0	1.446e+16	[3.194e+15, 8.187e+16]
COCDSup(190hPa)	Q0	242781	0	1.46e+16	[7.946e+15, 4.443e+16]
COCDSup(190hPa)	Q1	16789	0	1.37e+16	[7.172e+15, 2.081e+16]
COCDSup(190hPa)	Q2	64337	0	1.414e+16	[3.194e+15, 8.187e+16]
COCDSup(314hPa)		323907	0	2.647e+16	[3.189e+15, 1.952e+17]

Version 6 Performance and Test Report

COCDSup(314hPa)	Q0	242781	0	2.693e+16	[1.005e+16, 1.431e+17]
COCDSup(314hPa)	Q1	16789	0	2.401e+16	[1.284e+16, 4.208e+16]
COCDSup(314hPa)	Q2	64337	0	2.539e+16	[3.189e+15, 1.952e+17]
COCDSup(478hPa)		323907	0	3.774e+16	[1.377e+16, 2.908e+17]
COCDSup(478hPa)	Q0	242781	0	3.851e+16	[1.908e+16, 1.975e+17]
COCDSup(478hPa)	Q1	16789	0	3.361e+16	[1.849e+16, 7.69e+16]
COCDSup(478hPa)	Q2	64337	0	3.593e+16	[1.377e+16, 2.908e+17]
COCDSup(684hPa)		314518	9389	4.748e+16	[2.266e+16, 4.279e+17]
COCDSup(684hPa)	Q0	241196	0	4.838e+16	[2.652e+16, 2.22e+17]
COCDSup(684hPa)	Q1	16094	0	4.286e+16	[2.638e+16, 7.789e+16]
COCDSup(684hPa)	Q2	57228	9389	4.497e+16	[2.266e+16, 4.279e+17]
COCDSup(932hPa)		281825	42082	5.518e+16	[1.868e+16, 1.473e+17]
COCDSup(932hPa)	Q0	224668	0	5.578e+16	[2.849e+16, 1.281e+17]
COCDSup(932hPa)	Q1	11896	0	5.277e+16	[3.439e+16, 9.009e+16]
COCDSup(932hPa)	Q2	45261	42082	5.281e+16	[1.868e+16, 1.473e+17]
COCDSupErr		30972691	1427309	6.451e+15	[2.889e+13, 4.71e+17]
COCDSupErr	Q0	23388667	0	5.053e+15	[3.401e+13, 2.166e+17]
COCDSupErr	Q1	1577374	0	7.548e+15	[3.513e+13, 1.182e+17]
COCDSupErr	Q2	6006650	1427309	1.16e+16	[2.889e+13, 4.71e+17]
COCDSupErr(0.1hPa)		323907	0	4.118e+13	[3.466e+13, 1.615e+14]
COCDSupErr(0.1hPa)	Q0	242781	0	3.935e+13	[3.466e+13, 1.163e+14]
COCDSupErr(0.1hPa)	Q1	16789	0	4.178e+13	[3.517e+13, 9.341e+13]
COCDSupErr(0.1hPa)	Q2	64337	0	4.793e+13	[3.579e+13, 1.615e+14]
COCDSupErr(3.3hPa)		323907	0	1.286e+14	[5.207e+13, 1.466e+15]
COCDSupErr(3.3hPa)	Q0	242781	0	1.045e+14	[5.207e+13, 1.158e+15]
COCDSupErr(3.3hPa)	Q1	16789	0	1.492e+14	[5.695e+13, 9.094e+14]
COCDSupErr(3.3hPa)	Q2	64337	0	2.139e+14	[6.032e+13, 1.466e+15]
COCDSupErr(16hPa)		323907	0	3.743e+14	[1.084e+14, 4.367e+15]
COCDSupErr(16hPa)	Q0	242781	0	2.989e+14	[1.084e+14, 3.697e+15]
COCDSupErr(16hPa)	Q1	16789	0	4.483e+14	[1.9e+14, 2.895e+15]
COCDSupErr(16hPa)	Q2	64337	0	6.395e+14	[1.953e+14, 4.367e+15]
COCDSupErr(47hPa)		323907	0	6.939e+14	[1.829e+14, 8.886e+15]
COCDSupErr(47hPa)	Q0	242781	0	5.339e+14	[1.829e+14, 7.764e+15]
COCDSupErr(47hPa)	Q1	16789	0	8.488e+14	[2.839e+14, 6.067e+15]
COCDSupErr(47hPa)	Q2	64337	0	1.257e+15	[2.69e+14, 8.886e+15]
COCDSupErr(103hPa)		323907	0	1.588e+15	[4.525e+14, 2.089e+16]
COCDSupErr(103hPa)	Q0	242781	0	1.243e+15	[4.525e+14, 1.728e+16]
COCDSupErr(103hPa)	Q1	16789	0	1.908e+15	[6.508e+14, 1.345e+16]
COCDSupErr(103hPa)	Q2	64337	0	2.808e+15	[6.16e+14, 2.089e+16]
COCDSupErr(190hPa)		323907	0	3.733e+15	[8.366e+14, 4.782e+16]
COCDSupErr(190hPa)	Q0	242781	0	2.841e+15	[8.366e+14, 4.264e+16]
COCDSupErr(190hPa)	Q1	16789	0	4.621e+15	[1.392e+15, 3.321e+16]
COCDSupErr(190hPa)	Q2	64337	0	6.866e+15	[1.187e+15, 4.782e+16]
COCDSupErr(314hPa)		323907	0	7.874e+15	[1.258e+15, 1.065e+17]
COCDSupErr(314hPa)	Q0	242781	0	5.877e+15	[1.258e+15, 9.349e+16]
COCDSupErr(314hPa)	Q1	16789	0	9.947e+15	[2.584e+15, 7.271e+16]
COCDSupErr(314hPa)	Q2	64337	0	1.487e+16	[2.089e+15, 1.065e+17]
COCDSupErr(478hPa)		323907	0	1.188e+16	[1.942e+15, 1.639e+17]
COCDSupErr(478hPa)	Q0	242781	0	8.917e+15	[1.942e+15, 1.375e+17]
COCDSupErr(478hPa)	Q1	16789	0	1.492e+16	[3.938e+15, 1.069e+17]
COCDSupErr(478hPa)	Q2	64337	0	2.225e+16	[3.774e+15, 1.639e+17]
COCDSupErr(684hPa)		314518	9389	1.794e+16	[5.938e+15, 3.084e+17]
COCDSupErr(684hPa)	Q0	241196	0	1.408e+16	[5.938e+15, 1.72e+17]

Version 6 Performance and Test Report

COCDSupErr(684hPa)	Q1	16094	0	2.131e+16	[9.354e+15, 9.308e+16]
COCDSupErr(684hPa)	Q2	57228	9389	3.326e+16	[9.46e+15, 3.084e+17]
COCDSupErr(932hPa)		281825	42082	2.513e+16	[7.967e+15, 4.386e+17]
COCDSupErr(932hPa)	Q0	224668	0	1.925e+16	[7.967e+15, 2.062e+17]
COCDSupErr(932hPa)	Q1	11896	0	3.083e+16	[1.167e+16, 1.135e+17]
COCDSupErr(932hPa)	Q2	45261	42082	5.284e+16	[1.201e+16, 4.386e+17]
COVMRLevSup		30711454	1688546	7.487e-08	[4.669e-10, 1.332e-06]
COVMRLevSup	Q0	23194535	0	7.582e-08	[1.381e-08, 1.332e-06]
COVMRLevSup	Q1	1563479	0	7.086e-08	[1.516e-08, 1.201e-06]
COVMRLevSup	Q2	5953440	1688546	7.22e-08	[4.669e-10, 1.287e-06]
COVMRLevSup(0.1hPa)		323906	1	1.445e-07	[2.208e-09, 2.484e-07]
COVMRLevSup(0.1hPa)	Q0	242781	0	1.447e-07	[1.125e-07, 2.484e-07]
COVMRLevSup(0.1hPa)	Q1	16789	0	1.447e-07	[1.189e-07, 2.271e-07]
COVMRLevSup(0.1hPa)	Q2	64336	1	1.44e-07	[2.208e-09, 2.439e-07]
COVMRLevSup(3.3hPa)		323906	1	2.635e-08	[1.143e-08, 7.403e-08]
COVMRLevSup(3.3hPa)	Q0	242781	0	2.552e-08	[2.105e-08, 5.352e-08]
COVMRLevSup(3.3hPa)	Q1	16789	0	2.754e-08	[2.252e-08, 4.567e-08]
COVMRLevSup(3.3hPa)	Q2	64336	1	2.919e-08	[1.143e-08, 7.403e-08]
COVMRLevSup(16hPa)		323907	0	2.137e-08	[1.212e-08, 5.731e-08]
COVMRLevSup(16hPa)	Q0	242781	0	2.082e-08	[1.381e-08, 4.691e-08]
COVMRLevSup(16hPa)	Q1	16789	0	2.265e-08	[1.529e-08, 4.319e-08]
COVMRLevSup(16hPa)	Q2	64337	0	2.311e-08	[1.212e-08, 5.731e-08]
COVMRLevSup(47hPa)		323907	0	2.39e-08	[1.511e-08, 8.999e-08]
COVMRLevSup(47hPa)	Q0	242781	0	2.336e-08	[1.757e-08, 4.096e-08]
COVMRLevSup(47hPa)	Q1	16789	0	2.499e-08	[1.892e-08, 3.288e-08]
COVMRLevSup(47hPa)	Q2	64337	0	2.567e-08	[1.511e-08, 8.999e-08]
COVMRLevSup(103hPa)		323907	0	3.903e-08	[1.663e-08, 1.697e-07]
COVMRLevSup(103hPa)	Q0	242781	0	3.97e-08	[2.257e-08, 8.547e-08]
COVMRLevSup(103hPa)	Q1	16789	0	3.722e-08	[2.682e-08, 5.174e-08]
COVMRLevSup(103hPa)	Q2	64337	0	3.696e-08	[1.663e-08, 1.697e-07]
COVMRLevSup(190hPa)		323907	0	6.252e-08	[2.715e-08, 3.428e-07]
COVMRLevSup(190hPa)	Q0	242781	0	6.494e-08	[3.417e-08, 2.114e-07]
COVMRLevSup(190hPa)	Q1	16789	0	5.638e-08	[3.561e-08, 8.714e-08]
COVMRLevSup(190hPa)	Q2	64337	0	5.499e-08	[2.715e-08, 3.428e-07]
COVMRLevSup(314hPa)		323907	0	8.262e-08	[3.833e-08, 5.137e-07]
COVMRLevSup(314hPa)	Q0	242781	0	8.604e-08	[4.685e-08, 4.287e-07]
COVMRLevSup(314hPa)	Q1	16789	0	7.269e-08	[4.419e-08, 1.21e-07]
COVMRLevSup(314hPa)	Q2	64337	0	7.233e-08	[3.833e-08, 5.137e-07]
COVMRLevSup(478hPa)		323907	0	9.434e-08	[4.368e-08, 5.592e-07]
COVMRLevSup(478hPa)	Q0	242781	0	9.696e-08	[5.404e-08, 5.125e-07]
COVMRLevSup(478hPa)	Q1	16789	0	8.434e-08	[5.449e-08, 1.816e-07]
COVMRLevSup(478hPa)	Q2	64337	0	8.706e-08	[4.368e-08, 5.592e-07]
COVMRLevSup(684hPa)		312713	11194	1.013e-07	[5.131e-08, 7.73e-07]
COVMRLevSup(684hPa)	Q0	240922	0	1.019e-07	[6.006e-08, 4.359e-07]
COVMRLevSup(684hPa)	Q1	15766	0	9.431e-08	[6.506e-08, 1.588e-07]
COVMRLevSup(684hPa)	Q2	56025	11194	1.007e-07	[5.131e-08, 7.73e-07]
COVMRLevSup(932hPa)		275886	48021	1.094e-07	[5.659e-08, 9.238e-07]
COVMRLevSup(932hPa)	Q0	220177	0	1.08e-07	[6.359e-08, 3.149e-07]
COVMRLevSup(932hPa)	Q1	11658	0	1.064e-07	[7.245e-08, 1.574e-07]
COVMRLevSup(932hPa)	Q2	44051	48021	1.173e-07	[5.659e-08, 9.238e-07]
COVMRLevSupErr		30711454	1688546	9.908e-09	[1.348e-09, 3.535e-07]
COVMRLevSupErr	Q0	23194535	0	9.086e-09	[1.348e-09, 3.228e-07]
COVMRLevSupErr	Q1	1563479	0	1.083e-08	[1.939e-09, 2.881e-07]

Version 6 Performance and Test Report

COVMRLevSupErr	Q2	5953440	1688546	1.287e-08	[1.865e-09, 3.535e-07]
COVMRLevSupErr(0.1hPa)		323906	1	2.599e-08	[2.148e-08, 8.741e-08]
COVMRLevSupErr(0.1hPa)	Q0	242781	0	2.48e-08	[2.148e-08, 6.288e-08]
COVMRLevSupErr(0.1hPa)	Q1	16789	0	2.683e-08	[2.226e-08, 5.488e-08]
COVMRLevSupErr(0.1hPa)	Q2	64336	1	3.026e-08	[2.23e-08, 8.741e-08]
COVMRLevSupErr(3.3hPa)		323906	1	5.57e-09	[2.757e-09, 4.252e-08]
COVMRLevSupErr(3.3hPa)	Q0	242781	0	4.735e-09	[2.757e-09, 3.291e-08]
COVMRLevSupErr(3.3hPa)	Q1	16789	0	6.463e-09	[3.097e-09, 2.699e-08]
COVMRLevSupErr(3.3hPa)	Q2	64336	1	8.487e-09	[3.266e-09, 4.252e-08]
COVMRLevSupErr(16hPa)		323907	0	4.409e-09	[1.645e-09, 3.684e-08]
COVMRLevSupErr(16hPa)	Q0	242781	0	3.683e-09	[1.645e-09, 2.696e-08]
COVMRLevSupErr(16hPa)	Q1	16789	0	5.273e-09	[2.412e-09, 2.1e-08]
COVMRLevSupErr(16hPa)	Q2	64337	0	6.923e-09	[2.631e-09, 3.684e-08]
COVMRLevSupErr(47hPa)		323907	0	3.807e-09	[1.348e-09, 3.773e-08]
COVMRLevSupErr(47hPa)	Q0	242781	0	3.116e-09	[1.348e-09, 2.693e-08]
COVMRLevSupErr(47hPa)	Q1	16789	0	4.546e-09	[1.939e-09, 1.971e-08]
COVMRLevSupErr(47hPa)	Q2	64337	0	6.224e-09	[1.865e-09, 3.773e-08]
COVMRLevSupErr(103hPa)		323907	0	4.972e-09	[1.783e-09, 4.726e-08]
COVMRLevSupErr(103hPa)	Q0	242781	0	4.141e-09	[1.783e-09, 2.934e-08]
COVMRLevSupErr(103hPa)	Q1	16789	0	5.865e-09	[2.528e-09, 1.987e-08]
COVMRLevSupErr(103hPa)	Q2	64337	0	7.872e-09	[2.441e-09, 4.726e-08]
COVMRLevSupErr(190hPa)		323907	0	6.732e-09	[2.217e-09, 6.109e-08]
COVMRLevSupErr(190hPa)	Q0	242781	0	5.749e-09	[2.217e-09, 2.999e-08]
COVMRLevSupErr(190hPa)	Q1	16789	0	7.938e-09	[3.468e-09, 2.111e-08]
COVMRLevSupErr(190hPa)	Q2	64337	0	1.013e-08	[3.339e-09, 6.109e-08]
COVMRLevSupErr(314hPa)		323907	0	8.003e-09	[2.47e-09, 7.525e-08]
COVMRLevSupErr(314hPa)	Q0	242781	0	7.118e-09	[2.47e-09, 2.642e-08]
COVMRLevSupErr(314hPa)	Q1	16789	0	9.142e-09	[4.131e-09, 1.875e-08]
COVMRLevSupErr(314hPa)	Q2	64337	0	1.105e-08	[3.88e-09, 7.525e-08]
COVMRLevSupErr(478hPa)		323907	0	7.041e-09	[2.807e-09, 6.146e-08]
COVMRLevSupErr(478hPa)	Q0	242781	0	6.7e-09	[2.909e-09, 2.637e-08]
COVMRLevSupErr(478hPa)	Q1	16789	0	7.196e-09	[2.879e-09, 2.327e-08]
COVMRLevSupErr(478hPa)	Q2	64337	0	8.289e-09	[2.807e-09, 6.146e-08]
COVMRLevSupErr(684hPa)		312713	11194	5.503e-09	[2.517e-09, 3.846e-08]
COVMRLevSupErr(684hPa)	Q0	240922	0	4.941e-09	[2.517e-09, 3.247e-08]
COVMRLevSupErr(684hPa)	Q1	15766	0	6.501e-09	[3.24e-09, 2.124e-08]
COVMRLevSupErr(684hPa)	Q2	56025	11194	7.637e-09	[3.108e-09, 3.846e-08]
COVMRLevSupErr(932hPa)		275886	48021	1.243e-08	[4.583e-09, 1.126e-07]
COVMRLevSupErr(932hPa)	Q0	220177	0	1.106e-08	[4.583e-09, 4.155e-08]
COVMRLevSupErr(932hPa)	Q1	11658	0	1.468e-08	[7.812e-09, 2.895e-08]
COVMRLevSupErr(932hPa)	Q2	44051	48021	1.87e-08	[8.342e-09, 1.126e-07]
COVMRSurf		323907	0	1.138e-07	[5.676e-08, 9.441e-07]
COVMRSurf	Q0	242781	0	1.123e-07	[6.394e-08, 3.923e-07]
COVMRSurf	Q1	16789	0	1.108e-07	[7.329e-08, 2.589e-07]
COVMRSurf	Q2	64337	0	1.2e-07	[5.676e-08, 9.441e-07]
COVMRSurfErr		323907	0	1.617e-08	[7.477e-09, 1.3e-07]
COVMRSurfErr	Q0	242781	0	1.487e-08	[7.477e-09, 4.95e-08]
COVMRSurfErr	Q1	16789	0	1.744e-08	[9.347e-09, 3.401e-08]
COVMRSurfErr	Q2	64337	0	2.072e-08	[9.191e-09, 1.3e-07]
num_CO_Func		323907	0	8.709	[0, 9]
CO_trapezoid_layers		2160	0	57.56	[1, 93]
CO_eff_press		2820817	95183	409.9	[1.259, 967.4]
CO_VMR_eff		2829540	86460	7.59e-08	[6.155e-09, 8.941e-07]

Version 6 Performance and Test Report

CO_VMR_eff	Q0	2152805	0	7.724e-08	[1.871e-08, 5.04e-07]
CO_VMR_eff	Q1	141268	0	6.977e-08	[2.229e-08, 1.992e-07]
CO_VMR_eff	Q2	535467	86460	7.213e-08	[6.155e-09, 8.941e-07]
CO_VMR_eff_err		2820817	95183	2.661e-08	[2.892e-09, 7.916e-07]
CO_VMR_eff_err	Q0	2152805	0	2.069e-08	[2.892e-09, 3.694e-07]
CO_VMR_eff_err	Q1	141268	0	3.177e-08	[4.042e-09, 2.772e-07]
CO_VMR_eff_err	Q2	526744	95183	4.944e-08	[3.986e-09, 7.916e-07]
CO_verticality		2820791	95209	0.4131	[-0.3166, 1.546]
CO_dof		322923	984	0.7243	[0, 1.454]
CO_ave_kern		26244000	0	0.0444	[-0.2551, 0.57]
CH4_total_column		323907	0	3.56e+19	[1.85e+19, 6.911e+19]
CH4_total_column	Q0	212097	0	3.565e+19	[1.912e+19, 4.046e+19]
CH4_total_column	Q1	9454	0	3.487e+19	[2.025e+19, 3.98e+19]
CH4_total_column	Q2	102356	0	3.555e+19	[1.85e+19, 6.911e+19]
CH4CDSup		30972691	1427309	3.754e+17	[3.344e+13, 2.756e+18]
CH4CDSup	Q0	20281379	0	3.759e+17	[3.344e+13, 1.217e+18]
CH4CDSup	Q1	900371	0	3.695e+17	[3.377e+13, 1.192e+18]
CH4CDSup	Q2	9790941	1427309	3.749e+17	[3.353e+13, 2.756e+18]
CH4CDSup(0.1hPa)		323907	0	6.373e+14	[1.839e+14, 1.565e+15]
CH4CDSup(0.1hPa)	Q0	212097	0	6.723e+14	[1.839e+14, 1.428e+15]
CH4CDSup(0.1hPa)	Q1	9454	0	3.84e+14	[1.864e+14, 1.395e+15]
CH4CDSup(0.1hPa)	Q2	102356	0	5.882e+14	[1.846e+14, 1.565e+15]
CH4CDSup(3.3hPa)		323907	0	7.925e+15	[3.089e+15, 1.793e+16]
CH4CDSup(3.3hPa)	Q0	212097	0	8.278e+15	[3.089e+15, 1.597e+16]
CH4CDSup(3.3hPa)	Q1	9454	0	5.343e+15	[3.142e+15, 1.545e+16]
CH4CDSup(3.3hPa)	Q2	102356	0	7.432e+15	[3.099e+15, 1.793e+16]
CH4CDSup(16hPa)		323907	0	4.273e+16	[2.652e+16, 7.013e+16]
CH4CDSup(16hPa)	Q0	212097	0	4.365e+16	[2.675e+16, 6.251e+16]
CH4CDSup(16hPa)	Q1	9454	0	3.606e+16	[2.72e+16, 6.045e+16]
CH4CDSup(16hPa)	Q2	102356	0	4.144e+16	[2.652e+16, 7.013e+16]
CH4CDSup(47hPa)		323907	0	1.246e+17	[9.044e+16, 1.725e+17]
CH4CDSup(47hPa)	Q0	212097	0	1.257e+17	[9.617e+16, 1.503e+17]
CH4CDSup(47hPa)	Q1	9454	0	1.165e+17	[9.889e+16, 1.466e+17]
CH4CDSup(47hPa)	Q2	102356	0	1.229e+17	[9.044e+16, 1.725e+17]
CH4CDSup(103hPa)		323907	0	2.409e+17	[1.31e+17, 3.863e+17]
CH4CDSup(103hPa)	Q0	212097	0	2.419e+17	[2.043e+17, 2.729e+17]
CH4CDSup(103hPa)	Q1	9454	0	2.349e+17	[2.128e+17, 2.636e+17]
CH4CDSup(103hPa)	Q2	102356	0	2.394e+17	[1.31e+17, 3.863e+17]
CH4CDSup(190hPa)		323907	0	3.762e+17	[2.148e+17, 8.886e+17]
CH4CDSup(190hPa)	Q0	212097	0	3.769e+17	[3.329e+17, 4.143e+17]
CH4CDSup(190hPa)	Q1	9454	0	3.744e+17	[3.47e+17, 4.073e+17]
CH4CDSup(190hPa)	Q2	102356	0	3.748e+17	[2.148e+17, 8.886e+17]
CH4CDSup(314hPa)		323907	0	5.285e+17	[3.996e+17, 1.002e+18]
CH4CDSup(314hPa)	Q0	212097	0	5.289e+17	[4.629e+17, 5.906e+17]
CH4CDSup(314hPa)	Q1	9454	0	5.251e+17	[4.823e+17, 5.842e+17]
CH4CDSup(314hPa)	Q2	102356	0	5.278e+17	[3.996e+17, 1.002e+18]
CH4CDSup(478hPa)		323907	0	6.929e+17	[5.387e+17, 1.371e+18]
CH4CDSup(478hPa)	Q0	212097	0	6.924e+17	[6.06e+17, 7.834e+17]
CH4CDSup(478hPa)	Q1	9454	0	6.864e+17	[6.204e+17, 7.641e+17]
CH4CDSup(478hPa)	Q2	102356	0	6.945e+17	[5.387e+17, 1.371e+18]
CH4CDSup(684hPa)		314518	9389	8.548e+17	[5.951e+17, 2.346e+18]
CH4CDSup(684hPa)	Q0	205984	0	8.548e+17	[7.641e+17, 9.686e+17]
CH4CDSup(684hPa)	Q1	9267	0	8.526e+17	[7.709e+17, 9.398e+17]

Version 6 Performance and Test Report

CH4CDSup(684hPa)	Q2	99267	9389	8.551e+17	[5.951e+17, 2.346e+18]
CH4CDSup(932hPa)		281825	42082	1.011e+18	[3.727e+17, 1.835e+18]
CH4CDSup(932hPa)	Q0	183518	0	1.012e+18	[8.647e+17, 1.161e+18]
CH4CDSup(932hPa)	Q1	7897	0	1.018e+18	[9.252e+17, 1.13e+18]
CH4CDSup(932hPa)	Q2	90410	42082	1.009e+18	[3.727e+17, 1.835e+18]
CH4CDSupErr		30972691	1427309	1.23e+16	[8.019e+11, 5.651e+17]
CH4CDSupErr	Q0	20281379	0	1.175e+16	[8.075e+11, 5.869e+16]
CH4CDSupErr	Q1	900371	0	1.168e+16	[8.019e+11, 5.932e+16]
CH4CDSupErr	Q2	9790941	1427309	1.35e+16	[8.056e+11, 5.651e+17]
CH4CDSupErr(0.1hPa)		323907	0	1.713e+13	[4.602e+12, 6.971e+14]
CH4CDSupErr(0.1hPa)	Q0	212097	0	1.723e+13	[4.602e+12, 3.87e+13]
CH4CDSupErr(0.1hPa)	Q1	9454	0	9.737e+12	[4.62e+12, 3.574e+13]
CH4CDSupErr(0.1hPa)	Q2	102356	0	1.76e+13	[4.617e+12, 6.971e+14]
CH4CDSupErr(3.3hPa)		323907	0	2.507e+14	[9.066e+13, 7.687e+15]
CH4CDSupErr(3.3hPa)	Q0	212097	0	2.511e+14	[9.066e+13, 5.076e+14]
CH4CDSupErr(3.3hPa)	Q1	9454	0	1.602e+14	[9.251e+13, 4.647e+14]
CH4CDSupErr(3.3hPa)	Q2	102356	0	2.584e+14	[9.149e+13, 7.687e+15]
CH4CDSupErr(16hPa)		323907	0	1.367e+15	[7.83e+14, 2.992e+16]
CH4CDSupErr(16hPa)	Q0	212097	0	1.334e+15	[7.83e+14, 2.028e+15]
CH4CDSupErr(16hPa)	Q1	9454	0	1.091e+15	[8.088e+14, 1.823e+15]
CH4CDSupErr(16hPa)	Q2	102356	0	1.459e+15	[7.92e+14, 2.992e+16]
CH4CDSupErr(47hPa)		323907	0	3.813e+15	[2.664e+15, 7.186e+16]
CH4CDSupErr(47hPa)	Q0	212097	0	3.661e+15	[2.682e+15, 4.559e+15]
CH4CDSupErr(47hPa)	Q1	9454	0	3.387e+15	[2.82e+15, 4.252e+15]
CH4CDSupErr(47hPa)	Q2	102356	0	4.167e+15	[2.664e+15, 7.186e+16]
CH4CDSupErr(103hPa)		323907	0	8.133e+15	[4.335e+15, 1.284e+17]
CH4CDSupErr(103hPa)	Q0	212097	0	7.797e+15	[6.344e+15, 8.931e+15]
CH4CDSupErr(103hPa)	Q1	9454	0	7.614e+15	[6.758e+15, 8.653e+15]
CH4CDSupErr(103hPa)	Q2	102356	0	8.878e+15	[4.335e+15, 1.284e+17]
CH4CDSupErr(190hPa)		323907	0	1.113e+16	[6.425e+15, 1.958e+17]
CH4CDSupErr(190hPa)	Q0	212097	0	1.055e+16	[9.13e+15, 1.181e+16]
CH4CDSupErr(190hPa)	Q1	9454	0	1.077e+16	[9.618e+15, 1.186e+16]
CH4CDSupErr(190hPa)	Q2	102356	0	1.237e+16	[6.425e+15, 1.958e+17]
CH4CDSupErr(314hPa)		323907	0	1.551e+16	[1.202e+16, 2.729e+17]
CH4CDSupErr(314hPa)	Q0	212097	0	1.465e+16	[1.225e+16, 1.682e+16]
CH4CDSupErr(314hPa)	Q1	9454	0	1.5e+16	[1.331e+16, 1.663e+16]
CH4CDSupErr(314hPa)	Q2	102356	0	1.733e+16	[1.202e+16, 2.729e+17]
CH4CDSupErr(478hPa)		323907	0	2.093e+16	[1.601e+16, 3.565e+17]
CH4CDSupErr(478hPa)	Q0	212097	0	1.98e+16	[1.655e+16, 2.702e+16]
CH4CDSupErr(478hPa)	Q1	9454	0	2.017e+16	[1.713e+16, 2.45e+16]
CH4CDSupErr(478hPa)	Q2	102356	0	2.334e+16	[1.601e+16, 3.565e+17]
CH4CDSupErr(684hPa)		314518	9389	2.632e+16	[1.788e+16, 4.445e+17]
CH4CDSupErr(684hPa)	Q0	205984	0	2.511e+16	[2.065e+16, 4.554e+16]
CH4CDSupErr(684hPa)	Q1	9267	0	2.569e+16	[2.15e+16, 4.417e+16]
CH4CDSupErr(684hPa)	Q2	99267	9389	2.889e+16	[1.788e+16, 4.445e+17]
CH4CDSupErr(932hPa)		281825	42082	3.986e+16	[1.555e+16, 5.349e+17]
CH4CDSupErr(932hPa)	Q0	183518	0	3.849e+16	[3e+16, 5.629e+16]
CH4CDSupErr(932hPa)	Q1	7897	0	3.802e+16	[2.96e+16, 5.252e+16]
CH4CDSupErr(932hPa)	Q2	90410	42082	4.282e+16	[1.555e+16, 5.349e+17]
CH4VMRLevSup		30711466	1688534	1.404e-06	[1.226e-07, 5.137e-06]
CH4VMRLevSup	Q0	20111517	0	1.414e-06	[1.398e-07, 2.099e-06]
CH4VMRLevSup	Q1	892433	0	1.333e-06	[1.412e-07, 2.022e-06]
CH4VMRLevSup	Q2	9707516	1688534	1.39e-06	[1.226e-07, 5.137e-06]

Version 6 Performance and Test Report

CH4VMRLevSup(0.1hPa)		323907	0	4.888e-07	[1.226e-07, 1.202e-06]
CH4VMRLevSup(0.1hPa)	Q0	212097	0	5.157e-07	[1.417e-07, 1.129e-06]
CH4VMRLevSup(0.1hPa)	Q1	9454	0	2.949e-07	[1.436e-07, 1.069e-06]
CH4VMRLevSup(0.1hPa)	Q2	102356	0	4.509e-07	[1.226e-07, 1.202e-06]
CH4VMRLevSup(3.3hPa)		323907	0	5.926e-07	[2.394e-07, 1.32e-06]
CH4VMRLevSup(3.3hPa)	Q0	212097	0	6.179e-07	[2.394e-07, 1.173e-06]
CH4VMRLevSup(3.3hPa)	Q1	9454	0	4.055e-07	[2.435e-07, 1.134e-06]
CH4VMRLevSup(3.3hPa)	Q2	102356	0	5.575e-07	[2.402e-07, 1.32e-06]
CH4VMRLevSup(16hPa)		323907	0	1.036e-06	[6.319e-07, 1.676e-06]
CH4VMRLevSup(16hPa)	Q0	212097	0	1.057e-06	[6.615e-07, 1.493e-06]
CH4VMRLevSup(16hPa)	Q1	9454	0	8.818e-07	[6.722e-07, 1.444e-06]
CH4VMRLevSup(16hPa)	Q2	102356	0	1.006e-06	[6.319e-07, 1.676e-06]
CH4VMRLevSup(47hPa)		323907	0	1.438e-06	[9.563e-07, 2.081e-06]
CH4VMRLevSup(47hPa)	Q0	212097	0	1.451e-06	[1.121e-06, 1.724e-06]
CH4VMRLevSup(47hPa)	Q1	9454	0	1.351e-06	[1.154e-06, 1.686e-06]
CH4VMRLevSup(47hPa)	Q2	102356	0	1.418e-06	[9.563e-07, 2.081e-06]
CH4VMRLevSup(103hPa)		323907	0	1.635e-06	[8.844e-07, 2.949e-06]
CH4VMRLevSup(103hPa)	Q0	212097	0	1.643e-06	[1.383e-06, 1.844e-06]
CH4VMRLevSup(103hPa)	Q1	9454	0	1.6e-06	[1.459e-06, 1.793e-06]
CH4VMRLevSup(103hPa)	Q2	102356	0	1.624e-06	[8.844e-07, 2.949e-06]
CH4VMRLevSup(190hPa)		323907	0	1.718e-06	[1.175e-06, 3.306e-06]
CH4VMRLevSup(190hPa)	Q0	212097	0	1.721e-06	[1.52e-06, 1.889e-06]
CH4VMRLevSup(190hPa)	Q1	9454	0	1.705e-06	[1.583e-06, 1.839e-06]
CH4VMRLevSup(190hPa)	Q2	102356	0	1.712e-06	[1.175e-06, 3.306e-06]
CH4VMRLevSup(314hPa)		323907	0	1.757e-06	[1.395e-06, 3.556e-06]
CH4VMRLevSup(314hPa)	Q0	212097	0	1.758e-06	[1.577e-06, 1.93e-06]
CH4VMRLevSup(314hPa)	Q1	9454	0	1.749e-06	[1.626e-06, 1.91e-06]
CH4VMRLevSup(314hPa)	Q2	102356	0	1.756e-06	[1.395e-06, 3.556e-06]
CH4VMRLevSup(478hPa)		323907	0	1.78e-06	[1.477e-06, 3.512e-06]
CH4VMRLevSup(478hPa)	Q0	212097	0	1.78e-06	[1.613e-06, 1.983e-06]
CH4VMRLevSup(478hPa)	Q1	9454	0	1.774e-06	[1.639e-06, 1.943e-06]
CH4VMRLevSup(478hPa)	Q2	102356	0	1.781e-06	[1.477e-06, 3.512e-06]
CH4VMRLevSup(684hPa)		312713	11194	1.798e-06	[1.226e-06, 4.685e-06]
CH4VMRLevSup(684hPa)	Q0	204458	0	1.797e-06	[1.614e-06, 2.028e-06]
CH4VMRLevSup(684hPa)	Q1	9195	0	1.796e-06	[1.65e-06, 1.965e-06]
CH4VMRLevSup(684hPa)	Q2	99060	11194	1.799e-06	[1.226e-06, 4.685e-06]
CH4VMRLevSup(932hPa)		275886	48021	1.816e-06	[8.634e-07, 3.921e-06]
CH4VMRLevSup(932hPa)	Q0	179860	0	1.816e-06	[1.558e-06, 2.087e-06]
CH4VMRLevSup(932hPa)	Q1	7772	0	1.82e-06	[1.653e-06, 2.013e-06]
CH4VMRLevSup(932hPa)	Q2	88254	48021	1.817e-06	[8.634e-07, 3.921e-06]
CH4VMRLevSupErr		30711466	1688534	3.703e-08	[7.738e-09, 1.383e-06]
CH4VMRLevSupErr	Q0	20111517	0	3.687e-08	[7.745e-09, 3.17e-07]
CH4VMRLevSupErr	Q1	892433	0	3.295e-08	[7.793e-09, 1.024e-07]
CH4VMRLevSupErr	Q2	9707516	1688534	3.775e-08	[7.738e-09, 1.383e-06]
CH4VMRLevSupErr(0.1hPa)		323907	0	3.478e-08	[8.943e-09, 9.211e-07]
CH4VMRLevSupErr(0.1hPa)	Q0	212097	0	3.559e-08	[8.943e-09, 8.223e-08]
CH4VMRLevSupErr(0.1hPa)	Q1	9454	0	2.015e-08	[8.993e-09, 7.608e-08]
CH4VMRLevSupErr(0.1hPa)	Q2	102356	0	3.447e-08	[9.025e-09, 9.211e-07]
CH4VMRLevSupErr(3.3hPa)		323907	0	3.505e-08	[1.317e-08, 5.743e-07]
CH4VMRLevSupErr(3.3hPa)	Q0	212097	0	3.573e-08	[1.317e-08, 7.356e-08]
CH4VMRLevSupErr(3.3hPa)	Q1	9454	0	2.317e-08	[1.336e-08, 6.728e-08]
CH4VMRLevSupErr(3.3hPa)	Q2	102356	0	3.475e-08	[1.326e-08, 5.743e-07]
CH4VMRLevSupErr(16hPa)		323907	0	4.625e-08	[2.791e-08, 5.222e-07]

Version 6 Performance and Test Report

CH4VMRLevSupErr(16hPa)	Q0	212097	0	4.62e-08	[2.791e-08, 6.863e-08]
CH4VMRLevSupErr(16hPa)	Q1	9454	0	3.824e-08	[2.864e-08, 6.258e-08]
CH4VMRLevSupErr(16hPa)	Q2	102356	0	4.711e-08	[2.802e-08, 5.222e-07]
CH4VMRLevSupErr(47hPa)		323907	0	5e-08	[3.538e-08, 4.556e-07]
CH4VMRLevSupErr(47hPa)	Q0	212097	0	4.943e-08	[3.689e-08, 6.041e-08]
CH4VMRLevSupErr(47hPa)	Q1	9454	0	4.591e-08	[3.872e-08, 5.745e-08]
CH4VMRLevSupErr(47hPa)	Q2	102356	0	5.156e-08	[3.538e-08, 4.556e-07]
CH4VMRLevSupErr(103hPa)		323907	0	4.766e-08	[2.724e-08, 3.485e-07]
CH4VMRLevSupErr(103hPa)	Q0	212097	0	4.699e-08	[3.896e-08, 5.233e-08]
CH4VMRLevSupErr(103hPa)	Q1	9454	0	4.606e-08	[4.096e-08, 5.148e-08]
CH4VMRLevSupErr(103hPa)	Q2	102356	0	4.919e-08	[2.724e-08, 3.485e-07]
CH4VMRLevSupErr(190hPa)		323907	0	4.12e-08	[2.767e-08, 2.248e-07]
CH4VMRLevSupErr(190hPa)	Q0	212097	0	4.069e-08	[3.341e-08, 4.451e-08]
CH4VMRLevSupErr(190hPa)	Q1	9454	0	4.093e-08	[3.472e-08, 4.443e-08]
CH4VMRLevSupErr(190hPa)	Q2	102356	0	4.229e-08	[2.767e-08, 2.248e-07]
CH4VMRLevSupErr(314hPa)		323907	0	3.318e-08	[1.896e-08, 1.051e-07]
CH4VMRLevSupErr(314hPa)	Q0	212097	0	3.295e-08	[1.943e-08, 3.761e-08]
CH4VMRLevSupErr(314hPa)	Q1	9454	0	3.296e-08	[2.065e-08, 3.746e-08]
CH4VMRLevSupErr(314hPa)	Q2	102356	0	3.369e-08	[1.896e-08, 1.051e-07]
CH4VMRLevSupErr(478hPa)		323907	0	2.153e-08	[1.444e-08, 2.102e-07]
CH4VMRLevSupErr(478hPa)	Q0	212097	0	2.141e-08	[1.476e-08, 5.182e-08]
CH4VMRLevSupErr(478hPa)	Q1	9454	0	2.105e-08	[1.53e-08, 2.949e-08]
CH4VMRLevSupErr(478hPa)	Q2	102356	0	2.182e-08	[1.444e-08, 2.102e-07]
CH4VMRLevSupErr(684hPa)		312713	11194	2.019e-08	[1.325e-08, 2.351e-07]
CH4VMRLevSupErr(684hPa)	Q0	204458	0	1.99e-08	[1.604e-08, 5.791e-08]
CH4VMRLevSupErr(684hPa)	Q1	9195	0	2.123e-08	[1.649e-08, 5.643e-08]
CH4VMRLevSupErr(684hPa)	Q2	99060	11194	2.068e-08	[1.325e-08, 2.351e-07]
CH4VMRLevSupErr(932hPa)		275886	48021	4.283e-08	[2.951e-08, 2.657e-07]
CH4VMRLevSupErr(932hPa)	Q0	179860	0	4.212e-08	[3.657e-08, 5.435e-08]
CH4VMRLevSupErr(932hPa)	Q1	7772	0	4.26e-08	[3.736e-08, 5.316e-08]
CH4VMRLevSupErr(932hPa)	Q2	88254	48021	4.431e-08	[2.951e-08, 2.657e-07]
CH4VMRSurf		323907	0	1.822e-06	[7.719e-07, 5.194e-06]
CH4VMRSurf	Q0	212097	0	1.822e-06	[1.543e-06, 2.102e-06]
CH4VMRSurf	Q1	9454	0	1.819e-06	[1.65e-06, 2.026e-06]
CH4VMRSurf	Q2	102356	0	1.823e-06	[7.719e-07, 5.194e-06]
CH4VMRSurfErr		323907	0	5.091e-08	[3.526e-08, 2.758e-07]
CH4VMRSurfErr	Q0	212097	0	5.034e-08	[4.452e-08, 6.317e-08]
CH4VMRSurfErr	Q1	9454	0	5.054e-08	[4.538e-08, 5.863e-08]
CH4VMRSurfErr	Q2	102356	0	5.212e-08	[3.526e-08, 2.758e-07]
num_CH4_Func		323907	0	9.873	[0, 10]
CH4_trapezoid_layers_10func		2400	0	53.9	[1, 88]
CH4_eff_press_10func		3198046	41954	330.3	[1.429, 899.2]
CH4_VMR_eff_10func		3207832	32168	1.615e-06	[3.189e-07, 4.97e-06]
CH4_VMR_eff_10func	Q0	2100394	0	1.62e-06	[3.189e-07, 2.123e-06]
CH4_VMR_eff_10func	Q1	93283	0	1.581e-06	[3.247e-07, 2.002e-06]
CH4_VMR_eff_10func	Q2	1014155	32168	1.609e-06	[3.196e-07, 4.97e-06]
CH4_VMR_eff_10func_err		3198046	41954	4.916e-08	[9.716e-09, 1.494e-07]
CH4_VMR_eff_10func_err	Q0	2100394	0	4.912e-08	[9.716e-09, 8.425e-08]
CH4_VMR_eff_10func_err	Q1	93283	0	4.873e-08	[9.945e-09, 8.409e-08]
CH4_VMR_eff_10func_err	Q2	1004369	41954	4.93e-08	[9.805e-09, 1.494e-07]
CH4_verticality_10func		3198016	41984	0.5266	[-0.3359, 1.514]
CH4_dof		322923	984	0.8974	[0, 1.75]
CH4_ave_kern_10func		32400000	0	0.05198	[-0.2104, 0.8595]

Version 6 Performance and Test Report

olr		323907	0	230.8	[80.24,	392.3]
olr	Q0	322926	0	231	[80.24,	392.3]
olr	Q1	658	0	163.3	[89.4,	297]
olr	Q2	323	0	161.4	[81.83,	264.5]
spectralolr		5182528	1472	14.43	[0.0006532,	87.06]
spectralolr	Q0	5166816	0	14.44	[0.0006532,	87.06]
spectralolr	Q1	10544	0	10.22	[0.0009869,	55.83]
spectralolr	Q2	5168	1472	10.09	[0.001188,	46.06]
olr3x3		2915172	828	230.8	[78.97,	392.4]
olr3x3	Q0	2906334	0	231	[78.97,	392.4]
olr3x3	Q1	5931	0	163.5	[89.4,	297]
olr3x3	Q2	2907	828	161.4	[81.83,	264.5]
olr_err		323907	0	5.006	[5,	7]
olr_err	Q0	322926	0	5	[5,	5]
olr_err	Q1	658	0	7	[7,	7]
olr_err	Q2	323	0	7	[7,	7]
clrolr		323907	0	251	[88.43,	392.4]
clrolr	Q0	280015	0	255.1	[88.43,	392.4]
clrolr	Q2	43892	0	224.8	[90.37,	385.6]
clrolr_err		323907	0	12.71	[10,	30]
clrolr_err	Q0	280015	0	10	[10,	10]
clrolr_err	Q2	43892	0	30	[30,	30]
spectralclrolr		5182528	1472	15.69	[0.0007838,	87.08]
spectralclrolr	Q0	4480240	0	15.94	[0.0007838,	87.08]
spectralclrolr	Q2	702288	1472	14.05	[0.000831,	83.81]
ftpgeoqa		323907	0	0	[0,	0]
zengeoqa		323907	0	0	[0,	0]
demgeoqa		323907	0	0.01092	[0,	4]
all_spots_avg		323907	0	0.074	[0,	1]
retrieval_type		324000	0	0.1096	[0,	100]
SurfClass		323907	0	2.224	[0,	7]
IR_Precip_Est		323907	0	2.31	[0,	39.38]
IR_Precip_Est	Q0	322926	0	2.273	[0,	39.38]
IR_Precip_Est	Q1	658	0	14.56	[0,	33.71]
IR_Precip_Est	Q2	323	0	14.85	[0,	32.46]
IR_Precip_Est3x3		2915172	828	2.31	[0,	41.66]
IR_Precip_Est3x3	Q0	2906334	0	2.273	[0,	41.66]
IR_Precip_Est3x3	Q1	5931	0	14.53	[0,	33.71]
IR_Precip_Est3x3	Q2	2907	828	14.85	[0,	32.46]
IR_Precip_Est_Err		323907	0	0.4621	[0,	7.877]
IR_Precip_Est_Err	Q0	322926	0	0.4546	[0,	7.877]
IR_Precip_Est_Err	Q1	658	0	2.911	[0,	6.742]
IR_Precip_Est_Err	Q2	323	0	2.97	[0,	6.493]
TAirMWOnly		30972691	1427309	236.8	[165.8,	316.2]
TAirMWOnly	Q0	30575466	0	236.5	[165.8,	315.8]
TAirMWOnly	Q2	397225	1427309	258.8	[193.4,	316.2]
TAirMWOnly(0.1hPa)		323907	0	240.4	[217.6,	274.4]
TAirMWOnly(0.1hPa)	Q0	323907	0	240.4	[217.6,	274.4]
TAirMWOnly(3.3hPa)		323907	0	244.5	[226.9,	263.5]
TAirMWOnly(3.3hPa)	Q0	323907	0	244.5	[226.9,	263.5]
TAirMWOnly(16hPa)		323907	0	222.5	[195,	239.7]
TAirMWOnly(16hPa)	Q0	323907	0	222.5	[195,	239.7]
TAirMWOnly(47hPa)		323907	0	212.2	[182.9,	231.9]

Version 6 Performance and Test Report

TAirMWOnly(47hPa)	Q0	323907	0	212.2	[182.9,	231.9]
TAirMWOnly(103hPa)		323907	0	207.3	[181.8,	234.3]
TAirMWOnly(103hPa)	Q0	323907	0	207.3	[181.8,	234.3]
TAirMWOnly(190hPa)		323907	0	216.8	[189.9,	236.8]
TAirMWOnly(190hPa)	Q0	323907	0	216.8	[189.9,	236.8]
TAirMWOnly(314hPa)		323907	0	231.4	[203.1,	258.4]
TAirMWOnly(314hPa)	Q0	314141	0	231.2	[203.1,	251.5]
TAirMWOnly(314hPa)	Q2	9766	0	237	[208.5,	258.4]
TAirMWOnly(478hPa)		323907	0	251.9	[216.2,	277.8]
TAirMWOnly(478hPa)	Q0	314141	0	251.7	[216.2,	276.3]
TAirMWOnly(478hPa)	Q2	9766	0	258.4	[223.8,	277.8]
TAirMWOnly(684hPa)		314518	9389	268.7	[211.6,	295.4]
TAirMWOnly(684hPa)	Q0	304855	0	268.5	[211.6,	295.4]
TAirMWOnly(684hPa)	Q2	9663	9389	274.5	[236.5,	292.8]
TAirMWOnly(932hPa)		281825	42082	281.2	[234,	313.1]
TAirMWOnly(932hPa)	Q0	273360	0	281	[234,	313.1]
TAirMWOnly(932hPa)	Q2	8465	42082	287.5	[241.9,	312.7]
TAirMWOnlyErr		8261788	810212	2.573	[0.9841,	8.959]
TAirMWOnlyErr(1000hPa)		182070	141837	7.338	[3,	8.15]
TAirMWOnlyErr(400hPa)		314141	9766	2.011	[1.576,	3]
TAirMWOnlyErr(70hPa)		314141	9766	1.442	[1.259,	3]
TAirMWOnlyErr(7.0hPa)		314141	9766	1.602	[1.395,	3]
TAirMWOnlyErr(0.5hPa)		314141	9766	3.613	[2.395,	4.357]
MWSurfClass		323907	0	2.224	[0,	7]
sfcTbMWStd		1619540	648460	193.1	[75.15,	347.6]
sfcTbMWStd	Q0	1256568	0	191.1	[75.15,	313.2]
sfcTbMWStd	Q2	362972	648460	200	[82.83,	347.6]
EmisMWStd		1619540	648460	0.6913	[0.2751,	1.161]
EmisMWStd	Q0	1570710	0	0.6876	[0.2814,	1]
EmisMWStd	Q2	48830	648460	0.8115	[0.2751,	1.161]
EmisMWStdErr		1619540	648460	0.04861	[0.015,	1]
EmisMWStdErr	Q0	1570710	0	0.01903	[0.015,	1]
EmisMWStdErr	Q2	48830	648460	1	[1,	1]
Emis50GHz		323907	0	0.697	[0.2899,	1]
Emis50GHz	Q0	314141	0	0.6935	[0.3966,	1]
Emis50GHz	Q2	9766	0	0.81	[0.2899,	1]
totH2OMWOnlyStd		323907	0	19.66	[0.06155,	94.35]
totH2OMWOnlyStd	Q1	176898	0	25.13	[1.948,	72.35]
totH2OMWOnlyStd	Q2	147009	0	13.08	[0.06155,	94.35]
H2OCDMWOnly		30972691	1427309	7.06e+20	[1.17e+11,	3.799e+22]
H2OCDMWOnly	Q1	17185670	0	8.866e+20	[1.681e+15,	2.438e+22]
H2OCDMWOnly	Q2	13787021	1427309	4.809e+20	[1.17e+11,	3.799e+22]
H2OCDMWOnly(0.1hPa)		323907	0	7.58e+15	[6.525e+15,	8.189e+15]
H2OCDMWOnly(0.1hPa)	Q1	176898	0	7.719e+15	[6.555e+15,	8.189e+15]
H2OCDMWOnly(0.1hPa)	Q2	147009	0	7.412e+15	[6.525e+15,	8.179e+15]
H2OCDMWOnly(3.3hPa)		323907	0	7.484e+16	[6.67e+16,	8.46e+16]
H2OCDMWOnly(3.3hPa)	Q1	176898	0	7.304e+16	[6.67e+16,	8.446e+16]
H2OCDMWOnly(3.3hPa)	Q2	147009	0	7.701e+16	[6.672e+16,	8.46e+16]
H2OCDMWOnly(16hPa)		323907	0	2.064e+17	[2.038e+17,	2.246e+17]
H2OCDMWOnly(16hPa)	Q1	176898	0	2.044e+17	[2.038e+17,	2.193e+17]
H2OCDMWOnly(16hPa)	Q2	147009	0	2.088e+17	[2.038e+17,	2.246e+17]
H2OCDMWOnly(47hPa)		323907	0	4.206e+17	[4.188e+17,	4.237e+17]
H2OCDMWOnly(47hPa)	Q1	176898	0	4.21e+17	[4.188e+17,	4.237e+17]

Version 6 Performance and Test Report

H2OCDMWOnly(47hPa)	Q2	147009	0	4.202e+17	[4.188e+17, 4.223e+17]
H2OCDMWOnly(103hPa)		323907	0	7.618e+17	[7.071e+17, 1.023e+18]
H2OCDMWOnly(103hPa)	Q1	176898	0	7.769e+17	[7.071e+17, 1.023e+18]
H2OCDMWOnly(103hPa)	Q2	147009	0	7.435e+17	[7.071e+17, 1.011e+18]
H2OCDMWOnly(190hPa)		323907	0	6.069e+18	[2.311e+17, 6.123e+19]
H2OCDMWOnly(190hPa)	Q1	176898	0	6.722e+18	[2.311e+17, 3.077e+19]
H2OCDMWOnly(190hPa)	Q2	147009	0	5.284e+18	[2.954e+17, 6.123e+19]
H2OCDMWOnly(314hPa)		323907	0	7.523e+19	[2.05e+18, 1.315e+21]
H2OCDMWOnly(314hPa)	Q1	176898	0	8.789e+19	[4.475e+18, 7.625e+20]
H2OCDMWOnly(314hPa)	Q2	147009	0	5.999e+19	[2.05e+18, 1.315e+21]
H2OCDMWOnly(478hPa)		323907	0	4.679e+20	[5.151e+17, 5.042e+21]
H2OCDMWOnly(478hPa)	Q1	176898	0	5.296e+20	[3.697e+19, 3.735e+21]
H2OCDMWOnly(478hPa)	Q2	147009	0	3.937e+20	[5.151e+17, 5.042e+21]
H2OCDMWOnly(684hPa)		314518	9389	1.866e+21	[1.095e+15, 1.099e+22]
H2OCDMWOnly(684hPa)	Q1	176897	0	2.054e+21	[3.175e+19, 8.231e+21]
H2OCDMWOnly(684hPa)	Q2	137621	9389	1.625e+21	[1.095e+15, 1.099e+22]
H2OCDMWOnly(932hPa)		281825	42082	6.206e+21	[9.867e+11, 2.972e+22]
H2OCDMWOnly(932hPa)	Q1	176838	0	7.182e+21	[3.916e+20, 1.856e+22]
H2OCDMWOnly(932hPa)	Q2	104987	42082	4.561e+21	[9.867e+11, 2.972e+22]
totCldH20Std		323907	0	0.03035	[0, 15.67]
totCldH20Std	Q1	176897	0	0.03017	[5.963e-08, 0.4997]
totCldH20Std	Q2	147010	0	0.03057	[0, 15.67]
totCldH20StdErr		299257	24650	0.0162	[0.0005, 15.67]
totCldH20StdErr	Q1	176897	0	0.00179	[0.0005, 0.04648]
totCldH20StdErr	Q2	122360	24650	0.03702	[0.0005, 15.67]
satzen_amsu		323907	0	28.37	[1.739, 56.33]
satazi_amsu		323907	0	0.8704	[-180, 180]
MWHingeSurfFreqGHz		1680	0	82.94	[23.8, 183.3]
PrecipAA4_50km		0	323907	nan	[0, 0]
PrecipAA5_50km		0	323907	nan	[0, 0]
PrecipAA6_50km		0	323907	nan	[0, 0]
PrecipAA7_50km		0	323907	nan	[0, 0]
PrecipAA8_50km		0	323907	nan	[0, 0]
PrecipAA9_50km		0	323907	nan	[0, 0]
PrecipAA4_15km		0	2916000	nan	[0, 0]
PrecipAA5_15km		0	2916000	nan	[0, 0]
PrecipAA6_15km		0	2916000	nan	[0, 0]
PrecipAA7_15km		0	2916000	nan	[0, 0]
PrecipAA8_15km		0	2916000	nan	[0, 0]
PrecipAA9_15km		0	2916000	nan	[0, 0]
AMSU_A_4_Precip_Corr_50km		0	323907	nan	[0, 0]
AMSU_A_5_Precip_Corr_50km		0	323907	nan	[0, 0]
AMSU_A_6_Precip_Corr_50km		0	323907	nan	[0, 0]
AMSU_A_7_Precip_Corr_50km		0	323907	nan	[0, 0]
AMSU_A_8_Precip_Corr_50km		0	323907	nan	[0, 0]
AMSU_A_9_Precip_Corr_50km		0	323907	nan	[0, 0]
AMSU_A_4_Precip_Corr_15km		0	2916000	nan	[0, 0]
AMSU_A_5_Precip_Corr_15km		0	2916000	nan	[0, 0]
AMSU_A_6_Precip_Corr_15km		0	2916000	nan	[0, 0]
AMSU_A_7_Precip_Corr_15km		0	2916000	nan	[0, 0]
AMSU_A_8_Precip_Corr_15km		0	2916000	nan	[0, 0]
AMSU_A_9_Precip_Corr_15km		0	2916000	nan	[0, 0]
rain_rate_50km		0	323907	nan	[0, 0]

Version 6 Performance and Test Report

rain_rate_15km		0	2916000	nan	[0,	0]
lwCDSup		30972691	1427309	1.087e+18	[0,	2.367e+21]
lwCDSup	Q1	17185670	0	1.074e+18	[0,	4.46e+20]
lwCDSup	Q2	13787021	1427309	1.105e+18	[0,	2.367e+21]
lwCDSup(0.1hPa)		323907	0	0	[0,	0]
lwCDSup(0.1hPa)	Q1	176898	0	0	[0,	0]
lwCDSup(0.1hPa)	Q2	147009	0	0	[0,	0]
lwCDSup(3.3hPa)		323907	0	0	[0,	0]
lwCDSup(3.3hPa)	Q1	176898	0	0	[0,	0]
lwCDSup(3.3hPa)	Q2	147009	0	0	[0,	0]
lwCDSup(16hPa)		323907	0	0	[0,	0]
lwCDSup(16hPa)	Q1	176898	0	0	[0,	0]
lwCDSup(16hPa)	Q2	147009	0	0	[0,	0]
lwCDSup(47hPa)		323907	0	0	[0,	0]
lwCDSup(47hPa)	Q1	176898	0	0	[0,	0]
lwCDSup(47hPa)	Q2	147009	0	0	[0,	0]
lwCDSup(103hPa)		323907	0	0	[0,	0]
lwCDSup(103hPa)	Q1	176898	0	0	[0,	0]
lwCDSup(103hPa)	Q2	147009	0	0	[0,	0]
lwCDSup(190hPa)		323907	0	0	[0,	0]
lwCDSup(190hPa)	Q1	176898	0	0	[0,	0]
lwCDSup(190hPa)	Q2	147009	0	0	[0,	0]
lwCDSup(314hPa)		323907	0	5.571e+16	[0,	8.75e+20]
lwCDSup(314hPa)	Q1	176898	0	0	[0,	0]
lwCDSup(314hPa)	Q2	147009	0	1.227e+17	[0,	8.75e+20]
lwCDSup(478hPa)		323907	0	1.972e+18	[0,	2.267e+21]
lwCDSup(478hPa)	Q1	176898	0	9.993e+16	[0,	1.515e+20]
lwCDSup(478hPa)	Q2	147009	0	4.225e+18	[0,	2.267e+21]
lwCDSup(684hPa)		314518	9389	1.397e+18	[0,	2.063e+21]
lwCDSup(684hPa)	Q1	176897	0	2.656e+17	[0,	1.756e+20]
lwCDSup(684hPa)	Q2	137621	9389	2.852e+18	[0,	2.063e+21]
lwCDSup(932hPa)		281825	42082	1.403e+19	[0,	2.102e+21]
lwCDSup(932hPa)	Q1	176838	0	1.965e+19	[0,	3.309e+20]
lwCDSup(932hPa)	Q2	104987	42082	4.565e+18	[0,	2.102e+21]
lwCDSupErr		30972691	1427309	2.266e+17	[1e+16,	4.735e+20]
lwCDSupErr	Q1	17185670	0	2.236e+17	[1e+16,	8.919e+19]
lwCDSupErr	Q2	13787021	1427309	2.304e+17	[1e+16,	4.735e+20]
lwCDSupErr(0.1hPa)		323907	0	1e+16	[1e+16,	1e+16]
lwCDSupErr(0.1hPa)	Q1	176898	0	1e+16	[1e+16,	1e+16]
lwCDSupErr(0.1hPa)	Q2	147009	0	1e+16	[1e+16,	1e+16]
lwCDSupErr(3.3hPa)		323907	0	1e+16	[1e+16,	1e+16]
lwCDSupErr(3.3hPa)	Q1	176898	0	1e+16	[1e+16,	1e+16]
lwCDSupErr(3.3hPa)	Q2	147009	0	1e+16	[1e+16,	1e+16]
lwCDSupErr(16hPa)		323907	0	1e+16	[1e+16,	1e+16]
lwCDSupErr(16hPa)	Q1	176898	0	1e+16	[1e+16,	1e+16]
lwCDSupErr(16hPa)	Q2	147009	0	1e+16	[1e+16,	1e+16]
lwCDSupErr(47hPa)		323907	0	1e+16	[1e+16,	1e+16]
lwCDSupErr(47hPa)	Q1	176898	0	1e+16	[1e+16,	1e+16]
lwCDSupErr(47hPa)	Q2	147009	0	1e+16	[1e+16,	1e+16]
lwCDSupErr(103hPa)		323907	0	1e+16	[1e+16,	1e+16]
lwCDSupErr(103hPa)	Q1	176898	0	1e+16	[1e+16,	1e+16]
lwCDSupErr(103hPa)	Q2	147009	0	1e+16	[1e+16,	1e+16]
lwCDSupErr(190hPa)		323907	0	1e+16	[1e+16,	1e+16]

Version 6 Performance and Test Report

lwCDSupErr(190hPa)	Q1	176898	0	1e+16	[1e+16,	1e+16]
lwCDSupErr(190hPa)	Q2	147009	0	1e+16	[1e+16,	1e+16]
lwCDSupErr(314hPa)		323907	0	2.114e+16	[1e+16,	1.75e+20]
lwCDSupErr(314hPa)	Q1	176898	0	1e+16	[1e+16,	1e+16]
lwCDSupErr(314hPa)	Q2	147009	0	3.455e+16	[1e+16,	1.75e+20]
lwCDSupErr(478hPa)		323907	0	4.041e+17	[1e+16,	4.533e+20]
lwCDSupErr(478hPa)	Q1	176898	0	2.943e+16	[1e+16,	3.029e+19]
lwCDSupErr(478hPa)	Q2	147009	0	8.548e+17	[1e+16,	4.533e+20]
lwCDSupErr(684hPa)		314518	9389	2.871e+17	[1e+16,	4.126e+20]
lwCDSupErr(684hPa)	Q1	176897	0	6.01e+16	[1e+16,	3.511e+19]
lwCDSupErr(684hPa)	Q2	137621	9389	5.789e+17	[1e+16,	4.126e+20]
lwCDSupErr(932hPa)		281825	42082	2.808e+18	[1e+16,	4.204e+20]
lwCDSupErr(932hPa)	Q1	176838	0	3.93e+18	[1e+16,	6.617e+19]
lwCDSupErr(932hPa)	Q2	104987	42082	9.17e+17	[1e+16,	4.204e+20]
cIWSup		30972691	1427309	0	[0,	0]
cIWSup(0.1hPa)		323907	0	0	[0,	0]
cIWSup(3.3hPa)		323907	0	0	[0,	0]
cIWSup(16hPa)		323907	0	0	[0,	0]
cIWSup(47hPa)		323907	0	0	[0,	0]
cIWSup(103hPa)		323907	0	0	[0,	0]
cIWSup(190hPa)		323907	0	0	[0,	0]
cIWSup(314hPa)		323907	0	0	[0,	0]
cIWSup(478hPa)		323907	0	0	[0,	0]
cIWSup(684hPa)		314518	9389	0	[0,	0]
cIWSup(932hPa)		281825	42082	0	[0,	0]
satzen_hsb	0	323907	nan	[0,	0]	
satazi_hsb	0	323907	nan	[0,	0]	
tsurf_forecast		323907	0	281.6	[197.4,	326]
Forecast_Wind_U		323907	0	0.114	[-24.11,	22.25]
Forecast_Wind_V		323907	0	0.4194	[-24.7,	22.91]
MODIS_emis		603576	1340424	0.9482	[0.6652,	0.996]
MODIS_emis_dev		603576	1340424	0.008472	[0,	0.1188]
MODIS_emis_qct		1296000	0	26.03	[0,	3712]
MODIS_emis_spots		4945728	12550272	0.9472	[0.6565,	0.996]
MODIS_emis_spots_dev		4945728	12550272	0.007006	[0,	0.1197]
MODIS_emis_10_hinge		1005960	2234040	0.9574	[0.646,	0.999]
MODIS_LST		124018	199889	273.7	[196.1,	332.4]
MODIS_LST_dev		124018	199889	1.636	[0,	15.95]
MODIS_LST_qct		1296000	0	70.56	[0,	1.281e+04]
MODIS_LST_spots		1038036	1877964	273.3	[195.4,	333.1]
MODIS_LST_spots_dev		1038036	1877964	1.211	[0,	17.38]
CO2ppmv		323907	0	373.2	[373.2,	373.2]
CO2ppmv	Q2	323907	0	373.2	[373.2,	373.2]
CO2ppmvErr		323907	0	7.464	[7.463,	7.464]
CO2ppmvErr	Q2	323907	0	7.464	[7.463,	7.464]
TSurfClim		323907	0	281.3	[204.6,	327.3]
TSurfAirClim		323907	0	280.6	[209.6,	314.1]
TAirClim		32390800	9200	237.5	[184.3,	326.3]
TAirClim(0.1hPa)		323907	0	239.4	[231.4,	259]
TAirClim(3.3hPa)		323907	0	244.4	[232.9,	256.5]
TAirClim(16hPa)		323907	0	219.6	[193,	228.2]
TAirClim(47hPa)		323907	0	210.8	[184.4,	225.2]
TAirClim(103hPa)		323907	0	206	[187.6,	224.8]

Version 6 Performance and Test Report

TAirClim(190hPa)	323907	0	215.7	[195.7,	227.3]	
TAirClim(314hPa)	323907	0	231.2	[208.7,	248.7]	
TAirClim(478hPa)	323907	0	252	[225.3,	269.1]	
TAirClim(684hPa)	323907	0	267.2	[189.5,	294.2]	
TAirClim(932hPa)	323907	0	277.5	[189.5,	316.8]	
H2OCDCLim	32390800	9200	9.053e+20	[1.681e+15,	2.086e+22]	
H2OCDCLim(0.1hPa)	323907	0	7.58e+15	[6.525e+15,	8.189e+15]	
H2OCDCLim(3.3hPa)	323907	0	7.484e+16	[6.67e+16,	8.46e+16]	
H2OCDCLim(16hPa)	323907	0	2.064e+17	[2.038e+17,	2.246e+17]	
H2OCDCLim(47hPa)	323907	0	4.206e+17	[4.188e+17,	4.237e+17]	
H2OCDCLim(103hPa)	323907	0	7.618e+17	[7.071e+17,	1.023e+18]	
H2OCDCLim(190hPa)	323907	0	5.093e+18	[1.057e+18,	2.428e+19]	
H2OCDCLim(314hPa)	323907	0	7.115e+19	[3.824e+18,	3.983e+20]	
H2OCDCLim(478hPa)	323907	0	4.366e+20	[3.188e+19,	2.599e+21]	
H2OCDCLim(684hPa)	323907	0	1.778e+21	[3.04e+19,	7.247e+21]	
H2OCDCLim(932hPa)	323907	0	5.759e+21	[3.027e+19,	1.554e+22]	
Tropo_CCI	322926	981	248.9	[193,	270.8]	
Tropo_CCI	Q0	50324	0	254.6	[194.6,	269.9]
Tropo_CCI	Q1	229691	0	248.7	[193,	270.8]
Tropo_CCI	Q2	42911	981	243.6	[194,	268.7]
Tropo_CCI_Est_Err		322926	981	0.5	[0.5,	0.5]
Strato_CCI		322926	981	211.5	[184.5,	231.8]
Strato_CCI	Q0	50324	0	209.6	[188.6,	231.2]
Strato_CCI	Q1	229691	0	211.8	[185.5,	231.8]
Strato_CCI	Q2	42911	981	211.5	[184.5,	231.6]
Strato_CCI_Est_Err		322926	981	0.5	[0.5,	0.5]
MoonInViewIR		323907	0	0	[0,	0]
pseudo_lapse_rate		2915172	828	4.724	[-10.36,	10.19]
TAirSCCNN	30972686	1427314	236.4	[157.2,	323.2]	
TAirSCCNN(0.1hPa)	323907	0	239.4	[231.4,	259]	
TAirSCCNN(3.3hPa)	323907	0	243.7	[223.7,	266.2]	
TAirSCCNN(16hPa)	323907	0	220.8	[192.4,	237.8]	
TAirSCCNN(47hPa)	323907	0	211.9	[181.5,	231.8]	
TAirSCCNN(103hPa)	323907	0	207	[183.4,	233.5]	
TAirSCCNN(190hPa)	323907	0	217	[188.6,	236.4]	
TAirSCCNN(314hPa)	323907	0	230.9	[205.1,	254.2]	
TAirSCCNN(478hPa)	323907	0	251.7	[222.3,	273.8]	
TAirSCCNN(684hPa)	314518	9389	268.6	[179.8,	293.7]	
TAirSCCNN(932hPa)	281825	42082	281.7	[216.3,	316.5]	
TAirCldyReg	30972691	1427309	236.2	[113.5,	384.3]	
TAirCldyReg(0.1hPa)	323907	0	239.4	[231.4,	259]	
TAirCldyReg(3.3hPa)	323907	0	243.4	[220.4,	270.4]	
TAirCldyReg(16hPa)	323907	0	221.3	[193.3,	238.4]	
TAirCldyReg(47hPa)	323907	0	212.3	[183.8,	232.3]	
TAirCldyReg(103hPa)	323907	0	207.2	[181.2,	233.1]	
TAirCldyReg(190hPa)	323907	0	216.7	[188.7,	237.7]	
TAirCldyReg(314hPa)	323907	0	231.2	[204.6,	253.4]	
TAirCldyReg(478hPa)	323907	0	251.4	[220.1,	272.9]	
TAirCldyReg(684hPa)	314518	9389	267.9	[136.7,	334.1]	
TAirCldyReg(932hPa)	281825	42082	280.1	[161.4,	364.1]	
H2OCDSCCNN	30972686	1427314	7.152e+20	[3.585e+14,	1.969e+22]	
H2OCDSCCNN(0.1hPa)	323907	0	5.244e+15	[1.401e+15,	1.577e+16]	
H2OCDSCCNN(3.3hPa)	323907	0	5.041e+16	[1.579e+16,	1.351e+17]	

Version 6 Performance and Test Report

H2OCDSCCNN(16hPa)	323907	0	1.404e+17	[4.572e+16, 4.051e+17]
H2OCDSCCNN(47hPa)	323907	0	2.875e+17	[8.928e+16, 8.371e+17]
H2OCDSCCNN(103hPa)	323907	0	5.255e+17	[1.507e+17, 1.561e+18]
H2OCDSCCNN(190hPa)	323907	0	4.242e+18	[2.121e+17, 2.629e+19]
H2OCDSCCNN(314hPa)	323907	0	6.174e+19	[5.451e+17, 7.329e+20]
H2OCDSCCNN(478hPa)	323907	0	4.334e+20	[3.393e+18, 3.573e+21]
H2OCDSCCNN(684hPa)	314518	9389	1.89e+21	[7.771e+18, 8.615e+21]
H2OCDSCCNN(932hPa)	281825	42082	6.386e+21	[5.398e+19, 1.613e+22]
H2OCDCLdyReg	30972691	1427309	6.606e+20	[2.927e+08, 7.583e+22]
H2OCDCLdyReg(0.1hPa)	323907	0	4.884e+15	[6.205e+14, 2.895e+16]
H2OCDCLdyReg(3.3hPa)	323907	0	4.76e+16	[5.285e+15, 2.431e+17]
H2OCDCLdyReg(16hPa)	323907	0	1.32e+17	[1.57e+16, 7.386e+17]
H2OCDCLdyReg(47hPa)	323907	0	2.696e+17	[3.227e+16, 1.519e+18]
H2OCDCLdyReg(103hPa)	323907	0	4.896e+17	[6.763e+16, 2.754e+18]
H2OCDCLdyReg(190hPa)	323907	0	4.014e+18	[1.266e+15, 2.069e+19]
H2OCDCLdyReg(314hPa)	323907	0	6.076e+19	[2.994e+16, 4.382e+20]
H2OCDCLdyReg(478hPa)	323907	0	3.967e+20	[1.112e+17, 5.41e+21]
H2OCDCLdyReg(684hPa)	314518	9389	1.687e+21	[2.861e+12, 1.472e+22]
H2OCDCLdyReg(932hPa)	281825	42082	6.041e+21	[2.127e+15, 3.815e+22]
TSurfSCCNN	323907	0	281.7	[196.5, 332.9]
TSurflRet	323907	0	281.7	[196.5, 332.9]
TSurfAirlRet	323907	0	278.9	[196.4, 336.1]
TAirlRet	30972691	1427309	236.7	[156.8, 322.9]
TAirlRet(0.1hPa)	323907	0	239.6	[229.5, 264.5]
TAirlRet(3.3hPa)	323907	0	244	[226.1, 263.6]
TAirlRet(16hPa)	323907	0	222	[193.7, 239]
TAirlRet(47hPa)	323907	0	212.5	[182.1, 232.5]
TAirlRet(103hPa)	323907	0	207.1	[182.7, 234]
TAirlRet(190hPa)	323907	0	217.1	[187.3, 236.7]
TAirlRet(314hPa)	323907	0	231.1	[204.1, 257.9]
TAirlRet(478hPa)	323907	0	251.9	[221.1, 275.1]
TAirlRet(684hPa)	314518	9389	268.7	[178.6, 294.3]
TAirlRet(932hPa)	281825	42082	281.7	[216.2, 316.6]
H2OCD1Ret	30972691	1427309	7.152e+20	[3.585e+14, 1.969e+22]
H2OCD1Ret(0.1hPa)	323907	0	5.244e+15	[1.401e+15, 1.577e+16]
H2OCD1Ret(3.3hPa)	323907	0	5.041e+16	[1.579e+16, 1.351e+17]
H2OCD1Ret(16hPa)	323907	0	1.404e+17	[4.572e+16, 4.051e+17]
H2OCD1Ret(47hPa)	323907	0	2.875e+17	[8.928e+16, 8.371e+17]
H2OCD1Ret(103hPa)	323907	0	5.255e+17	[1.507e+17, 1.561e+18]
H2OCD1Ret(190hPa)	323907	0	4.242e+18	[2.121e+17, 2.629e+19]
H2OCD1Ret(314hPa)	323907	0	6.174e+19	[5.451e+17, 7.329e+20]
H2OCD1Ret(478hPa)	323907	0	4.334e+20	[3.393e+18, 3.573e+21]
H2OCD1Ret(684hPa)	314518	9389	1.89e+21	[7.771e+18, 8.615e+21]
H2OCD1Ret(932hPa)	281825	42082	6.386e+21	[5.398e+19, 1.613e+22]
O3CDInit	0	32400000	nan	[0, 0]
O3CDInit(0.1hPa)	0	323907	nan	[0, 0]
O3CDInit(3.3hPa)	0	323907	nan	[0, 0]
O3CDInit(16hPa)	0	323907	nan	[0, 0]
O3CDInit(47hPa)	0	323907	nan	[0, 0]
O3CDInit(103hPa)	0	323907	nan	[0, 0]
O3CDInit(190hPa)	0	323907	nan	[0, 0]
O3CDInit(314hPa)	0	323907	nan	[0, 0]
O3CDInit(478hPa)	0	323907	nan	[0, 0]

Version 6 Performance and Test Report

O3CDInit(684hPa)	0	323907	nan	[0,	0]
O3CDInit(932hPa)	0	323907	nan	[0,	0]
numHingesSurfFG	323907	0	39	[39,	39]
freqEmisFG	12632412	19767588	1380	[649.3,	2632]
freqEmisFG(649)	323907	0	649.3	[649.3,	649.3]
freqEmisFG(725)	323907	0	724.6	[724.6,	724.6]
freqEmisFG(909)	323907	0	909.1	[909.1,	909.1]
freqEmisFG(1163)	323907	0	1163	[1163,	1163]
freqEmisFG(1205)	323907	0	1205	[1205,	1205]
freqEmisFG(1639)	323907	0	1639	[1639,	1639]
freqEmisFG(2174)	323907	0	2174	[2174,	2174]
freqEmisFG(2381)	323907	0	2381	[2381,	2381]
freqEmisFG(2500)	323907	0	2500	[2500,	2500]
freqEmisFG(2632)	323907	0	2632	[2632,	2632]
emisIRFG	12632412	19767588	0.9709	[0.6652,	0.999]
emisIRFG(649)	323907	0	0.9573	[0.9067,	0.999]
emisIRFG(725)	323907	0	0.9639	[0.9117,	0.9971]
emisIRFG(909)	323907	0	0.9829	[0.9176,	0.9949]
emisIRFG(1163)	323907	0	0.9728	[0.6652,	0.996]
emisIRFG(1205)	323907	0	0.9721	[0.6652,	0.996]
emisIRFG(1639)	323907	0	0.9743	[0.9472,	0.9899]
emisIRFG(2174)	323907	0	0.9644	[0.8015,	0.9958]
emisIRFG(2381)	323907	0	0.9607	[0.7379,	0.9943]
emisIRFG(2500)	323907	0	0.9627	[0.7145,	0.9875]
emisIRFG(2632)	323907	0	0.9648	[0.6905,	0.9865]
freqEmisInit	9360	2640	1380	[649.3,	2632]
emisIRInit	0	16200000	nan	[0,	0]
rhoIRInit	0	16200000	nan	[0,	0]
FracLandPlusIce	323907	0	0.4363	[0,	1]
CldClearParam	2915172	828	-5.815e-10	[-27.62,	30.5]
CC1_Noise_Amp	323907	0	1.242	[0.3333,	42.02]
Tsurf_4_CC1	323907	0	281.7	[196.5,	332.9]
TotCld_4_CC1	323907	0	0.5068	[0,	1]
CC1_RCode	323907	0	0	[0,	0]
CC2_RCode	323584	323	0.002033	[0,	1]
Phys_RCode	323249	658	0.001036	[0,	5]
TotCld_below_500mb	323249	658	0.2888	[0,	1]
Phys_resid_AMSUA	3875112	984888	0.1355	[-56.83,	59.91]
Phys_resid_IR_window_790	322926	981	-0.4007	[-39.72,	32.37]
Phys_resid_IR_window_844	322926	981	-0.2411	[-39.07,	35]
Phys_resid_IR_window_917	322926	981	-0.005794	[-30.72,	36.89]
Phys_resid_IR_window_1231	322926	981	-0.1232	[-31.01,	36.85]
Phys_resid_IR_window_2513	322914	993	0.397	[-23.69,	70.58]
Phys_resid_IR_window_2616	322898	1009	0.7106	[-43.61,	114.9]
CBTmOBT1231	2909241	6759	-0.5178	[-24.8,	80.09]
CBTmOBT1231s	2909241	6759	-0.355	[-24.8,	80.09]
CC_noise_eff_amp_factor	323842	65	12.08	[0.3333,	1203]
CC1_noise_eff_amp_factor	323842	65	33.2	[0.3333,	2224]
CC1_Resid	323907	0	1.417	[0.09384,	29.42]
CCfinal_Resid	323907	0	0.598	[0.07768,	28.17]
CCfinal_Noise_Amp	323907	0	1.241	[0.3333,	42.02]
Tdiff_IR_MW_ret	323249	658	0.6288	[0,	45.8]
Tdiff_IR_4CC1	323249	658	0.9673	[0.001355,	50.02]

Version 6 Performance and Test Report

TSurfdiff_IR_4CC1	323249	658	4.706	[0, 71.4]
TSurfdiff_IR_4CC2	323249	658	4.706	[0, 71.4]
AMSU_Chans_Resid	323249	658	0.2482	[7.749e-07, 17.25]
TotCld_4_CCfinal	323907	0	0.4574	[0, 1]
Surf_Resid_Ratio	323186	721	1.379	[0.002192, 56.27]
Temp_Resid_Ratio	323186	721	1.74	[0.2008, 36.28]
Water_Resid_Ratio	322966	941	1.118	[0.005691, 15.98]
Cloud_Resid_Ratio3x3	2602728	313272	0.1759	[0, 391.6]
Cloud_Resid_Ratio	289192	34715	0.1759	[0, 363.6]
O3_Resid_Ratio	322962	945	0.568	[0.000134, 7.498]
CO_Resid_Ratio	322923	984	0.2792	[0, 16.74]
CH4_Resid_Ratio	322923	984	0.5595	[0, 19.48]
MWCheck_Resid_Ratio	322962	945	0.2753	[0.01305, 4.287]
invalid	323907	0	0	[0, 0]
MW_ret_used	323907	0	0.003029	[0, 1]
bad_clouds	323907	0	0	[0, 0]
Start_Clim	323907	0	2.702	[2, 5]
Startup	323907	0	4	[4, 4]
cld_surf_fallback	323249	658	0.1586	[0, 1]
nchan_big_ang_adj	323907	0	0.08368	[0, 85]
bad_llb	323907	0	0	[0, 0]
bad_llb_amssu	323907	0	0	[0, 0]
bad_llb_hsb	323907	0	1	[1, 1]
bad_llb_airs	323907	0	0	[0, 0]
bad_llb_vis	323907	0	0.49	[0, 1]
forecast	323907	0	0	[0, 0]
no_psurf_guess	323907	0	0	[0, 0]
bad_temps	323907	0	0	[0, 0]
bad_h2o	323907	0	0	[0, 0]
bad_o3	323907	0	0.003029	[0, 1]
bad_co	323907	0	0.006076	[0, 2]
no_tuning	0	323907	nan	[0, 0]
no_ang_corr	323907	0	0	[0, 0]
no_mw	323907	0	0	[0, 0]
no_initial	323907	0	1	[1, 1]
no_final	323907	0	0	[0, 0]
mw_fpe	323907	0	0	[0, 0]
cloudy_reg_fpe	323907	0	0	[0, 0]
initial_fpe	323907	0	0	[0, 0]
final_fpe	323907	0	0	[0, 0]
MWPrecip	0	323907	nan	[0, 0]
MWsurf_T0	323907	0	0.1787	[-150.3, 174.7]
MWsurf_Tinf	323907	0	4.323	[-216.7, 194.5]
MWsecant_ratio	186450	137457	1.122	[1, 1.813]
MWseaice_conc	323907	0	0.1343	[0, 1]
MWresidual_temp	323907	0	1.604	[0.001373, 423.3]
MWresidual_mois	323907	0	215.9	[0.0347, 1.001e+06]
MWresidual_AMSUA	4858620	1380	0.02031	[-119.5, 66.35]
MWresidual_HSB	1619540	460	0	[0, 0]
MWiter_temp	323907	0	2.058	[1, 12]
MWiter_mois	323907	0	4.019	[1, 16]
mw_ret_code	323907	0	0.5741	[0, 36]
sccnn_ret_code	323907	0	0	[0, 0]

Version 6 Performance and Test Report

cloudy_reg_ret_code	323907	0	0	[0,	0]
Cloudy_Reg_FOV_chan	323907	0	1301	[1301,	1301]
Cloudy_Reg_FOV	323907	0	5.018	[1,	9]
Cloudy_Reg_FOV_BT	323907	0	265.5	[189.8,	315.2]
Cloudy_Reg_Score	323907	0	0.9222	[0.8024,	1.77]
cloud_ice	323907	0	0	[0,	0]
icc_too_cloudy	323907	0	0	[0,	0]
icc_low_contrast	0	323907	nan	[0,	0]
icc_bad_rad	323907	0	0	[0,	0]
icc_contrast	0	323907	nan	[0,	0]
bad_1st	0	323907	nan	[0,	0]
bad_1st_surf	323907	0	1	[1,	1]
bad_1st_cc	323907	0	0	[0,	0]
bad_1st_regres	0	323907	nan	[0,	0]
bad_1st_phys	0	323907	nan	[0,	0]
fcc_too_cloudy	323249	658	0	[0,	0]
fcc_low_contrast	323249	658	0	[0,	0]
fcc_bad_rad	323249	658	0	[0,	0]
fcc_contrast1	323907	0	1.241	[0.3333,	42.02]
fcc_contrast2	322926	981	1.203	[0.3333,	45.3]
bad_final	323907	0	0	[0,	0]
bad_final_cc	323907	0	0.002031	[0,	1]
bad_final_ir	323249	658	0.0009992	[0,	1]
bad_final_surf	323907	0	0	[0,	0]
bad_final_temp	323907	0	0	[0,	0]
bad_final_h2o	323907	0	0	[0,	0]
bad_final_o3	323249	658	0.0009992	[0,	1]
bad_final_cloud	0	323907	nan	[0,	0]
bad_cc_cld_ret	0	323907	nan	[0,	0]
MW_IR_ret_differ	322926	981	0	[0,	0]
bad_MW_low_resid	322926	981	0	[0,	0]
MW_low_atm_resid	322926	981	0.2482	[7.749e-07,	17.25]
final_AMSU_ret	323907	0	0	[0,	0]
final_HSB_ret	323907	0	3	[3,	3]
final_cloud_ret	323907	0	0.349	[0,	1]
final_cloud_spot_ret3x3	2915172	828	0.1046	[0,	1]
final_surf_ret	322926	981	0	[0,	0]
final_temp_ret	322926	981	0	[0,	0]
final_h2o_ret	322926	981	6.193e-06	[0,	1]
final_o3_ret	322926	981	3.097e-06	[0,	1]
final_ch4_ret	322926	981	4.955e-05	[0,	3]
final_co_ret	322926	981	3.406e-05	[0,	3]
final_co2_ret	0	323907	nan	[0,	0]
bad_vis_rad	323907	0	0	[0,	0]
bad_vis_cal	323907	0	0	[0,	0]
bad_vis_det_temp	323907	0	0	[0,	0]
bad_scan_hd_temp	323907	0	0	[0,	0]
Initial_CC_score	323907	0	0.9222	[0.8024,	1.77]
Initial_CC_subscores	2267356	972644	0.9361	[0.3101,	30.27]
sccnn_bt_corr	647816	184	3.392	[-14.7,	68.01]
sccnn_bt_corr_freq	647816	184	2224	[2216,	2231]
relayer_num_nonpos_coef_h2o	323907	0	9.262e-06	[0,	3]
relayer_num_nonpos_coef_o3	323907	0	0	[0,	0]

Version 6 Performance and Test Report

relayer_num_nonpos_coef_co	323907	0	1.544e-05	[0,	5]
relayer_num_nonpos_coef_ch4	323907	0	3.705e-05	[0,	1]
relayer_num_knots	323907	0	33.53	[27,	34]
relayer_degree	323907	0	4	[4,	4]
relayer_runge_kutta_bits	323907	0	0.001235	[0,	8]
Num_Fill_Chан_Cloudy_Reg	323907	0	0.008722	[0,	1]
Num_Fill_Chан_SCCNN	323907	0	0.0002809	[0,	1]
Num_Fill_Chан_Ang_Adj	323907	0	0.004816	[0,	1]
Doppler_shift_ppm	323907	0	-0.01041	[-1.255,	1.242]
spectral_clear_indicator	2916000	0	0.3157	[-2,	2]
num_clear_spectral_indicator	323907	0	0.1128	[-1,	9]
orbit_phase_deg	10799	1	177.7	[0.04301,	360]
shift_y0	183583	17	-13.51	[-13.72,	-13.36]
scan_freq	25680022	2378	1337	[649.6,	2665]
LlcProc	25682400	0	0	[0,	0]
LlcCleanReason	25682400	0	0	[0,	0]
L1C_Reconst_Bias	0	570720	nan	[0,	0]
L1C_Reconst_Dev	0	570720	nan	[0,	0]

4.3. *Cloud cleared radiances ('airiccf')*

Fieldname	Qual	NumGood	NumBad	Mean	[Min,	Max]
<hr/>								
radiances		717303340	53168660	39.13	[-155.6,	334.8]	
radiances	Q0	263131176	0	35.01	[0.004028,	199.7]	
radiances	Q1	242225138	0	37.49	[0.001404,	183.6]	
radiances	Q2	211947026	53168660	46.11	[-155.6,	334.8]	
radiances(650)		322908	999	46.4	[8.688,	89.81]	
radiances(650)	Q0	274036	0	47.07	[28.75,	60.69]	
radiances(650)	Q1	28313	0	43.24	[26.81,	58.69]	
radiances(650)	Q2	20559	999	41.75	[8.688,	89.81]	
radiances(790)		322926	981	97.49	[14,	197.6]	
radiances(790)	Q0	45365	0	109.4	[14,	197.6]	
radiances(790)	Q1	109711	0	107.8	[17.94,	176.2]	
radiances(790)	Q2	167850	981	87.54	[14.47,	197.4]	
radiances(844)		322926	981	90.99	[11.62,	192.7]	
radiances(844)	Q0	46140	0	103.1	[11.62,	192.7]	
radiances(844)	Q1	94419	0	103.6	[15.19,	174.6]	
radiances(844)	Q2	182367	981	81.4	[11.62,	192.2]	
radiances(917)		322926	981	81.04	[8.625,	177.8]	
radiances(917)	Q0	50500	0	93.34	[8.625,	177.7]	
radiances(917)	Q1	88402	0	93.27	[10.72,	161.1]	
radiances(917)	Q2	184024	981	71.78	[8.758,	177.8]	
radiances(1231)		322926	981	39.43	[1.887,	109.7]	
radiances(1231)	Q0	63366	0	48.18	[1.887,	109.7]	
radiances(1231)	Q1	116457	0	42.5	[2.535,	97.12]	
radiances(1231)	Q2	143103	981	33.05	[1.898,	107.1]	
radiances(2513)		322914	993	0.621	[-0.01611,	5.401]	
radiances(2513)	Q0	77695	0	0.8163	[0.00647,	4.176]	
radiances(2513)	Q1	84319	0	0.775	[0.002319,	4.001]	
radiances(2513)	Q2	160900	993	0.4461	[-0.01611,	5.401]	
radiances(2616)		322898	1009	0.4882	[-0.01093,	5.229]	

Version 6 Performance and Test Report

radiances(2616)	Q0	73989	0	0.6514	[0.004395,	4.04]
radiances(2616)	Q1	79210	0	0.5985	[0.001526,	3.578]
radiances(2616)	Q2	169699	1009	0.3656	[-0.01093,	5.229]
radiances(2665)		322809	1098	0.3907	[-0.01575,	4.073]
radiances(2665)	Q0	72775	0	0.5282	[0.006348,	3.385]
radiances(2665)	Q1	87393	0	0.4706	[0.002319,	3.063]
radiances(2665)	Q2	162641	1098	0.2862	[-0.01575,	4.073]
radiance_err		717303340	53168660	1.799	[0.0003242,	176.2]
radiance_err	Q0	263131176	0	0.2623	[0.0003242,	2.016]
radiance_err	Q1	242225138	0	1.147	[0.0003242,	5.312]
radiance_err	Q2	211947026	53168660	4.452	[0.0003242,	176.2]
radiance_err(650)		322908	999	0.6744	[0.2188,	36.25]
radiance_err(650)	Q0	274036	0	0.2846	[0.2188,	1]
radiance_err(650)	Q1	28313	0	1.375	[0.7266,	2.594]
radiance_err(650)	Q2	20559	999	4.906	[1.719,	36.25]
radiance_err(790)		322926	981	4.864	[0.08105,	99.33]
radiance_err(790)	Q0	45365	0	0.5991	[0.08105,	1.719]
radiance_err(790)	Q1	109711	0	2.709	[0.8438,	4.812]
radiance_err(790)	Q2	167850	981	7.425	[1.344,	99.33]
radiance_err(844)		322926	981	5.028	[0.09375,	96.42]
radiance_err(844)	Q0	46140	0	0.5974	[0.09375,	1.734]
radiance_err(844)	Q1	94419	0	2.725	[0.7344,	4.922]
radiance_err(844)	Q2	182367	981	7.34	[1.203,	96.42]
radiance_err(917)		322926	981	4.695	[0.03369,	90.87]
radiance_err(917)	Q0	50500	0	0.5702	[0.03369,	1.691]
radiance_err(917)	Q1	88402	0	2.612	[0.5391,	4.984]
radiance_err(917)	Q2	184024	981	6.827	[0.9844,	90.87]
radiance_err(1231)		322926	981	2.341	[0.01221,	37.61]
radiance_err(1231)	Q0	63366	0	0.4486	[0.01221,	1.217]
radiance_err(1231)	Q1	116457	0	1.58	[0.1797,	3.934]
radiance_err(1231)	Q2	143103	981	3.799	[0.3027,	37.61]
radiance_err(2513)		322914	993	0.06363	[0.0005035,	2.27]
radiance_err(2513)	Q0	77695	0	0.01193	[0.0005035,	0.1042]
radiance_err(2513)	Q1	84319	0	0.05598	[0.0005112,	0.3157]
radiance_err(2513)	Q2	160900	993	0.0926	[0.0005112,	2.27]
radiance_err(2616)		322898	1009	0.05359	[0.000351,	2.739]
radiance_err(2616)	Q0	73989	0	0.00932	[0.000351,	0.08679]
radiance_err(2616)	Q1	79210	0	0.04436	[0.0003586,	0.2757]
radiance_err(2616)	Q2	169699	1009	0.0772	[0.0003586,	2.739]
radiance_err(2665)		322809	1098	0.04205	[0.0004883,	2.3]
radiance_err(2665)	Q0	72775	0	0.008081	[0.0004883,	0.1083]
radiance_err(2665)	Q1	87393	0	0.03567	[0.0004959,	0.2294]
radiance_err(2665)	Q2	162641	1098	0.06067	[0.0004959,	2.3]
CldClearParam		2915172	828	-5.157e-10	[-27.62,	32.75]
nominal_freq		570720	0	1337	[649.6,	2665]
scanang		323907	0	-0.04109	[-47.91,	47.83]
satheight		10800	0	714.5	[703.7,	730.3]
satroll		10800	0	-0.0004961	[-0.03416,	0.03116]
satpitch		10800	0	-0.02367	[-0.03092,	-0.007053]
satyaw		10800	0	-0.0006888	[-0.03821,	0.03502]
satzen		323907	0	28.08	[1.73,	55.83]
satazi		323907	0	0.02965	[-180,	180]
solzen		323907	0	90.55	[14.77,	165.2]

Version 6 Performance and Test Report

solazi	172264	151643	-52.04	[-180,	180]
glintlat	5353	5447	7.832	[-65.87,	75.93]
glintlon	5353	5447	-0.7059	[-180,	180]
sun_glint_distance	323907	0	1.554e+04	[0,	3e+04]
nadirTAI	10800	0	3.055e+08	[3.054e+08,	3.055e+08]
sat_lat	10800	0	-1.526	[-81.87,	81.87]
sat_lon	10800	0	-0.4735	[-180,	180]
scan_node_type	10800	0	66.51	[65,	68]
topog	323907	0	343.1	[-82.4,	5805]
topog_err	323907	0	32.41	[0,	1437]
landFrac	323907	0	0.3314	[0,	1]
landFrac_err	323907	0	0.03044	[0,	0.471]
ftpgeoqa	323907	0	0	[0,	0]
zengeoqa	323907	0	0	[0,	0]
demgeoqa	323907	0	0.01092	[0,	4]
satgeoqa	10800	0	0	[0,	0]
glintgeoqa	10800	0	1.025	[0,	77]
moongeoqa	10800	0	9.259e-05	[0,	1]
CalFlag	25682400	0	0.8156	[-128,	57]
CalScanSummary	10800	0	0.1836	[-128,	24]
CalChanSummary	570720	0	0.9731	[-128,	58]
ExcludedChans	570720	0	0.7792	[0,	6]
orbit_phase_deg	10799	1	177.7	[0.04301,	360]
shift_y0	183583	17	-13.51	[-13.72,	-13.36]
scan_freq	25680022	2378	1337	[649.6,	2665]
Doppler_shift_ppm	323907	0	-0.01041	[-1.255,	1.242]
NeN_L1B	556824	13896	0.2972	[0.0009686,	48.33]
NeN_L1B_Static	570720	0	0.3893	[0.001041,	12.62]
dust_flag	323907	0	-0.636	[-1,	1]
CC_noise_eff_amp_factor	323842	65	12.08	[0.3333,	1203]
CC1_noise_eff_amp_factor	323842	65	33.2	[0.3333,	2224]
CC1_Resid	323907	0	1.417	[0.09384,	29.42]
CCfinal_Resid	323907	0	0.598	[0.07768,	28.17]
TotCld_4_CCfinal	323907	0	0.4574	[0,	1]
CCfinal_Noise_Amp	323907	0	1.241	[0.3333,	42.02]
invalid	323907	0	0	[0,	0]
all_spots_avg	323907	0	0.074	[0,	1]
MW_ret_used	323907	0	0.003029	[0,	1]
bad_clouds	323907	0	0	[0,	0]
retrieval_type	324000	0	0.1096	[0,	100]

Copyright 2013. All rights reserved.